



HAL
open science

La semicarbazide-sensitive amine oxydase : son rôle dans la différenciation cellulaire des chondrocytes et des cellules musculaires lisses vasculaires et son implication dans des pathologies articulaires et cardiovasculaires

Anna Filip

► To cite this version:

Anna Filip. La semicarbazide-sensitive amine oxydase : son rôle dans la différenciation cellulaire des chondrocytes et des cellules musculaires lisses vasculaires et son implication dans des pathologies articulaires et cardiovasculaires. Human health and pathology. Université de Lorraine, 2014. English. NNT : 2014LORR0244 . tel-01751265

HAL Id: tel-01751265

<https://hal.univ-lorraine.fr/tel-01751265>

Submitted on 29 Mar 2018

HAL is a multi-disciplinary open access archive for the deposit and dissemination of scientific research documents, whether they are published or not. The documents may come from teaching and research institutions in France or abroad, or from public or private research centers.

L'archive ouverte pluridisciplinaire **HAL**, est destinée au dépôt et à la diffusion de documents scientifiques de niveau recherche, publiés ou non, émanant des établissements d'enseignement et de recherche français ou étrangers, des laboratoires publics ou privés.



AVERTISSEMENT

Ce document est le fruit d'un long travail approuvé par le jury de soutenance et mis à disposition de l'ensemble de la communauté universitaire élargie.

Il est soumis à la propriété intellectuelle de l'auteur. Ceci implique une obligation de citation et de référencement lors de l'utilisation de ce document.

D'autre part, toute contrefaçon, plagiat, reproduction illicite encourt une poursuite pénale.

Contact : ddoc-theses-contact@univ-lorraine.fr

LIENS

Code de la Propriété Intellectuelle. articles L 122. 4

Code de la Propriété Intellectuelle. articles L 335.2- L 335.10

http://www.cfcopies.com/V2/leg/leg_droi.php

<http://www.culture.gouv.fr/culture/infos-pratiques/droits/protection.htm>



Ecole Doctorale BioSE (Biologie-Santé-Environnement)

Thèse

Présentée et soutenue publiquement pour l'obtention du titre de

DOCTEUR DE L'UNIVERSITE DE LORRAINE

Mention : « Sciences de la Vie et de la Santé »

par

Anna FILIP

La semicarbazide-sensible amine oxydase : son rôle dans la différenciation cellulaire des chondrocytes et des cellules musculaires lisses vasculaires et son implication dans des pathologies articulaires et cardiovasculaires

Date de soutenance : 10 décembre 2014

Membres du jury :

Rapporteurs :

Virginie MATTOT, CR «UMR_8161 CNRS-Université Lille-Nord, Lille »
Magali CUCCHIARINI, Associate Prof «Saarland University Medical Center, Hamburg»

Examineurs :

Soraya TALEB, CR «UMR_970 INSERM HEGP, Paris»
Bruno Fève, PU-PH «UMR S_938 INSERM-Université Paris»
Didier MAINARD, PU-PH «UMR_7365 CNRS-Université de Lorraine, Nancy»
Jacques MAGDALOU, DR «UMR_7365 CNRS-Université de Lorraine, Nancy»
Directeur de thèse
Patrick LACOLLEY, DR «UMR_1116 INSERM-Université de Lorraine, Nancy»
Directeur de thèse
Nathalie MERCIER, MCU «UMR_1116 INSERM-Université de Lorraine, Nancy»
Co-directeur de thèse

Travail effectué aux laboratoires UMR_1116 INSERM-Université de Lorraine; « Défaillance Cardiovasculaire Aigue et Chronique » et UMR_7365 CNRS-Université de Lorraine ; « Ingénierie Moléculaire et Physiopathologie Articulaire (IMoPA) »,
Faculté de Médecine, Vandœuvre-lès-Nancy.

Acknowledgments

Mes travaux ont été réalisés au laboratoire UMR_1116 INSERM «Défaillance Cardiovasculaire Aigue et Chronique » et au laboratoire UMR_7365 CNRS « Ingénierie Moléculaire et Physiopathologie Articulaire (IMoPA) » à la faculté de médecine de l'Université de Nancy entre 2011 et 2014.

Au terme de ces travaux, je tiens avant tout à adresser mes remerciements les plus chaleureux à tous ceux qui m'ont aidée au cours de leur réalisation.

Tout d'abord, je tiens à remercier très sincèrement Monsieur le Directeur de thèse **Jacques Magdalou** pour m'avoir donné la possibilité d'effectuer un stage avant commencer ma thèse. Je le remercie d'avoir accepté de diriger ma thèse au lieu de prendre sa retraite, et de m'avoir suivie pendant ces trois ans. J'en profite pour lui exprimer ma plus profonde gratitude pour son implication constante, son soutien financier et scientifique.

Je tiens à manifester ma gratitude à Monsieur le Directeur de thèse **Patrick Lacolley** qui m'a fait l'honneur de m'accueillir et m'a permis de réaliser ces travaux dans son laboratoire. Je lui suis très reconnaissante pour sa confiance, son soutien financier et scientifique, ses précieuses remarques et pour son encouragement continu malgré toutes les difficultés que j'ai pu rencontrer durant cette période.

Je tiens à remercier très sincèrement Madame le Co-Directeur de thèse **Nathalie Mercier** pour son intérêt et son implication dans ma thèse. Je la remercie pour m'avoir fait bénéficier de ses conseils, de sa grande curiosité et rigueur scientifique ainsi que pour son aide lors de la réalisation de ces travaux. Je la remercie plus spécialement pour les nombreuses discussions et suggestions précieuses, pour m'avoir appris toutes les expériences de biologie moléculaire et cellulaire. Je la remercie pour sa disponibilité, la confiance qu'elle m'a accordée et son soutien à tous les niveaux tout au long de la thèse. Je la remercie pour la patience et le courage dont elle a fait preuve lors de la correction de ce manuscrit.

Je tiens à remercier Monsieur le Professeur **Bruno Fève** pour tous les conseils et toutes les idées qu'il a pu apporter durant ce travail. Je le remercie également pour m'avoir fait l'honneur de participer au jury de cette thèse.

Je remercie Mesdames et Messieurs les membres du jury de m'avoir fait l'honneur d'évaluer ma thèse, mes rapporteurs Madame le Docteur **Virginie Mattot** qui m'a suivi au cours de ma thèse en tant que membre de mon comité de suivi de thèse et Madame le Docteur **Magali Cucchiarini** pour son expertise ; mes examinateurs, Monsieur le Professeur **Bruno Fève**, Madame le Docteur **Soraya Talèb** et Monsieur le Professeur **Didier Mainard**, directeur de la fédération de recherche

J'adresse un grand merci à Madame le Docteur **Armelle Ropars** pour avoir suivi ce travail en tant que membre du comité de suivi de thèse, pour tous les conseils et les conversations scientifiques concernant mon travail.

Je remercie très cordialement mes collaborateurs :

- Parisiens spécialistes de l'athérosclérose, Monsieur le Professeur **Ziad Mallat**, Madame le Docteur **Soraya Taleb** et **Yacine Haddad** en espérant que cette collaboration sera très prochainement fructueuse.
- De Finlande, spécialiste de la SSAO, Madame le Professeur Sirpa Jalkanen d'où le projet SSAO et athérosclérose a débuté.
- Du Biopôle (laboratoire UMR_7365 CNRS « Ingénierie Moléculaire et Physiopathologie Articulaire (IMoPA) »), spécialistes du cartilage, le Docteur **Arnaud Bianchi** et le Docteur **Astrid Pinzano**, pour tous leurs conseils, les idées et les expériences qu'ils ont apportés et qui enrichissent ce travail.

J'adresse mes remerciements aux membres de l'équipe «UMR_1116 INSERM-Université de Lorraine» où j'ai passé d'agréables moments en leur compagnie. Leur bonne humeur et leur aide m'ont été très précieuses lors de ce parcours professionnel. En particulier, je remercie sincèrement **Simon N Thornton** pour toutes les corrections en anglais et lui exprime également toute ma reconnaissance pour sa bonne humeur et ses conseils scientifiques dans cette thèse. Je remercie **Carlos Labat** pour m'avoir aidée dans le domaine des statistiques.

Je tiens à remercier chaleureusement mes amies, **Karima Ait Aissa** et **Jérémy Lagrange** de m'avoir montré la voie. Qu'ils trouvent ici l'expression de ma profonde sympathie et de mes sincères remerciements pour m'avoir aidée dans les moments difficiles, notamment avec l'administration française... et pour les bons moments que nous avons passés ensemble.

Je tiens également à remercier **Huguette Louis, Cécile Łakomy, Z'hor Ramdane-Cherif, Anne Pizard, Elodie Rousseau, Audrey Isch** et **Véronique Regnault**, pour m'avoir encouragée et aidée avec l'agréable mais difficile langue française, et de m'avoir appris toutes les expressions sans lesquelles je ne pourrais pas survivre en France! Je les remercie pour leur patience et leur courage.

Je tiens également à la remercier **Gina Youcef, Narimane Al Kattani, et Véronique Laplace** pour la bonne humeur lors des déjeuners partagés au labo et merci tout particulièrement à **Véronique** de s'être aussi bien occupée de mes souris.

Je suis contente d'avoir rencontré **Amel Mohamadi, Simon Toupance, Delphine Lambert et Ekatarina Belozertseva** et je les remercie pour les moments de convivialité partagés.

A tous mes amis en France, je vous témoigne toute mon amitié. Je tiens également à exprimer toute ma reconnaissance à **Annie Callot** pour moments passés à Châtel qui m'ont reposée et détendue et pour m'avoir accompagnée tout au long de ces années. Elle m'a aidée dans l'apprentissage de la langue français, la découverte de la culture française, et toutes les petites choses de la vie pendant mon séjour en France. Je remercie **Xiaojian Zhou, Xinjun Li, Weigang Zhao** et **Carmen Tallez** pour leur bonne humeur et pour les bons moments que nous avons passés ensemble.

Et enfin, je dédie cette thèse à ma chère famille, **ma maman** et **mon mari** que je remercie du fond du coeur pour avoir toujours cru en moi, pour m'avoir accompagnée et pour m'avoir apporté le réconfort nécessaire avant, maintenant et toujours. Je les remercie d'avoir fait preuve d'écoute et de compréhension. Je tiens à leur adresser par ces quelques mots toute mon affection et ma reconnaissance.

Dziękuję mojej mamie za to, że nauczyła mnie pracować i tego, że nie ma drogi na skróty. Dziękuję jej za to, że we mnie wierzyła i że nauczyła mnie wiary w siebie.

Szczególnie dziękuję mojemu mężowi, za przygodę, która rozpoczęła się we Francji. Za jego wsparcie i niekończący się optymizm. Za to, że do mojego doktoratu miał podejście jak Wanda Rutkiewicz do kolegi w górach.

”Bo tak naprawdę – w górach nikt nikomu nie pomoże, nie weźmie na plecy i nie zniesie na dół wyczerpanego kolegi. Może jedynie zmobilizować tego drugiego, by sięgnął do swoich rezerw. Może stworzyć, być może złudne poczucie bezpieczeństwa, przywrócić wiarę we własne siły, zachęcić do dalszego działania.”

(Wanda Rutkiewicz)

Za wszystkie podróże i wycieczki... szczególnie za góry... i za to, że zalicza się do tej pierwszej grupy ludzi.

“ Kiedyś ktoś mnie zapytał: - Dlaczego chodzisz po górach? ” Odpowiedziałem, że ludzi można podzielić a) na tych, którym nie trzeba tej pasji tłumaczyć, b) na tych, którym się jej nie wytłumaczy ”

(Piotr Pustelnik)

I za to, że jest zachłanny na życie (nawet, jeśli są to jednodniowe wyjazdy...)

“ W ciągu miesiąca intensywnego życia w górach przeżywa się tyle, co zwyczajnie w czasie kilku lat; to jest zajecie dla ludzi zachłannych na życie – życia człowiekowi jest za mało. ”

(Jerzy Kukuczka)

Prosta rzecz, śnić ten sen...

Dla mojej Gwiazdki, na którą czekałam całe cztery lata!

Table of Contents

Acknowledgments.....	2
Table of Contents	7
Résumé de la Thèse.....	12
List of Abbreviations.....	24
List of Figures.....	27
List of Tables.....	31
Context	32
I. Introduction.....	34
1. Amine oxidases.....	35
1.1. Amine oxidases.....	35
1.1.1. FAD-containing amine oxidases	35
1.1.2. TPQ-containing amine oxidases	36
<i>DAO</i>	36
<i>Lysyl oxidase</i>	36
<i>SSAO</i>	37
1.2. The semicarbazide-sensitive amine oxidase	38
1.2.1. Gene and protein structure of SSAO	38
1.2.1.1. Cloning of the gene	38
1.2.1.2. Protein domains and active sites	41
1.2.1.3. Soluble forms of SSAO/VAP-1	43
1.2.2. TPQ and enzymatic reaction mechanisms	44
1.3. Enzymatic reaction of SSAO	46
1.3.1. Substrates (MA, BZM)	46
1.3.2. Products of SSAO reaction.....	48
<i>Aldehydes</i>	48
<i>Hydrogen peroxide</i>	49
<i>Ammonia</i>	49

1.3.3.	Inhibitors	49
1.4.	Protein expression of SSAO in different tissues	50
1.5.	The role of SSAO in different cells/tissues	51
1.5.1.	Adipocytes (glucose uptake and cell differentiation).....	51
1.5.2.	Vascular smooth muscle cells.....	53
1.5.3.	Endothelial cells of high endothelial venules	54
1.5.4.	Chondrocytes.....	57
1.6.	Expression and activity of SSAO in pathological conditions.....	57
	<i>Diabetes</i>	58
	<i>Atherosclerosis</i>	58
	<i>Other diseases associated with SSAO</i>	59
2.	Cartilage.....	61
2.1.	Physiology of cartilage.....	61
2.2.	Articular cartilage function.....	62
2.3.	Structure of the hyaline cartilage.....	62
2.3.1.	Chondrocytes.....	64
2.3.2.	Extracellular matrix (ECM) components.....	65
2.3.2.1.	Collagens	67
2.3.2.2.	Proteoglycans	68
2.4.	Cartilage formation	69
2.4.1.	Long bone development.....	69
2.4.2.	Markers of chondrocyte differentiation.....	71
	<i>Condensation</i>	71
	<i>Proliferation</i>	73
	<i>Maturation and hypertrophy</i>	73
	<i>Apoptosis</i>	74
2.4.3.	Transcriptional factors of chondrogenesis	75
2.4.3.1.	Sox9	75
2.4.3.2.	Runx2.....	75
2.5.	Diseases of joints and cartilage degradation.....	76
2.5.1.	Osteoarthritis (OA)	76
2.5.3.	Animal models of cartilage diseases	79
3.	Vascular Part.....	81
3.1.	General structure and function of blood vessels	81

3.1.1. Vein.....	83
3.1.2. Artery.....	83
3.1.3. Capillaries	85
3.2. Structure of an aorta	86
3.2.1. Intima	86
3.2.1.1. EC.....	86
3.2.2. Media.....	86
3.2.2.1. Vascular smooth muscle cells.....	87
3.2.2.2. vSMC differentiation and phenotype changing	88
3.2.2.3. ECM	89
3.2.3. Adventitia	90
3.3. Remodeling of the arterial wall	90
3.4. Diseases of the vascular system	91
3.4.1. Atherosclerosis - Inflammatory disease of arterial blood vessels.....	91
3.4.1.1. Endothelial cell dysfunction	92
3.4.1.2. Cell types involved in atherosclerosis	92
3.4.1.3. Atherosclerotic plaque characterization	94
3.4.1.4. Animal models of atherosclerosis – <i>ApoE</i> ^{-/-} mice	95
II. Working hypothesis and objectives	97
III. Materials and methods	99
1. Models.....	99
1.1. Human cartilage	99
1.2. Animals	99
1.2.1. Normal rats.....	99
1.2.2. Models of cartilage degradation: MIA.....	100
1.2.3. WT and knock out <i>SSAO</i> ^{-/-} mice	100
1.2.4. Model of atherosclerosis: <i>ApoE</i> ^{-/-} <i>SSAO</i> ^{-/-} double knock out mice.....	101
1.3. Cells: models of hypertrophic differentiation	102
1.3.1. Primary cell culture of rat chondrocytes and hypertrophic differentiation protocol	102
1.3.2. Progressive passage of rat chondrocytes	103
1.3.3. ATDC5	103
2. Common methods.....	104
2.1. Histology and Immunohistochemistry	104

2.2.	Western blot.....	106
2.3.	RNA isolation	108
2.4.	RT- and real time qPCR.....	108
3.	Specific methods	111
3.1.	SSAO activity.....	111
3.1.1.	Homogenates preparation for SSAO activity measurement.....	111
3.1.2.	SSAO activity measurement	111
3.2.	Measurement of 2-Deoxy-D-glucose uptake	112
3.3.	MTT.....	113
3.4.	Atherosclerotic lesion quantification in aorta.....	113
3.5.	Atherosclerotic plaque quantification in the aortic sinus	113
3.6.	Mesurement of cytokines.....	114
3.7.	Mice genotyping.....	114
3.8.	Experiments performed in collaboration	115
3.9.	Statistical analysis.....	116
IV.	Cartilage and chondrocyte differentiation.....	117
1.	Hypothesis	118
2.	Objectives and strategies	119
3.	Results	121
3.1.	The presence of SSAO in rat cartilage	121
3.1.1.	SSAO expression in healthy cartilage of Wistar rats.	121
3.1.2.	SSAO is present in the rat growth plate	123
3.2.	The role of SSAO in cartilage	124
3.2.1.	Model of chondrocyte terminal differentiation.....	124
3.2.1.1.	ATDC5.....	125
3.2.1.2.	Primary rat chondrocytes culture.....	129
3.2.2.	Expression and enzyme activity of SSAO.....	140
3.2.2.1.	SSAO in ATDC5.....	140
3.2.2.2.	SSAO expression and activity during primary chondrocyte differentiation.....	141
3.2.3.	Effect of SSAO inhibition on terminal chondrocyte differentiation	147
3.2.4.	The role of SSAO in terminal chondrocyte differentiation.....	151
3.3.	The presence of SSAO in human OA cartilage.....	152
3.3.1.	SSAO in human more and less diseased cartilage	152
3.3.2.	Expression and activity of SSAO in human more and less diseased cartilage.....	155

3.4.	Presence of SSAO in cartilage of the MIA rat model of cartilage degradation	157
4.	Discussion	160
5.	Conclusions.....	167
6.	Perspectives.....	169
V.	Vascular and atherosclerosis studies	171
1.	Hypothesis	172
2.	Objectives and Strategies	174
3.	Results	176
3.1.	Role of SSAO in plaque development: Invalidation of SSAO in <i>ApoE</i> ^{-/-} mice	176
3.1.1.	Lipid profile in <i>ApoE</i> ^{-/-} and <i>ApoE</i> ^{-/-} <i>SSAO</i> ^{-/-} mice.....	176
3.1.2.	Kinetics of disease development.....	177
3.1.3.	Phenotype of atherosclerosis plaques and media	180
3.1.3.1.	α-actin expression in media of aortic sinus.....	180
3.1.3.2.	Lymphocyte infiltration in media of aortic sinus.....	181
3.1.3.3.	Monocyte/macrophage presence in media of aortic sinus	183
3.1.3.4.	Collagen content in the media and the plaque of the aortic sinus.....	183
3.1.4.	Exploration of pro- and anti-inflammatory profiles	184
-	in spleen	184
-	in aorta	187
3.1.5.	Exploration of the VSMC phenotype	188
3.1.6.	Role of SSAO in cellular trafficking in <i>ApoE</i> ^{-/-} <i>SSAO</i> ^{-/-} mice vs <i>ApoE</i> ^{-/-} mice.....	188
-	in mice under HFD	188
4.	Discussion	192
5.	Conclusion	198
6.	Perspectives.....	200
VI.	General discussion	202
VII.	References.....	205
Annex.	232

Résumé de la Thèse

Situation du sujet

Contexte scientifique de la SSAO

La « semicarbazide-sensitive amine oxidase » (SSAO) est une enzyme à topaquinone qui transforme les amines primaires (comme la méthylamine et la benzylamine) en aldéhyde, peroxyde d'hydrogène et ammoniacque.

La SSAO connue aussi sous le nom de VAP-1 (Vascular Adhésion Protein 1) possède des propriétés d'adhésion qui permettent aux leucocytes de migrer à travers l'endothélium des capillaires post lymphatiques, des vaisseaux lymphatiques et des veinules vers les tissus inflammatoires.

La forme membranaire est exprimée dans différents tissus. Nous avons préalablement montré que la SSAO augmente au cours de la différenciation des CMLV (El Hadri et al., 2002). Nous avons également montré qu'elle pouvait accélérer la différenciation adipocytaire (Mercier et al., 2001). Plusieurs études ont suggéré une participation de la SSAO dans l'organisation de la matrice extracellulaire (MEC) *via* l'établissement de pontages (crosslinks) ou en modifiant la synthèse ou l'organisation d'autres composants matriciels tels que les protéoglycanes (Mercier et al., 2006 ; 2007 ; 2009). Enfin, la SSAO pourrait également participer à l'oxydation des LDL et à l'inflammation, *via* notamment la forme soluble de la SSAO après clivage et libération dans le plasma. La SSAO soluble plasmatique est augmentée chez les patients atteints de maladies cardiovasculaires (Boomsma et al., 1997) et inflammatoires (Kurkijarvi et al., 1998).

De par son expression différenciation-dépendante et ses potentiels rôles dans l'organisation matricielle, nous faisons l'hypothèse que la SSAO est un candidat très intéressant qui pourrait participer à la différenciation des CMLV et par conséquent à l'organisation matricielle.

Nous nous intéresserons également au rôle de la SSAO dans la différenciation des chondrocytes, les seules cellules présentes dans la matrice cartilagineuse. Cet état différencié qui est responsable de l'homéostasie de la matrice extracellulaire est susceptible d'être modifié et à l'origine de pathologies articulaires comme l'arthrose.

Contexte scientifique et principaux objectifs sur le cartilage

La MEC joue un rôle important dans de nombreux tissus, en particulier dans le cartilage et le vaisseau, où elle assure non seulement les propriétés mécaniques (élasticité) mais également des propriétés physiologiques assurant l'intégrité et la fonctionnalité de l'ensemble. L'intégrité de ce réseau macromoléculaire peut être modifiée au cours du vieillissement ou dans des situations pathologiques conduisant à des affections de type articulaire (arthrose, arthrite).

L'homéostasie du cartilage est assurée par la synthèse de molécules matricielles tissu- spécifiques par les chondrocytes en fonction de leur état de différenciation.

Les chondrocytes matures sont caractérisés par la synthèse de collagène II et de protéoglycanes tels que l'agrécan. Lorsque les chondrocytes entrent en différenciation terminale (stade hypertrophique) en réponse à l'inflammation ou à d'autres facteurs, leur phénotype est caractérisé par la synthèse de collagène X et l'expression de métalloprotéinases. Le cartilage perd progressivement ses propriétés mécaniques, ce qui contribue à la progression de la maladie (Dreier, 2010; Goldring et al., 2006).

La MEC est affectée au cours du vieillissement ou des pathologies sus-nommées, impliquant une dédifférenciation des cellules pourrait aboutir à l'apoptose en réponse à des stimulations pro-inflammatoires par exemple (arthrite).

Nous avons récemment mis en évidence l'expression de la SSAO dans des chondrocytes de rat en culture et sur des explants de cartilage par RT-PCR quantitative et immunohistochimie. La SSAO est également détectée dans la synovie et le tissu adipeux de Hoffa qui participent activement dans la progression de l'inflammation durant l'arthrose.

Le premier objectif du projet est de démontrer l'implication de la SSAO dans la différenciation chondrocytaire. Le deuxième objectif est d'étudier le rôle de la SSAO dans le développement de maladies osteoarticulaires comme l'arthrose.

Contexte scientifique et principaux objectifs sur la partie vasculaire

L'homéostasie de la paroi artérielle est assurée par la synthèse de molécules matricielles tissus spécifiques par les cellules musculaires lisses vasculaires (CMLV) en fonction de leur état de différenciation. La modification phénotypique des CMLV est un processus réversible essentiel au bon fonctionnement du système cardiovasculaire. Un déséquilibre entre le phénotype prolifératif/synthétique et contractile peut conduire au développement et/ou à la progression de maladies vasculaires en réponse à des signaux environnementaux anormaux. Ainsi, les CMLV peuvent se dédifférencier et migrer dans la néointima comme dans l'athérosclérose ou bien s'hypertrophier et modifier leurs propriétés contractiles comme dans l'hypertension artérielle, accompagnée de modifications de la matrice extracellulaire (MEC). Le stress oxydant a une place importante dans le maintien de la différenciation des CMLV. En excès, il peut induire une augmentation de la prolifération des CMLV (Sung et al., 2005) et une calcification vasculaire *via* une différenciation ostéogénique des CMLV (Byon et al., 2008). En revanche, une diminution du stress oxydant peut conduire à la dédifférenciation des CMLV comme dans les souris Nox4^{-/-} (Clemens et al., 2007).

La SSAO est fortement exprimée à la membrane des CMLV, des adipocytes et des cellules endothéliales lymphatiques. Son rôle exact n'est pas connu mais nous pensons qu'elle pourrait être impliquée dans la différenciation cellulaire comme dans l'adipocyte (Mercier et al., 2002). Notre groupe a suggéré une participation de la SSAO dans l'organisation de la MEC *via* l'établissement des cross-links ou en modifiant la synthèse ou l'organisation d'autres composants matriciels tels que les protéoglycanes (Mercier et al., 2006, 2007, 2009). La SSAO pourrait ainsi contribuer au remodelage vasculaire observé dans des pathologies liées à l'âge.

L'athérosclérose est une maladie inflammatoire chronique des grosses artères caractérisée par un épaissement intimal qui se développe par infiltration et prolifération des CML, de monocytes-macrophages et de lymphocytes (Dzau et al., 2002, Wang et al., 2012). Le développement de l'athérosclérose est favorisé par différents événements comme le stress oxydatif qui active la prolifération cellulaire et la peroxydation lipidique. Il a été montré qu'*in vivo*, l'incubation de méthylamine et de la forme soluble de SSAO dans le milieu de culture pouvait induire une cytotoxicité sur les cellules endothéliales (Yu et al., 1993) et à un moindre degré sur les CML (Langford et al., 2001) et une apoptose des CMLV (Hernandez et al., 2006).

Le premier objectif du projet est de démontrer l'implication de la SSAO et des remaniements matriciels du tissu artériel dans un exemple de pathologie liée au vieillissement tissulaire et à l'inflammation : l'athérosclérose.

Le deuxième est d'étudier le rôle de la SSAO dans la différenciation des CMLV et la réponse inflammatoire.

Stratégie et méthodologie générale

<u>Cartilage</u>	<u>Vaisseaux</u>
Approche intégrée <i>in vivo</i>	
- Cartilage arthrosique humain - Modèle animal d'arthrose :	Modèles animaux d'inactivation de la SSAO :
- Rat wistar traité par le monoiodoacétate	1. Géniques : Souris non traitées ApoE-/-SSAO-/- versus ApoE-/- 2. Fonctionnelle : Souris traitées par : - Inhibiteur de la SSAO : Semicarbazide - Anticorps fonctionnels anti-SSAO => étude du trafic des cellules immunitaire (injection de PBMC)
Prélèvement des tissus :	
- Cartilage de genou et tête fémorale	- Sang/plasma - Cœur - Aorte thoracique et abdominale - Tissu adipeux - Rate - Poumon
Approche mécanistique <i>in vitro</i> : modèles de différenciation cellulaire	
- Culture primaire de chondrocytes de rat - Lignée chondrocytaire murine ATDC5	- Culture de splénocytes stimulés par LPS et INFg => mesure de cytokine et Réponse régulatrice et effectrice dépendante des LT
Identification des événements moléculaires en modulant l'expression et l'activité de la SSAO par	
- Inhibiteur sélectif de la SSAO : LJP1586	- SCZ - anti-SSAO anticorps
Méthodologie	
Histologie : coloration histochimiques	
- bleu alcian => protéoglycans - Safranin O => protéoglycans - HES => morphologie des cellules	- Oil red O => quantification des plaques - rouge sirius => collagène

Protéines	
- Immunohistochimie SSAO Collagène X	- Immunohistochimie : α -actin, CD3+, MOMA-2, sm-MHC - Western blot : GAPDH, α -actin, sm-MHC
Activité de la SSAO	
- Méthode radiochimique	- Méthode fluorimétrique
Expression des gènes	
- RT-qPCR	- RT-qPCR - PCR classique (génotypage)
Méthodes spécifiques	
- transport de déoxy-glucose tritié	- profil lipidique

Résultats obtenus

Résultats obtenus et discussion sur le cartilage

La mise en évidence de la présence de la SSAO dans le cartilage de rat Wistar

Dans la première étape de notre recherche, nous avons localisé de la SSAO dans le cartilage du genou chez le rat Wistar. Ensuite, nous avons étudié le niveau d'expression de la SSAO et l'activité de la SSAO dans le cartilage de genou et la tête fémorale de rat Wistar.

Après la confirmation par histochimie (Safranine O et HES coloration) d'une bonne qualité du cartilage, une étude par immunohistochimie en utilisant un anticorps anti-SSAO a été effectuée. Elle a révélé la présence de la SSAO dans le cartilage et dans l'os sous-chondral. Nous pouvons remarquer que l'expression de la SSAO est moins prononcée dans le cartilage par rapport à l'os. Ceci est sûrement dû l'absence de vaisseaux sanguins dans le cartilage. Ensuite, nous avons détecté et quantifié l'ARNm codant pour l'expression du gène de la SSAO est significativement plus faible dans le cartilage de la tête fémorale (19 fois) et de cartilage de genou (33 fois) par rapport au tissu adipeux utilisé comme contrôle positif.

L'activité enzymatique de la SSAO a été détectée dans le cartilage de la tête fémorale et le cartilage du genou avec des niveaux seulement 3 fois et 7 fois plus faible respectivement que dans le tissu adipeux.

Très peu d'études ont montré une expression ou une activité de la SSAO dans le cartilage. Lyles GA, (1985) a rapporté de l'activité de la SSAO dans le cartilage, mais il n'a pas exploré le rôle de SSAO dans ce tissu conjonctif. Nos expériences confirment que la SSAO est exprimée sous

une forme active dans le cartilage articulaire, mais à un niveau plus faible que celui mesuré dans d'autres tissus tels que le tissu adipeux ou l'aorte. Ce travail a donc porté sur l'étude du rôle de la SSAO dans le cartilage articulaire et notamment dans la différenciation chondrocytaire. La SSAO a précédemment été impliquée dans la différenciation adipocytaire.

La mise au point de condition de la différenciation terminale de la chondrocytes in vitro

La différenciation chondrocytaire est un événement-clé dans l'homéostasie du cartilage. Pour étudier le rôle de la SSAO dans ce processus nous avons cherché un modèle de différenciation terminale des chondrocytes, *in vitro*. Nous avons testé la lignée murine chondrocytaire ATDC5 et la culture primaire chondrocytes articulaire de rat Wistar.

- La mise au point de conditions de culture ATDC5- une lignée chondrocytaires de souris immortalisée, connue pour mimer la différenciation endochondrale dans certaines conditions de culture

Dans la littérature nous avons trouvé différentes conditions de culture cellulaire (Choi et al., 2011, Iftikhar et al., 2010, Altaf et al., 2006). Lors de l'ensemencement, Les cellules ont été cultivées dans 10 % de SVF, en présence de L-glutamine, transferrine, et de sélénite de sodium. A confluence, J0, nous avons fait varier la concentration de sérum (2%, 5%) en présence d'insuline et d'ascorbate pendant 21 jours. Nous avons choisi de nous placer à 5 % de sérum pour les autres expériences car nous avons eu un meilleur rapport expression de SSAO/ degré de différenciation.

- La mise au point de conditions de culture primaire des chondrocytes de rat

Gartland *et al.* (2005) ont réussi à initier la différenciation terminale des chondrocytes costochondraux de rat. En nous inspirant de cette publication et d'autres (Altaf et al, 2006) nous avons établi le protocole suivant : les cellules sont isolées et cultivées en 10 % de SVF, en présence de L-glutamine (essentielle pour la croissance normale des cellules en général), de transferrine (agissant comme un transporteur d'électron), et de sélénite de sodium (puissant anti-oxydant). A confluence, J0 : nous avons fait varier la concentration de sérum (2%, 5%, 10%) en présence d'insuline (activant le transport de glucose, d'acides aminés et la synthèse protéique et d'acides nucléique) et d'ascorbate

(cofacteur essentiel à différentes classes d'enzymes notamment dans celles impliquées dans la synthèse du collagène) et nous avons testé deux milieux DMEM/F-12 et α MEM. Nous avons choisi le milieu DMEM/F-12 contenant 2 % de sérum pour les autres expériences car nous avons eu un meilleur rapport d'expression de SSAO/ degré de différenciation. Nous avons ensuite testé l'effet d'une supplémentation combinée en insuline et en ascorbate sur la différenciation et l'expression de la SSAO.

Finalement nous avons mis au point les conditions de culture permettant la différenciation des chondrocytes de rat au cours de laquelle l'expression et l'activité de la SSAO. Une bonne différenciation est caractérisée par la diminution de l'expression du collagène II, de Sox 9 et de l'agrécan (marqueurs chondrocytaires) indispensables pour permettre l'augmentation de l'expression du collagène X et de la MMP13 - marqueurs du phénotype d'hypertrophie (stade de différenciation terminale chondrocytaire et de minéralisation) en accord avec la littérature (Zuscik et al., 2008). Le profil de différenciation terminale a été meilleur dans les cultures des chondrocytes de rat Wistar que dans la lignée ATDC5. Ainsi les études suivantes ont été réalisées avec ce modèle.

La SSAO semble donc être impliquée dans le stade de maturation terminale des chondrocytes hypertrophiques en situation physiologique. Est-elle seulement un marqueur de différenciation ou joue-t-elle un véritable rôle dans la différenciation terminale ?

Modulation de l'activité de la SSAO

Afin de répondre à cette question, nous avons évalué l'effet de la modulation de l'activité de la SSAO par un inhibiteur spécifique (LJP1586 [Z-3-Fluoro-2-(4-methoxybenzyl)allylamine Hydrochloride] (O'Rourke, 2008)) sur la différenciation terminale chondrocytaire.

Nous avons mesuré le niveau d'expression et d'activité de l'enzyme. Notons qu'aucune activité enzymatique de la SSAO n'a été détectée dans les cellules traitées par le LJP (1 μ M), montrant l'efficacité de l'inhibiteur. De plus, les cellules traitées par LJP, montrent une différenciation plus tardive par rapport aux contrôles. Notamment l'augmentation de l'expression du collagène X, MMP13, OPN et ALP a été retardée dans les cellules traitées par l'inhibiteur par rapport aux cellules contrôles.

Des expériences préliminaires ont été débutées pour tenter d'expliquer par quels mécanismes la SSAO pourrait favoriser la différenciation chondrocytaire. Une première hypothèse est que la SSAO pourrait, comme dans d'autres types cellulaires (adipocytes, CMLv), augmenter le transport de glucose dans les chondrocytes. Il est connu qu'au cours de l'hypertrophie, une augmentation du transport de glucose a

été mis en évidence. Le transport de déoxyglucose tritié a donc été mesuré dans des chondrocytes en culture primaires traités ou non par le LJP à J21. Notre premier résultat montre que le transport basal de glucose est diminué dans les cellules traitées chroniquement par le LJP à J21. La stimulation aiguë (1h) par la BZM ne semble pas augmenter le transport de glucose dans les chondrocytes non traités ou traité par le LJP. Comme indiqué dans la littérature, une stimulation de 24h par l'IL1 α induit une augmentation du transport de glucose partiellement inhibée par le LJP. Si ces résultats sont confirmés par la suite, ceci suggèrera qu'une inhibition de la SSAO pourrait être employé pour limiter l'hypertrophie chondrocytaire lors d'une inflammation articulaire. De plus, un traitement plus long par la BZM devrait être testé car la régulation du transport de glucose pourrait passer par des effets géniques.

La SSAO joue donc un rôle dans la différenciation terminale des chondrocytes. L'hypertrophie constitue également un fait marquant de la pathologie arthrosique. En effet, le processus de différenciation terminale des chondrocytes est réactivé dans l'arthrose. Il est donc très intéressant d'étudier le changement de l'activité de la SSAO dans le cartilage arthrosique.

L'activité de la SSAO dans le cartilage arthrosique humain

Nous avons obtenu des prélèvements têtes fémorales de patients arthrosiques ayant subits la mise en place d'une prothèse. Sur une même tête fémorale, nous avons distingué et prélevé du cartilage érodé par la maladie et du cartilage non érodé sur les zones non portantes. Par la suite, nous avons étudié l'expression des marqueurs d'hypertrophie comme le collagène X, MMP13 et d'ostéopontine (OPN) et nous avons remarqué comme attendu, l'augmentation d'expression de ces marqueurs dans le cartilage plus malade. De façon intéressante, nous avons montré une augmentation de l'activité et de l'expression de la SSAO dans le cartilage plus malade en comparant avec le cartilage supposé sain. En conclusion, l'expression de la SSAO augmente dans le cartilage arthrosique où les chondrocytes entrent en différenciation terminale. Donc la SSAO pourrait être considérée comme une cible thérapeutique ou bien un marqueur d'arthrose.

La mise au point d'un modèle de rat traité au monosodique iodoacétate (MIA)

Pour étudier le rôle de la SSAO dans le processus de la dégradation du cartilage, nous avons utilisé un modèle animal d'arthrose en injectant au niveau des articulations du genou du monoiodoacétate (MIA 0,3 mg). Ce produit induit une détérioration progressive du cartilage. L'efficacité du traitement a été suivie par immunohistochimie. L'expression des marqueurs de différenciation terminale a été réalisée par PCR quantitative. Nous avons notamment trouvé

une diminution d'expression des tous ces marqueurs. L'expression de la SSAO est également fortement diminuée alors que son activité a été augmentée dans le cartilage dégradé par MIA.

Ces résultats préliminaires montrent que le traitement des rats par la dose de MIA utilisée (0.3 mg) est trop forte et probablement induit l'apoptose des chondrocytes, diminuant ainsi toutes les synthèses d'ARNm. La SSAO étant une protéine très stable, la baisse d'expression de l'enzyme ne semble pas encore se répercuter sur le niveau protéique et donc son activité (directement corrélée à son niveau d'expression protéique). C'est pourquoi différentes doses plus faibles de MIA doivent être testés.

Conclusion et perspectives

Dans ce travail nous avons montré que la SSAO est exprimée dans le cartilage de rat et le cartilage humain sous forme active. Nos études *in vitro* ont montré que la SSAO joue un rôle dans la différenciation terminale des chondrocytes et l'inhibition de son l'activité enzymatique a retardé ce processus. Nous envisageons de confirmer nos résultats obtenus avec le LJP avec l'emploi d'un SiRNA dirigé contre la SSAO. D'autre part, nous souhaiterions également étudier l'effet d'une surexpression de la SSAO dans des chondrocytes en culture. Enfin, pour évaluer le rôle potentiel de la SSAO dans le développement, le cartilage des embryons de souris SSAO^{-/-} pourraient être comparé à celui des souris WT. Les expériences de transport de glucose devront être répétées.

Par ailleurs, nous avons aussi montré que l'expression et l'activité enzymatique de la SSAO sont augmentées dans le cartilage arthrosique humain. De même, dans un modèle d'arthrose chez le rat induit par le MIA, nous avons trouvé une augmentation de l'activité de la SSAO dans le cartilage dégradé, par rapport cartilage sain. Des expériences complémentaires pourraient être réalisées en adaptant la dose de MIA en absence ou en présence d'un inhibiteur de la SSAO pour voir si l'inhibition de la SSAO pourrait diminuer le développement de l'arthrose induit par le MIA.

Dans un prochain travail, notre objectif est de démontrer l'implication de la SSAO dans l'homéostasie de la matrice cartilagineuse et le remaniement matriciel qui s'opère lors de certaines pathologies liées à l'inflammation et au vieillissement. Ceci passe par l'identification du ou des substrats naturels et des cibles protéiques de cette enzyme. Cette connaissance de la nature des substrats et ligands de l'enzyme doit nous conduire à une meilleure compréhension du rôle de cette protéine dans ces tissus.

Résultats obtenus et discussion sur la partie vasculaire

La SSAO, également appelée VAP-1, est augmentée aux sites d'inflammation et participe à l'adhésion des lymphocytes à l'endothélium des veinules et des vaisseaux lymphatiques. Nous souhaitons déterminer si la SSAO a un rôle important dans les mécanismes clés des pathologies liées au vieillissement et à l'inflammation (athérosclérose).

Ainsi, nous avons supposé que la SSAO pourrait participer au développement de l'athérosclérose *via* les produits enzymatiques qu'elle génère. Pour rechercher une implication potentielle de la SSAO dans la formation des plaques d'athérosclérose, nous avons produit des souris ApoE^{-/-}-SSAO^{-/-} double KO, initialement générées dans le laboratoire du Pr S. Jalkanen (MediCity, Université de Turku). Nous avons étudié la progression de la formation des plaques chez des souris de 15 et de 25 semaines. Notre hypothèse était que l'absence de SSAO limiterait le développement de l'athérosclérose.

Préalablement, nous avons montré que l'activité de la SSAO chez les souris ApoE^{-/-} n'est pas modifiée par rapport aux souris WT.

Phénotype des souris APOE^{-/-} déficientes en SSAO

Paradoxalement à l'âge de 25 semaines, les souris ApoE^{-/-}-SSAO^{-/-} présentent une augmentation significative de 50 % de la surface de plaque dans le sinus aortique et l'aorte associée à une diminution de 80 % de l'expression de l' α -actine spécifique des CML dans la média au niveau du sinus aortique par rapport aux souris ApoE^{-/-}. Aucune modification de l'infiltration des lymphocytes T et des monocytes/ macrophages dans la paroi artérielle, ni de modification du profil cytokinique pro- (TNF α et de l'INF γ) et anti-inflammatoire (l'IL10 et du TGF β) de la rate n'ont été observées chez les souris ApoE^{-/-} et ApoE^{-/-}-SSAO^{-/-} PCR quantitative et par immunohistochimie.

Pour confirmer que l'absence de la SSAO cause une augmentation de la surface des plaques dans le sinus aortique, nous avons généré un second groupe de souris ApoE^{-/-} et ApoE^{-/-}SSAO^{-/-} à partir des souris SSAO^{-/-} et ApoE^{-/-} envoyées par Sirpa Jalkanen. Ces animaux maintenus jusqu'à 15 et 25 semaines à Nancy, ont présenté le même phénotype que précédemment mais plus précocement, c'est à dire une augmentation significative de la surface de plaques dans le sinus aortique à 15 semaines. Probablement, cette différence est provoquée par un changement d'environnement d'élevage.

Recherche du mécanisme impliqué dans l'augmentation des plaques induit par l'absence de la SSAO

1- Modification du profil lipidique ?

L'absence de la SSAO n'a pas changé le profil lipidique chez les souris femelles ApoE^{-/-} de 15 semaines et de 25 semaines.

2- Modifier le trafic des cellules immunitaires ?

Notre collaboratrice, Dr S. Taleb à Paris, a montré que des souris de 12 semaines nourries avec un régime riche en graisses pendant 4 semaines ne présentent pas d'augmentation de surface de plaque dans le sinus aortique des souris ApoE^{-/-}SSAO^{-/-} comparé aux souris ApoE^{-/-}. Par contre, nous observons une modification dans la distribution des « peripheral bone marrow cells (PBMC) » en particulier dans le sang et l'aorte. Ces résultats ne sont pas reproduits ni dans des souris ApoE^{-/-} traitées par le semicarbazide pendant un mois ni dans des souris ApoE^{-/-} traitées par un anticorps pendant 2 jours anti-SSAO ayant préalablement subi un régime riche en graisses. Les souris nourries avec un régime normal ne montrent pas non plus de modification dans la distribution des PBMC.

3- Modification du profil immunitaire ?

Nous avons étudié le changement du profil inflammatoire chez les souris ApoE^{-/-}SSAO^{-/-} femelles de 25 semaines par rapport à des souris contrôles. Dans les rates nous n'avons pas trouvé de modification d'expression de cytokines pro- (TNF- α et de l'INF- γ) ou anti-inflammatoires (l'IL10 et du TGF- β) chez les souris ApoE^{-/-}SSAO^{-/-} par comparaison avec les souris ApoE^{-/-}. Par contre dans les aortes des souris ApoE^{-/-}SSAO^{-/-} femelles de 15 semaines, au niveau protéique nous avons trouvé une diminution des FGF β , GM-CSF, INF γ , IL1 β , MIP-

3 α et RANTES et une augmentation MCP-1. Chez les souris femelles ApoE^{-/-}SSAO^{-/-} de 25 semaines, nous avons trouvé une diminution de FGF β et une augmentation de l'IL5 et du VEGF. Des études de phénotype des CML montrent une diminution de smMHC dans les aortes de souris femelles ApoE^{-/-}SSAO^{-/-} de 15 semaines. A 25 semaines, les aortes de souris femelles ApoE^{-/-}SSAO^{-/-} montre une diminution significatif de sm-MCH par rapport aux souris contrôles suggérant une diminution de la différenciation des CMLV.

Conclusion et perspectives

Nos résultats principaux ont montré que l'absence de la SSAO chez les souris ApoE^{-/-} augmente significativement le développement de l'athérosclérose. Nous expliquons ce phénotype par (i) une modification du profil inflammatoire dans l'aorte mais pas dans la rate. (ii) une redirection du trafic des cellules immunitaires vers la plaque explique en partie ce phénotype (iii) ainsi qu'une dédifférenciation des CML dans l'aorte des souris ApoE^{-/-}SSAO^{-/-}.

Dans nos perspectives à court termes, nous souhaitons étudier le rôle de la SSAO dans la modulation du phénotype des CML *in vitro*, induite par l'inflammation.

List of Abbreviations

% – percent	COMP – cartilage oligomeric protein
°C – degree Celsius	CXCL4 – CXC chemokines ligand 4
A – adrenaline	D2, D3, D4 – protein domain
ADAMTS4 – aggrecanase-1	DA – dopamin
ADAMTS5 – aggrecanase-2	DAO – diamine oxidases
AGEs – advanced glycation end-products	DMSO – Dimethyl sulfoxide
Aggr – aggrecan	DNA – deoxyribonucleic acid
ALP – alkaline phosphatase	E.C. – enzyme classification
AO – Amine oxidases	EC – endothelial cells
AOC – copper-dependent amine oxidase	ECAO – Escherichia coli amine oxidase
ApoE – apolipoprotein E	ECM – extracellular matrix
ATDC5 – mouse immortalized chondrogenic cell line	ECM – extracellular matrix
bFGF – basic fibroblast growth factor	ED9 – embryonic day 9
BMI – body mass index	EDTA – ethylene diamine tetraacetate
BMP – bone morphogenetic growth factor	ES – embryonic stem cells
BSA – bovine serum albumin	FACS – Flow cytometry
BTT-2052 – (1S,2S)-2-(1- methylhydrazino)-1-indanol	FAD - flavin adenine dinucleotide
BZM – benzylamine	FBS – fetal bovine serum
CD – cluster of differentiation of immune cells	FGF – fibroblast growth factor
CD45.1 – cell population	Fgfr3 – fibroblast growth factor receptor
cDNA – complementary deoxyribonucleic acid	For – forward primer
CHF – congestive heart failure	GAG – glycosaminoglycan
Coll II – collagen type II	GAPDH – glyceraldehyde 3-phosphate dehydrogenase
	GLUT1 – glucose transporter 1
	GLUT4 – glucose transporter 4

GM-CSF – granulocyte macrophage-colony stimulating factor

h – hours

HA – hyaluronan or hyaluronic acid

HES – Hematoxylin-Erythrosin-Saffron ()

HEV – high endothelial venules

HFD – high fat diet

hVAP-1 – human vascular adhesion molecule 1

IDDM – insulin-dependent diabetes mellitus

IHC – immunohistochemistry

IL-1 – interleukin 1

IL-10 – interleukin 10

IL-12 – interleukin 12

IL-17 – interleukin 17

IL-18 – interleukin 18

IL-1 β – interleukin-1 β

IL-4 – interleukin 4

IL-5 – interleukin 5

INF γ – interferon γ

kDa - kilodaltons

KO – Knockout mouse

LDL – low-density lipoprotein

Ldlr – low-density lipoprotein receptor

LJP 1586 – Z-3-fluoro-2-(4-methoxybenzyl)allylamine hydrochloride

LOX – Lysyl oxidase

LOXL2 – lysyl oxidase like-2

LPS – Lipopolysaccharide

M – mol/l

M1 and M2 – macrophages subtypes

MA – methylamine

MAO – monoamine oxidases

MCP-1 – chemokine monocyte chemoattractant protein-1

M-CSF – macrophage colony-stimulating factor

MG – methylglyoxal

MIA – monosodium iodoacetate

min – minutes

MIP-1 α – macrophage inflammatory protein 1 α

MIP-3 α – macrophage inflammatory protein 3 α

MMP1 – matrix metalloproteinase-1

MMP13 – matrix metalloproteinase-13

MMP8 – matrix metalloproteinase-8

MMP9 – matrix metalloproteinase-9

MOMA – monocyte/macrophage

mRNA – messenger ribonucleic acid

MTT – 3-(4,5 dimethyl-2-thiazolyl)-2,5-diphenyl-2H-tetrazolium bromide

Mttp – microsomal triglyceride transfer protein

mVAP-1 – mouse vascular adhesion molecule 1

NA – noradrenalin

N-cadherin – neural cadherin

N-CAM – neural cell adhesion molecule

Neor – neomycin-resistance cassette.

NIDDM – non-insulin-dependent diabetes mellitus

NK cells – Natural killer cells

NO – nitric oxide

OA – osteoarthritis

OPN – osteopontin

oxLDL – oxidized low-density lipoprotein

PBMC – peripheral bone marrow cells
PBS – Phosphate buffered saline
PMNs – polymorphonuclear cells
(leukocyte/granulocytes)
RANTES – regulated on activation,
normal T-cell-expressed and –secreted
(chemokine ligand 5)
RAO – retina-specific amine oxidase
Rev – reverse reverse
RNA – ribonucleic acid
ROS – reactive oxygen species
RPS29 – ribosomal protein S29
RT – room temperature
RT- qPCR – real time quantitative
polymerase chain reaction
Runx2 (Cbfa1) – runt-related transcription
factor 2 (core binding factor alpha-1)
SCZ – semicarbazide
SEM – standard error of the mean
sm-MHC – smooth muscle myosin heavy
chain
sm- α -actin – smooth muscle α -actin
Sox9 – member of the SOX transcription
factors family encoded by (SRY (sex
determining region Y)-box 9)

SSAO – semicarbazide-sensitive amine
oxidase
sSSAO – soluble form of semicarbazide-
sensitive amine oxidase
sVAP-1 – soluble vascular adhesion
molecule 1
T75 – tissue culture flasks 75 cm²
TGF β – transforming growth factor beta
T_h1 – T helper 1
T_h2 – T helper 2
T_m – melting temperature
TNF α – tumor necrosis factor alpha
TPQ – 2, 4, 5-trihydroxyphenylalanine
quinone
trypt – tryptamine
v/v – volume/volume
VAP-1 – vascular adhesion molecule 1
VEGF – vascular endothelial growth factor
VLDL – very low-density lipoprotein
VSMC – vascular smooth muscle cells
w/v – weight/volume
WB – western blot
WT – wild type mice, strain C57Black
 β -PEA – β -phenylethylamine

List of Figures

Figure I-1. Enzymatic reaction catalysed by amine oxidases.	35
Figure I-2. Classification of amine oxidases.....	37
Figure I-3. The main features of mVAP-1 gene.	39
Figure I-4. Structure of porcine AOC genes.....	40
Figure I-5. Stereo views of hVAP-1.	42
Figure I-6. The conserved motifs of semicarbazide sensitive amine oxidases.....	43
Figure I-7. The TPQ biogenesis and the amine oxidases catalytic reaction	45
Figure I-8. Some compounds that have been shown to be SSAO substrates	47
Figure I-9. Structure of Z-3-fluoro-2-(4-methoxybenzyl)allylamine hydrochloride (LJP1586)	50
Figure I-10. The leukocyte-extravasation cascade.	55
Figure I-11. A model of the action of vascular adhesion protein 1 during leukocyte–endothelial-cell interaction.	56
Figure I-12. The three types of cartilage.	62
Figure I-13. Articular cartilage morphology.	64
Figure I-14. Chondrocyte morphology.	65
Figure I-15. The network of extracellular matrix (ECM) components in cartilage.....	66
Figure I-16. Diagram of adult articular cartilage	67
Figure I-17. Model of proteoglycan aggregate and aggrecan molecule.	68
Figure I-18. Overview of a bone formation by endochondral ossification.....	70
Figure I-19. Growth plate morphology.....	71
Figure I-20. Model of chondrogenesis during the development of long bones with main markers of each stage	73
Figure I-21. Model of chondrocytes differentiation in growth plate during the development of long bones with main markers of each stage.	74
Figure I-22. Schematic normal and OA joint	77
Figure I-23. Schematic model of osteoarthritis development	78
Figure I-24. The vascular system of the human body.	82
Figure I-25. The structure of the artery and vein.....	84
Figure I-26. The capillary vessels	85

Figure I-27. The tunica media organization.....	87
Figure I-28. The contractile or synthetic vascular smooth muscle cells.....	88
Figure I-29. Types of vascular remodeling.....	91
Figure I-30. The atherosclerosis progression.	94
Figure III-1. Protocol of PBMC injection	116
Figure IV-1. SSAO in articular cartilage of a normal rat.....	122
Figure IV-2. Expression and activity of SSAO in articular cartilage of rats.	123
Figure IV-3. SSAO in the growth plate of a normal rat.....	124
Figure IV-4. Phase-contrast microscopy of ATDC5 in culture.	126
Figure IV-5. Sox9 expression during ATDC5 terminal differentiation.	127
Figure IV-6. Collagen II (A) and aggrecan (B) mRNA expression.	128
Figure IV-7. Collagen X (A) and MMP13 (B) mRNA expression.	129
Figure IV-8. The protocol used for chondrocytes differentiation.	130
Figure IV-9. Phase-contrast microscopy of rat chondrocytes in culture.....	131
Figure IV-10. Sox9 expression in rat chondrocytes.	132
Figure IV-11. Collagen I and II expression in rat chondrocytes.	133
Figure IV-12. Aggrecan and versican expression in rat chondrocytes.....	134
Figure IV-13. Collagan X expression in rat chondrocytes.	135
Figure IV-14. The chondrocyte culture protocols.....	136
Figure IV-15. Phase-contrast microscopy of rat chondrocytes in culture, as a function of time and culture medium composition.	137
Figure IV-16. Sox9 expression in rat chondrocytes.	138
Figure IV-17. Collagen I (A) and II (B) expression during rat chondrocyte terminal differentiation ...	139
Figure IV-18. Aggrecan (A) and versican (B) expression during rat chondrocyte terminal differentiation.	139
Figure IV-19. Collagen X (A) and MMP13 (B) expression during rat chondrocyte terminal differentiation	140
Figure IV-20. SSAO expression during rat chondrocyte terminal differentiation	141
Figure IV-21. SSAO expression and activity during rat chondrocyte terminal differentiation.....	142
Figure IV-22. Sox9 (A) and collagen II (B) expression during rat chondrocyte terminal differentiation	143
Figure IV-23. Collagen X (A) and MMP13 (B) expression during rat chondrocyte terminal differentiation	144
Figure IV-24. Expression of SSAO as a function of terminal cell differentiation in primary chondrocyte culture	146

Figure IV-25. Cell viability	148
Figure IV-26. SSAO activity and SSAO mRNA expression.	149
Figure IV-27. Expression of pre-hypertrophy/hypertrophy markers.	150
Figure IV-28. Expression of hypertrophy markers.....	150
Figure IV-29. Glucose transport.....	152
Figure IV-30. Characteristic of less/more diseased cartilage.	153
Figure IV-31. Expression of SSAO in human OA cartilage.....	154
Figure IV-32. SSAO enzymatic activity in a human OA cartilage.	155
Figure IV-33. Expression of chondrocyte terminal differentiation markers.	156
Figure IV-34. Expression of chondrocyte terminal differentiation markers in rat knee cartilage.	157
Figure IV-35. SSAO expression in rat knee cartilage.....	158
Figure IV-36. SSAO enzymatic activity in rat knee cartilage.....	158
Figure V-1. Triglyceride, LDL cholesterol and total cholesterol concentrations in	177
Figure V-2. Plaque quantification after oil red O staining in the aortic sinus from 15 week-old female mice.	178
Figure V-3. Plaque quantification after oil red O staining in the thoracic aorta from 15 week-old female mice.	178
Figure V-4. Plaque quantification after oil red O staining in the aortic sinus from 25 week-old female mice.	179
Figure V-5. Plaque quantification after oil red O staining in the thoracic aorta from 25 week-old female mice.	179
Figure V-6. α -actin staining in the aortic sinus of young, 15 week-old female mice.	180
Figure V-7. α -actin IHC staining in the aortic sinus of old, 25 week-old female mice.....	181
Figure V-8. Lymphocyte infiltration to plaques and tunica media in the aortic sinus of young, 15 week-old female mice.	182
Figure V-9. Lymphocyte infiltration to plaques and tunica media in the aortic sinus of 25 female week-old mice.	182
Figure V-10. Monocyte/macrophage infiltration to plaques in the aortic sinus of 25 week-old female mice.	183
Figure V-11. Collagen content in plaques and tunica media in the aortic sinus of 25 week-old female mice.	184
Figure V-12. Expression of pro-inflammatory markers (TNF α and IFN γ) and anti-inflammatory markers (TGF β and IL10) in spleen from <i>ApoE</i> ^{-/-} and <i>ApoE</i> ^{-/-} <i>SSAO</i> ^{-/-} 15 week-old female mice.....	185
Figure V-13. Expression of pro-inflammatory markers (TNF α and IFN γ) and anti-inflammatory markers (TGF β and IL10) in the spleen from <i>ApoE</i> ^{-/-} and <i>ApoE</i> ^{-/-} <i>SSAO</i> ^{-/-} 25 week-old female mice.....	186

Figure V-14. Mouse atherosclerosis array was preformed with abdominal aortas from 15 week-old female mice.	187
Figure V-15. Western blot was performed to study protein presence in abdominal aortas from 25 week-old female mice.	188
Figure V-16. General characteristic of <i>ApoE</i> ^{-/-} and <i>ApoE</i> ^{-/-} <i>SSAO</i> ^{-/-} young female mice.	189
Figure V-17. CD45.1 peripheral bone marrow cells (PBMC) distribution in <i>ApoE</i> ^{-/-} and <i>ApoE</i> ^{-/-} <i>SSAO</i> ^{-/-} young female mice.	190
Figure V-18. Immune cell populations in <i>ApoE</i> ^{-/-} and <i>ApoE</i> ^{-/-} <i>SSAO</i> ^{-/-} young mice.	190
Figure V-19. General WT and <i>SSAO</i> ^{-/-} 15 week-old female mice characteristics.	201
Figure V-20. General WT and <i>SSAO</i> ^{-/-} 25 week-old female mice characteristics.	201
Figure V-1. The general schema of the consequences of SSAO action.	204

List of Tables

Table I-1. Collagen and proteoglycan distributions in extracellular matrix of cartilage	66
Table I-2. Animal models of atherosclerosis. Selected mouse models of atherosclerosis progression and regression.	95
Table III-1. Diagram of the experiment and mouse experimental groups.	101
Table III-2. The protocols used for chondrocyte differentiation.	103
Table III-3. The chondrocyte culture protocols.	103
Table III-4. Protocol of immunohistochemical studies.	104
Table III-5. The list of antibodies used to immunohistochemical studies.	106
Table III-6. The list of antibodies used in WB.	107
Table III-7. Protocols of RNA isolation.	108
Table III-8. Primer sequences used for RT-qPCR rat cDNA analysis.	109
Table III-9. Primer sequences used for RT-qPCR human cDNA analysis	110
Table III-10. Primer sequences used for RT-qPCR mouse cDNA analysis.	110
Table III-11. The protocols of protein homogenate preparation.	111

Context

The incidence of age-related diseases, such as those concerning joints (osteoarthritis, arthritis) and cardiovascular diseases (atherosclerosis, arteriosclerosis) is increasing in recent years.

Osteoarthritis affects 9 to 10 million French people, or about 17% of the population. This is the most common rheumatic disease. Indeed, joint diseases account for 50% of chronic diseases affecting people over the age of 60 in the world while cardiovascular disease is the leading cause of death for the whole world. Some risk factors appear to be involved in the onset of these diseases, such as age, sex, obesity, but whose incidence is increasing, which has a tendency to aggravate the balance sheet over the years. Thus, its socio-economic impact is very important. So this is a real public health problem that needs to be overcome.

Age- and sex-standardized incident rates for symptomatic hand, hip, and knee OA have been estimated to be 100, 88, and 240 cases per 100,000 person-years, respectively, with incidence rates rising sharply after the age of 50 and levelling off after the age of 70 years (Neogi et al., 2013).

Atherosclerosis is a systemic multi-factorial disease that concerns different territories of the vascular tree and most epidemiologic data refer to one in particular and not on its totality. Nevertheless, it can be noticed that although coronary heart disease (CHD) mortality peaked in the 1960s and then declined dramatically, CHD remains the leading cause of death in both men and women (Pasternack et al., 2004). The Data on noncoronary atherosclerotic vascular disease (AVD) are far less available compared with data on CHD.

According to WHO, cardiovascular diseases are the leading cause of death worldwide, accounting for 30% of overall mortality. In France, they come second after cancer, with more than 145,000 deaths per year. Atherosclerosis is one of the main causes in France. It is an insidious phenomenon that begins in childhood and progresses silently made can be the starting point of the majority of cardiovascular diseases. It is known for its consequences, mainly myocardial infarction and angina pectoris, but also stroke, aortic aneurysm, arteritis obliterans lower limb and renal hypertension. Its main risk factors identified by the large INTERHEART

study in 2004 remain valid: high levels of bad cholesterol, physical inactivity, obesity, diabetes, smoking, alcohol, hypertension, age, and family history. Except for the last two factors, effective prevention, based on diet and lifestyle changes, is essential and effective to reduce these risk factors. They are associated with medication if necessary (antidiabetics, antihypertensives, etc.) (Dossier de presse de la FRM, l'athérosclérose, 2012).

The research presented here aims to determine whether the SSAO could play an important role in the key mechanisms involved in diseases associated with aging and inflammation (arthritis, atherosclerosis). Identification of substrates or inhibitors of target proteins would help to better understand the involvement of SSAO in the organization of the extracellular matrix of cartilage and blood vessels.

In this case, we see the SSAO as a possible therapeutic target. Thus, antibodies blocking adhesion function of SSAO inhibitors or selective blocking of SSAO activity could be used as drugs. It will therefore be of major interest to develop novel inhibitors of SSAO. On the other hand, SSAO may be proven to be a predictive marker of the development of these diseases?

This work fits perfectly into the CPER 2014-2020 Science and Technology for Health, which is being drafted, subproject Bioengineering for Health. This sub-project aims, through trans-disciplinary approaches to decipher the mechanisms of enzymes involved in detoxification, repair and regulation. Moreover this project is included in the network « Réseau cartilage » settled with the Universities of the « Grande Région ».

It is an unifying project that brings together two of the research groups of the “federation de recherche” UMR 3209 FR, particularly involved in basic and functional study of the extracellular matrix, in direct contact with highly prevalent pathologies including aging and overweight which are major risk factors. It is also in collaboration with hospital services (Orthopaedics, Rheumatology, Cardiovascular). This federation allows optimization of material and human resources that contributes to enhance the quality of the research.

I. Introduction

The mechanical properties of tissues are provided by the tissue components: extracellular matrix (ECM) and cells. Moreover, the proper functioning of tissues depends on the cell phenotype and the ECM composition. In addition, the ECM production can be changed during modulation of the cell phenotype. The tissues where the ECM plays particular functions are cartilage and blood vessels. In cartilage, chondrocytes during hypertrophic differentiation change protein expression and this can have effects on cartilage properties. Whereas in arteries, vascular smooth muscle cell (VSMC) phenotype can change from differentiated to synthetic leading to modification of the mechanical properties of the tissue.

As described in the literature, semicarbazide-sensitive amine oxidase (SSAO) is present in many tissues but in some its role has not yet been elucidated. It is known that SSAO participates in glucose transport (adipocytes, vascular smooth muscle cells) and in cell differentiation (adipocytes). Nevertheless, its role, in cartilage and VSMC has not been shown.

However, because of its enzymatic reaction which leads to the production of highly reactive aldehydes and hydrogen peroxide we can speculate that SSAO may contribute to the development of disease.

In this work we are interested in the role of SSAO in cartilage and arteries and its implication in disease such as osteoarthritis and atherosclerosis.

1. Amine oxidases

1.1. Amine oxidases

The amine oxidases (AO) are a large group of enzymes which catalyse the oxidative deamination of an aliphatic or an aromatic amine with dioxygen to form the corresponding aldehyde, ammonia and hydrogen peroxide. These products, depending on environment and concentration, can play many roles and show different degrees of toxicity (*refer to the paragraph: SSAO generated products*). Depending on the enzyme, an endogenous or xenobiotic (delivered to the organism with food or drugs) mono-, di- or polyamines can be substrates of AO (Gong et al., 2006; Strolin et al., 2007) (Fig. I-1).

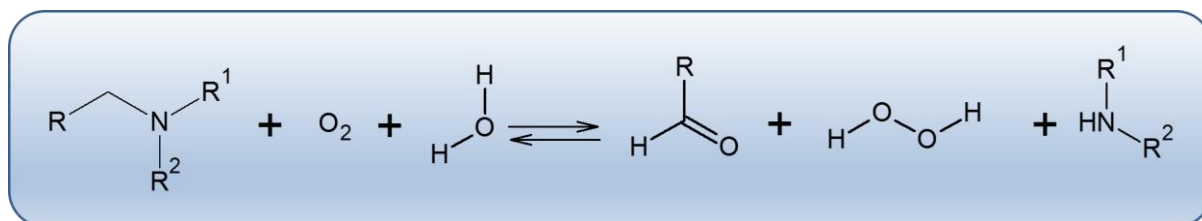


Figure I-1. Enzymatic reaction catalysed by amine oxidases.

The *Enzyme commission (E.C.) classification* classifies enzymes according to the nature of their catalytic enzyme reaction. The family of the amine oxidases contains two groups of enzymes which are divided depending on their cofactor: flavine adenine dinucleotide (FAD) and topa-quinone (TPQ) (Fig. I-2). Enzymatic activity, substrates, inhibitors and tissue expressions are well characterized for many of these AO. Nevertheless, their biological roles are not completely understood.

1.1.1. FAD-containing amine oxidases

To the first group belong the enzymes using FAD as cofactor like monoamine oxidase A, monoamine oxidase B and polyamine oxidases. These enzymes accept organic primary,

secondary or tertiary amines as substrates, including phenylethylamine (C₈H₁₁N), *n*-butylamine (C₄H₁₁N), ethylamine (C₂H₇N), amylamine (C₅H₁₃N), benzylamine (C₇H₉N), tyramine (C₈H₁₁NO), dopamine (C₈H₁₁NO₂) and kynuramine (C₉H₁₂N₂O). They are inhibited by pargyline (C₁₁H₁₃N) and clorgyline (C₁₃H₁₅C₁₂NO).

1.1.2. TPQ-containing amine oxidases

The group of enzymes using topa-quinone includes copper containing AO. These enzymes catalyse the deamination of a primary amine in trihydroxyphenylalanyl- and copper-dependent reactions. As substrates they accept histamine (C₅H₉N₃), putrescine (C₄H₁₂N₂), benzylamine (C₇H₉N), cadaverine (C₅H₁₄N₂), dopamine (C₈H₁₁NO₂), tryptamine (C₁₀H₁₂N₂), phenylethylamine (C₈H₁₁N) and spermine (C₁₀H₂₆N₄).

The enzymes from this group are sensitive for carbonyl-reactive compounds like semicarbazide (CH₅N₃O), therefore they are named semicarbazide-sensitive amine oxidases (SSAO).

This name refers to the entire group, to the diamine oxidases, lysyl oxidase, and cell surface and soluble forms of SSAO until better characterization of its members (Finney et al., 2014).

DAO

Diamine oxidases are enzymes expressed in a variety of tissues such as kidney, placenta, thymus and intestine. The *DAO* gene is composed of 5 exons and 4 introns. The important element of the active site, like in other TPQ-dependent amine oxidase, contains a tyrosine which undergoes a conversion to a topaquinone (Chassande et al., 1994). DAOs metabolize putrescine, cadaverine and histamine. Like others enzymes in this group they are sensitive to semicarbazide (Jalkanen et al., 2001).

Lysyl oxidase

Lysyl oxidase (*LOX*) is expressed in human placenta, skin and aorta. Some reports suggest that LOX is a secreted (46 to 32 kDa) protein which catalyzes the oxidation of peptidyl lysine to α -amino adipic- δ -semialdehyde, the precursor to the covalent crosslinkages that stabilize fibers of elastin and collagen. LOX uses a copper ion as a cofactor which is crucial during the first TPQ-dependent half-reaction (Kagan et al., 1991).

SSAO

SSAO refers to cellular or soluble forms of semicarbazide-sensitive amine oxidase (SSAO; AOC3; EC 1.4.3.6) which, like other enzymes from this family, carries out the oxidative deamination of primary aliphatic or aromatic amines into the corresponding aldehydes, hydrogen peroxide and ammonia (Lyles, 1996; Jalkanen et al., 2001; O'Sullivan et al., 2004). Nevertheless, a large number of studies on cellular and soluble forms of SSAO have highlighted their dissimilarity from other members of the copper-containing AO.

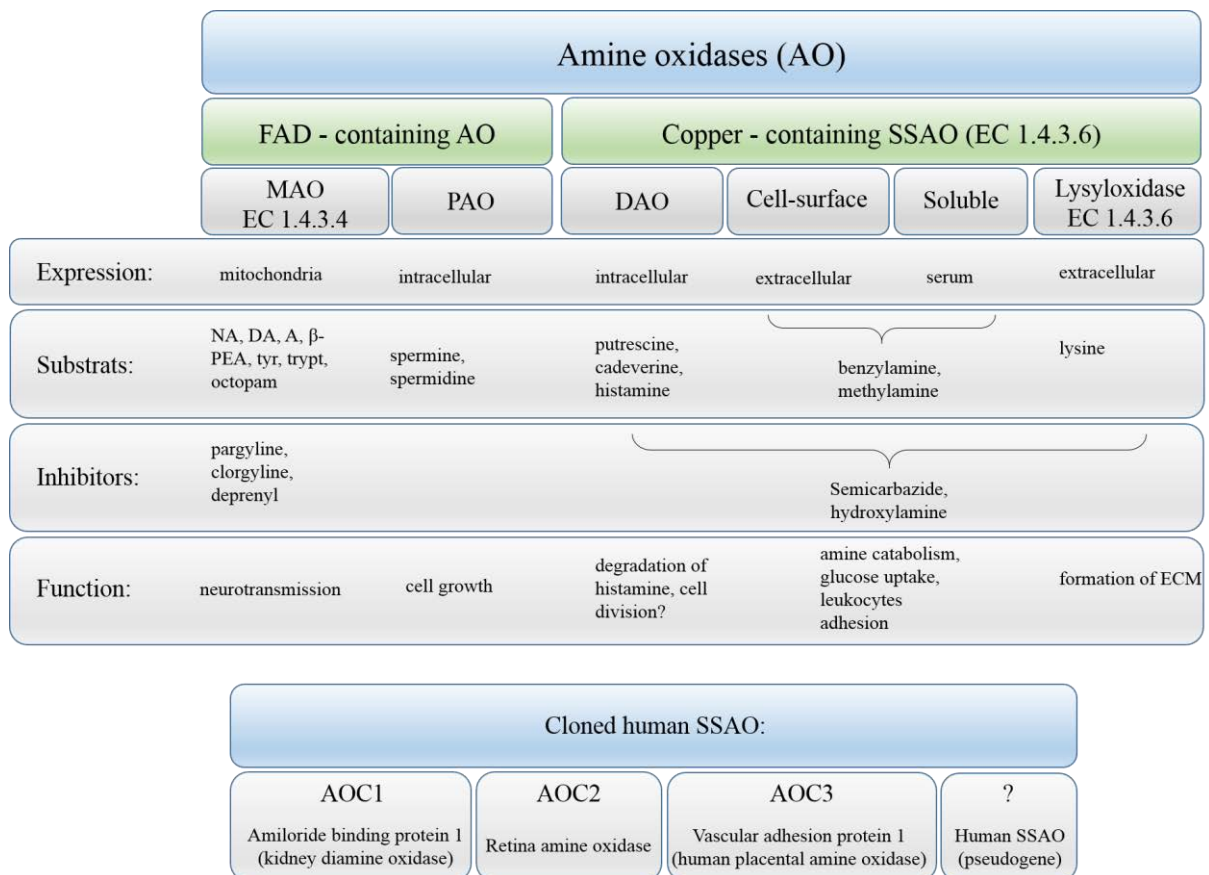


Figure I-2. Classification of amine oxidases. NA, noradrenaline; DA, dopamine; A, adrenaline; β -PEA, β -phenylethylamine; trypt, tryptamine, ECM, extracellular matrix; AOC, amine oxidase, copper-dependent (from Jalkanen et al., 2001).

1.2. The semicarbazide-sensitive amine oxidase

SSAO has been known for many years and its activity has been detected in many tissues (eg aorta, adipose tissue). Nevertheless, its physiological tissue-dependent role was far from clear until 1998 when cloning of SSAO elucidated some protein features that suggested the role of this protein.

1.2.1. Gene and protein structure of SSAO

1.2.1.1. Cloning of the gene

For many years now a lot of work has been devoted to cloning AO. *SSAO* was cloned for the first time in 1998 from human gut smooth muscle and since then, in many other tissues in different species.

Mu et al., (1994) cloned bovine liver amine oxidase and they reported the nucleotide sequence of bovine serum amine oxidase and its predicted protein sequence. Moreover, Høgdall et al., (1998) reported that the nucleotide sequence of a bovine lung cDNA was similar but not identical to the cDNA sequence of copper-containing amine oxidase from liver described by Mu et al., in 1994. This result was explained by different mechanisms of gene expression ensuring tissue-specific expression of the different forms.

Cloning of the human *SSAO* was first reported in the placenta (Zhang et al., 1996). The studies of Imamura et al., (Imamura et al., 1997 and 1998) on the human retinal amine oxidase gene (*AOC2*) revealed its localization on chromosome 17, in 17q21.

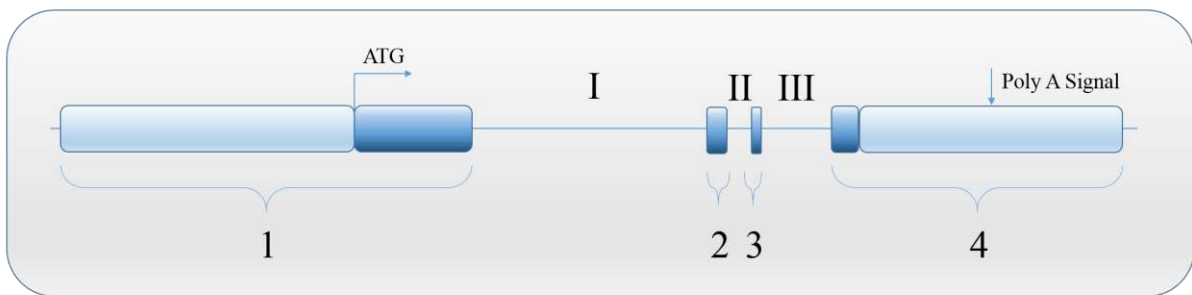
In 1998, Smith et al., cloned *SSAO*/vascular adhesion molecule 1 (*VAP-1*) from human gut smooth muscle. The protein obtained from the open-reading frame in the *VAP-1* cDNA encoded a 763-amino acid protein of 84.6kD.

In 1998, Cronin et al., reported two alternatively spliced transcripts of human copper-containing AO pseudogene in liver and placenta.

In the same year, Bono et al., (1998) cloned and characterized the mouse kidney *VAP-1*. The amplified 800-bp fragment has shown 80% amino acid identity to human hVAP-1. Moreover, they determined the nucleotide sequence, structural organization and chromosomal localization in the genome of a gene encoding for mouse *VAP-1*. The *mVAP-1* gene is composed of four

exons separated by three introns and encodes a protein with high identity to copper-containing amine oxidases. The active site is composed of two important histidines that coordinate a copper atom located in exon 1. Moreover, exon 1 includes 8 putative glycosylation sites which are probably essential for adhesive properties of the enzyme (Bono et al., 1998). The main features of the gene are presented in figure I-3.

A



B

Exon		Intron	
Number	Size (bp)	Number	Size (bp)
1	5528	I	3179
2	286	II	346
3	130	III	906
4	3982		

Figure I-3. The main features of *mVAP-1* gene. A: A schematic diagram of the mouse *VAP-1* gene. The four exons are represented by boxes and Arabic numerals. The introns are represented as a straight continuous line and in Roman numerals. B: Intron-exon boundaries of the *mVAP-1* gene (adapted from Bono et al., 1998).

Morris et al., (1997) reported the cloning of cDNA from rat adipocytes, encoding an integral membrane protein, the sequence of which is very closely related to serum AO. Ochiai et al., (2005) determined that the cDNA sequence of SSAO was 3556 bp in length and encoded 763 amino acids giving a calculated protein molecular weight of 85 kDa.

Schwelberger (2004 and 2006) cloned four genes encoding for a porcine copper-containing amine oxidase (Fig. I-4). *AOC1* encodes DAO. The *AOC2*, *AOC3* *AOC4* genes have four exons each and are tandemly arranged on the same chromosome that encodes for the retina-specific

AO (RAO), vascular adhesion protein-1 (VAP-1) and probably a soluble form of VAP-1 respectively. The author proposed that *AOC4* encoding a protein of 762 amino acid residues, is mainly expressed in the liver and had features of a secretory protein that could be a good candidate for plasma AO. Nevertheless, other reports indicated that a soluble form of VAP-1 could be the result of a proteolytic release of the large extracellular part of the membrane associated AOC3 gene product (Abella et al., 2004; Stolen et al., 2004a; Schwelberger, 2007).

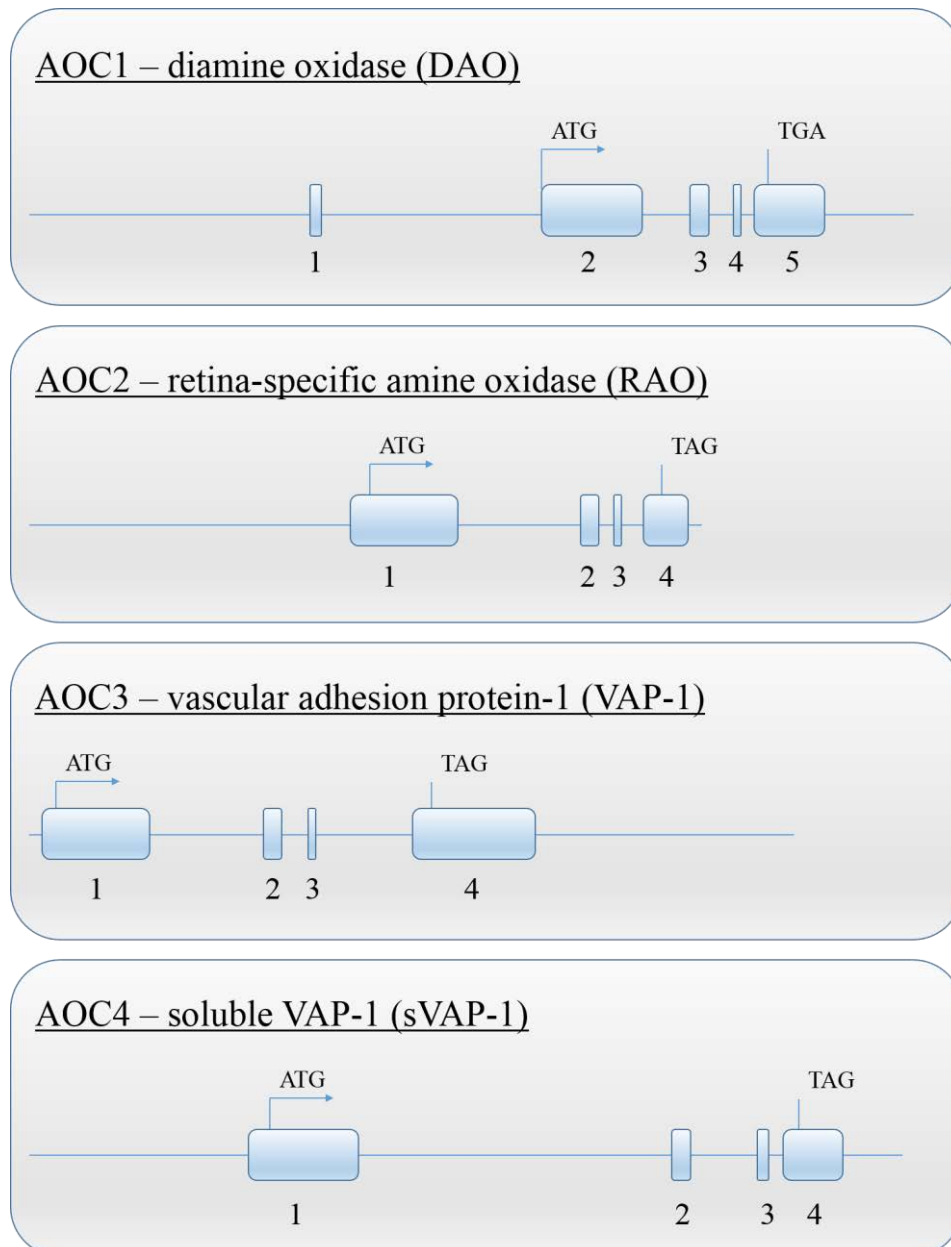


Figure I-4. Structure of porcine AOC genes. Exons are shown as numbered boxes and the coding regions are indicated by the translation start and stop codons (adapted from Schwelberger, 2006).

Cloning and sequencing of the SSAO full-length cDNA from the murine adipose cell line 3T3-L1 have shown that this cDNA encodes the murine homolog of the human placental AO. It is also the homolog of a partial rat adipocyte cDNA and corresponds to a major integral glycoprotein of the adipocyte plasma membrane (Moldes et al., 1999).

Recently, a shorter splice variant of VAP-1, VAP-1 Δ 3 from human lung was cloned and it is about 130 amino acids shorter than VAP-1. The authors suggested that the VAP-1 Δ 3-isoform could serve as a regulatory mechanism whereby leukocytes trafficking can be decreased *via* reducing the number of functional cell-surface VAP-1 molecules available for the process of transmigration (Kaitaniemi et al., 2013).

1.2.1.2. Protein domains and active sites

The SSAO enzyme group consists of many isoforms depending on the species, tissues and substrate specificity.

The Human VAP-1 (hVAP-1) from gut smooth muscle has a molecular mass of 90 kDa (per monomer) and 170-180 kDa (per dimer). It shows a strong identity with the other copper-containing AO, especially with the bovine serum amine oxidase (81%) and the rat adipocyte SSAO (83%) (Morris et al., 1997). The intracellular domain was composed of four amino acids, the membrane-spanning domains (transmembrane helix) contained a region of 23 predominantly hydrophobic amino acids (residues 5–27) and a large glycosylated extracellular domain composed of domains D2, D3 and D4 with 12 putative N-glycosylated and 6 putative O-glycosylated sites (Fig. I-5) (Salminen et al., 1998; Smith et al., 1998; Airene et al., 2005).

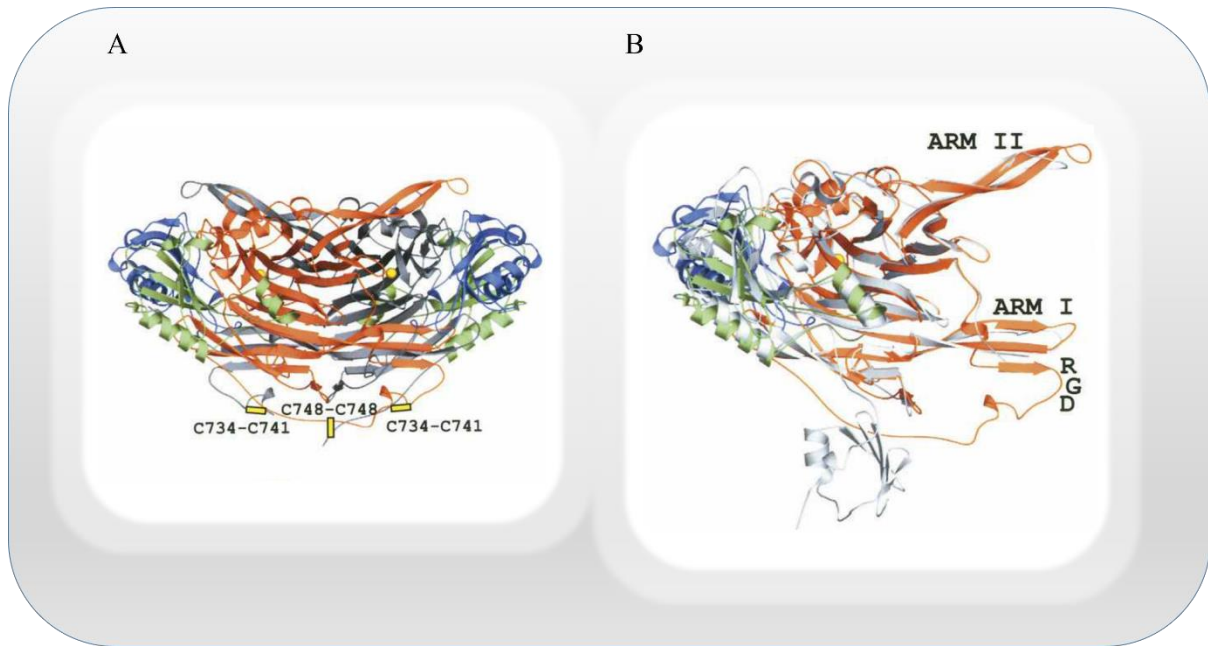


Figure I-5. Stereo views of hVAP-1. A: A ribbon diagram of the dimer is shown. B: A monomer of hVAP. The b-hairpin arms I and II, the RGD motif, and the disulfide bridges are indicated. The ribbons for hVAP-1 were drawn with domain-specific coloring: D2, green; D3, blue; D4 of subunit A, orange; and D4 of subunit B, gray. The *Escherichia coli* AO (ECAO) ribbon is in gray. The copper atom of the active site is shown as a yellow sphere (from Airene et al., 2005).

The mouse VAP-1 (mVAP-1) is a 765-amino acid protein with six putative N-glycosylation and six putative O-glycosylation sites. The mVAP-1 from gut smooth muscle is larger than hVAP-1 from the same tissue. The mVAP-1 represents 110- and 220 kDa and this can be due to species-specific glycosylation differences (Bono et al., in 1998).

Despite differences between species, large part of the proteins show homologies. Studies of Cai and Klinman have shown that the active site of the enzyme has remained practically unchanged during evolution (Cai et al., 1994).

VAP-1 is heart-shaped, the type II membrane homodimeric protein is short, four amino acids in length, a cytoplasmic NH₂ terminus, a single membrane-spanning domain and a large COOH-terminal extracellular part containing the active site (Smith et al., in 1998; Salminen et al., 1998; Airene et al., 2005; Jalkanen et al., 2001). Each monomer of hVAP-1 is composed with three domains: D2 (residues 55-169), D3 (residues 170-300) and D4 (residues 301-761). The D2 domain is highly conserved in all known copper-containing amine oxidase, nevertheless the D4 domain is the most conserved domain in the SSAOs (Fig. I-6). These residues are

involved in topaquinone generation (TPQ471) and positioning (Tyr372, Asn470), in the catalytic reaction (Asp386), coordination of the copper ion (His520, His522, His684), metal binding site (Asp529, Asp673) and lining the active site cavity (Asn470) (Salminen et al., 1998; Airenne et al., 2005; Lunelli et al., 2005). The D4 domain contains the RGD at positions 726 to 728, and the tripeptide is known to play role in lymphocyte adhesion. Nevertheless it is not indispensable for VAP1-dependent adhesion (Salmi et al., 2000). The active site is deeply buried within the protein and accessible via a cavity formed by the D3 and D4 domains.

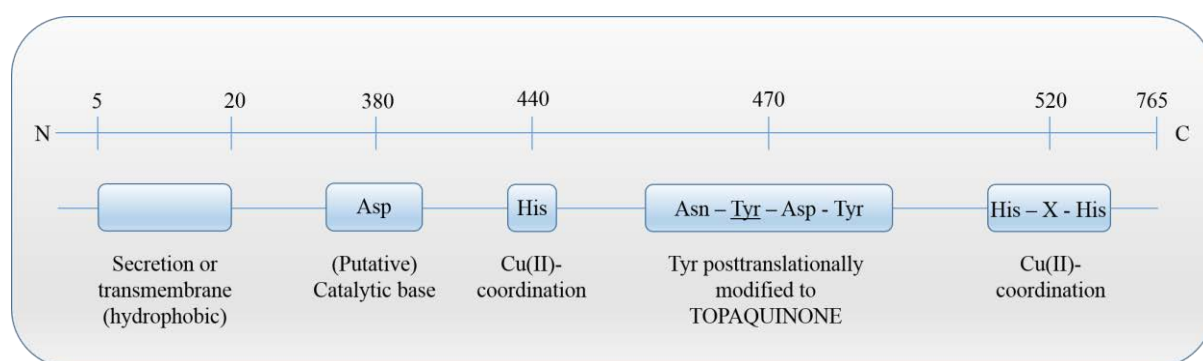


Figure I-6. The conserved motifs of semicarbazide sensitive amine oxidases (SSAO) (adapted from Jalkanen et al., 2001).

1.2.1.3. Soluble forms of SSAO/VAP-1

Several works have already confirmed the presence of a soluble form of SSAO (sSSAO). This soluble form of SSAO has been found in man, presumably resulting from the proteolytic cleavage of membrane-bound hVAP-1 (Abella et al., 2004; Stolen et al., 2004a). This hypothesis is supported by the sequence of the membrane domain of SSAO/VAP-1 with the intracellular NH₂-terminal end characterized by a region containing 23 predominantly hydrophobic amino acids. The amino acid residue at position 19 was proposed as the cleavage site (Smith et al., 1998). In 2005, Jakobsson et al., produced and crystallized an N-terminally truncated, human sSSAO containing 29 residues.

The sources of sSSAO were suggested to be the endothelial cells of high endothelial venules, adipocytes (Stolen et al., 2004a) and vascular smooth muscle cells (Göktürk et al., 2003).

The level of sSSAO is low in human and rodents plasma compared to cow or pig. It increases in inflammatory diseases like atherosclerosis.

1.2.2. TPQ and enzymatic reaction mechanisms

Essential for the deamination reaction carried out by SSAO, is the topa-quinone (TPQ) cofactor. SSAO uses a tyrosine residue as a redox cofactor, that is post-translationally modified to 2, 4, 5-trihydroxyphenylalanine quinone (TPQ) (Janes et al., 1990; Klinman, 1996; McGuirl et al., 1999). As for the TPQ precursor, a residue of tyrosine situated in the active site with a consensus sequence (Asn-Tyr-Asp/Glu) was indicated (Mu et al., 1992). During the post-translational modification leading to the topa-quinone formation, a functional copper binding site, which is preserved through evolution, and oxygen play an essential role.

The enzymatic reaction can be divided into two half-reactions (Fig. I-7). First, the reduction of TPQ by the substrate takes place. The primary amine group of the substrate is trapped in a covalent bond to the TPQ residue and a Schiff base is formed. Then hydrolysis takes place and an aldehyde is released. The reduced cofactor is attached to aminoquinol-Cu(II). In the second oxidative half-reaction, copper participates in an electron transfer between TPQ-aminoquinol and molecular oxygen. The TPQ is re-oxidated by molecular oxygen with a concomitant release of hydrogen peroxide and ammonia (Jalkanen et al., 2001; Dawkes et al., 2001; Klinman et al., 2003; Dubois et al., 2005).

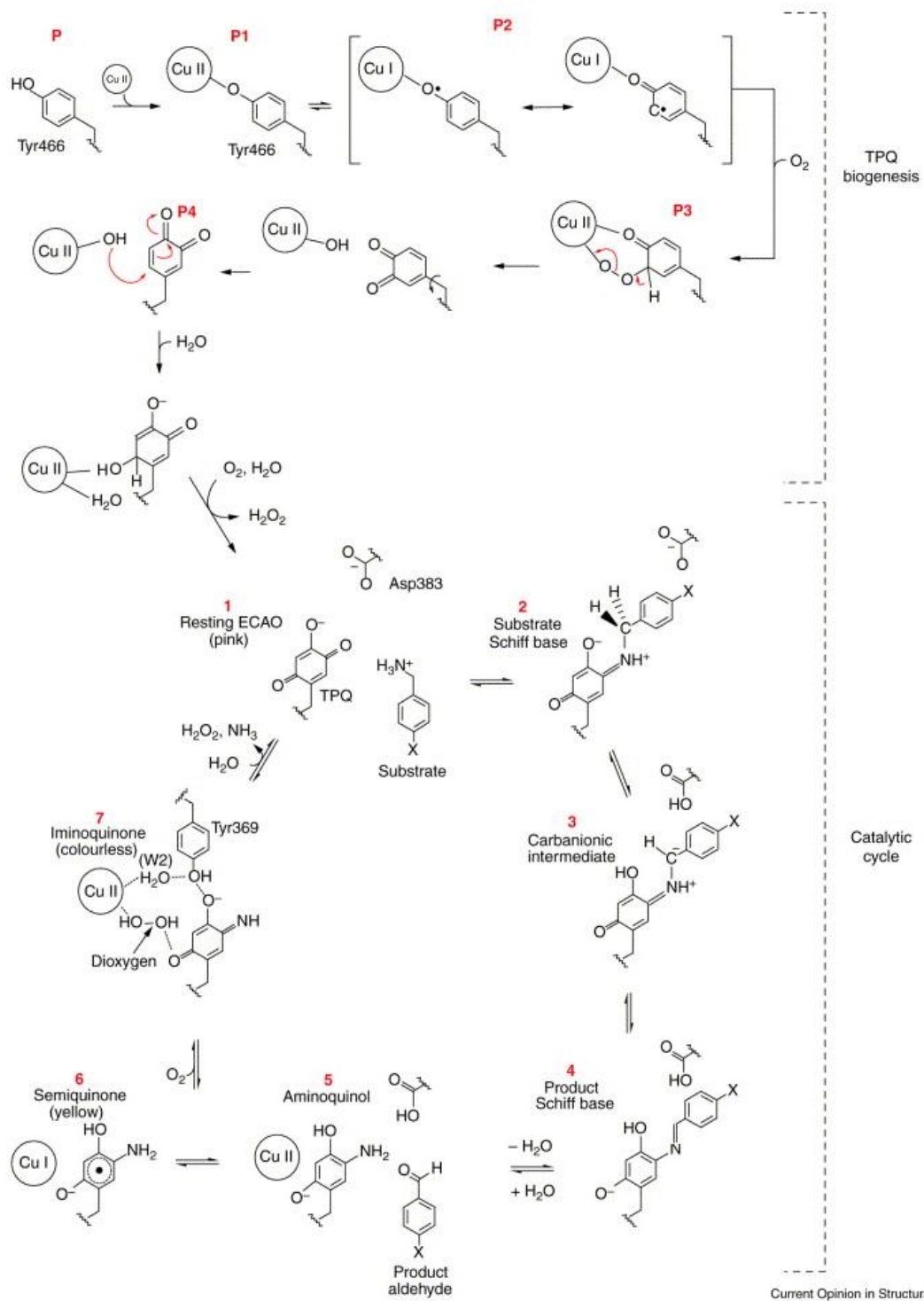


Figure I-7. The TPQ biogenesis and the amine oxidases catalytic reaction (adapted from Dawkes et al., 2001).

1.3. Enzymatic reaction of SSAO

1.3.1. Substrates (MA, BZM)

The substrates can be divided into two groups. The first group includes endogenous substances. In 1965, McEven mentioned the ability of SSAO to metabolize methylamine (MA), what was confirmed by Precious and colleagues using homogenates of rat aorta and human umbilical artery (Precious et al., 1988; Yu et al., 1993). MA is produced from adrenaline (Schayer et al., 1952), sarcosine, creatinine (Davis et al., 1961; Yu et al., 1993), lecithin or choline deamination (Zeisel et al., 1983 and 1985; Precious et al., 1988). It was also reported that cigarette smoke contains methylamine. Moreover, nicotine can induce the release of adrenaline and by metabolic reaction more methylamine is produced (Yu et al., 1998). Methylamine can also be delivered to the organism through food and drinks (Zeisel et al., 1986). Aminoacetone, another SSAO substrate (Lyles et al., 1992), derives from glycine or threonine metabolism (Bird et al., 1984; Elliott, 1960). The physiological substrates are believed to include also 2-phenylethylamine (McEnen, 1965a and 1965b), tyramine (Young et al, 1982), dopamine (Lizcano et al., 1991a) and histamine.

The second group of SSAO substrates contains xenobiotic amines such as mescaline and primaquine (O'Sullivan et al., 2004) and can be delivered with the diet or medical treatment.

SSAO has also been referred to as benzylamine oxidase. Indeed, benzylamine (BZM) is well deaminated by SSAO and in many studies it is used as a substrate of this enzyme (Clarke et al., 1982; Lizcano et al., 1991b).

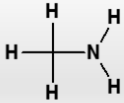
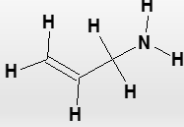
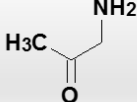
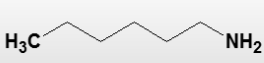
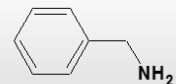
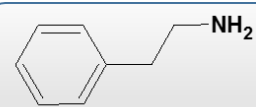
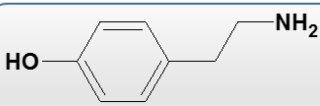
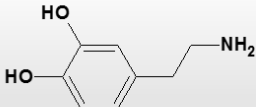
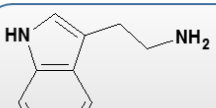
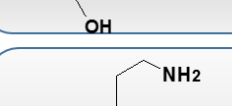
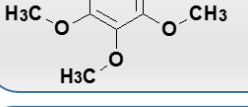
SUBSTRATES	COMMENTS
	<p>Methylamine</p> <p>Endogenous and xenobiotic. Not a substrate for MAO.</p>
	<p>Allylamine</p> <p>Xenobiotic. Not a substrate for MAO. Highly toxic product.</p>
	<p>Aminoacetone</p> <p>Endogenous. Not a substrate for MAO.</p>
	<p><i>n</i>-Pentylamine</p> <p>Xenobiotic. Also MAO-B substrate.</p>
	<p>Benzylamine</p> <p>Xenobiotic. Also MAO-B substrate.</p>
	<p>2-Phenethylamine</p> <p>Trace amine. Also MAO-B substrate.</p>
	<p>Tyramine</p> <p>Endogenous and xenobiotic. Also MAO A and B substrate.</p>
	<p>Dopamine</p> <p>Endogenous. Also MAO A and B substrate.</p>
	<p>5-Hydroxytryptamine</p> <p>Substrate in dental pulp. MAO-A substrate.</p>
	<p>Mescaline</p> <p>Xenobiotic. Also MAO substrate.</p>
	<p>Primaquine</p> <p>Xenobiotic. Also MAO substrate.</p>

Figure I-8. Some compounds that have been shown to be SSAO substrates (adapted from O'Sullivan et al., 2004).

1.3.2. Products of SSAO reaction

The enzymatic action mediated by SSAO produces hydrogen peroxide, ammonia and aldehyde. Depending on the substrate used, aldehydes with different levels of toxicity can be formed. For example, the deamination of endogenous methylamine results in the formation of formaldehyde. Additionally, the increase of SSAO activity causes an accumulation of generated products and affects surrounding cells. There are many reports concerning the toxicity of SSAO products which are involved in endothelial damage, protein cross-linkage and atherosclerosis (Boor et al., 1990; Yu et al., 1992, 1993 and 1996; Callingham et al., 1995).

Aldehydes

Divers aldehydes, for example formaldehyde and methylglyoxal formed by deamination of methylamine and aminoacetone (Yu et al., 1997, 1998a) respectively, manifest high cytotoxicity.

Formaldehyde is a very reactive molecule, and a low amount can be quickly metabolized by the aldehyde dehydrogenase. Nevertheless, in higher concentrations it is capable of inducing intra- and inter-molecular cross-linkages between proteins and between proteins and DNAs (Yu et al., 1998).

A rich literature exists around the influence of formaldehyde on tissues. In 2004, Gubisne-Haberle et al., reported that after incubation with SSAO-containing tissue extracts or slices, methylamine (MA) was converted into formaldehyde and thus reacted with lysine residues and induced protein cross-linkages. Chronic rat treatment with MA increases oxidative stress and vascular damage (Deng et al., 1998 and 1999) while inhibition of SSAO activity decreases atherogenesis (Yu et al., 2002). An increase of SSAO-catalyzed MA turnover has been found to be associated with vulnerability for atherosclerosis in mice (Yu et al., 1998). SSAO-mediated deamination has been shown to be toxic toward endothelial cells *in vitro*. Moreover, this effect was reduced when a SSAO selective inhibitor was used (Yu et al., 1993). Through its catalytic action, the membrane as well as the soluble forms of SSAO induce cell death in cultured smooth muscle cells (Hernandez et al., 2006; Solé et al., 2008).

Massive exposure to methylamine after an industrial accident was lethal to humans (Gubisne-Haberle et al., 2004).

Methylglyoxal is another bioactive aldehyde which can quickly cross-link proteins. Additionally, it was shown by Mathys et al., (2002), that SSAO mediates the synthesis of methylglyoxal- advanced glycation end-products.

Taken together, aldehydes are able to cause damage of proteins by formation of cross-links between them and play a role in the formation of advanced glycation end-products (AGEs). Chronic exposure of proteins to these aldehydes may cause direct cytotoxic damage leading to diseases.

Hydrogen peroxide

Hydrogen peroxide is a known regulator of gene expression (Sies et al., 2014). Nevertheless, oxidative stress can be initiated and propagated by hydrogen peroxide overproduction and its conversion to hydroxyl free radicals (Fenton reaction: $\text{H}_2\text{O}_2 + \text{Fe}^{2+} \rightarrow \cdot\text{OH} + \text{OH}^- + \text{Fe}^{3+}$) (Muzykantov, 2001). Free radicals can also be generated from formaldehyde in the presence of H_2O_2 ($2\text{HCHO} + \text{H}_2\text{O}_2 \rightarrow 2\text{H}^\cdot + 2\text{C}=\text{O} + 2\text{H}_2\text{O}$). Moreover, increases of H_2O_2 concentration can contribute to oxidative stress and therefore cytotoxicity thus to disease progression such as atherosclerosis and osteoarthritis (Deng et al., 1998; Yu et al., 2003, Breton-Romero et al., 2014).

Ammonia

Ammonia in high concentrations is neurotoxic due to its excitatory actions on glutamate-receptors in the brain (Albrecht, 1998).

1.3.3. Inhibitors

In order to define SSAO functions, many attempts to generate selective inhibitors have been performed. Previously, developed inhibitors were divided into several groups: hydrazine-type inhibitors (semicarbazide), inhibitors with nitrogen-containing heterocyclic core such as allylamines, amino acid derivatives, benzamides, oxime-based inhibitors (Dunkel, 2011). Nevertheless, most of the known inhibitors exhibit a lack of selectivity with respect to other copper-containing AOs, and to FAD-dependent MAO (Matyus et al., 2004). Others have

potential for toxicity upon prolonged administration. First developed as an antibiotic, LJP1586 (Z-3-fluoro-2-(4-methoxybenzyl)allylamine hydrochloride) has been shown to be a potent and a selective SSAO inhibitor (O'Rourke et al., 2008) (Fig. I-9). There exists also an alternative manner to inhibit SSAO activity such as with peptide inhibitors which bind to SSAO/VAP-1, small interfering RNAs that downregulate SSAO expression, and function-blocking antibodies.

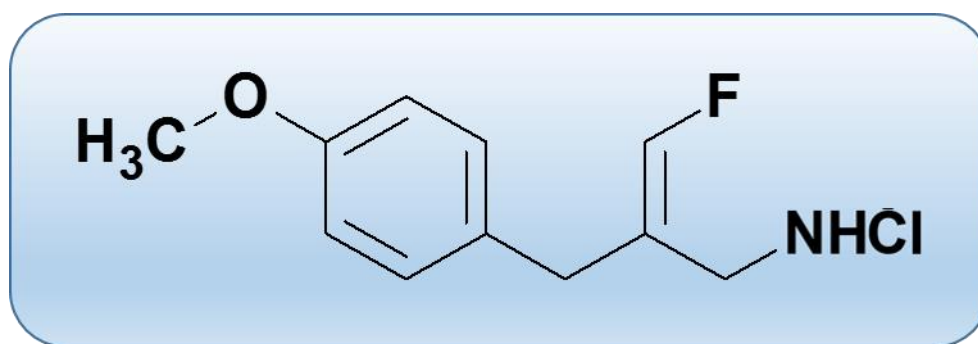


Figure I-9. Structure of Z-3-fluoro-2-(4-methoxybenzyl)allylamine hydrochloride (LJP1586) (from O'Rourke et al., 2008).

1.4. Protein expression of SSAO in different tissues

Over the past forty years, the presence of SSAO has been reported in many diverse tissues. The first major source of SSAO was in large arteries. VAP-1 was found in the media layer of large vessels such as the aorta (Salmi et al., 1993). It was demonstrated in bovine and rabbit aorta (Lyles, 1996), rat aorta (Gubisne-Haberle et al., 2004) and next in human vasculature (Lewinsohn, 1984). Further studies associated a SSAO presence in the aorta with smooth muscle cells layer (VSMC) (Lewinsohn, 1984; Lyles et al., 1985; Precious et al., 1988). SSAO activity measured in VSMC from pig and rat cultured *in vitro* confirmed this association (Hysmith et al., 1987; Blicharski et al., 1990). Moreover, several studies have reported that SSAO is mainly localized in the plasma membrane of cells in rat aorta (Wibo et al., 1980), in pig aortic SMC (Hysmith et al., 1988a; 1988b) and in human tonsil VSMC (Jaakkola et al., 1999). SSAO was also shown to be present in non-vascular smooth muscle (Lewinsohn, 1981) and mouse small intestine (Gubisne-Haberle et al., 2004).

Recently we can find reports about SSAO/VAP-1 expression in foetal tissues. Already during the early stage of human foetal development (7 weeks) SSAO is detectable in the smooth muscle layer of the aortic and gut wall, smooth muscle and fat cells in different organs. VAP-1

expression in primary lymphoid organs was seen in thymus and in secondary lymphoid organs, the spleen was positive for VAP-1 presence. Moreover, a study has confirmed the active form of VAP-1 in foetal tissues (Salmi et al., 2006).

In 2008, Valente et al., showed that SSAO/VAP-1 is expressed during mouse embryonic development. Expression of VAP-1 is already detected at embryonic day 9 (ED9) in the myocardial progenitor cells of the ventricular wall of the heart. Then at ED14, VAP-1 was found in the heart, aorta, pulmonary vessels and vessels and arteries of the lung. In later stages of embryonic development, VAP-1 was detected also in the sensory organs, smooth muscle tissue and skeletal elements.

Another major source of SSAO is white and brown adipose tissues. SSAO was detected in rat adipocytes (Barrand et al., 1982 and 1984a; Raimondi et al., 1991), and localized in plasma membranes of rat brown adipose tissue (Barrand et al., 1984b).

Salmi et al., (1993) have reported high expression of SSAO/VAP-1 in endothelial cells of high endothelial venules (HEV).

For the first time the presence of SSAO activity in non-vascularized tissues such as rat articular cartilage was reported in 1987 by Lyles and Berti (1987) and in odontoblast by Norqvist and Oreland (1981, 1982).

1.5. The role of SSAO in different cells/tissues

SSAO is expressed in many tissues, extensively in adipocytes and in the vasculature, particularly in smooth muscle cells. SSAO has been found in endothelial cells of high endothelial venules of peripheral lymph nodes. An increase in the soluble form of SSAO was found in serum of patients with inflammatory diseases like atherosclerosis or inflammatory liver disease. There exist many reports about the role of SSAO in these tissues.

1.5.1. Adipocytes (glucose uptake and cell differentiation)

It has been observed that *AOC3* gene expression increases during adipogenesis (Moldes et al., 1999; Subra et al., 2003). In adipocytes, it has been reported previously that SSAO played a role in glucose transport. Glucose transport is stimulated in rat adipocytes treated with benzylamine in the presence of vanadate. Nevertheless, this effect is totally abolished with a

SSAO inhibitor. In addition, benzylamine promoted also the translocation of GLUT4 to the plasma membrane in rat adipocytes (Enrique-Tarancon et al., 1998; Morris et al., 1997). The oxidation of tyramine – another SSAO substrate, in the presence of vanadate synergistically stimulated glucose transport in adipocytes by peroxovanadate formation. Moreover, studies have shown that peroxovanadate which is a powerful insulin-mimetic compound can be generated by exo-, but also endogenous hydrogen peroxide, the product of SSAO enzymatic action (Marti et al., 1998). The same group has shown that *in vivo* administration of benzylamine and vanadate decreased plasma glucose levels in rats, suggesting an effect on glucose deposition in the whole animal body (Enrique-Tarancon et al., 2000).

Morin et al., (2001), have confirmed that SSAO activity is localized on the human adipocyte membranes and reported its insulin-like interaction with glucose and lipid metabolism. *In vitro*, SSAO-dependent oxidation of amines stimulates glucose transport and inhibits lipolysis (Iglesias-Osma et al., 2005). Adipocyte treatment with TNF-alpha which increases obesity-linked insulin resistance and decreases insulin-stimulated glucose transport, causes a decrease in SSAO expression in those cells (Mercier et al., 2003).

Yu et al., (2004), have confirmed that inhibition of SSAO decreases glucose transport in adipocytes obtained from SSAO inhibitor pre-treated mice. The weight gain in obese diabetic KKAY mice treated with a selective SSAO inhibitor was significantly decreased more so than in control mice that were not treated with the SSAO inhibitor. In addition, SSAO-mediated oxidation of methylamine and aminoacetone induces glucose uptake by adipocytes and as a result causes a transient reduction of blood glucose.

The effect of glucose uptake inducted by administration of SSAO substrates is totally absent in adipocytes from *AOC3* KO mice. This observation proves that SSAO-dependent oxidation and production of peroxide hydrogen is necessary to modulate an insulin-like effect of the amines (Bour et al., 2007; Stolen et al., 2005).

In addition, Iglesias-Osma et al., (2004 and 2005) have shown for the first time that methylamine increases *in vivo* glucose disposal, and exhibits an antihyperglycaemic action which is not mediated by a clear effect on insulin secretion.

Moreover, SSAO is involved in terminal differentiation and development of adipocytes. *In vitro* pre-adipocytes exposed to a SSAO substrate like methylamine increase cell differentiation depending on treatment time and dose of the substrate. Moreover, this effect is abolished by

catalase, what indicates that SSAO activity accelerates cell differentiation via hydrogen peroxide production (Mercier et al., 2001; Fontana E et al., 2001; Carpené et al., 2006).

1.5.2. Vascular smooth muscle cells

It has been shown that SSAO is strongly expressed in vascular smooth muscle cells (VSMC) and El Hadri has suggested in 2002, that this amine oxidase can have a role in the cell differentiation process. It was reported that SSAO mRNA expression and its enzymatic activity increased during VSMC differentiation. Moreover, the activation of SSAO by methylamine regulates glucose uptake in differentiated VSMCs and increases glucose transporter 1 (GLUT1) expression at the cell surface. Likewise, SSAO activation stimulates the glucose transport in adipocytes and its inhibition abolishes this process. This effect has been found during VSMC treatment with methylamine. Addition of catalase to the culture medium results in an inhibition of glucose transport through a diminution of the membrane expression of GLUT1. However, SSAO-dependent VSMC differentiation was not confirmed in this study.

Increased aldehyde and H₂O₂ production by SSAO in the presence of MA was shown to induce cytotoxicity of VSMC. In the presence of MA, cells underwent apoptosis by caspase-3 stimulation. However, the number of caspase-3 positive cells was significantly decreased when SSAO activity was inhibited with semicarbazide. Moreover, SSAO catalytic activity in the presence of MA induced vascular cell death by p53 phosphorylation. In addition, the increased VSMC apoptosis was associated with increased aldehyde formation and not with H₂O₂ (Hernandez et al., 2006, Sole et al., 2008).

Many *in vivo* studies were devoted to clarify the role of SSAO in arterial wall.

The pharmacological inhibition of AO (almost complete inhibition of SSAO and strong inhibition of LOX) by semicarbazide in rats caused a reduction in vessel diameter and in elastin insoluble content. In addition, treated rats presented an increase of ECM components other than collagen and insoluble elastin in the arterial wall, increased arterial stiffness, and a decreased pressure of carotid artery rupture (Mercier et al., 2007 and 2009). Studies of Landford et al., (1999) have shown that SSAO inhibition in rats causes degenerative medial changes, decrease of mature elastin and collagen and disorganization of the elastin architecture. Nevertheless, the total amounts of elastin and collagen were unchanged.

Comparison of genetically modified mice with WT control mice has delivered much interesting information. *SSAO*^{-/-} mice with a 129S6 genetic background did not show differences in distensibility, wall stress, neither in medial thickness nor in medial cross sectional area. However, the lumen diameter was significantly increased in *SSAO*^{-/-} mice compared to *SSAO*^{+/+} mice. Parameters in SSAO deficient mice such as arterial stiffness, mechanical resistance, LOX activity elastic fibre morphology, elastin and collagen content and vascular reactivity were unchanged (Mercier et al., 2006). Mice overexpressing SSAO in VSMC present decreases of mechanical properties, mean arterial pressure (MAP) and increases of pulse pressure. In addition, problems with blood pressure regulation and abnormal structure of the elastic fibres were found (Gokturk et al., 2003 and 2007). Reported by Stolen et al., SSAO overexpression in endothelial cells with methylamine administration, increased glucose uptake and increased diabetes-like complications. Particularly, AGE product formation, elevated blood pressure and modification in the atherosclerotic lesion formation were found (Yu et al., 1997b; Stolen et al., 2004b).

Activation of SSAO by its substrate increases glucose uptake through H₂O₂. Nonetheless, other products such as ammonia and aldehydes are concomitantly generated. As indicated in the chapter “*Enzymatic action of SSAO, products*”, high concentrations of H₂O₂ induce oxidative stress, and aldehydes, derived from methylamine and aminoacetone, which are toxic.

1.5.3. Endothelial cells of high endothelial venules

Immune responses are dependent on tightly controlled lymphocyte trafficking in the body. Lymphocytes enter the inflamed tissues by recognizing and binding to the endothelial cells in specialized postcapillary venules called high endothelial venules (HEV), then they migrate between the endothelial cells into surrounding tissues. This process of tethering, rolling, activation, firm adhesion and transmigration is presented in figure I-10.

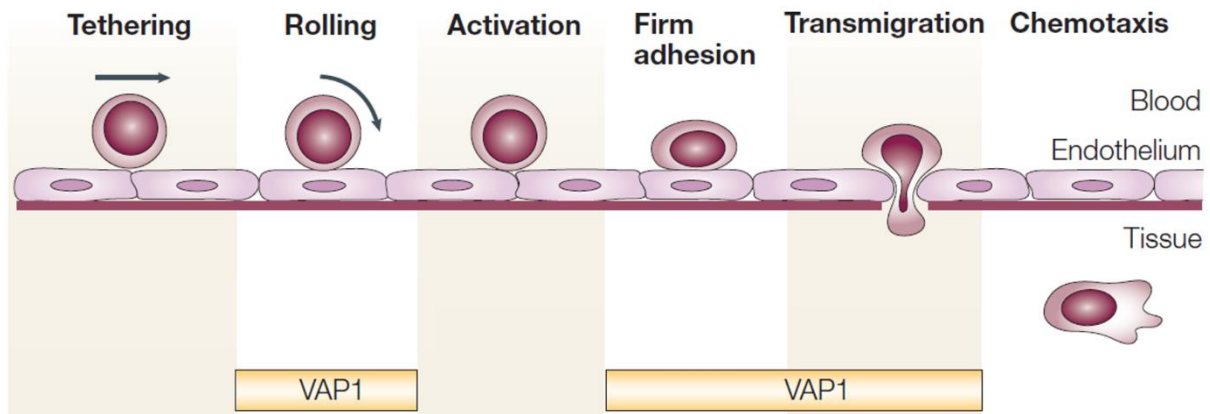


Figure I-10. The leukocyte-extravasation cascade. The different phases of the multistep adhesion cascade that supports leukocyte exit from the blood into the tissues. Vascular adhesion protein 1 is involved at many steps by binding to leukocytes and by producing bioactive end products, such as hydrogen peroxide (from Salmi et al., 2012).

Salmi and Jalkanen have reported that vascular adhesion protein 1 (VAP-1) is strongly expressed at the luminal side of the endothelial cells in HEV-like venules in inflamed synovial membranes. Nevertheless, in this type of vessel, VAP-1 can be expressed on EC surface also under non-inflammatory conditions. In most other vessels, such as flat-walled venules, VAP-1 is translocated from cytoplasmatic vesicles to the luminal surface only upon induction of inflammation. Nevertheless, VAP-1 was not detected on the luminal surface of large vessels (e.g. aorta, vena cava) or on the surface of infiltrating leukocytes. Then the role of VAP-1 to be a specific recognition element for leukocytes was proposed (Fig. I-11) (Salmi et al., 1992; Salmi et al., 1993; Salmi et al., 2012).

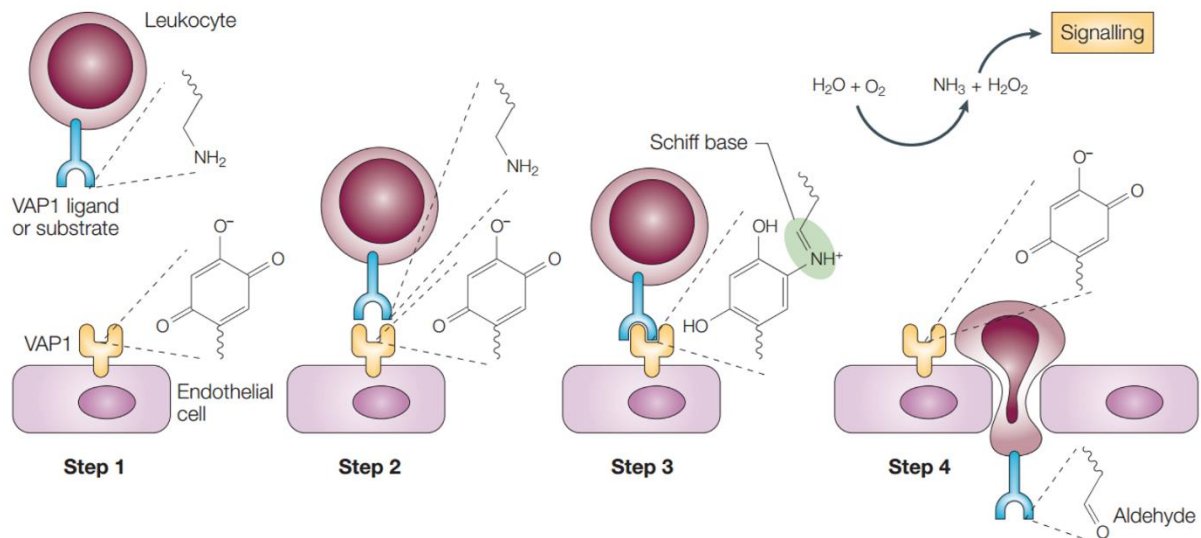


Figure I-11. A model of the action of vascular adhesion protein 1 during leukocyte–endothelial-cell interaction. A four-step model of the action of vascular adhesion protein 1 (VAP-1) in the interaction between leukocytes and endothelial cells is shown. In step 1, VAP-1 is present at the surface of the endothelial cell, and a freely flowing leukocyte expresses a VAP-1 ligand or substrate. In step 2, VAP-1 binds the leukocyte through a cell-surface epitope, the function of which can be inhibited by specific antibody. In step 3, this interaction guides the leukocyte substrate into the catalytic centre of VAP-1, and in the presence of water (H₂O) and oxygen (O₂), a Schiff base is formed. In step 4, the catalytic reaction leads to an aldehyde modification of the leukocyte substrate and to the release of hydrogen peroxide (H₂O₂) and ammonia (NH₃), which can trigger various signalling pathways in both cell types. The molecular interactions between a lymphocyte cell-surface amine (NH₂) and the TOPA-quinone in VAP-1 are highlighted (from Salmi et al., 2012).

Many reports exist about the enzymatic and non-enzymatic roles of VAP-1 in leukocyte migration. This aspect was mainly studied using the monoclonal anti-VAP1 antibody which does not inhibit its enzymatic activity but impaired lymphocyte binding (Yoong et al., 1998; Salmi et al., 2001; Lalor et al., 2002; Bonder et al., 2005). VAP-1 enzymatic activity is mostly involved in leukocyte-endothelial cell contacts. When enzymatic activity of VAP-1 was inhibited, impaired rolling, firm adhesion and transendothelial migration of leukocytes were observed (Salmi et al., 2001; Lalor et al., 2002; Koskinen et al., 2004).

Tohka et al., (2001), have shown the role of VAP-1 in the accumulation of granulocytes in inflamed tissues by mediating continuous slow rolling and cell adhesion. An anti-VAP1 antibody treatment has induced an impaired granulocyte-dependent inflammatory response *in vivo*, in mice. Moreover, blocking of VAP-1 increases the velocity of rolling granulocytes and decreases the number of firmly adherent cells to the vascular wall.

Mice models were used to study the role of VAP-1 in leukocytes trafficking and homing. Mice overexpressing VAP-1 on the EC surface show an increase of lymphocyte binding to this cells (Stolen et al., 2004b). While VAP1-deficient mice did not shown any changes under normal conditions, but in inflamed tissues cell migration was damaged. Lack of VAP-1 caused lymphocytes and granulocytes to roll faster. Moreover, not a large number of cells were firmly adherent nor underwent transmigration (Koskinen et al., 2007; Stolen et al., 2005).

In 2005, Merinen at al., reported that migration of the different subsets of leukocytes to the site of inflammation could be decreased by targeting VAP-1 in acute and chronic conditions.

1.5.4. Chondrocytes

Lyles and Bertie in 1986 have reported the enzymatic activity of SSAO in rat cartilage, nevertheless they did not explore its role in this tissue.

In our research, we have shown that SSAO mRNA expression as well as its activity increases in a cell differentiation-depended manner. (*Please see the chapter “results, chondrocytes differentiation”*).

1.6. Expression and activity of SSAO in pathological conditions

As described above, the membrane form of SSAO/VAP-1 is expressed in many different tissues. Moreover, under normal conditions, the soluble form of SSAO/VAP-1 (sSSAO) circulates in the plasma. In humans, normal activity of sSSAO is in the range of 150-550 mU/l and it remains well regulated and stable until 60 years old. Nevertheless, activity of sSSAO is increased under inflammatory conditions. Until now several diseases such as: diabetes mellitus (type 1 and type 2), congestive heart failure or liver cirrhosis were associated with significant increase of plasma SSAO activity (Boomsma et al., 2005). As described in “*Enzymatic action of SSAO, products*” increased enzymatic action of SSAO causing accumulation of aldehydes and H₂O₂ contributes to the cytotoxicity, tissue damage and disease progression.

Thus increased sSSAO could cause progression of the disease or provoke other tissue damage.

Diabetes

Diabetes is an important disease where there is an association with increased levels of soluble SSAO.

Many reports exist about increased levels of the soluble form of SSAO in serum of patients with diabetes. Plasma SSAO is significantly increased in patients with type I diabetes as well with type II. Moreover, a correlation between plasma SSAO level and age, duration of diabetes and plasma glucose was found. Nevertheless, no differences were found in plasma SSAO when patients were divided into groups depending on the absence or presence of complication (Boomsma et al., 1999). Other studies have shown that in diabetic patients with retinopathy, activity of plasma SSAO was significantly increased compared to those without this complication. The urinary concentration ratio of methylamine/creatinine was lower in patients with complications, however statistical analysis did not show a significant relation between methylamine/creatinine and SSAO (Gronvall-Nordquist et al., 2001).

Furthermore, Meszaros in 1999 confirmed that plasma SSAO was elevated in patients with non-insulin-dependent diabetes mellitus (NIDDM) and with insulin-dependent diabetes mellitus (IDDM) compared to controls. Interestingly, he reported a positive correlation between serum SSAO and BMI. Serum SSAO activity was significantly increased in obese patients with NIDDM, IDDM and NIDDM with hypertension compared to only obese patients.

These studies confirm that SSAO is elevated in diabetes. The increased SSAO activity leads to diabetes-like complications such as advanced glycation end product formation, elevated blood pressure, atherosclerosis development and nephropathy (Stolen et al., 2004b).

Atherosclerosis

Numerous studies suggest that diabetes causes vascular complications via elevated levels of plasma SSAO activity.

It was reported that SSAO activity in serum of non-insulin-dependent diabetes mellitus (NIDDM) patients without vascular complication was significantly higher compared to controls, and significantly lower compared to the NIDDM patients with macro-angiopathy (Meszaros et al., 1999).

It is known that toxic products are generated by SSAO via the reaction of oxidative deamination. The methylglyoxal (MG) formed as a result of SSAO-dependent oxidation of aminoacetone is cytotoxic, and probably through protein modification induces cell apoptosis.

Studies of Mathys et al., (2002) have shown that methylglyoxal (MG) which is formed as a result of SSAO-dependent oxidation of aminoacetone, reacts with cell proteins to form AGEs whose presence was related to increased SSAO activity. Moreover, the aortas from diabetic rats injected with aminoacetone presented greater amounts of argpyrimidine (one of the AGEs) than non-treated rats in the smooth muscle layer of aortas. Thus increased SSAO activity in plasma affects the arterial wall and its structure.

In addition, atherosclerosis development induced by an atherosclerotic diet increased by twofold in mice treated with methylamine (a SSAO substrate) compared to atherosclerosis in non-treated mice. Nevertheless, mice overexpressing SSAO in endothelial cells presented a significant decrease in the number of atherosclerotic lesions whereas the atherosclerotic area remained unchanged. These results suggested that SSAO activity modifies atherosclerotic plaque formation without an increase in lesion formation (Stolen et al., 2004b).

Taken together, increased plasma SSAO activity is responsible for arterial damage, and since the level of serum SSAO activity was shown to be associated with the severity of atherosclerosis it has been proposed that determination of sSSAO activity could be marker of atherosclerosis (Karadi et al., 2002).

Other diseases associated with SSAO

Plasma SSAO activity was proposed also to be changed in patients with congestive heart failure (CHF). In order to study this hypothesis, the SSAO activity was compared to relevant parameters of CHF. As suspected, plasma SSAO was significantly increased in patients with CHF compared to the controls. Further studies have shown that elevated plasma SSAO is associated with increased mortality in patients with chronic heart failure (Boomsma et al., 1997 and 2000). Thus studies of plasma SSAO levels may be useful in generation of medical treatments preventing vascular endothelial damage and heart failure.

Also, it is known that SSAO increases in inflamed tissues, for example during liver inflammatory disease. In plasma of patients with inflammatory liver disorders the serum form

of SSAO is significantly increased compared to healthy controls, but levels of sSSAO were unchanged in patients with rheumatoid arthritis or inflammatory bowel disease. In addition, the authors compared sSSAO levels in different liver diseases and the highest values were found in patients with primary cirrhosis and active cirrhosis due to alcoholic liver disease. In further studies authors have studied sSSAO levels in patients with acute and chronic liver disease. They have shown that serum levels of SSAO in chronic liver disease are increased but stay unchanged in acute fulminant hepatic failure caused by paracetamol-induced massive hepatic necrosis (Kurkijarvi et al., 1998 and 2000).

Another inflammatory disease tested for SSAO was arthritis. The laboratory studies showed that SSAO plays an important role in arthritis and its activity is needed for inflammation. In a rat model with induced arthritis, inhibition of SSAO by oral administration of BTT-2052 significantly reduced the clinical inflammation in a dose-dependent manner. Moreover, in a mouse model of arthritis the lack of SSAO (transgenic *SSAO*^{-/-} mice) or SSAO activity inhibition significantly reduced clinical inflammation (Marttila-Ichihara et al., 2006).

Taken together, all those reports show that SSAO is increased in many different diseases and could be implicated in disease development by its enzymatic reaction where toxic products are generated.

2. Cartilage

2.1. Physiology of cartilage

Cartilage is a flexible connective tissue composed of chondrocytes, the only cell type present in the tissue. Depending on the mechanical and structural properties, three types of cartilage can be distinguished: hyaline, elastic and fibrocartilage. These types of cartilage are different with respect to cell arrangement as well as to the extracellular matrix (ECM) composition (Fig. I-12).

Hyaline cartilage occurs in the vertebrate skeleton as articular cartilage on the ends of bone where they form joints (diarthrodial joints), costal cartilage and growth plates by which long bones grow during childhood. Moreover, hyaline cartilage is present in craniofacial structures, the trachea and bronchial tubes, the sternum, ribs and the tip of the nose. It is extremely strong, but very flexible and elastic. It is characterized by a high content of type II collagen and proteoglycans and by a hierarchical structure. In this cartilage type, chondrocytes often form clusters. The main function of hyaline cartilage is the reduction of friction at joints, the longitudinal growth of bones and support.

Fibrous cartilage (fibrocartilage) is also associated with the skeletal system. It is present in the meniscus of the knee, the *anulus fibrosus* of the intervertebral discs of the spine, the mandibular condyle in the temporomandibular joint and the symphysis pubis. It has been reported that this kind of cartilage occurs temporarily at fracture sites upon healing. Fibrocartilage is a tough form of cartilage that consists of chondrocytes, scattered among clearly visible dense bundles of collagen fibres within the matrix. The principal function of this cartilage type between the adjacent vertebrae is the absorption of shock.

Elastic cartilage is present in the ear pinna, external auditory meatus, eustachian tube and epiglottis. In elastic cartilage, the chondrocytes are located in a threadlike network of elastic fibres within the matrix of the cartilage. It helps to maintain the shape and flexibility of the organ (Sugiki et al., 2007; Mizuno et al., 2014).

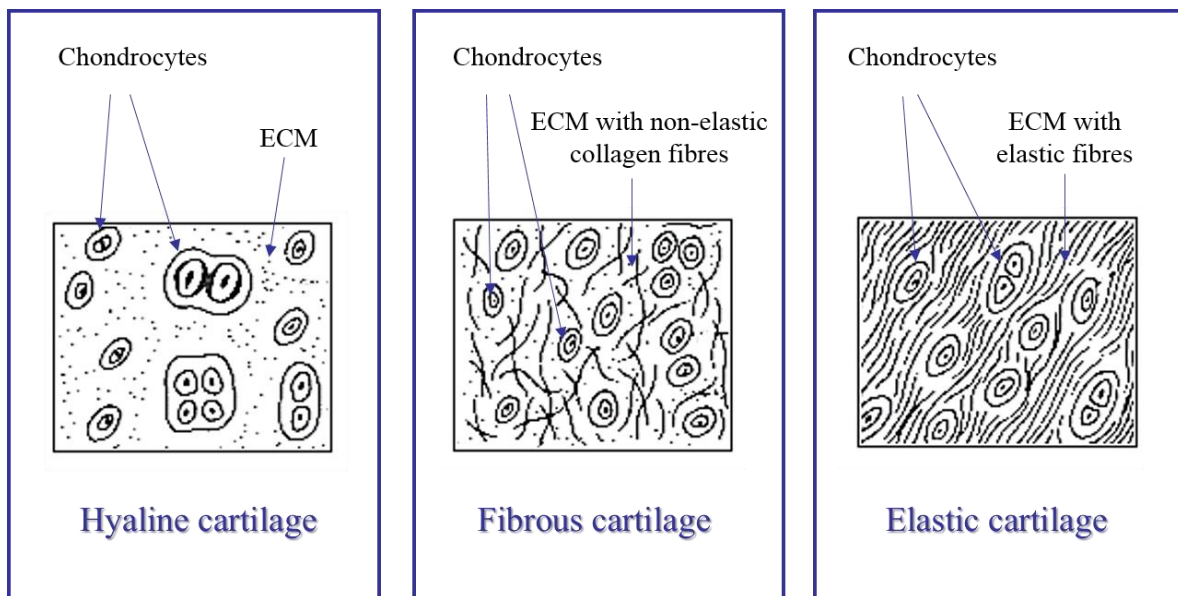


Figure I-12. The three types of cartilage. Schematic cartilage types were adapted from the University of the Western Cape, Department of Biodiversity & Conservation Biology website.

2.2. Articular cartilage function

Bones are characterized by rigidity and strength. Nevertheless, its painless movements are possible owing to a thin layer of articular cartilage. The first principal function of cartilage is the protection of the two opposing bones, ensuring a smooth surface which provides low friction between the two bones. In this aspect, this connective tissue with viscoelastic properties has a unique capacity to resist high loads without structure damage.

During movement, cartilage and the interstitial fluid show a large compression. Then the liquid phase flows out the ECM to the synovial space. When the pressure on the cartilage dissipates, the fluid in the synovial cavity is slowly drawn back into the extracellular matrix framework (Paulsen et al., 1999; Pearle et al., 2005; Quinn et al., 2013; Hunziker et al., 2014).

2.3. Structure of the hyaline cartilage

Articular cartilage is avascular, without nerves and lymphatic vessels. It consists of 2 phases: a fluid phase made up of up to 70% of water, and a solid phase composed of 20% type II collagen, 6% proteoglycans and 4% other organic molecules (Carter et al., 2003). The fluid phase comprises mainly water with inorganic ions such as chloride, potassium, sodium and calcium.

The solid phase comprises mainly proteoglycan aggregates, collagens, and in smaller quantities noncollagenous proteins and glycoproteins. The components of the solid phase retain the water and provide the unique mechanical properties through negative electrostatic repulsion forces. The only types of cells resident the cartilage network are chondrocytes and they constitute less than 2% of the total cartilage volume. Depending on the chondrocyte phenotype and the ECM components, several zones of cartilage can be determined from the surface to the bone: the superficial zone, the middle transitional zone, the middle deep zone and the calcified cartilage zone (Fig. I-13) (Wong et al., 2003). These zones are characterized by various collagen organizations and different amounts of proteoglycans. The thin superficial (tangential) zone, which makes up 10-20% of articular cartilage, is characterized by a high number of flattened chondrocytes and the highest collagen content (Palfrey et al., 1966). Collagen type II and type IX fibres are packed tightly and aligned parallel to the articular surface. This structure gives the resistance for shear stress, tensile stiffness, strength and resistance for compressive forces imposed by articulation (Buckwalter et al., 2005). This zone stays in direct contact with the synovial fluid. Under the superficial (tangential) zone, is the middle (transitional) zone which takes place and represents 40% to 60% of the total articular cartilage volume. Proteoglycans and collagens are the main constituents of this zone. The collagen fibres are arranged obliquely. Chondrocytes, in contrast to those of the layer above, are more dispersed with a rounder shape. This zone is characterized by its resistance to compressive forces of the deep zone where the collagen fibrils are arranged perpendicular to the articular surface. This zone makes about 30% of the total cartilage volume. It contains less water and more proteoglycans compared to the middle zone. The proteoglycans increase resistance to compressive forces of this zone. The cells form typical columns which are oriented in parallel to the collagen fibres and perpendicular to the joint line. The calcified cartilage makes a link between the deep cartilage zone and the bone. The transition line (tidemark) is well visible. This zone plays a role in anchoring the cartilage into the bone by fibres of collagen from the deep zone (Paulsen et al., 1999; Pearle et al., 2005; Palfrey et al., 1966; Wong et al., 2003; Carter et al., 2003).

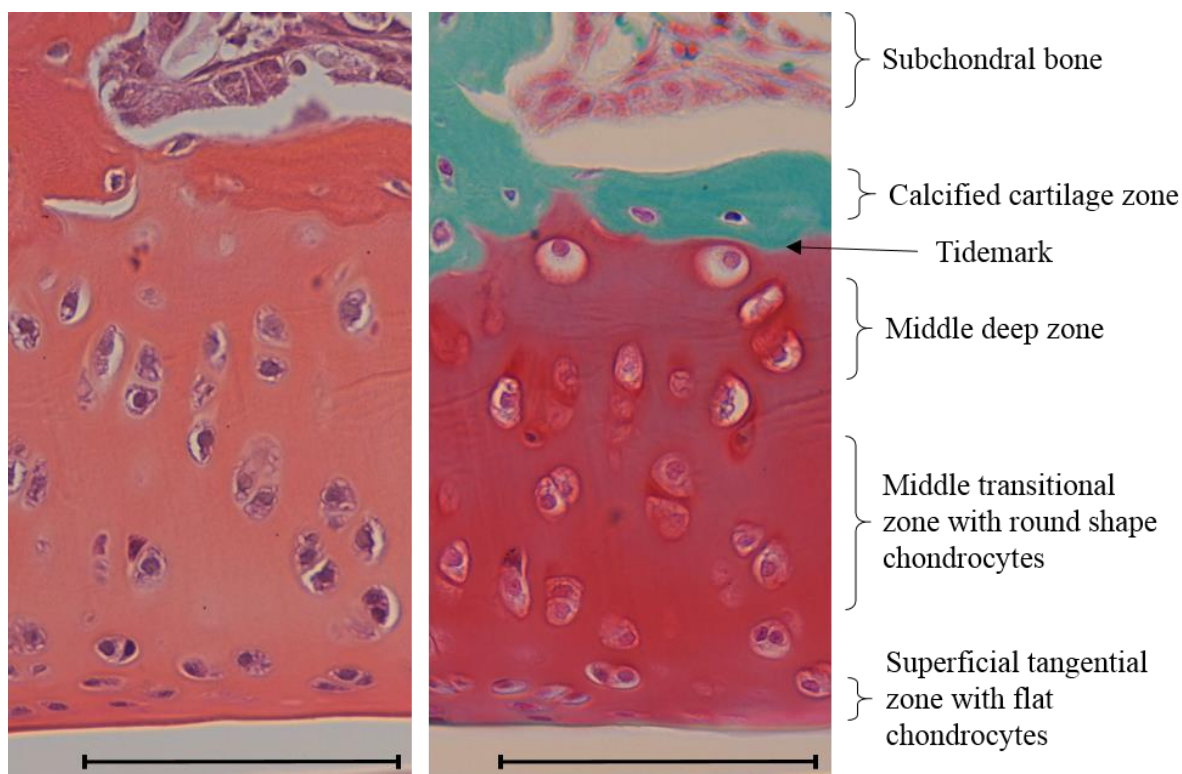


Figure I-13. Articular cartilage morphology. Histologic examination of the cross sections of Wistar rat articular cartilage stained with HES (morphology), Safranin O (proteoglycan content), respectively. The micrographs were taken using DMD 108 Leica microscope with original magnification 40x. The scale on the micrographs represents 100 μ m (authors: A. Filip, A. Pinzano, personal communication).

2.3.1. Chondrocytes

The chondrocytes come from mesodermal origin mesenchymal stem cells. These cells are highly specialized and metabolically active. The size, shape, number and metabolic activity of chondrocytes are different depending on the zone where the cells are located. The chondrocytes from the superficial zone are characterized by a specific flat shape, smaller size and higher density compared to the chondrocytes in deeper cartilage zone (Palfrey et al., 1966). Synthesis of ECM is the principal role of chondrocytes, and components of the ECM are different depending on the zone considered. Chondrocytes rarely enter in cell-to-cell contact for communication between them, nevertheless they are able to receive and react to stimuli such as growth factors, cytokines, mechanical loads and hydrostatic pressures (Fig. I-14).

Beside the synthesis of ECM, chondrocytes are limited in proliferation. This has great influence for self-healing. Their survival depends on an optimal chemical and mechanical environment.

Articular cartilage is avascular. Chondrocytes are nourished by synovial fluid diffusion through the matrix by mechanical forces (Ruhlen et al., 2014).

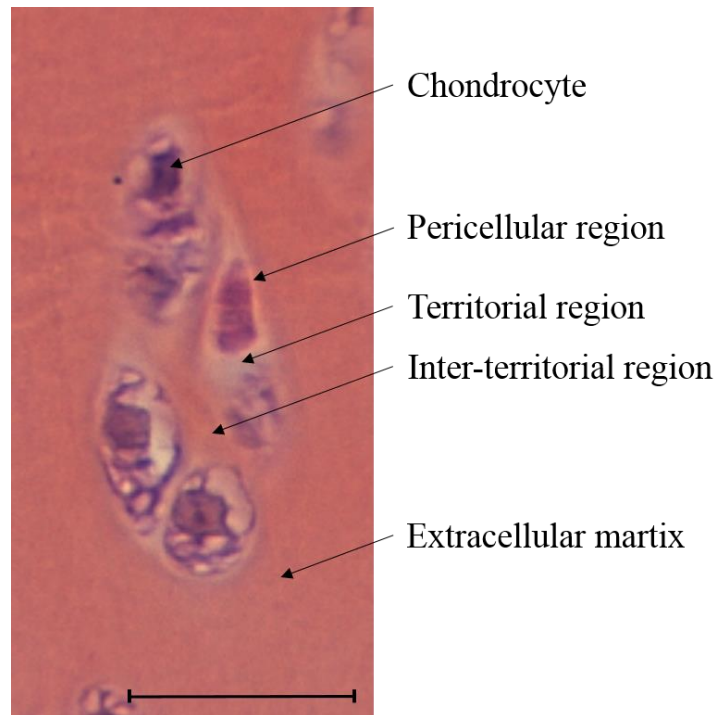


Figure I-14. Chondrocyte morphology. Histologic examination of a cross section of Wistar rat articular cartilage stained with HES. The micrographs were taken using DMD 108 Leica microscope with original magnification 40x, the scale on the micrographs represents 25 μ m (authors: A. Filip, A. Pinzano, personal communication).

2.3.2. Extracellular matrix (ECM) components

Cartilage is particularly rich in extracellular matrix (Fig. I-15). Approximately 20% of cartilage weight consists of extracellular matrix which contains proteoglycans, collagens and, in less quantity, noncollagenous proteins, glycoproteins, lipids and phospholipids, the amounts of each varies between zones (Table I-1). Integrity of the cartilage network is indispensable for the function of this tissue.

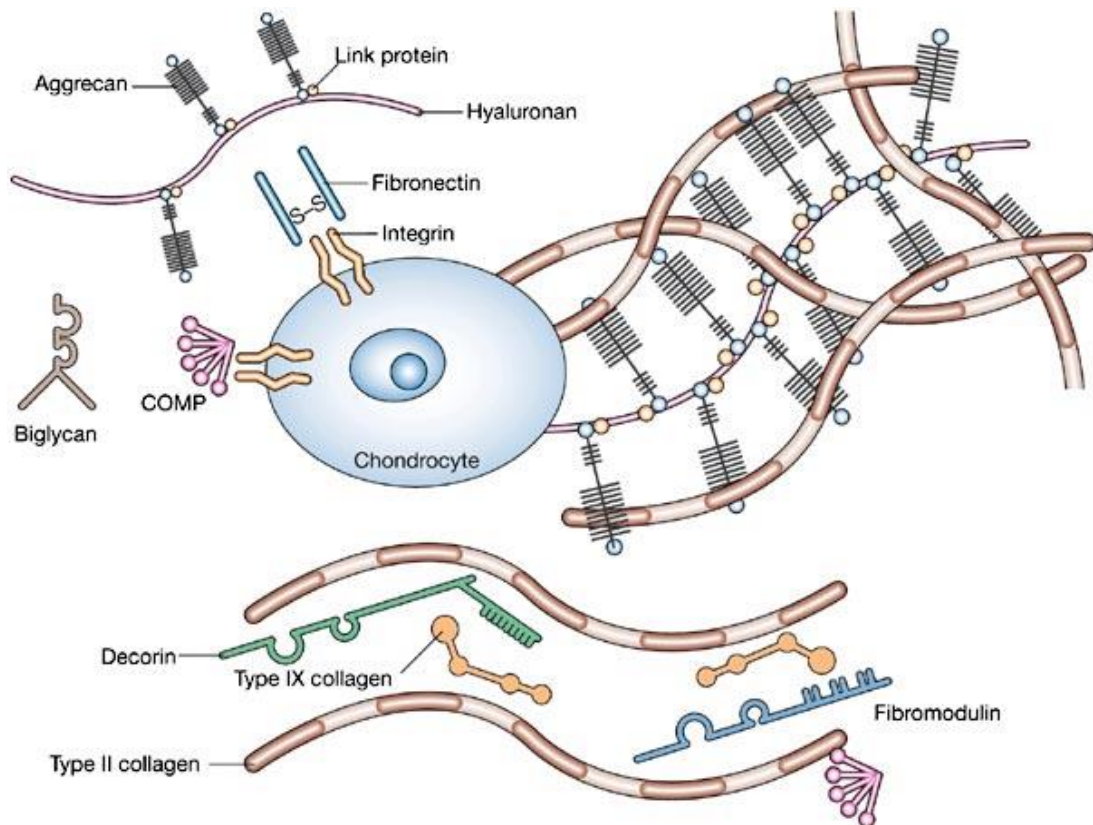


Figure I-15. The network of extracellular matrix (ECM) components in cartilage (from Chen et al., 2006).

Table I-1. Collagen and proteoglycan distributions in extracellular matrix of cartilage (Paulsen et al., 1999). The regions for each zone are indicated in figure I-14.

Articular cartilage		Collagens					Proteoglycans			
		I	II	II	VI	IX	XI	C4S	C6S	KS
Articular surface		-	++	++	-	++	-	+	+	+
Upper zone	pericellular	-	+++	++	++	+	-	++	++	++
	territorial	-	++	+	+	++	+	++	++	+
	interterritorial	-	++	+	-	++	-	+	+	++
Middle zone	pericellular	-	+++	++	++	+	-	++	++	++
	territorial	-	++	+	+	++	+	++	++	+
	interterritorial	-	++	+	-	++	-	+	+	+
Deep zone	pericellular	-	+++	+	++	+	-	++	++	++
	territorial	-	++	-	+	++	+	++	++	+
	interterritorial	-	++	-	-	++	-	+	+	++

2.3.2.1. Collagens

Collagens are the extracellular matrix components which contribute to the tensile behaviour of cartilage. Collagen fibre orientation depends on cartilage zone (Fig. I-16). In articular cartilage, the main collagen is type II. Collagen type II represents approximately 90% of the collagens in articular cartilage. This concentration differs according to the tissue. As an example, in meniscus collagen type I is predominant.

The other collagen types present in cartilage are III, VI, IX and XI and they contribute only for a minor proportion and their role is limited to helping to form and stabilize the type II collagen fibril network.

The collagen structure comprises a region consisting of 3 polypeptide chains (α -chains) which form a triple helix stabilizing the matrix. The polypeptide chains are constituted mainly with glycine and proline residues. The hydroxyprolines ensure the stability *via* hydrogen bonds along the length of the molecule (Paulsen et al., 1999; Pearle et al., 2005; Bruckner et al., 1989).

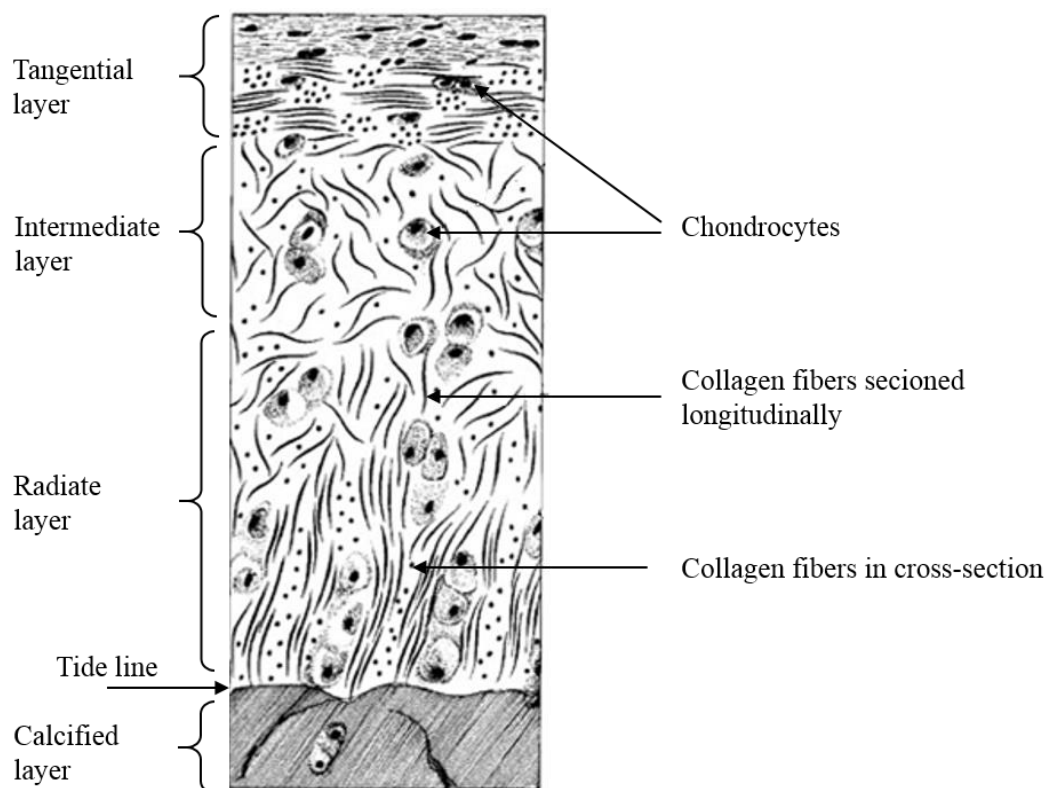


Figure I-16. Diagram of adult articular cartilage showing four layers and arrangement of chondrocytes and collagenous fibers (from Anatomy and Physiology of Equine Joints of Wayne McIlwraith).

2.3.2.2. Proteoglycans

The hyaline cartilage is characterized by a high content of proteoglycans which represent approximately 15% of the wet weight of the tissue. Proteoglycans are large molecules comprising a protein core and serine residues plus several glycosaminoglycans. Glycosaminoglycans are linked by covalent binding to the protein core. Specifically chondroitin sulfate and keratin sulfates as are found in aggrecans. These sulphate groups insure the negative charge of the macromolecule. These large substances create a network by interactions with hyaluronan (HA) as well as with collagens. Altogether they are responsible for the turgid nature of cartilage with osmotic properties. Compaction of the proteoglycans influences the swelling pressure and liquid phase movements during compressions.

In cartilage, aggrecan is the most abundant proteoglycan. It contains three globular domains and it forms proteoglycan aggregates composed of a central filament of HA with up to 100 molecules of aggrecan which interacts with the link protein part of aggrecan (Fig. I-17) (Morgelin et al., 1988). Other less abundant and smaller proteoglycans like versican, decorin, biglycan and fibromodulin are also present in cartilage (Pearle et al., 2005; S. Shibata et al., 2003; Kamiya et al., 2006; Roughley, 2006).

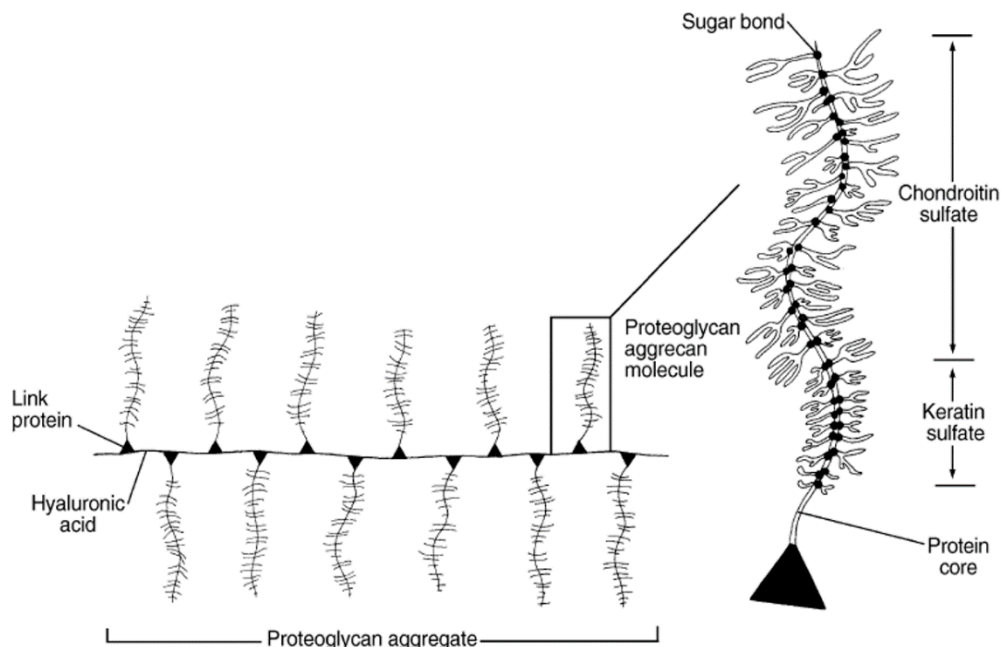


Figure I-17. Model of proteoglycan aggregate and aggrecan molecule. Aggrecan in ECM exists as proteoglycan aggregates which are composed of a central filament of hyaluronic acid with up to a hundred aggrecan molecules radiating from it. Each interaction is stabilized by the presence of a link protein that is accessible to most proteinases (from Pearle et al., 2005).

2.4. Cartilage formation

Mesenchymal “stem” cells which are specified as osteo-chondro-progenitors in the process of differentiation, give rise to osteocytes and chondrocytes (Lee et al., 2004). Chondrocytes are the one resident cell type in cartilage.

2.4.1. Long bone development

During embryogenesis most bones are formed and two types of bone development can be considered. Intramembranous ossification generates the flat bones such as those of the skull and clavicles. It involves the direct development of osteoblasts from mesenchymal tissue without an intervening cartilage model. By endochondral ossification, all long bones are formed (Fig. I-18). This synthesis is initiated during foetal life and continues until final bone formation. Bone formation starts by the creation of the cartilage model of the future bone and subsequently the primary centre of ossification is formed. In length, bones grow by proliferation, maturation, calcification and ossification of the cartilage network. The bone girth is increased by the apposition of new bone on the surface of the shaft.

The centre of ossification expands lengthwise from the cartilage framework and a secondary centre of ossification is formed at the ends of the bone. Two centres of ossification are separated by a cartilaginous growth plate which disappears and is replaced by bone in the final stage of bone creation. In mature bone, the cartilage covers the ends of the bone and this articular cartilage remains the only form present in bone (Young, 1962; Wong et al., 2003; Otto et al., 1997; Erlebecher et al., 1995; Kronenberg, 2003).

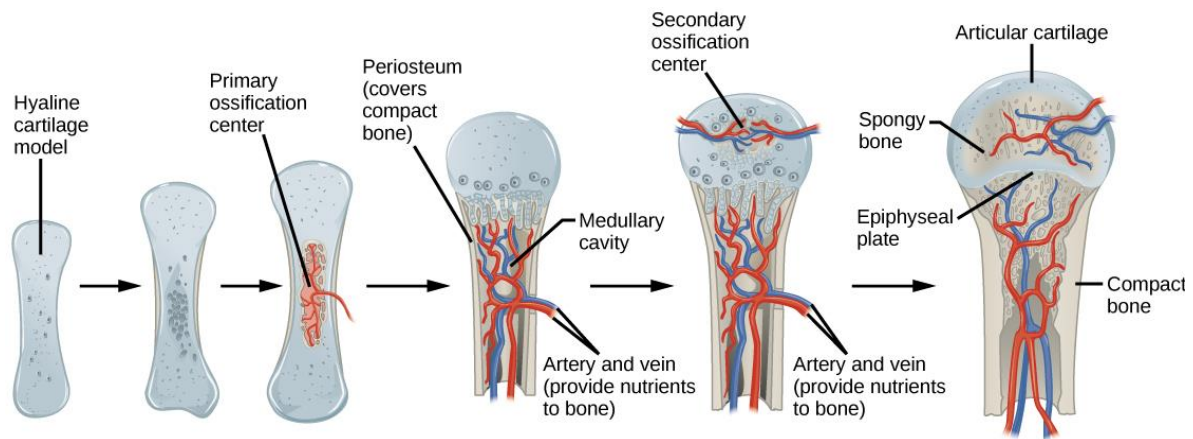


Figure I-18. Overview of a bone formation by endochondral ossification (from the Rice University, Bone Formation and Development website).

Chondrocytes are the only cell type which forms in the growth plate (Fig. I-19). The chondrocytes arise in the embryo from the prechondrocytic mesenchymal cells and subsequently undergo migration to presumptive skeletogenic sites from the cranial neural crest, paraxial mesoderm, and lateral plate mesoderm and formation of cell mass *condensations* (Mau et al., 2007; DeLise et al., 2000). Then cells undergo chondrogenesis and newly arising chondrocytes enter differentiation. Their morphology and arrangement depend on the stage of the cell's lifespan which can be divided into proliferation, maturation, hypertrophy, and ossification steps (Zwilling, 1972; Wallis et al., 1996; de Crombrughe et al., 2000; Roach et al., 2000).

First, chondrocytes undergo proliferation and form columns of flattened cells, moreover they are stimulated by matrix synthesis containing strictly defined components (Fukumoto et al., 2003). In the next step, proliferation is stopped. Cell size increases but all chondrocytes remain in multicellular clusters, in columns parallel to the long axis of the bone. Chondrocytes enter a period of high secretory activity, they deposit around themselves ECM components.

In the hypertrophic zone chondrocytes are bigger with round shape and are characterized by secretion of molecules degrading ECM components. Following the hypertrophic zone, calcification is initiated (Kirsch et al., 1997) and chondrocytes undergo programmed cell death (Bronckers et al., 1996; Horton et al., 1998; Roach et al., 2000). The ECM surrounding the chondrocytes is removed and then cells responsible for the expansion of the ossification enter (Sugiki et al., 2007).

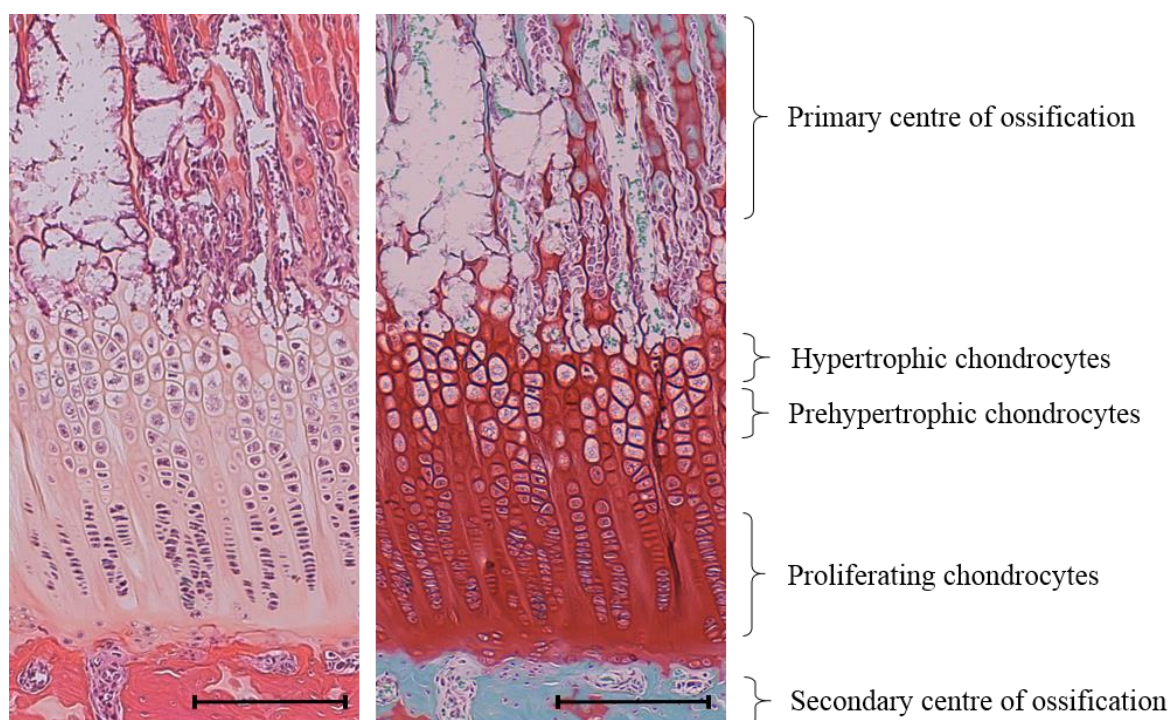


Figure I-19. Growth plate morphology. Histologic examination of the cross sections of Wistar rat growth plate stained with HES (morphology), Safranin O (proteoglycan content) respectively. The micrographs were taken using DMD 108 Leica microscope with original magnification 10x, the scale on the micrographs represents 200 μ m (authors: A. Filip, A. Pinzano, personal communication).

2.4.2. Markers of chondrocyte differentiation

Every stage of chondrocyte maturation and terminal differentiation, as well chondrogenesis are characterized by expression of specific markers (Fig. I-20).

Condensation

The mesenchymal cells undergo condensation which is regulated by cell–cell and cell–matrix interactions. Collagens type I, III and V are the main fibrillar components of undifferentiated mesenchymal progenitor cells (Mau et al., 2007, DeLise et al., 2000). Expression of cell adhesion molecules, neural cadherin (N-cadherin), neural cell adhesion molecule (N-CAM) and FGF- β are responsible for the initiation of interaction between cells and the surrounding matrix. Studies have shown that several fibroblast growth factor families play important roles in limb initiation, development but also mediate outgrowth (Martin et al., 1998; Tickle et al., 2001; Burdan et al., 2009). In the FGF-8 conditional knockout mouse, skeletal defects were found and FGF-10 null mice presented important reductions or disappearance of limbs. Moreover, the

various mutations in receptors like *Fgfr3*, 1 or 2 led to skeletal dysplasia. (Tickle et al., 2002). In 2001, Kawakami et al., have shown that FGF-dependent limb initiation was controlled by Wnt signals. The three forms of *Wnt* genes through β -catenin act as key regulators of the FGF-8/FGF-10 loop that directs limb initiation. The *Wnt-2b* and *Wnt-8c* genes activate FGF-10, and *Wnt-3a* gene mediates the induction of FGF-8 in the limb ectoderm by FGF-10.

The bone morphogenetic protein (BMP) growth factor initiates chondroprogenitor cell determination and differentiation and is important for precartilaginous condensation (Sugiki et al., 2007). Moreover, it favours proliferation and prevents late hypertrophic differentiation (Shea et al., 2003; Zou et al., 1997). BMP in a later stage of differentiation plays a role in chondrocyte maturation and in hypertrophy (Pizette et al., 2000; Niswander, 2002).

Cells, by products of the extracellular matrix rich in hyaluronan, type I and II collagens, fibronectin, cartilage oligomeric protein (COMP), tenascin and syndecan, increase cell–matrix interactions (Ma et al., 2003; DeLise et al., 2000; Sandell et al., 1994a). Besides, FGF- β , expression of the transcription factor Sox9 is necessary for mesenchymal condensation followed by chondrogenesis (see in “Transcriptional factors of chondrogenesis-Sox9”) (de Crombrughe et al., 2000 and 2001; Lefebvre et al., 2001; Zhao et al., 1997).

When cells are differentiated into chondrocytes, expression of collagens type I, III and V is strongly decreased in favour of the expression of the aggrecan and collagen type II and in less quantity collagens type IX and XI (Sandell et al., 1994a and 1994b). Cells are small with an uniform shape. They avoid proliferating and cell-cell interaction. Large spaces in this zone correspond to the extracellular matrix (DeLise et al., 2000; von der Mark et al., 1976).

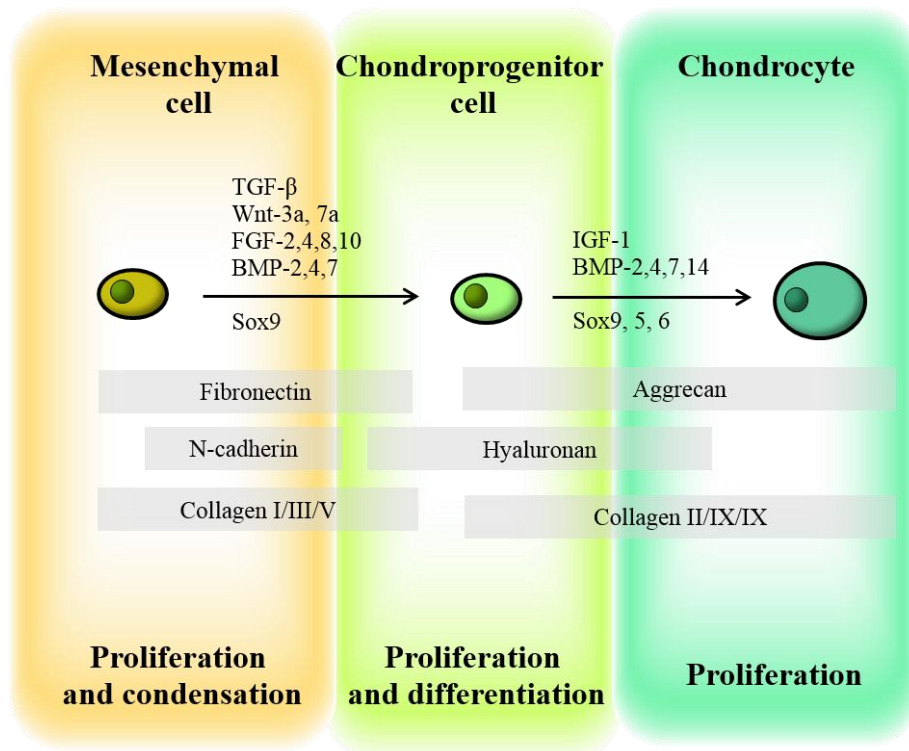


Figure I-20. Model of chondrogenesis during the development of long bones with main markers of each stage (adapted from Goldring et al., 2006).

Proliferation

Cell condensation is followed by chondrocyte proliferation induced by secretion of Sox9 and two other transcription factors of this family, namely Sox5 and Sox6 (Akiyama et al., 2002). Expression of Sox9 induces type II collagen expression, the main marker of proliferating chondrocytes. The Sox9 transcript is abundantly present until chondrocytes mature and enter prehypertrophy (Zhao et al., 1997; Seki et al., 2003; Lefebvre et al., 1997). The early proliferative stage is characterized by collagen VI and matrilin 1 expression which is not detected during hypertrophic differentiation. In this step cells divide several times and form longitudinal columns. Their shape is changed, they are flat and enter into cell-cell interactions.

Maturation and hypertrophy

Mature chondrocytes are characterized by a high expression of type II collagen and aggrecan, the two main components of extracellular matrix. It was reported that Runx2 is required for chondrocytes maturation and then it stimulates the chondrocyte terminal differentiation (Enomoto et al., 2004). Its expression, as well as Indian Hedgehog expression, is not well

detectable in the proliferation zone, nevertheless it increases in pre- and hypertrophic chondrocytes (Ushijima et al., 2014). Expression of type II collagen and aggrecan is decreased in pre-hypertrophic chondrocytes. Meanwhile, the expression of prehypertrophic markers such as collagen X (Bruckner et al., 1989) and hypertrophic markers like matrix metalloproteinase expression, mainly MMP13 which causes degradation of collagen-proteoglycan framework, increase. Following hypertrophy, chondrocytes enter terminal hypertrophy. The expression of alkaline phosphatase (role in mineralization) and osteopontin (role in cell-matrix interaction during endochondral ossification) increase (Fig. I-21) (Kirsch et al., 1997; Dreier et al., 2008).

Vitamin A accelerates hypertrophic differentiation and further matrix mineralization (Dreier, 2010).

The presence of vascular growth factor (VEGF) indicates angiogenesis required for the replacement of cartilage by bone.

The terminal chondrocytes differentiation is controlled by regulating factors as growth factors and thyroid hormone, estrogen, androgen, vitamin D and glucocorticoids.

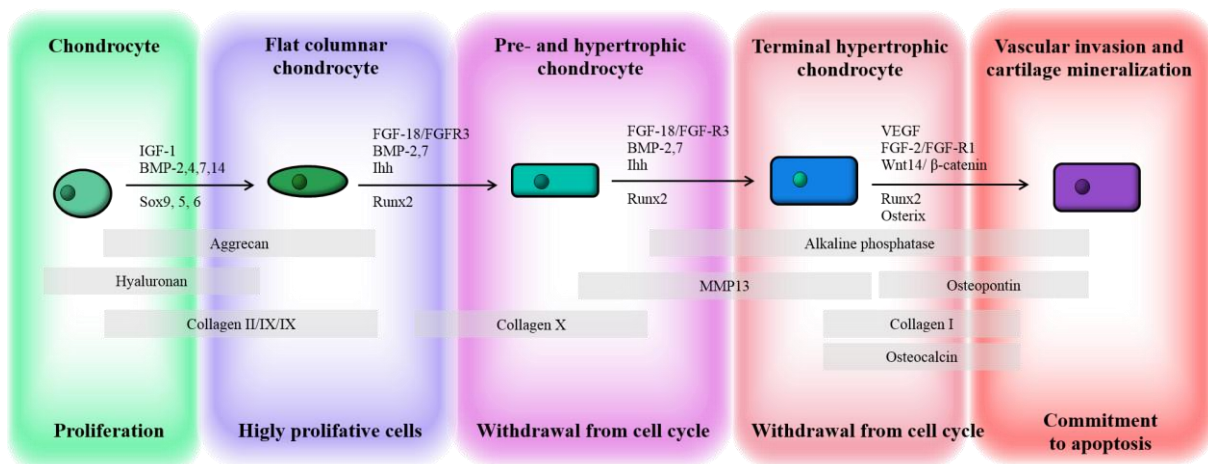


Figure I-21. Model of chondrocytes differentiation in growth plate during the development of long bones with main markers of each stage (adapted from Goldring et al., 2006).

Apoptosis

After invasion of blood vessels from subchondral bone the hypertrophic chondrocytes undergo apoptosis, programmed cell death. Then the mineralized template is remodelled into bone.

2.4.3. Transcriptional factors of chondrogenesis

2.4.3.1. Sox9

Sox9 is a member of the SOX transcription factor family and like other family members, Sox9 plays a crucial role during development. There are many reports about the role of Sox9 during embryogenesis in many tissues. In cartilage, this protein is essential for the first stage of tissue formation (Pritchett et al., 2011). During chondrogenesis, *Sox9* is expressed in chondroprogenitors and differentiated chondrocytes, but its expression rapidly shuts down in chondrocytes undergoing hypertrophic differentiation (Ng et al., 1997; Zhao et al., 1997). Sox9 binds to target sites in promoters of cartilage-specific genes like *Col2a1* (Lefebvre et al., 1997).

Other studies elucidated that mouse embryo chimeras derived from *Sox9*^{-/-} embryonic stem (ES) cells did not express chondrocyte-specific markers. Chondrogenic differentiation of *Sox9*^{-/-} ES cells is disrupted, Sox9-deficient cells do not reach maturation characterised by round-shape cells and a high expression of collagen II (Hargus et al., 2008).

More recent studies have shown that Sox9 was required for maintaining column proliferation. It delays cell hypertrophy and prevents *Runx2* expression (Dy, 2012).

2.4.3.2. Runx2

Runx2 (runt-related transcription factor 2) also called Cbfa1 (core binding factor alpha-1), a member of runt-domain gene family, is an essential transcription factor for osteoblast differentiation. In cartilage, Runx2 positively regulates chondrocytes maturation to the hypertrophic phenotype and it is expressed by immature and prehypertrophic chondrocytes (Yoshida et al., 2004). Moreover, Runx2 plays an important role in the process of endochondral ossification. Komori et al and Otto et al., in 1997 reported that *Runx2*^{-/-} mice died soon after birth and exhibited a lack of bone formation due to the absence of osteoblast differentiation. Further studies have shown that *Runx2*^{-/-} chondrocytes show the adipocyte phenotype over time in culture. Mature chondrocytes in normal conditions do not undergo the transdifferentiation into adipocytes which indicates a role of Runx2 in chondrocyte maturation (Enomoto et al., 2004).

2.5. Diseases of joints and cartilage degradation

As described above chondrogenesis and terminal chondrocytes differentiation in physiological conditions is related to bone development and cartilage formation. In adults, the process is resumed at the site of stress-related injuries like fractures of bone or articular cartilage. Endochondral bone fracture, through new cartilage formation and its replacement by bone, is repaired. However, the cartilage damage and initiation of the terminal differentiation of resident chondrocytes leads to the loss of functional cartilage and development of cartilage degradation such as in osteoarthritis (Zuscik et al., 2008).

2.5.1. Osteoarthritis (OA)

Osteoarthritis is a degenerative joint disease which is characterized by the degradation of cartilage at the ends of the long bones. This is a noninflammatory chronic disease, nevertheless the inflammation status which frequently appears during injury, increases during the development of OA.

As a result, the bones lose their protection against friction. The cartilage become stiff and the bones begin to rub against each other. This causes pain and difficulties in movement (Fig. I-22). With time, joint replacements should be necessary. Other clinical manifestations of this pathology are sensitivity, stiffness, crunching, joint locking and sometimes local inflammation. OA increases with age but it is not age-dependent. Body weight, sex and biomechanical instability are included in the multitude of factors exacerbating this disease. The most common features of OA are cartilage oedema, cartilage surface deformation and its degradation, chondrocyte proliferation and proteoglycan content reduction, fibrillation, subchondral bone thickening, osteophyte formation, synovial intimal cell hyperplasia and synovial fibrosis (Rieppo et al., 2003).

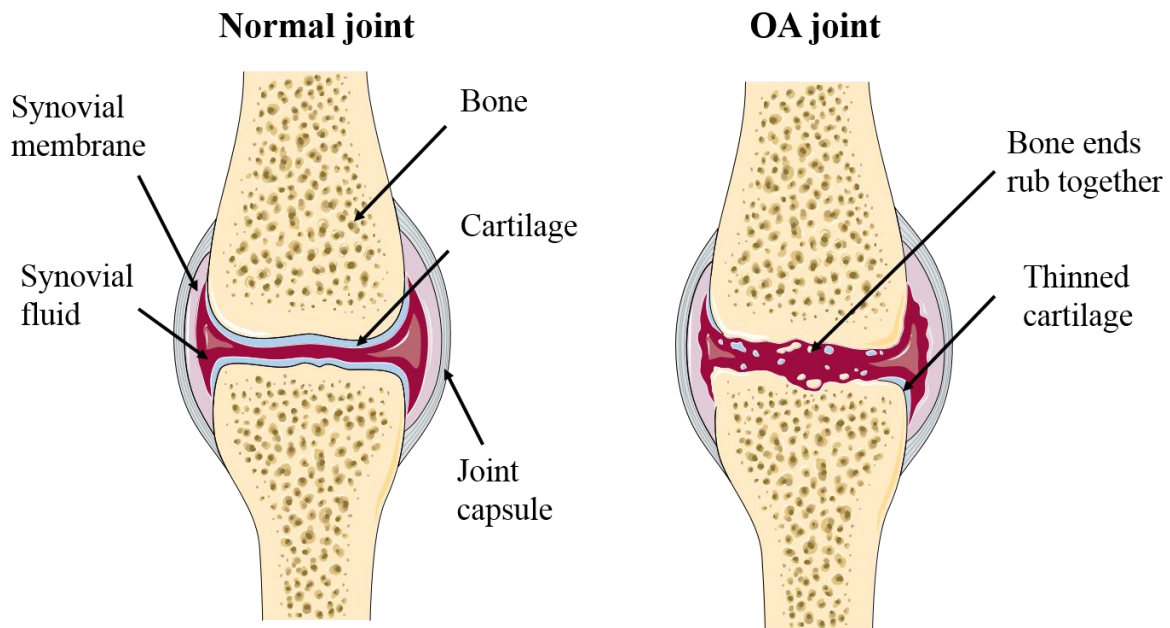


Figure I-22. Schematic normal and OA joint (from Powerpoint image bank, Servier website).

2.5.2. Molecular mechanisms of OA

In healthy articular cartilage, chondrocytes are characterized by a stable phenotype and low proliferation. They avoid terminal differentiation. The balance between biosynthesis and degradation of extracellular matrix components is tightly controlled. In OA the balance in ECM-cell interaction is disturbed with an increase in the degradation process. The pivotal event at the origin of OA is the activation of chondrocytes to a proliferation phase (Crelin et al., 1960). It is induced by a modification of extracellular matrix components. As it was shown, changes in the environment of chondrocytes have an impact on cell phenotype. Decreases of proteoglycan content and destabilization of the collagen framework leads to chondrocyte proliferation.

On a molecular level, the first stage of the disease is characterized by releasing the catabolic pro-inflammatory cytokines by the synovium. This stimulates the chondrocytes to increase the production of ECM components in order to heal injured tissue (Aigner et al., 1997; Martel-Pelletier et al., 1999). Nevertheless, the prolonged presence of those cytokines (IL-1, TNF α , IL-17, and IL-18 as well as PGE $_2$) causes an increase in collagenases (MMP1, MMP8, MMP9, and MMP13) and aggrecanases (ADAMTS4 and ADAMTS5), which leads to ECM component

degradation (Goldring, 2000a and 2000b; Smith et al., 2006; Bertrand et al., 2010; Sherwood et al., 2014).

As a result, chondrocytes enter terminal differentiation. Remodelling of cartilage matrix by proteases, vascularization and focal calcification of articular cartilage with calcium hydroxyapatite crystal formation takes place. This process is similar to chondrocyte hypertrophic differentiation during endochondral ossification (growth plate). Moreover, the signalling molecules implicated in growth plate chondrocyte differentiation may be involved in OA development (Fuerst et al., 2009a and 2009b).

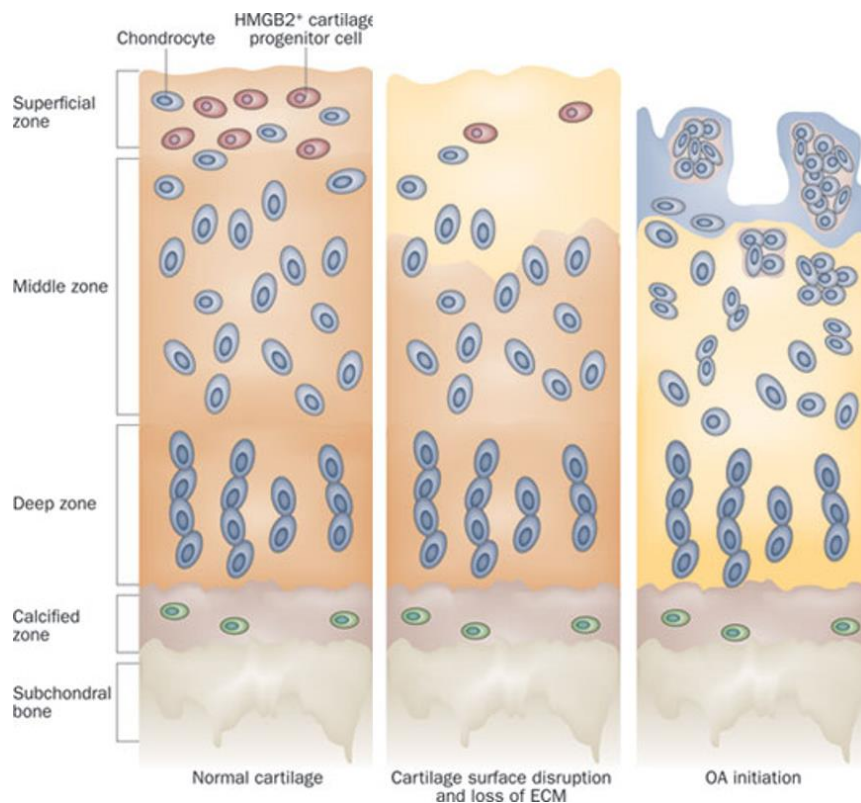


Figure I-23. Schematic model of osteoarthritis development (adapted from Lotz and Carames, 2011).

In the literature, many studies about OA development report a change of chondrocyte phenotype. The first feature is chondrocyte hypertrophy, after mineralization and subsequently the break down of cartilage.

The activated chondrocytes following proliferation and maturation enter hypertrophy which is followed by mineralization. This process indicates that chondrocyte hypertrophic differentiation in the growth plate and during osteoarthritis development are partially characterized by the same features (Fig. I-23). On the other hand, only few publications have shown that during OA, chondrocytes decrease expression of Sox9 and aggrecan but do not increase the main marker of pre-hypertrophic chondrocytes such as collagen X.

2.5.3. Animal models of cartilage diseases

In order to study cartilage degradation during osteoarthritis development, several animal models of this disease have been established and are well characterized (Gregory et al., 2012; Little et al., 2012).

Animal models of OA are a powerful tool to study the implication of selected compounds (SSAO for example) in cartilage degradation and could be useful to characterize new targets for disease treatment as well as evaluation of potential antiarthritic drugs for clinical use.

Animal models of OA can be divided into two groups. The first group concerns animals which develop osteoarthritis in the knee joint (guinea pigs, transgenic models) and the second contains animals where cartilage degradation is induced.

OA can be caused by surgically-induced instability of joints as well by elicitation of cartilage degradation through intra-articular iodoacetate, papain or collagenase injections. Iodoacetate affects cell metabolism, papain induces degradation of proteoglycans abundantly present in cartilage ECM, and collagenase affects joint structures like tendons and ligaments but also collagen present in the ECM of cartilage. Administration of oral or parenteral quinolone antibiotics has the capacity to cause articular cartilage degeneration in the mid-zone in growing animals (Bendele et al., 2001).

All animal models of OA have advantages and limitations. The suitable model of OA needs to be adapted to the experiment requirements. The principal differences between the models are time and degree of cartilage degradation. Nevertheless, the homogeneity of cartilage damage and proximity to the human OA are variable depending on the OA experimental model.

The monosodium iodoacetate (MIA) animal model of cartilage degradation is well established and widely used in a number of different species such as guinea pigs (Williams et al., 1985),

horses (Penraat et al., 2000), mice (Van Der Kraan et al., 1989) and rats (Bove et al., 2003). Iodoacetate is a metabolic inhibitor of glyceraldehyde-3-phosphatedehydrogenase activity in chondrocytes resulting in disruption of glycolysis and eventual cell death. MIA treatment induces increased reactive oxygen species (ROS) production and mitochondria-mediated caspase-3 activation. Depending on the dose and injection frequency, as well as time of exposition to MIA, the degree of cell and cartilage degradation can be modulated (Van Der Kraan et al., 1989; Jiang et al., 2012).

3. Vascular Part

3.1. General structure and function of blood vessels

The vascular system of the human body is the network of blood vessels that begins and ends with the heart (Fig. I-24). All living tissues and cells are near to blood vessels which form a network throughout the body and allow nutrients in the blood to flow from the heart to every cell and then back to the heart. The crucial function of this system is to connect all cells with organs of exchange such as the lungs, the liver, small intestine and kidneys.

Three types of blood vessels can be appointed: the arteries, capillaries and veins. These blood vessels have different structures which depends on the function, nevertheless all consist of a layered wall surrounding a central blood containing space (lumen).

Briefly, blood leaves the heart through the arteries to the various tissues and organs. Blood in the arteries, except in the pulmonary artery, is oxygenated. Then, the exchange of gases (oxygen and carbon dioxide), nutrients and products of metabolism between blood and tissue fluid through capillaries takes place. Subsequently, deoxygenated blood leaves the capillary vessels and goes back to the heart via veins, except in the pulmonary vein, which leaves the lungs and contains oxygenated blood.

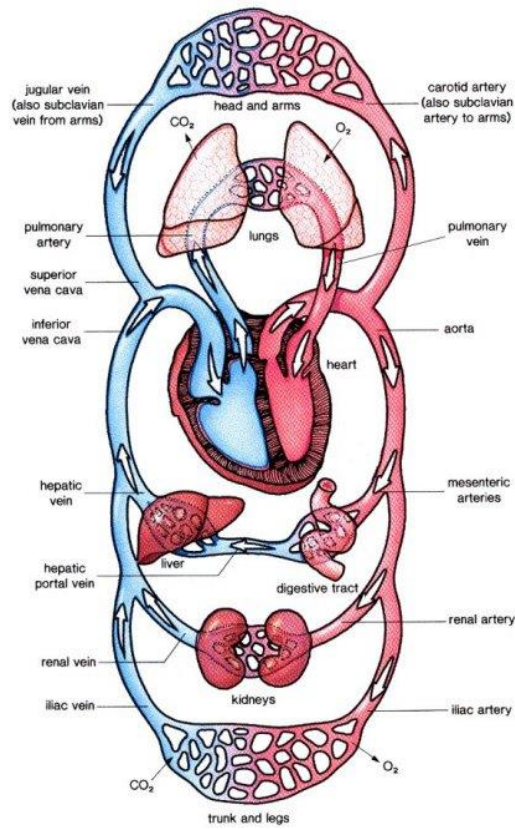


Figure I-24. The vascular system of the human body. Adapted from Human Circulatory System, RevisionWorld web site.

3.1.1. Vein

As briefly described above, the main function of the veins is to transfer blood to the heart. Deoxygenated blood from the tissues drains into venules that connect to larger veins and these go to the heart. The pulmonary vein transfers oxygenated blood from the lungs to the left atrium while the veins associated with the small intestine carry digested food *via* the liver to the inferior vena cava. The diameter is small in the venules and progressively increases as the veins approach the heart.

The function-dependent structure of veins is different to the arteries (Fig. I-25). Blood pressure after passing the capillaries is much lower than pressure exerted by the heartbeat. So veins differ from arteries in that the middle muscular wall is thinner than in arteries. Additionally in veins semi-lunar valves prevent backflow of blood.

3.1.2. Artery

Arteries can be divided up with respect to their size into large, middle arteries and the smallest-arterioles. The main function of arteries is blood transport from the heart to organs. Oxygenated blood by each heartbeat enters the large arteries, then the arterioles. In this system, the arteries show a progressive diminution in diameter as they recede from the heart, from about 25 mm in the aorta to 0.3 mm in some arterioles.

The wall of the arteries consists of three distinct layers: tunica adventitia (outer layer), tunica media (middle layer) and tunica intima (inner layer).

Compared to veins, several differences can be appointed in artery function-dependent structure (Fig. I-25). The arteries receive blood under high pressure, their structure thus needs to be able to stretch with every heartbeat. The middle layer of arteries containing elastic connective tissue is more resistant and thicker compared to this part in veins. Nevertheless, the proportion and structure of different arteries changes with the size and function of the particular artery. For example, the tunica media in arterioles contains less elastic fibers but more smooth muscle cells than that of the aorta (Burton, 1954).

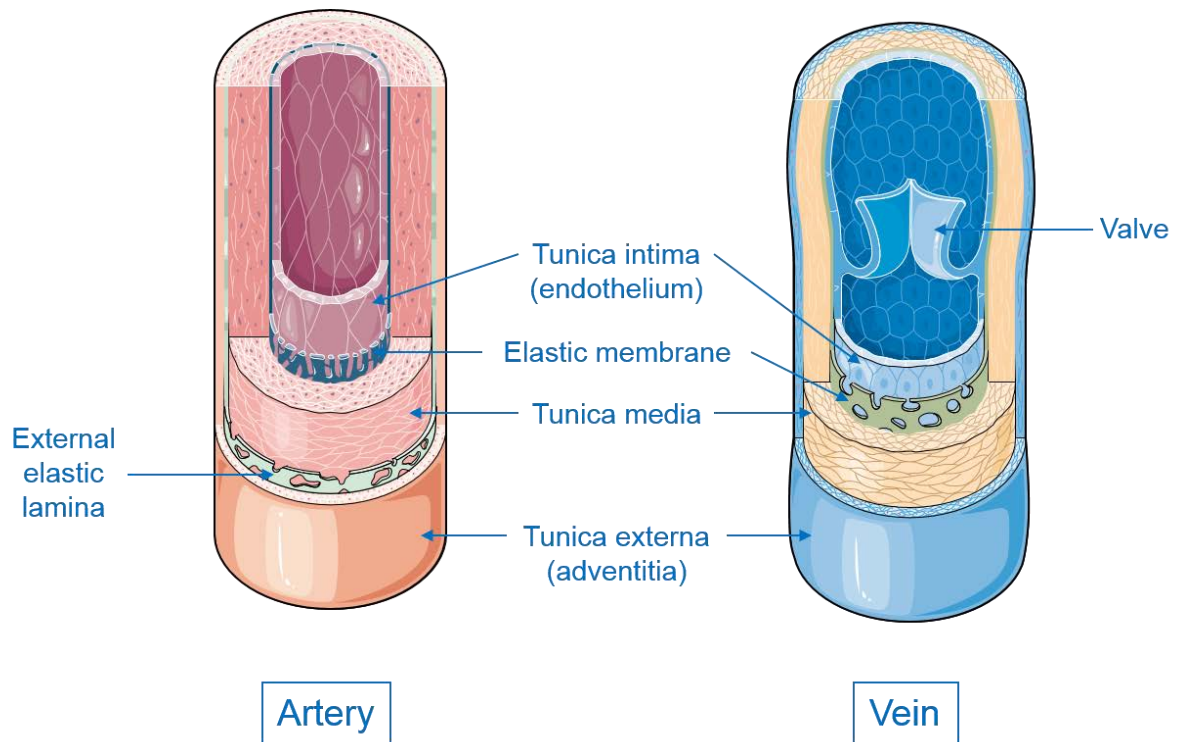


Figure I-25. The structure of the artery and vein. The three layers: tunica intima, tunica media and tunica adventitia are indicated in the schematic. The tunica intima is composed with endothelial cells and is in direct contact with the blood. The tunica media is composed with vascular smooth muscle cells framed with layers of elastic fibers and surrounded by collagen fibers and other extracellular matrix protein. Function-dependent structure of the tunica media in artery is different in two types of blood vessels. In artery, where the blood pressure is higher this tunica is more developed and gives mechanical properties like strength and elasticity. The tunica media is separated from the inner and the outer tunica by elastic membrane. The tunica adventitia is composed with collagen and fibroblasts, elastic fibers and contains vasa vasorum (adapted from Powerpoint image bank, Servier website).

3.1.3. Capillaries

Exchange of gases, nutrients and products of cellular metabolism takes place in the capillaries through the capillary endothelium. The structure of this wall, similar to that of the tunica intima, is formed with a layer of endothelial cells resting on a basement membrane. The diameter of capillaries is large enough to permit the red blood cells to squeeze through in single file. Moreover, the presence of specialized junctions, gaps or fenestrations support the function of the capillaries. Features of those structures facilitate the principal function which is promotion of the exchange of nutrients and metabolic end-products between the blood and the cells of the interstitial tissues (Fig. I-26).

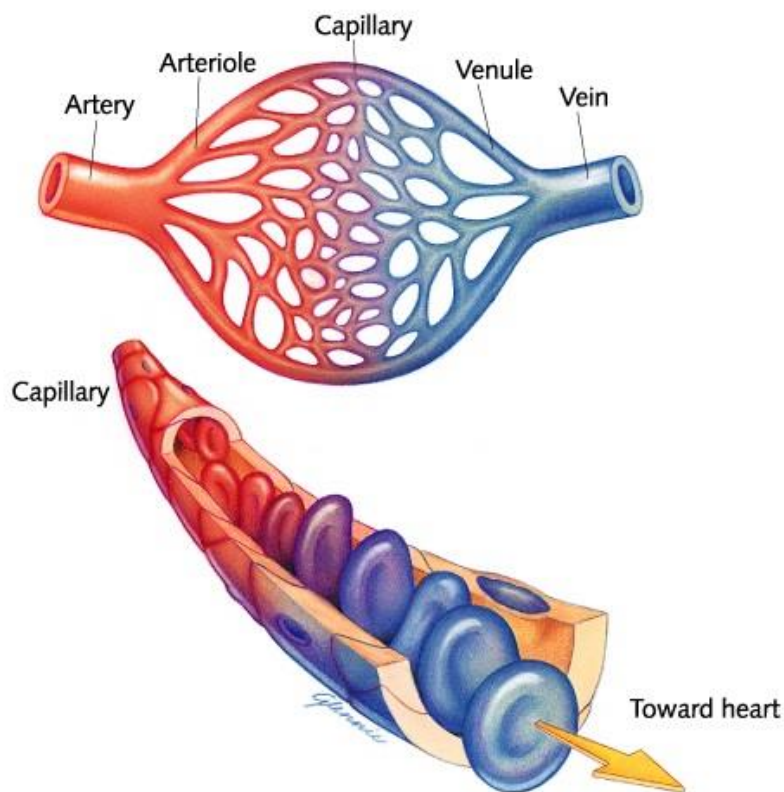


Figure I-26. The capillary vessels (adapted from Mosby, Inc. and derived items copyright, 2003)

3.2. Structure of an aorta

3.2.1. Intima

The tunica intima is the inner layer of closely packed endothelial cells in all blood vessels. Flat endothelial cells from tunica intima are separated from the tunica media by a layer of connective tissue, the basement membrane which anchors the cells to the arterial wall.

The main role of the intima is to decrease friction between the blood components and the blood vessel wall and to separate the blood from the tunica media.

3.2.1.1. EC

Endothelial cells arise from the hemangioblast. They show phenotypic variation depending on their localization in the vascular tree and type of blood vessel (arteries and veins). Endothelial cells from different blood vessels can be distinguished depending on different marker expressions. Moreover, the cell response for the same stimuli can be different depending on the localation of the ECs. ECs react with physical and chemical stimuli within the circulation and regulate hemostasis, vasomotor tone and immune and inflamatory responses.

The anticoagulant barrier between the blood and the tunica media, created by the endothelium, is crucial for the proper functioning of blood vessels. Structure and functional integrity provided by the endothelial layer is semi-permeable and can control the transfer of selected molecules and cells. Nonetheless, it is also a multifunctional endocrin organ (Cines et al., 1998; Sumpio et al., 2002).

Because endothelial cells provide many essential functions, endothelial dysfunction, activation or injury leads to vascular diseases and can promote the development of chronic inflammatory conditions, such as atherosclerosis.

3.2.2. Media

The tunica media is the thicker middle layer containing elastic connective tissue. It is separated from the tunica intima by the internal elastic lamellae and from the tunica adventitia by the external elastic lamellae. The media is supplied with two sets of nerves. The first stimulates the muscles to relax and in result allows extension. The second stimulates contraction of the vascular smooth muscle and in result the artery becomes narrower.

This layer contains elastic fibers with smooth muscle cells which are embedded in a ground substance rich in proteoglycans. The outer layer of the media is penetrated by branches of the vasa vasorum (Fig. I-27).

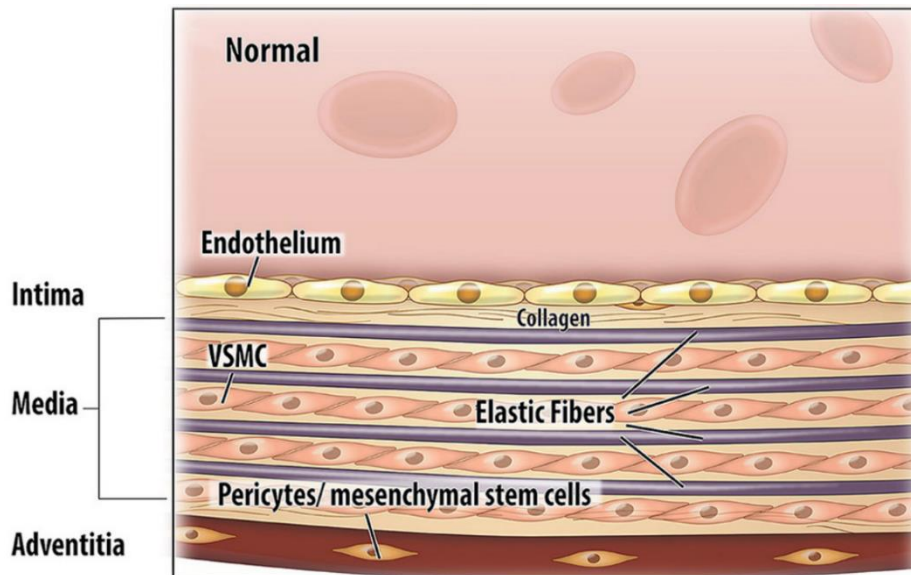


Figure I-27. The tunica media organization. Vascular smooth muscle cells form several layers which are separated with elastic fibers. The collagen fibers (mainly collagen type I and III), proteoglycans and others protein fill the extracellular space and provide the unique mechanical properties of arterial wall (adapted from Van Varik et al., 2012).

3.2.2.1. Vascular smooth muscle cells

Vascular smooth muscle cells are highly specialized cells whose main functions are the contraction and the regulation of blood vessel tone, blood pressure and blood flow. In the tunica media of healthy arteries the smooth muscle cells exhibit a low rate of proliferation, low synthetic activity and express well-defined contractile proteins and signaling molecules. The extracellular matrix proteins form the elastic fibers and provide the mechanical proprieties of artery (Lacolley et al., 2012).

In normal artery spindle-shape VSMC are characterized by expression of contractile-specific proteins. The SM-alpha-actin is a widely expressed marker. Other markers such as SM-MHC, calponin, SM-22 alpha, h-caldesmon, metavinculin, telokin and smoothelin are also characteristic for differentiated VSMC (Kemp et al., 1991; Birukov et al., 1993; Huber, 1997; Roy et al., 2001; Morgan et al., 2001; Owens et al., 1997, 1998 and 2004).

3.2.2.2. vSMC differentiation and phenotype changing

Vascular smooth muscle cells are able to change their phenotype from contractile to proliferative, inflammatory and synthetic, in response to inflammatory mediators, growth factors, mechanical influences and cell-cell or cell-extracellular matrix interactions (Mano et al., 1999; Owens et al., 2004; Alexander et al., 2012). Each VSMC phenotype is characterized by the expression of characteristic markers (Fig. I-28).

Activated vSMC change morphology, they are bigger than quiescent cells, and increase production of extracellular matrix components like collagen III, fibronectin, matrix metalloproteinases, osteopontin (Giachelli et al., 1995) and tropomyosin-4 (Abouhamed et al., 2003). They are characterized by an increase in proliferation rate, migration and a decrease in the expression of specific contractile markers (Kemp et al., 1991; Polisenio et al., 2006; Boehm et al., 2001). These features play a role in vascular repair but nevertheless they can lead also to the development of vascular diseases like atherosclerosis, hypertension and neointima formation. Many reports exist about VSMC phenotype changing during cardiovascular disease development.

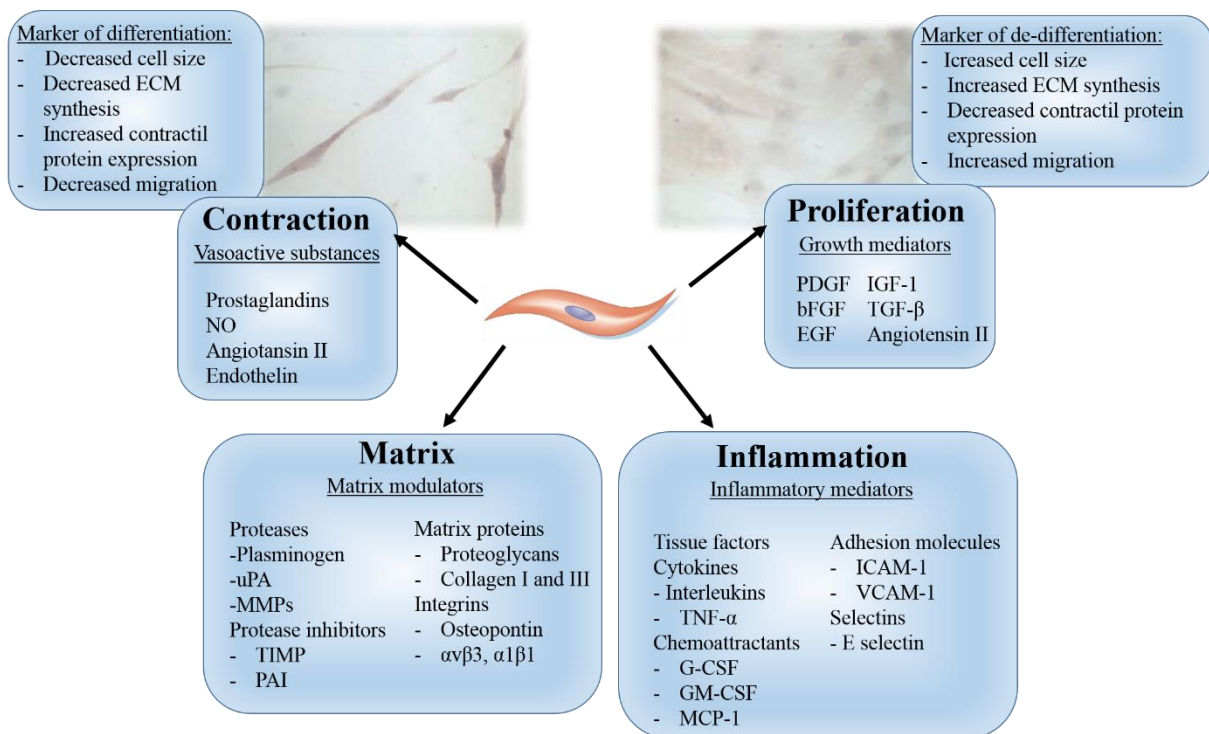


Figure I-28. The contractile or synthetic vascular smooth muscle cells. Contractile VSCM are small and have characteristic spindle-shape, in contrast synthetic cells are bigger and present rhomboid-like shape. Below the picture of appropriate cell phenotype, the main markers are listed. (Adapted from: Dzau et al., 2002; Rzucidlo et al., 2007).

3.2.2.3. ECM

The major mechanical properties of arteries are assured by extracellular matrix protein synthesized by SMC. Indeed, in tunica media the two main ECM proteins, elastin and collagen, are responsible for the major features of this tissue – elasticity and resistance. The elastic fibers are constituted with the elastin and associated proteins. Its quantity is different depending on the artery and its distance from the heart. The second major proteins of tunica media ECM are collagen I and III which give tensile force to the blood vessels.

Elastin

Elastin is a polymer of linear polypeptide chains and constitutes more than 50% of the dry weight of the aorta. During aging, aorta elasticity decreases because of degenerative changes in elastin (Atanasova et al., 2012).

With age the concentration of elastine decreases, nevertheless its amount remains unchanged. This process is due to an increase of other extracellular matrix proteins such as collagen.

Collagen

In aorta many types of collagens were detected, such as collagen type I, III, IV, V, VI and VIII. Nevertheless, collagens type I and type III constitute about 80-90% of the total amount of collagen. These long, fibrous structural proteins are formed with three polypeptide strands, the alpha chains which are twisted together to form a triple helix stabilized by hydrogen bonds. Collagen is important for function and mechanical properties of arteries like tensile strength and stiffness (Berillis, 2013). With age, its content increases in arteries, moreover its structure is changed because of an increase in cross-links between collagens fibres. The cross-link process can be due to an increase of cross-linking amino-acids or accumulation of advanced glycation end-products as a result of glycation and oxidizing reactions (Tsamis et al., 2013).

3.2.3. Adventitia

The tunica adventitia is the outer layer which anchors a blood vessel to the surrounding tissues. This tunica is formed with irregularly arranged collagen bundles, scattered fibroblasts, elastic fibers and contains vasa vasorum and vasa nervi.

3.3. Remodeling of the arterial wall

Arterial remodeling refers to the structural and functional changes of the vessel wall size or cross-sectional area within the external elastic lamina that occur in response to aging, injury or disease. This process is stimulated by different pathophysiological mechanisms that are dependent on each other and that have an influence on the cellular and non-cellular components of the arterial wall. As the main mechanisms involved in arterial remodeling, endothelial dysfunction, hyperplasia of the tunica intima and tunica media, changes in collagens and elastin content, fibrosis and arterial calcification can be listed. The phenotype can change because VSMC can increase proliferation and their migration, thus contribute to the thickening of the arterial wall. Moreover, synthetic VSMC induce an increase in vascular tone, an ECM modification and calcification (Virmani et al., 1991; Safar et al., 1998; Ward et al., 2000).

Arterial remodeling can be divided into atherosclerosis which is an inflammatory process initiated by accumulation of lipids and plaques formation, and arteriosclerosis which is associated with aging and cardiovascular, metabolic or inflammatory diseases (Libby, 2002; Libby et al., 2011). In addition, arterial remodeling can be inward or outward but also can be hypertrophic, eutrophic or hypotrophic. Whereas, arterial hypertrophic or hypotrophic remodeling is characterized by thickening or thinning of the vascular wall, respectively, in the case of eutrophic arterial remodeling the thickness of the vessel wall remain unchanged (Fig. I-29) (O'Rourke et al., 2007).

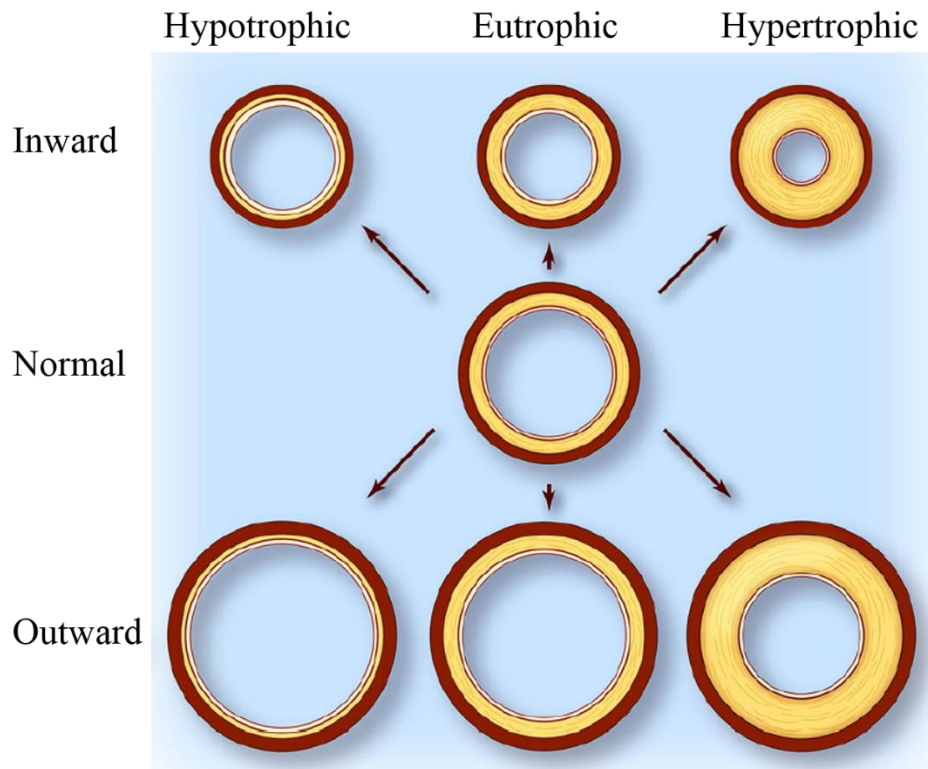


Figure I-29. Types of vascular remodeling. Different types of arterial remodeling are presented: hypotrophic (left column), eutrophic (center column) and hypertrophic (right column). In addition remodeling can be either inward or outward (adapted from van Varik et al., 2012).

3.4. Diseases of the vascular system

3.4.1. Atherosclerosis - Inflammatory disease of arterial blood vessels

Atherosclerosis which is a chronic disease with subsequent cardiovascular complications such as myocardial infraction, ischemic heart failure and stroke, is a major cause of death in Western populations. Several risk factors can be listed such as: hypertension, diabetes, serum total and low-density lipoprotein cholesterol and smoking (Hahn et al., 2009).

Atherosclerosis of the arterial wall refers to the development of atheromatous plaques in the inner lining of the arteries. Accumulation and oxidation of low-density lipoprotein within the arterial wall initiate a complex series of biochemical and inflammatory/immunomodulatory reactions involving multiple cell types ultimately leading to the development of unstable atherosclerotic plaques. This disease is due to aging and cellular senescence (Wang et al., 2012).

3.4.1.1. Endothelial cell dysfunction

Development of atherosclerosis begins with tunica intima dysfunction. As the first stage of atherosclerosis is intimal xanthomas or intimal thickening, where the intimal xanthomas are fatty streak accumulation of foam cells and intimal thickening is the accumulation of VSMCs in an absence of lipid or foam cells (Rosenfeld et al., 2000).

As atherosclerosis is an aging-associated disease, it seems to be important to look at time-dependent endothelium changes. Aged ECs have many features associated with cellular senescence (Khaidakov et al., 2011; Shi et al., 2004; Asai et al., 2000). Moreover, those changes are accompanied by modulation in cytoskeleton integrity, proliferation, cell migration and angiogenesis.

It was shown that aged ECs decrease production of NO and increase endothelin-1 (Donato et al., 2009). Endothelial cell aging is associated with a loss of EC function and an increase of proinflammatory and proapoptotic stage, that consequently increase monocytes migration into the arterial wall.

3.4.1.2. Cell types involved in atherosclerosis

Monocytes/macrophages

As macrophages are innate immune effectors, their reaction is not initiated by antigenic specificity (Boyle, 2005). Monocytes patrolling blood vessel enter in the arterial wall. Under stimulation by ECs and VSMC which release M-CSF (macrophage colony-stimulating factor), monocytes differentiate into activated macrophages. Then, other stimulators like scavenger receptors interact with macrophages causing, oxLDL uptake and further foam cell formation. Two subtypes of macrophages can be appointed, M1 and M2. The first sort prevail, M1 secrete pro-inflammatory cytokines (IL-1), tumor necrosis factor alpha (TNF α) and reactive oxygen species. Action of M1 leads to plaque development by recruitment of immune cells, oxidation of LDL and an increase in foam cell formation (Hansson, 2005). The second subunit, macrophage M2, secretes interleukin-10 (IL-10) and transforming growth factor beta (TGF β) indicative of an anti-inflammatory character (Gordon, 2003).

T lymphocytes

T lymphocytes, after binding with vascular adhesion molecules, infiltrate intima and enter into contact with antigen-presenting cells. Subsequently, they differentiate into two subtypes: T

helper 1 (T_h1) or T helper 2 (T_h2) cells (Taleb et al., 2008). T_h1 cells prevail in plaques and produce pro-inflammatory cytokines and chemokines, which in consequence favor atherosclerotic lesion progression and plaque vulnerability (Hansson et al., 2006). While T_h2 cells indicate an anti-atherosclerotic character through elaboration of anti-inflammatory cytokines such as IL-4, IL-5 or IL-10 which probably suppress the inflammatory response (Mallat et al., 1999).

Mast cells

Mast cells are responsible for increasing vascular permeability by the secretion of various vasoactive substances and further promoting immune cell recruitment. Moreover, mast cells produce cytokines such as TNF α , and can activate or even induce apoptosis of SMCs, macrophages and ECs (Sun et al., 2007).

Smooth muscle cells

Following vascular injury, SMCs change their quiescent contractile phenotype for a proliferative synthetic phenotype. Proliferating SMCs induce intimal thickening and participate in the development of fibrous cap atheromas (Clarke et al., 2006).

In consequence, ECM protein synthesis and the number of cells increase. After the intensified proliferation, SMCs irreversibly lose the ability of multiplication what is sign of cell senescence. Moreover, in the lesion place, under stimuli like secretion of growth factors from immune cells, pro-inflammatory molecules including endothelial growth factor (VEGF), TNF α and IL-1 β promote inflammation (Doran et al., 2008).

Platelets

Platelets mediate inflammation status in early and late stages of atherosclerosis (Weyrich et al., 2009). At the earliest stage of atherosclerosis, activated platelets *via* the cell surface protein CD40 and its ligand, mediate endothelial cell activation (Henn et al., 1998).

Additionally, activated platelets *via* secretion of inflammatory molecules like RANTES, CXC chemokines ligand 4 (CXCL4), macrophage inflammatory protein (MIP-1 α) or IL-1 β , recruit and activate immune cells, activate the phenotype switch of SMC and promote proteolysis through secretion of MMPs (Gleissner et al., 2008).

3.4.1.3. Atherosclerotic plaque characterization

The initial stage of atherosclerotic lesion development includes endothelium activation, SMC activation, immune cells recruitment and infiltration to the intima. LDL enters the intima and its oxidation takes place, and the resultant oxLDL is formed. Monocytes differentiate into macrophages and take up oxLDL. When cells are full of oxLDL, they form foam cells. VSMC proliferate and migrate into the intima and intimal thickening progresses (Steinberg et al., 2002a and 2002b; Perrotta et al., 2013). Proliferative/synthetic SMC forms a fibrous cap.

Inflammation progresses and immune cells are recruited. The extracellular matrix synthesis by SMCs and foam cell formation significantly increase the size of the necrotic core and narrow the lumen. Cells from the necrotic core stimulate the increase of inflammation status and enhanced the immune response. In fact atherosclerotic plaque development and rupture of the fibrotic cap takes place. Following blood contact with the necrotic core, a thrombus is formed and extends into the vessel lumen, where it can impede blood flow (Fig. I-30).

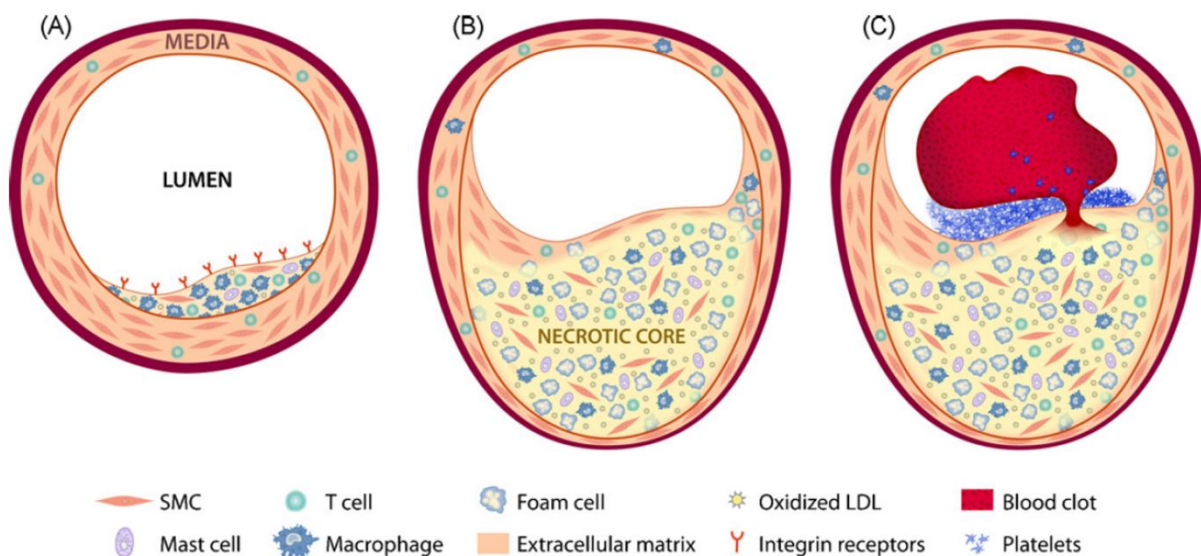


Figure I-30. The atherosclerosis progression. A: An early stage of atherosclerosis characterized by intima xanthomas; ECs activation, VSMC phenotype switch, monocytes/macrophages presence and foam cells formation. B: Well developed atherosclerotic plaque with necrotic core, fibrous cap atheroma and highly narrowed lumen. C: The atherosclerotic plaque rupture following fibrous cap rupture and blood contact with fibrous cap and necrotic core. In result platelet aggregation, thrombosis and artery occlusion (adapted from Bui et al., 2009).

3.4.1.4. Animal models of atherosclerosis – *ApoE*^{-/-} mice

In order to study plaque development during atherosclerosis, several animal models of this disease have been established and well characterized (Jawien et al., 2004; Gete et al., 2012; Moor et al., 2013). Animal models of atherosclerosis allow the study of the implication of selected molecules (in our study SSAO) in disease development.

Several models of atherosclerosis have been developed (Table I-2).

Table I-2. Animal models of atherosclerosis. Selected mouse models of atherosclerosis progression and regression. *ApoE*, apolipoprotein E; *Ldlr*, low-density lipoprotein receptor; *Mttp*, microsomal triglyceride transfer protein large subunit; VLDL, very low-density lipoprotein (Adapted from Moor et al., 2013).

Mouse model	Model features	Lipoprotein profile
Progression		
<i>ApoE</i> ^{-/-} mice	Spontaneous development of complex plaques when mice are fed on a chow diet; and acceleration of plaque formation when mice are fed on a Western diet	Intestinally derived remnant lipoprotein particles
<i>Ldlr</i> ^{-/-} mice	Development of plaques following a cholesterol and fat-enriched diet; and lipoprotein profile similar to that of humans	VLDL and LDL
Regression		
Aortic transplant mice	Rapid regression of atherosclerosis; but requires surgical procedure, for example, the transplantation of aortas from <i>ApoE</i> ^{-/-} mice to wild-type mice	Lipid levels revert to the levels in wild-type mice
Reversa mice	An <i>Ldlr</i> ^{-/-} mouse-based platform that shows inducible reversal of hyperlipidaemia after conditional inactivation of <i>Mttp</i>	Lipid levels revert to nearly the levels that are observed in wild-type mice
Reconstitution of <i>ApoE</i> ^{-/-} mice with APOE	The inducible regression of atherosclerosis by adenoviral delivery of <i>ApoE</i> to the liver or by correcting a hypomorphic allele of the <i>ApoE</i> gene	Lipid levels revert to nearly the levels that are observed in wild-type mice

The most popular and available in our laboratory is the *ApoE*^{-/-} model of atherosclerosis. These mice are homozygous for the *ApoE* mutation which significantly increases cholesterol levels in total plasma that are age and sex independent.

II. Working hypothesis and objectives

Hypothesis

The extracellular matrix plays a major role in the homeostasis of numerous tissues, including vascular and cartilage tissues. Any alteration of the matrix network profoundly change its structure and function which in turn affects cell phenotype and leads to generative diseases, such as atherosclerosis or osteoarthritis.

SSAO catalyzes the oxidation of primary amines with the release of potential harmful electrophilic products, aldehydes and hydrogen peroxide that can react with matrix components and induce their degradation. Its implication in differentiation and inflammation, and in other actions, such as glucose intake, has already been demonstrated in adipocytes and VSMC. However, for this latter type of vascular cell, the molecular mechanism for differentiation must be better precised.

- It is hypothesized that SSAO could contribute to the development of atherosclerosis.

In chondrocytes of cartilage, expression of SSAO has been reported, but, until now, the role of this enzyme has not been elucidated.

- It is hypothesized that the enzyme, by its activity, would participate in cartilage homeostasis and pathology.

Objectives

The main goal of this work is to determine the role of SSAO in

- 1- the differentiation of two types of cells: VSMC associated with blood vessels, and chondrocytes, the only cells in cartilage,
- 2- extracellular matrix remodeling, in relation with two main diseases, atherosclerosis and osteoarthritis.

For this purpose, a pluridisciplinary strategy will be used: cell and molecular biology, biochemistry, animal models, and histology. A close partnership has been established between the two research laboratories of the Federation de Recherche 3209 (Unité mixte Université de Lorraine-INSERM U 961 «Risque cardiovasculaire, rigidité-fibrose et hypercoagulabilité» and UMR Université de Lorraine CNRS 7561 «Physiopathologie, Pharmacologie et Ingénierie Articulaires») and the clinical departments (cardiology, orthopaedics) of the CHU in Nancy.

III. Materials and methods

1. Models

1.1. Human cartilage

Articular cartilage samples were obtained from three patients (women with a mean age 71 ± 5 years) undergoing total knee joint replacement in collaboration with the “Service de Chirurgie Orthopédique et Traumatologique”. The study was approved by our local Research Institution review board (Commission de la Recherche Clinique, registration number UF 9757-CPRC 2004 – Cellules souches et Chondrogenèse). The protocol conforms with the ethical guidelines of the Declaration of Helsinki, and written informed consent was obtained from each patient. Cartilage biopsies were taken from the injured area and from the macroscopically unaffected area distant to the damaged zone. The samples were kept frozen at -80°C until used or placed in paraformaldehyde for histological analysis.

1.2. Animals

1.2.1. Normal rats

All experiments were performed in accordance with national animal care guidelines and were pre-approved by a local ethics committee. Male Wistar rats (100-150 g) were obtained from Charles River (L'Arbresle, France). They were housed under controlled temperature and light cycle conditions with food and water *ad libitum*. The Wistar rats were anesthetized with 3.5% of isoflurane in oxygen and put to death by cervical dislocation. Thoracic aortas and perigonadal adipose tissues were excised for a positive source of SSAO. Cartilage samples

were taken from hips and knee joints for histology, enzyme activity and mRNA expression. Hips were used also for isolated chondrocyte cell culture.

1.2.2. Models of cartilage degradation: MIA

All experiments were performed in accordance with national animal care guidelines and were pre-approved by a local ethics committee. Male Wistar rats (150-175 g) were obtained from Charles River (L'Arbresle, France). They were housed under controlled temperature and light cycle conditions with food and water *ad libitum*. After acclimatization time the Wistar rats were anesthetized with 3.5% of isoflurane in oxygen and MIA-dependent cartilage degradation was induced by single intra-articular injection of 0.3 mg of monosodium iodoacetate (MIA; Sigma, St. Louis, MO, USA) through the infrapatellar ligament of the right knee. MIA was dissolved in sterile physiologic saline and administered in a volume of 50µl using a 27gauge needle. The left contralateral control knee was injected with 50µl of physiologic saline. Two weeks after injection the Wistar rats were anesthetized with 3.5% of isoflurane in oxygen and put to death by cervical dislocation. The knee joint, knee and femoral head cartilage were dissected and used to further studies.

1.2.3. WT and knock out *SSAO*^{-/-} mice

All experiments were performed in accordance with national animal care guidelines and were pre-approved by a local ethics committee. Mice were housed under controlled temperature and light cycle conditions with food and water *ad libitum*.

SSAO^{-/-} knock out mice with a C57BL6/J background were generously given by S. Jalkanen and established as previously described in Stollen et al., 2005. Briefly, gene targeting techniques were used to disrupt the mouse *SSAO/AOC3* gene by replacing a portion of its first exon with a neomycin-resistance (Neor) cassette. Mice homozygous for the null mutation were produced and this mutation was maintained in a pure C57 background.

WT and *SSAO*^{-/-} 15 or 25 week-old female mice were anesthetized with 3.5% of isoflurane in oxygen and put to death by cervical dislocation. The aortas from 15 week-old or 25 week-old were excised and washed in a physiological serum at room temperature supplemented with 1% penicillin/ streptomycin/neomycin (P/S) and 7.5mg/l Amphotericin B (Sigma-Aldrich,

Missouri, USA). The tissues around the aortas were precisely dissected and the aortas were opened longitudinally. Then the aortas were washed twice in the same but sterile physiological serum at room temperature and put in culture. RPMI 1640 (Gibco, Life Technology, Saint Aubin, France) culture medium containing 1% P/S, 2.5mg/l of Amphotericin B and 1ng/ml of TNF α (Sigma-Aldrich, Saint-Quentin Fallavier, France) was used (Table III-1). Then aortas were incubated for 24 or 48 hours in a 37°C, 5% CO₂ humidified cell culture incubator. Subsequently the culture medium were collected, the aortas were washed in cold sterile PBS. The samples were kept frozen at -80°C until used.

Table III-1. Diagram of the experiment and mouse experimental groups.

Mouse experimental groups					
Age [week-old]	Genotype	Time of treatment			
		24 hours		48 hours	
		Non treatment	TNF α	Non treatment	TNF α
15	WT	2	2	6	6
	<i>SSAO</i> ^{-/-}	6	5	6	6
25	WT	3	4	7	7
	<i>SSAO</i> ^{-/-}	10	11	12	13

1.2.4. Model of atherosclerosis: *ApoE*^{-/-} *SSAO*^{-/-}-double knock out mice

The *SSAO*^{-/-} mice were crossbred with *ApoE*^{-/-} knock out mice with a C57BL6/J background commercially available from The Jackson Laboratory (Charles River, L'Arbresle, France). The first generation of double knock out mice (*ApoE*^{-/-}*SSAO*^{-/-}) selected by genotyping were kept until 15 or 25 weeks-old and then mice were anesthetized with 3.5% of isoflurane in oxygen and put to death by cervical dislocation. Heart, kidney and spleen were embedded into OCT,

frozen and kept at -80°C. Thoracic aortas, lung, perigonadal adipose tissue, liver, spleen and kidney were kept frozen at -80°C until use.

1.3. Cells: models of hypertrophic differentiation

1.3.1. Primary cell culture of rat chondrocytes and hypertrophic differentiation protocol

Chondrocytes were isolated from femoral head cartilage of 100-150 g Wistar rats with 2 mg/ml pronase in 0.9% (w/v) NaCl supplemented with 1% penicillin/ streptomycin/neomycin (P/S) stabilized solution (Sigma-Aldrich, Saint-Quentin Fallavier, France) for 2 hours. Subsequently, cartilage sections were digested with 1.5 mg/ml collagenase in DMEM/F-12 containing 10% fetal bovine serum (FBS) (Dominique Dutscher, Issy-les-Moulineaux, France), 1% P/S overnight in a 37°C, 5% CO₂ humidified cell culture incubator. The chondrocytes were collected by centrifugation and plated at 1.3×10^4 cells/cm² in DMEM/F-12 with 1% P/S, 20 mM L-glutamine, 5.2 nM sodium selenite and human 10 µg/ml transferrin (all provided by Sigma-Aldrich, Saint-Quentin Fallavier, France) (growth medium) containing 10% decomplemented FBS. Cells were cultured for 4-5 days until confluence. The medium was changed every 2 days. All experiments were performed after the initial passage. Cells were removed with trypsin (0.25%, Life Technologies SAS, Saint Aubin, France) and seeded at 2×10^3 cells/cm² in 6-well plates for RNA and 6×10^3 cells/cm² in T-75 flasks for measurement of SSAO activity. At confluence, chondrocytes were switched to growth medium presented in Table III-2 and III-3 for different periods of time up to the 21st day, in the absence or the presence of 1 µM LJP 1586 [Z-3-Fluoro-2-(4-methoxybenzyl)allylamine hydrochloride], a selective SSAO inhibitor. We verified this concentration did not alter cell viability with 3-(4,5 dimethyl-2-thiazolyl)-2,5-diphenyl-2H-tetrazolium bromide (MTT).

Cells were observed at several time points of the culture by phase contrast microscope (Nikon DIAPHOT 300, Tokyo, Japan) and corresponding pictures were recorded (Nis-Elements BR 3.2 software, Champigny sur Marne, France) at magnification x10.

Table III-2. The protocols used for chondrocyte differentiation.

Protocol	Medium	FBS	Supplements	Medium	FBS	Supplements	Supplements
1	DMEM/F12	10 %	P/S L-glutamine Transferine Sodium selenite	DMEM/F12	10 %	P/S L-glutamine Transferine Sodium selenite	+ insulin (10µg/ml)
2				α-MEM	2 %		+ insulin
3				α-MEM	5 %		+ insulin

Table III-3. The chondrocyte culture protocols.

Protocol	Medium	FBS	Supplements	Medium	FBS	Supplements	Supplements
4	DMEM/F12	10 %	P/S L-glutamine Transferine Sodium selenite	DMEM/F12	2%	P/S L-glutamine Transferine Sodium selenite	-
5							+ Insulin (2µg/ml) + Ascorbic acid (37.5µg/ml)

1.3.2. Progressive passage of rat chondrocytes

All experiments were performed for passage 1 until 5 accordingly to protocol 5 presented in table 3. After an initial passage cells were removed with trypsin (0.25%, Life Technologies SAS, Saint Aubin, France) and seeded at 2×10^3 cells/cm² in 6-well plates for RNA, 6×10^3 cells/cm² in T-75 flasks for measurement of SSAO activity and 6×10^3 cells/cm² in T-75 flasks for the next passage. At confluence, chondrocytes were switched to growth medium supplemented with only 2% FBS, 2 µg/ml insulin and 37.5 µg/ml 2-phospho-L-ascorbic acid for period of time up to the 21st day.

1.3.3. ATDC5

Cells were seeded at 2×10^3 cells/cm² in 6-well plates for RNA and 6×10^3 cells/cm² in T-75 flasks for measurement of SSAO activity. At confluence, ATDC5 were switched to growth medium supplemented with 2% of 5% FBS, 2 µg/ml insulin and 37.5 µg/ml 2-phospho-L-ascorbic acid for different periods of time up to the 21st day.

Cells were observed at several time points of the culture by phase contrast microscope (Nikon DIAPHOT 300, Tokyo, Japan) and corresponding pictures were recorded (Nis-Elements BR 3.2 software, Champigny sur Marne, France) at magnification x10.

2. Common methods

2.1. Histology and Immunohistochemistry

Tissue samples were fixed and appropriately prepared for histological analysis.

Chemical staining was performed for the tissue sections. Cartilage sections were stained with Hematoxylin-Erythrosin-Saffron (HES) to evaluate their cellular and morphologic aspect and with Safranin O to evaluate proteoglycan content. The sinus aortic sections were stained with Sirius red to evaluate collagen content in ECM.

Then immunohistochemical staining was performed accordingly to the protocols presented in table III-4, using antibodies listed in table III-5 in the described condition.

Table III-4. Protocol of immunohistochemical studies.

Cartilage	Vascular
Fixing and embedding the tissue	
<ul style="list-style-type: none"> - Fixation: 48 hours in 4% (w/v) paraformaldehyde - Decalcification: 0.34 M ethylene diamine tetraacetate in water - Embedding medium: paraffin - Storage: RT 	<ul style="list-style-type: none"> - Fixation: 4 hours in 4% (w/v) paraformaldehyde, 24h in sucrose 30% (w/v) - Embedding medium: OCT - Storage: -80°C
Cutting and mounting the section	
- 5 µm thick slices were cut with a microtome	- 10 µm thick slices were cut with a cryostat
Deparaffinizing and rehydrating the section	
<ul style="list-style-type: none"> - Deparaffinization: 2.5 min in toluene - Hydration: 2.5 min in ethanol: 100%, 96% and 70% (v/v) 	<ul style="list-style-type: none"> - 5 min at RT - 15 min of fixation with 4% PFA - Washing for 5 min with TBST with 0.1% Triton

	- Washing twice for 5min in TBST 0.5%
Antigen retrieval	
- 10 mM sodium citrate buffer	---
Peroxidase inhibition	
- 30 min 3% H ₂ O ₂ in TBST 0.5%	- 5 min 3% H ₂ O ₂ in TBST 0.5%
Immunohistochemical staining	
<p>Incubation:</p> <ul style="list-style-type: none"> - 1h 5% BSA at RT - I° antibody at 4°C overnight - Washing 3 times for 15min in TBST 0.5% - 1h II° antibody at RT - Washing 3 times for 15min in TBST 0.5% 	<p>Incubation:</p> <ul style="list-style-type: none"> - 10 min with Dako block or 10% goat serum in 0.05% TBSA at RT - I° antibody at 4°C overnight - Washing 3 times for 15min in TBST 0.5% - 30 min II° antibody at RT - Washing 3 times for 15min in TBST 0.5%
Detection	
<ul style="list-style-type: none"> - 10 min of incubation with Horseradish peroxidase/Streptavidin (Dako) - Washing 3 times for 5min in TBST 0.5% - 10 min of incubation with 3,3'-diaminobenzidine (DAB, Thermo Scientific, Villebon sur Yvette, France) - Washing 2 times in tap water 	<ul style="list-style-type: none"> - 10 min of incubation with 3,3'-diaminobenzidine (DAB, Thermo Scientific, Villebon sur Yvette, France) - Washing 2 times in destilated water - 45 s of incubation with Hematoxylyne
Dehydrating and stabilizing with mounting medium	
<ul style="list-style-type: none"> - Hydration: 2.5 min in ethanol: 70%, 95% and 100% (v/v) - Incubation in toluene 2x 5 min - Slides mounting with Eukit 	- Slides mounting with Eukit
Viewing the staining under the microscope	
DMD 108 Leica microscope with a magnification 10x, 20x and 40x	Nikon DIAPHOT 300, Tokyo, Japan

Table III-5. The list of antibodies used to immunohistochemical studies.

I° Antibody	References	dilution	Incubation condition	II° Antibody	Incubation condition
In cartilage studies					
Anti-SSAO	Santa Cruz Biotechnology H43, sc-28642	1/50	Overnight, 4°C	Anti-rabbit	2h, RT
Anti-collagen X	Abcam, ab58632	1/20	Overnight, 4°C	Anti-rabbit	2h, RT
In vascular studies					
Anti- α -actin	Sigma A5228	1/1	1h, 4°C	Anti-rabbit	30 min, RT
Anti-MOMA	Chemicon MAB1852	1/100	Overnight, 4°C	Anti-rat	30 min, RT
Anti-CD3+	Abbiotech 250590	1/200	Overnight, 4°C	Anti-rabbit	30 min, RT

2.2. Western blot

Culture media were discarded from the culture plates. The cells were washed twice with cold PBS, harvested and homogenized in 250 μ l of lysis buffer (20 mM Tris-HCl, pH 7.5 containing 5mM EDTA, 150 mM NaCl, 1% Triton X100, 0.1% Tween 20, 1mM DTT) supplemented with fresh protease inhibitor cocktail (Complete, Mini, EDTA-free, Roch Diagnostics GmbH). After 30 min incubation on ice, the samples were centrifuged for 15 min at 4°C, at 10,000 g. Supernatants were collected and kept at -80°C until use.

SDS/PAGE was performed with a Mini-PROTEAN Tetra Cell, Mini Trans-Blot Module, and PowerPac Basic Power Supply (Bio-Rad).

Proteins were incubated at 95°C for 5 min, separated by SDS PAGE and transferred to nitrocellulose (Hybond-C Extra, Nitrocellulose, supported, 0.45 micron, Amersham, Biosciences catalog No. RPN2020E). The membrane was incubated with a blocking buffer:

5% non-fat dry milk, 0.1% (w/v) Tween 20 in TBS buffer (10 mM Tris-Base and 15 mM NaCl, pH 7.5) for 2h at room temperature. The membrane was blotted with a primary antibody (listed in Table III-6) in TBS buffer containing 5% non-fat dry milk and 0.1% Tween 20. After four washes, the membrane was incubated with an appropriate secondary antibody in the blocking buffer for 2 h. Following three washes in TBS buffer containing 0.1% Tween 20, the protein bands were visualized using the Chemiluminescence Kit (Immun-Star™ WesternC™ Chemiluminescence Kit #170-5070 Bio-Rad) on a Fujifilm Luminescent Image Analyzer LAS4000 System.

Table III-6. The list of antibodies used in WB.

I° Antibody	References	dilution	Incubation condition	II° Antibody	Incubation condition
<i>In cartilage studies</i>					
Anti-SSAO	Santa Cruz Biotechnology H43, sc-28642	1/1000	Overnight, 4°C	Anti-rabbit	2h, RT
Anti-collagen X	Abcam, ab58632	1/500	Overnight, 4°C	Anti-rabbit	2h, RT
<i>In vascular studies</i>					
Anti- α -actin	Sigma A5228	1/400	2h, RT	Anti-mouse	2h, RT
Anti-smMCH	BioMedical Technologies, BT-562	1/500	2h, RT	Anti-rabbit	2h, RT
Anti-GAPDH	Santa Cruz Biotechnology	1/500	2h, RT	Anti-mouse	2h, RT
Anti- α -tubulin	Sigma	1/500	2h, RT	Anti-mouse	2h, RT

2.3. RNA isolation

Cells and tissue were homogenized in buffer (RLT buffer containing 1% of β -mercaptoethanol) or crushed in liquid nitrogen and suspended in Isol-RNA lysis reagent respectively. This suspension was collected and kept at -80°C until RNA purification. Protocols and details are given in table III-7.

Table III-7. Protocols of RNA isolation.

Sample type	cells	tissues
Material quantity	6 well plate	< 100 mg
	3 washes with cold PBS	
Buffer volume	300 μl /well of RLT buffer containing 1% of β -mercaptoethanol	<i>1 ml of Isol-RNA Lysis Reagent (5 Prime, VWR International, Fontenay-sous-Bois, France)</i>
homogenization	Cell scraper Ten times up/down with 23 gauge needle.	- crushed in liquid nitrogen - tissue-lyser for 15 min
RNA extraction and purification	Qiagen Rneasy Mini Kit (Courtaboeuf, France)	Isol-RNA protocol
RNA concentration	spectrophotometric analysis using NanoDrop, 260nm	spectrophotometric analysis using NanoDrop, 260nm

2.4. RT- and real time qPCR

cDNAs were synthesized from 1 μg of total RNA (Thermo Scientific, Villebon sur Yvette, France). For real-time PCR analysis, 12.5 μl of SYBR Green PCR Master Mix (Marnes-la-Coquette, France), 300 nM of each sense and anti-sense primer (Table 8, 9 and 10), and 250 ng of cDNA were used in a total reaction volume of 25 μl .

The sequences of primers for rat, human and mouse genes of interest are shown in table III-8, III-9 and III-10, respectively. The gene encoding *RPS29*, which codes for a ribosomal protein, was shown previously to be invariable in TGF- β 1-challenged chondrocytes and used as a standard in cartilage studies and *GAPDH* in vascular studies. RT-qPCR was carried out using

an iCycler iQ thermal cycler (My iQ Single-Color Real-Time PCR Detection System, Bio-Rad, Marnes-la-Coquette, France) according to the manufacturer's instructions. Each sample was tested in duplicate. The methods of $2^{-\Delta\Delta C_t}$ was used for calculation.

$$2^{-\Delta\Delta C_t} = 2^{-[(C_{t, target gene} - C_{t, reference gene})_{sample} - (C_{t, target gene} - C_{t, reference gene})_{control}]}$$

Table III-8. Primer sequences used for RT-qPCR rat cDNA analysis (cartilage studies).

Marker		Sequences 5' – 3'	product length	T_m
Sox9	For	CTGAAGAAGGAGAGCGAGGA	84 bp	58.53
	Rev	GGTCCAGTCATAGCCCTTCA		58.80
Coll II	For	TCCCTCTGGTTCTGATGGTC	161 bp	58.43
	Rev	CTCTGTCTCCAGATGCACCA		59.10
Aggr	For	CAACCTCCTGGGTGTAAGGA	89 bp	58.64
	Rev	TGTAGCAGATGGCGTCGTAG		59.62
Coll X	For	TTCATCCCATACGCCATAAAG	103 bp	55.81
	Rev	AGGGACCTGGGTGTCCTC		59.88
MMP13	For	AGGCCTTCAGAAAAGCCTTC	226 bp	58.08
	Rev	GAGCTGCTTGTCAGGTTTC		59.12
SSAO	For	TTCAACCCTGCCACATCCA	79 bp	59.15
	Rev	GAGTTGCCGACACACACTG		59.07
RPS29	For	CTCTAACCGCCACGGTCTGA	174 bp	61.59
	Rev	ACTAGCATGATTGGTATCAC		52.46
ALP	For	GAACGTCAATTAACGGCTGA	50 bp	56.47
	Rev	CAGATGGGTGGGAAGAGGT		58.30
OPN	For	GGCTTACGGACTGAGGTCAA	78 bp	59.39
	Rev	AGGTCCTCATCTGTGGCATC		59.16

Table III-9. Primer sequences used for RT-qPCR human cDNA analysis (cartilage studies).

Marker		Sequences 5' – 3'	product length	T_m
RPS29	For	GGGTCACCAGCAGCTCGAGA	594 bp	64.02
	Rev	CAGACACGACAAGAGCGAGA		59.76
Coll X	For	TGCCCACAGGCATAAAAAGGCC	161 bp	65.70
	Rev	TGGTGGTCCAGAAGGACCTGGG		65.65
MMP13	For	TGGTGGTGATGAAGATGATTG	162 bp	56.68
	Rev	TCTAAGCCGAAGAAAGACTGC		58.04
OPN	For	GCCGAGGTGATAGTGTGGTT	125 bp	59.75
	Rev	ATTCAACTCCTCGCTTTCCA		57.14

Table III-10. Primer sequences used for RT-qPCR mouse cDNA analysis (vascular studies).

Marker		Sequences 5' – 3'	product length	T_m
GAPDH	For	AACTTTGGCATTGTGGAAGG	132 bp	56.79
	Rev	GGATGCAGGGATGATGTTCT		57.35
TNF α	For	GTAGCCACGTCGTAGCAAAC	118 bp	57.14
	Rev	CTGGCACCAGTGTGGTTGTC		54.55
IFN γ	For	GCCACGGCACAGTCATTGAAA	261 bp	62.01
	Rev	TCGCCTTGCTGTTGCTGAAGA		62.84
TGF β	For	AGCAACAATTCCTGGCGTTACCTT	221 bp	63.34
	Rev	TGGGCTCGTGGATCCACTTC		61.90
IL-10	For	GGCGCTGTCATCGATTCT	111 bp	58.32
	Rev	ATTCATTCATGGCCTTGTAGACAC		59.36

3. Specific methods

3.1. SSAO activity

3.1.1. Homogenates preparation for SSAO activity measurement

Cells and tissue were homogenized in a sodium phosphate buffer (80mM Na₂HPO₄, 20mM NaH₂PO₄, pH 7.4) respectively by sonication and crushed in liquid nitrogen respectively. Details are given in the table III-11. This suspension was collected and kept at -80°C until determination of the SSAO enzymatic activity by a radiometric assay.

Table III-11. The protocols of protein homogenate preparation.

Sample type	cells	tissues
Material quantity	1 T75	< 100 mg
	3 washes with cold PBS	
Buffer volume	500 µl / T75	30 µl/mg
Homogenization	Sonication 30s	- crushed in liquid nitrogen - tissue-lyser for 15 min

3.1.2. SSAO activity measurement

SSAO activity was determined using a radiochemical assay in tissue or cell homogenates in 100 mM sodium phosphate buffer (pH 7.4), with some modifications. The reaction was initiated by addition of 0.1 mM (0.1µCi) [7-¹⁴C]benzylamine hydrochloride (Perkin Elmer, NEC835050UC, Villebon sur Yvette, France) as the substrate for 30 min at 37°C and stopped with HCl. Incubations were carried out with 0.5 mM pargyline hydrochloride (a selective MAO inhibitor), and/or 1 mM semicarbazide hydrochloride (SSAO inhibitor). Aldehyde extraction was performed by addition of 1 ml of toluene/ethylacetate for 30 min at 37°C. After 1 min centrifugation at 7,500xg, the organic fraction was taken for [¹⁴C]aldehyde quantification using TRI-CARB 2100TR Liquid Scintillation Analyzer (Perkin Elmer, Zaventem, Belgium). Duplicates were made for each sample. SSAO enzyme activity (expressed in nmol/h/mg) was

calculated from the activity measured in the presence of pargyline minus that measured with pargyline and semicarbazide.

The SSAO enzyme activity was calculated from the equation:

$$\begin{aligned} \text{SSAO activity} &= (\text{activity in presence of pargyline}) \\ &- (\text{activity in presence of pargyline and semicarbazide}) \end{aligned}$$

Aldehyde extraction was performed by addition of 1 ml of toluene/ethylacetate for 30 min at 37°C with stirring every 10 min. After 1 min centrifugation at 7,500 g, aliquot (700 µl) of the organic fraction was taken for [¹⁴C]aldehyde quantification using TRI-CARB 2100TR Liquid Scintillation Analyser, A Packard Bioscience Company. Duplicates were made for each sample.

3.2. Measurement of 2-Deoxy-D-glucose uptake

Glucose transport was determined by measuring the uptake of 2-deoxy-D-glucose (2-DG) (sigma), a non metabolizable analogue of glucose.

Mature chondrocytes (days 21) cultivated in 24 well plates, in the absence or in the presence of 1µM LJP1586, were washed twice with 1 ml of warmed Krebs ringer (KRH) buffer without glucose. Then, chondrocytes were pre-incubated with 500µl of KRH without glucose containing 0.2 % bovine serum albumine (BSA) per well, 2h before the measurement of glucose uptake. Semicarbazide was added in some wells at a final concentration of 1 mM 1h 30 before the measurement of glucose uptake. Half an hour after SCZ, 1 mM BZM was added in some wells for 1h. Finally, 0.5 µCi/ml [1,2³H]-2-DG (Perkin Elmer, NEC835050UC, Villebon sur Yvette, France) with a specific activity of 28 Ci/mmol, at 37°C for 30 min. The reaction was stopped by removing the medium and washing 3 times by 1 ml of ice cold PBS. Cells were solubilized in 500µl of 0.2 % SDS. 400µl were taken to count radioactivity in the presence of 2.5 ml of scintillant. A positive control was obtained in treating cells for 24h hours with IL-1β 10 ng/ml. Results were expressed in dpm.

3.3. MTT

Cell viability

Cell viability was established by the MTT reduction assay (Sigma Aldrich, Schnendorf, Germany). 3.5 mg/ml MTT was added to 300 μ l of culture medium. After a 4 hour treatment at 37°C, the medium was removed, and DMSO (250 μ l) was added in each well in order to dissolve the blue formazan crystals formed by the mitochondrial dehydrogenases. The intensity of the product colour, measured at 550 - 620 nm with a multi-plate reader (50 μ l in a 96-well plate), was directly proportional to the number of living cells in the culture. For this assay quadruplicates were made for each culture condition.

3.4. Atherosclerotic lesion quantification in aorta

Aortas from 25 week-old *ApoE*^{-/-} and *ApoE*^{-/-}*SSAO*^{-/-} mice were excised and washed in a cold physiological serum. Tissues around the aortas were precisely dissected and discarded and the aortas were opened longitudinally. Then oil red O staining was performed. Briefly, aortas were incubated in 70% (v/v) ethanol during 5 minutes, subsequently staining of fatty streaks with oil red o solution during 20 minutes was executed. Following 5 minutes of aortas incubation in 70% (v/v) ethanol several water baths were carried out. Then aortas were mounted face up on slides in glycerol-gelatin mounting medium.

3.5. Atherosclerotic plaque quantification in the aortic sinus

The slides with tissue sections were incubated for 20 minutes at room temperature. Then the tissue section were covered by oil red O solution (1 gram of oil red O powder dissolved in 200 ml of izopropanol and diluted with 132 ml of distilled water). Subsequently, the slides were washed three times per 2 min in tap water and a counterstaining using haematoxylin was performed.

After three baths in tap water slides were mounted with mounting medium and plaques surface was quantified with Histolab software.

3.6. Measurement of cytokines

Protein extraction and atherosclerosis array

Aortas were homogenated in 200 µl buffer (Ray Biotech) complemented with a protease inhibitor cocktail (Roche, Mannheim, Germany). Equal amounts of protein from 7 tissue lysates samples were taken and mixed, if necessary samples were diluted with blocking buffer (Ray Biotech). Mouse atherosclerosis antibody array 5Ray Biotech was performed according to the manufacturer's instructions. Briefly, membranes were incubated with blocking buffer for 30 minutes at room temperature with gentle rotation (0.75 cycle/sec). Subsequently, membranes were incubated with 250 µg of proteins during 5 hours at room temperature with gentle rotation (in the same condition). Then two washings were effected, a first washing was performed by adding 2ml of buffer I into the well with the membrane and incubated 5 minutes and repeated three times. Second washing was equally preformed with buffer II and repeated twice. Following washing, membranes were incubated with a biotinylated antibody cocktail during 2 hours at room temperature with gentle rotation and the washing procedure was repeated. When buffer II was discarded 2 ml of 1x HRP-Streptavidin was added into each membrane and incubated overnight at 4°C. The following day, the washing procedure (buffer I and II) and chemiluminescence detection were executed. Membranes were incubated for 2 minutes in 500µl of detection buffer (detection buffer C mixed with detection buffer D (v/v)) and exposure was performed.

3.7. Mice genotyping

Mice were anesthetized with isoflurane and a section of the tail (~2mm long) was clipped off. A genotyping procedure was carried out using the Kapa mouse genotyping kit (Kapa Biosystems) accordingly to the manufacturer's indications. Briefly, DNA was extracted from the mouse tail by incubation it with KAPA Extract Enzyme Buffer supplemented with KAPA Express Extract ENZYME for 10 minutes at 75°C, followed by deactivation of the protease for 5 minutes at 95°C. PCR reaction was performed with 12.5 µl of KAPA2G Fast HotStart Genotyping Mix, 1µl of DNA from mouse tail and primers in final concentration 0.5µM (primers for VAP-1 WT: GCC CAC AAG GAA GAA GAC AC and CAA ACA CCA GGG ACA GAA CC; primers for KO: GGC TGC TGA TCT CGT TCT TC and TCT GGA TTC ATC GAC TGT GG). PCR was run in the following condition, initial denaturation for 3

minutes at 95°C followed by 3-step cycling: 15 seconds at 95°C, 15 seconds at 62°C and 30 seconds at 72°C repeated 35 times. After 5 minutes at 72°C of final extension, PCR products were analyzed directly in a 2% agarose TBE-gel containing 0.003% of ethidium bromide (v/v) and amplification products were visualized by UV exposition. 604 pb product was obtained for VAP^{-/-} mice and 405 pb was obtained for WT mice, both were heterozygous.

3.8. Experiments performed in collaboration

Peripheral bone marrow cell preparation

Bone marrow cells were obtained from the femur and tibia. PBMC were isolated and washed twice in ice-cold RPMI 1640 (Life Technologies). Femoral and tibial bones taken from donor CD45.1 C57BL/6 or ApoE^{-/-} mice were rinsed, and the residual muscle on the bones was carefully removed. Bone marrow cells were prepared by flushing the bones with RPMI 1640, and the cell suspension was filtered through nylon mesh to remove aggregates and washed once before transfusion. Cells in ficol were used for mouse injection (Figure III-1).

CD45 is a member of the Protein Tyrosine Phosphatase (PTP) family. Its intracellular (COOH-terminal) region contains two PTP catalytic domains, and the extracellular region is highly variable due to alternative splicing. The CD45 isoforms detected in the mouse are cell type-, maturation-, and activation state-specific. The CD45 antigen is an essential regulator of leukocyte activation and development. The CD45 isoforms play complex roles in T-cell and B-cell antigen receptor signal transduction.

In our experiments we used young mice ApoE^{-/-} and ApoE^{-/-}SSAO^{-/-} CD45.2. However PBMC injected to those mice were CD45.1 which allows us to recognize the differences in the cell distribution.

Flow cytometry

The FACS procedure as previously described in Taleb et al., (2007) was carried out. Briefly, cells were isolated from spleen, blood and thoracic aorta suspended in ice cold PBS buffer. Then 1*10⁶ cells (from spleen or aorta) or 50 µl of blood were placed into each well, then 50 µl of ice cold PBS per well was added. In next step, cells were labeled with fluorescein isothiocyanate (FITC)-conjugated anti-CD4 (BD Bioscience, 553047), APC-conjugated anti-

CD3 (eBioscience, 17-0031-83) or PercP-Cy5.5-conjugated anti-CD45.1 (BD Bioscience, 560580) antibodies. Then cells were incubated during 30 minutes at 4°C. Following incubation, cells were washed three times by centrifugation at 1500 rpm for 5 minutes and resuspend in 50 µl of in PBS buffer. The flow cytometry analysis were performed on the same day on an Epics XL flow cytometer (Beckman Coulter).

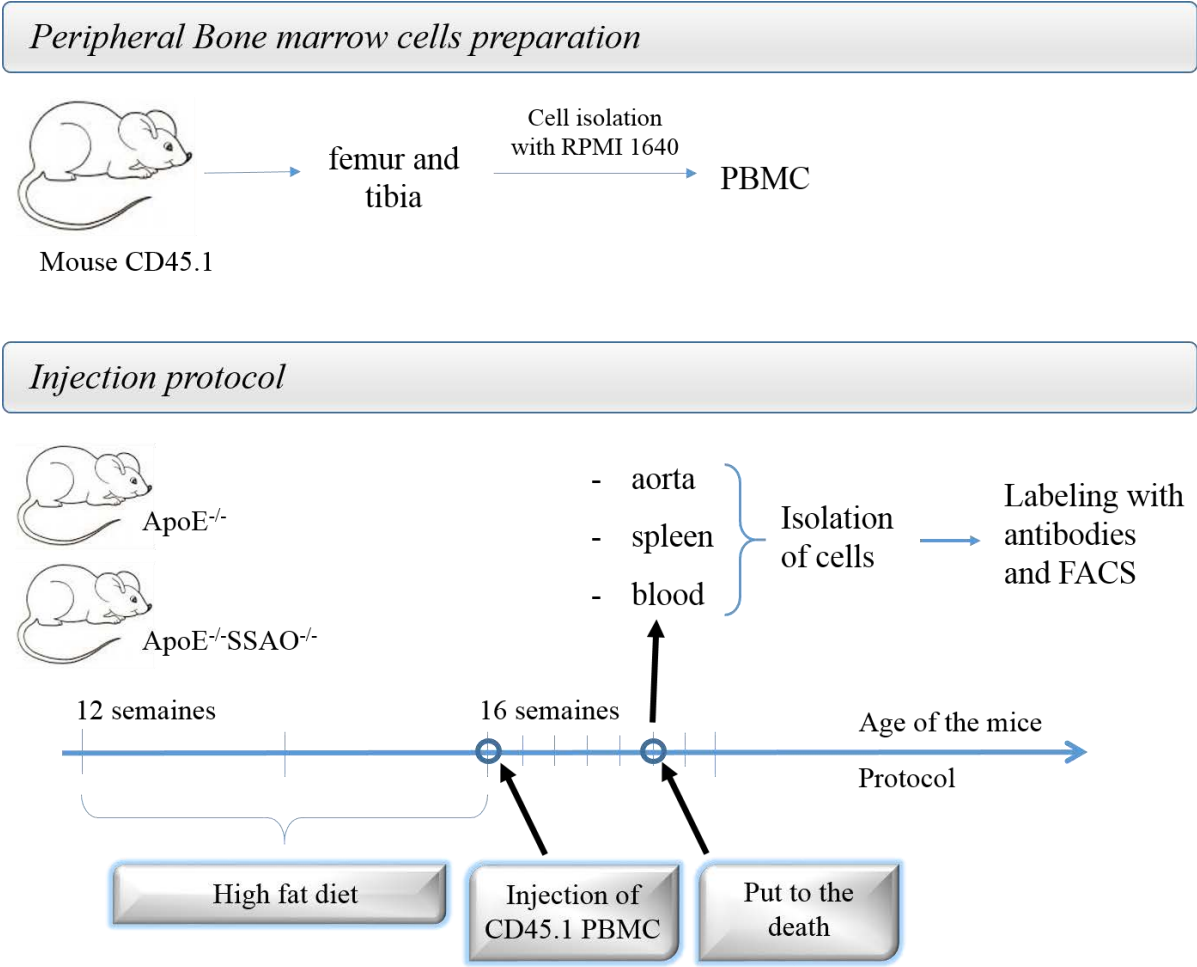


Figure III-1. Protocol of PBMC injection

3.9. Statistical analysis

All results represent the mean value ± SEM. All values were analysed by an Anova. P values less than 0.05 were considered significant. When results were significant, the different groups were compared by Fisher’s multiple-comparison test.

IV. Cartilage and chondrocyte differentiation

1. Hypothesis

There are many reports about the amine oxidases presence in cartilage and chondrogenic cell lines. Lyles *et al.*, in 1998 detected SSAO in rat cartilage, nevertheless they did not explore its role. Another amine oxidase from the same enzyme family, lysyl oxidase like-2 (LOXL2), was found in cartilage. Studies on its role have shown that inhibition of LOXL-2 enzymatic activity decreased ATDC5 (mouse immortalized chondrogenic cell line) hypertrophic differentiation (Iftikhar *et al.*, 2011).

The role of SSAO in adipocyte differentiation (Mercier *et al.*, 2001) and in glucose uptake during VSMC differentiation (El Hadri *et al.*, 2002) was already shown.

Thus we hypothesize that SSAO could play a role in chondrocyte terminal differentiation.

In addition, many articles have reported that the toxic components produced by the SSAO enzymatic reaction affect ECM components and tissue properties.

Our second hypothesis is that SSAO can be implicated in osteoarthritis development, where the terminal differentiation of chondrocytes is activated.

2. Objectives and strategies

In this work, we aimed (i) to confirm the presence of SSAO in cartilage in an active form, (ii) to find the relation between SSAO expression and chondrocyte terminal differentiation, and to demonstrate the role of SSAO in this process.

It was well described that SSAO is involved in the inflammatory response (Salmi et al., 2001a; 2001b and 2011) and its soluble form is abundantly present in blood serum in several diseases (Boomsma et al., 2003 and 2005). Marttila-Ichihara et al., (2006) have shown that inhibition of SSAO activity decreases the inflammatory status of arthritic paws. Moreover, it is known that non-physiological chondrocyte differentiation takes place during OA (Aigner et al., 1997; Martel-Pelletier et al., 1999). Thus, the second objective of this work was to demonstrate the presence of SSAO in OA of human cartilage.

This project had complementary approaches:

1) Presence of SSAO in the cartilage (ex vivo)

To confirm the presence of SSAO in cartilage, articular cartilage from Wistar rats was used to study:

- the expression of SSAO in cartilage (RT-qPCR and immunohistochemistry)
- the enzymatic activity of SSAO in cartilage and tissues used as positive controls (radiochemical assay)

in association with the cellular and morphologic aspects of cartilage (HES staining) and its proteoglycan content (Safranin O staining).

To check if SSAO could be regulated during OA, three independent human cartilage biopsies were analysed.

- The expression of SSAO in different graded diseased cartilage was measured by RT-qPCR and immunohistochemistry

- The enzymatic activity of SSAO in cartilage and tissues was used as positive controls (radiochemical assay)

in association with the cellular and morphologic aspect of cartilage (HES staining) and proteoglycan content (Safranin O staining)

- The expression of differentiation markers by chondrocytes (RT-qPCR and immunohistochemistry) as a function of the graded diseased cartilage.

2) *The role of SSAO in chondrocyte hypertrophic differentiation (in vitro)*

To characterise SSAO expression and activity during chondrocyte differentiation, we first had to established cell culture conditions using ATDC5 or chondrocytes from Wistar rats.

The phenotype throughout the cell culture (ATDC5 or rat chondrocytes) was evaluated by measuring:

- the expression of differentiation markers by (RT-qPCR)
- the expression of SSAO (RT-qPCR)
- the enzymatic activity of SSAO (radiochemical assay).

To investigate the involvement of SSAO in chondrocyte differentiation, the effect of a chronic SSAO stimulation by substrates or of chronic SSAO inactivation by selective inhibitors was evaluated on differentiation marker profiles in primary cell culture.

3) *SSAO expression and activity in OA rat cartilage (in vivo)*

To investigate the involvement of SSAO in cartilage degradation we used a MIA rat model and studied:

- the expression of terminal differentiation markers in diseased cartilage vs healthy cartilage (RT-qPCR)
- the enzymatic activity of SSAO (radiochemical assay)
- the expression of SSAO in cartilage (RT-qPCR and immunohistochemistry).

3. Results

3.1. The presence of SSAO in rat cartilage

In the first stage of our research, we localized SSAO in knee cartilage of Wistar rats.

Then we studied the level of SSAO expression and SSAO activity in cartilage from the knee and from the femoral head of Wistar rats.

3.1.1. SSAO expression in healthy cartilage of Wistar rats.

In order to confirm the expression of SSAO by chondrocytes we investigated the expression of SSAO in whole cartilage. Figure IV-1 shows a typical cartilage cross section of the knee joint. The cartilage matrix exhibited a good cellular and proteoglycan content as studied by hematoxylin/erythrosin/saffron (HES) and Safranin-O staining. Immunochemical staining using an anti-SSAO antibody revealed the presence of SSAO in the cartilage and in the sub-chondral bone. Staining was less pronounced in the cartilage, when compared to that of bone. This was probably due to the absence of vascularization in the cartilage matrix.

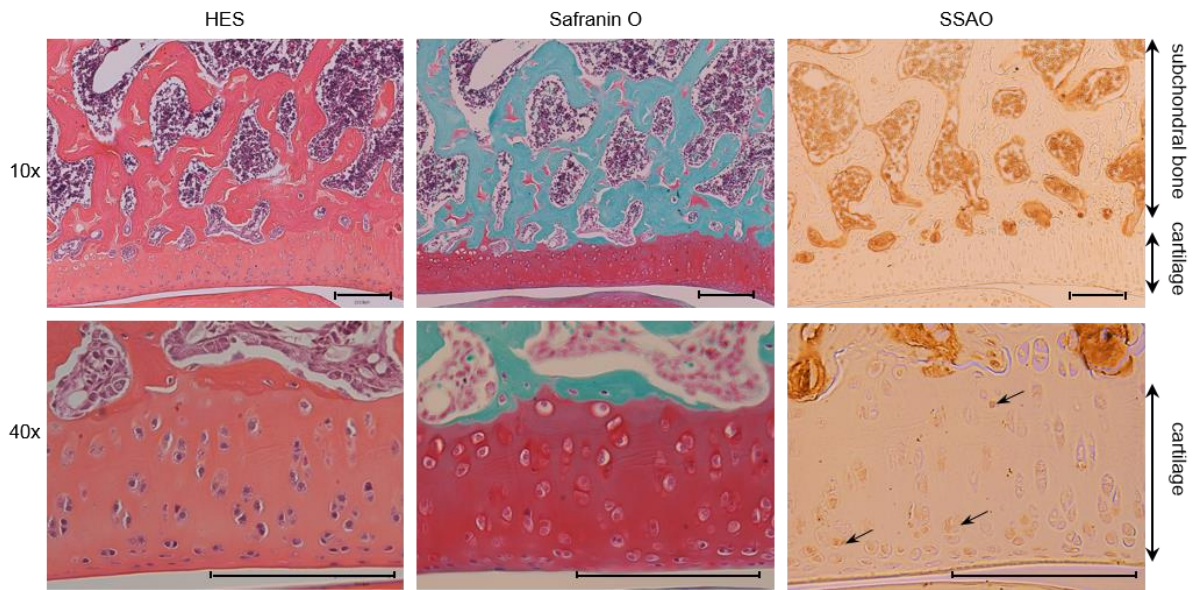


Figure IV-1. SSAO in articular cartilage of a normal rat. Histologic examination of the cross sections of Wistar rat knee joint stained with HES (morphology), Safranin O (proteoglycan content) and immunostained with an anti-SSAO antibody. Arrows indicate the expression of SSAO after immunostaining. The micrographs were taken using DMD 108 Leica microscope with original magnifications 10x and 40x. The scale represents 200 μ m.

Then the expression of SSAO at the gene level and SSAO activity were studied. SSAO was expressed in cartilage. However, it was significantly lower in femoral head cartilage (19 fold) and knee cartilage (33 fold), compared to adipose tissue used as a control (Fig. IV-2).

Enzyme activity, using radiolabeled benzylamine hydrochloride as the substrate, was detected in femoral head and knee cartilage. SSAO activity was only 3 fold (femoral head) and 7 fold (knee) lower than in adipose tissue.

Altogether, these experiments show that SSAO is expressed in an active form in articular cartilage, although at a lower level than in other tissues such as adipose tissue or aorta.

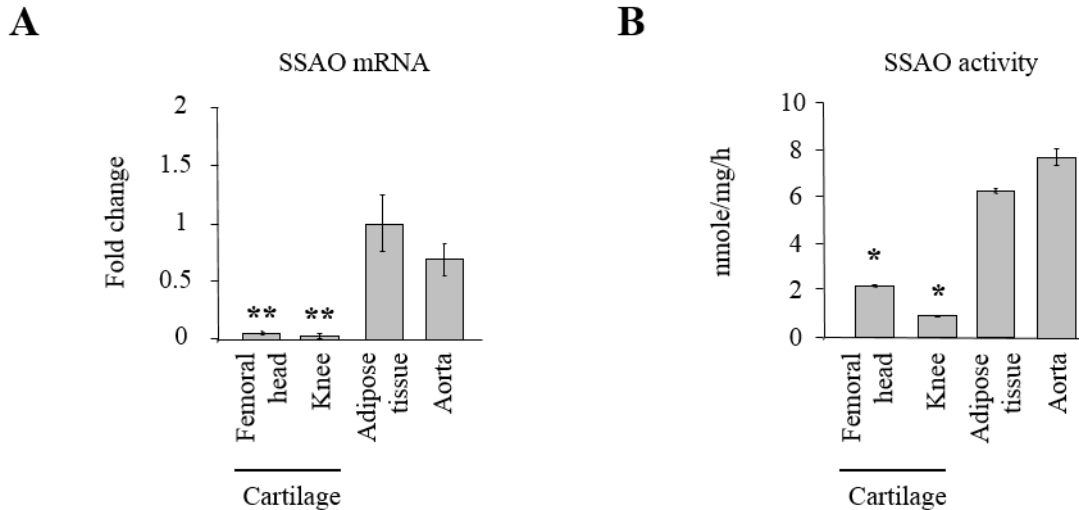


Figure IV-2. Expression and activity of SSAO in articular cartilage of rats. A: SSAO mRNA expression in cartilage, relatively to adipose tissue. Positive controls were run using thoracic aorta and adipose tissue. RPS29 mRNA expression was used as a gene reference. B: SSAO enzyme activity in cartilage, relatively to adipose tissue used as a positive control. The activity measured was 6.3 nmoles/h/mg. In the graphs, bars represent the mean value \pm SEM of three independent experiments performed in duplicate for real time qPCR and enzyme activity assay. Statistical significant P-values (* $P < 0.05$, ** $P < 0.01$) by Fisher's LDS Multiple-Comparison Test are shown in bold.

3.1.2. SSAO is present in the rat growth plate

Up until now nobody has suggested a role for SSAO in cartilage. Nevertheless, the function of SSAO in other tissues is well studied. Its role in adipocyte differentiation suggests that there is a possible role of SSAO in chondrocyte differentiation.

So the second stage of our research was to study the presence of SSAO in a femur growth plate from young Wistar rats (100-150g).

In the figure IV-3 we present a typical growth plate cartilage cross section. The cartilage matrix manifests a good cellularity (HES staining) and proteoglycan content (Safranin-O staining). The immunochemical staining revealed the presence of SSAO in chondrocytes in almost all zones of the growth plate.

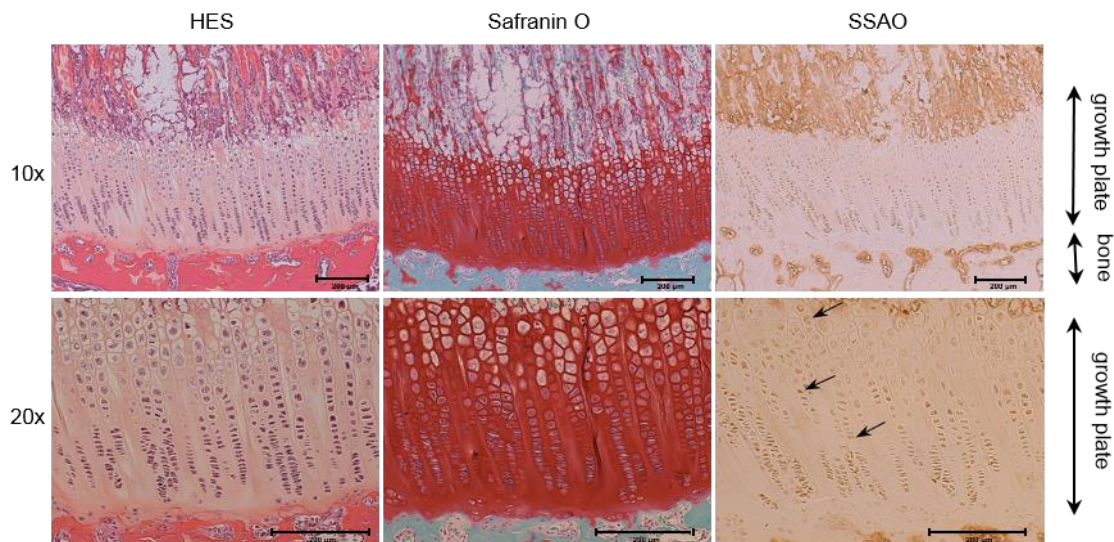


Figure IV-3. SSAO in the growth plate of a normal rat. Histologic examination of the cross sections of Wistar rat knee joint stained with HES (morphology), Safranin O (proteoglycan content) and immunostained with an anti-SSAO antibody. Arrows indicate the expression of SSAO after immunostaining. The micrographs were taken using DMD 108 Leica microscope with original magnifications 10x and 40x. The scale represents 200µm.

The results show that SSAO is expressed in the growth plate cartilage. Moreover, its amount seems to be higher than in articular cartilage examined in figure IV-1.

As SSAO is present in all zones of chondrocyte terminal differentiation, which is present in the growth plate, our hypothesis about implication of SSAO in chondrocytes hypertrophic differentiation has to be explored.

3.2. The role of SSAO in cartilage

The second stage of this work was to examine expression and activity of SSAO during chondrocyte terminal differentiation and to determine a possible role of SSAO in this process.

3.2.1. Model of chondrocyte terminal differentiation

For this purpose two models of chondrocyte differentiation have been used:

- the ATDC5 cell line which is derived from a mouse teratocarcinoma cells, and which exhibits a sequential development analogue for chondrocyte differentiation,
- rat chondrocytes.

3.2.1.1. ATDC5

ATDC5 were cultured in culture medium supplemented with 2% or 5% of FBS. In order to confirm their phenotype in culture, we have studied cell morphology and expression of chondrocyte markers: Sox9, collagen II and aggrecan, and terminal chondrocyte differentiation markers: collagen X, and MMP13.

In figure IV-4, the cells were observed under phase-contrast microscopy. At confluence stage (day 0) cells had a round shape and were similar to normal chondrocytes. At days 7, 14 and 21, the cells became progressively smaller, compared to day 0. At day 21, cells were not visible because of condensation degree.

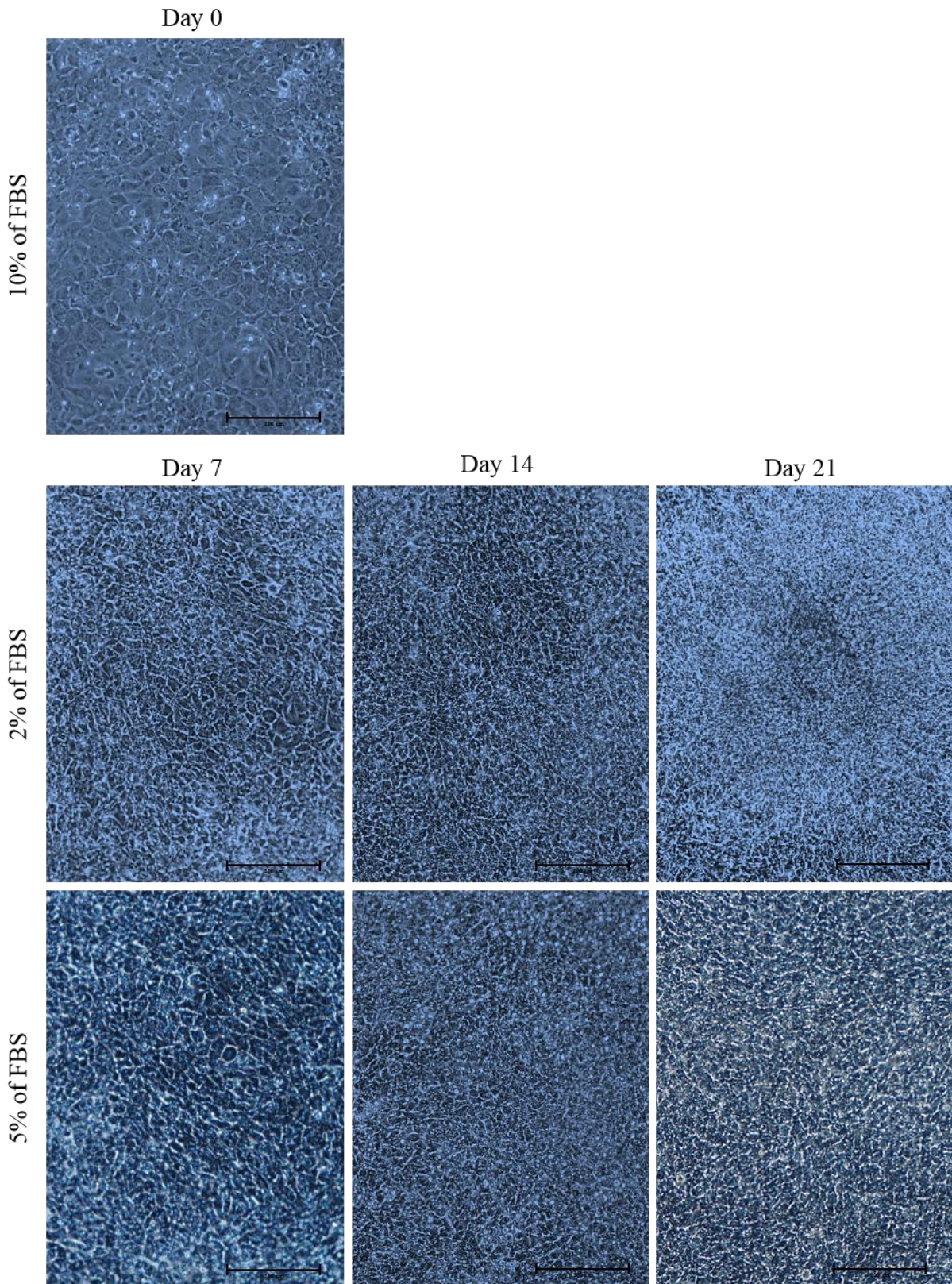


Figure IV-4. Phase-contrast microscopy of ATDC5 in culture. Representative photographs of ATDC5 in culture as a function of time and FBS concentrations. The micrographs were taken using Nikon Japan DIAPHOT 300 with magnification of 10x; the scale bar represents 200 μm.

In figure IV-5 expression of Sox9 by cells at different periods of time, from day 0 until day 21 is shown. Our results showed a 0.8 fold decrease in expression of Sox9 at day 21 in cells cultured in medium supplemented with 5% of FBS. Sox9 was transiently increased at day 7 with 2% FBS.

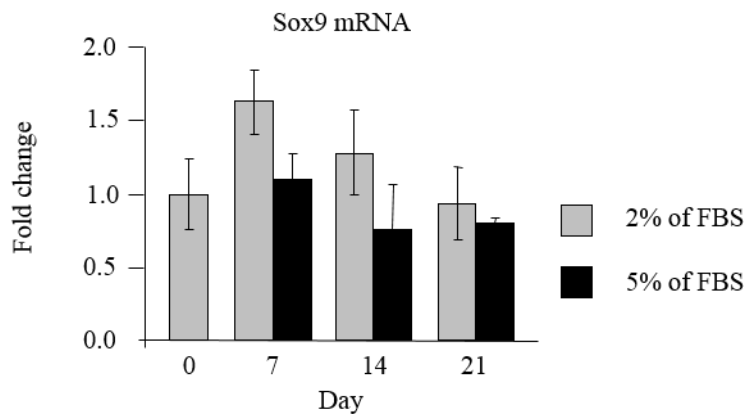


Figure IV-5. Sox9 expression during ATDC5 terminal differentiation. As a reference RPS29 mRNA expression was used. In the graph, bars represent the average value \pm SEM of three independent experiments performed in duplicate for real time qPCR. Statistics were calculated with respect to the day 0. Statistical significant P-values ($*P < 0.05$) by Student t-Test are shown in bold.

Subsequently we have studied the expression of chondrocyte markers like collagen II and aggrecan. Figure IV-6 shows that the expression of these two markers increased during culture time in 2% and 5% of FBS medium. ATDC5 are an immortalized cell line and not a primary cell culture. Therefore, differences in the expression of these markers were expected. Our results are similar to those reported by Iftikhar et al., (2011) in that respect.

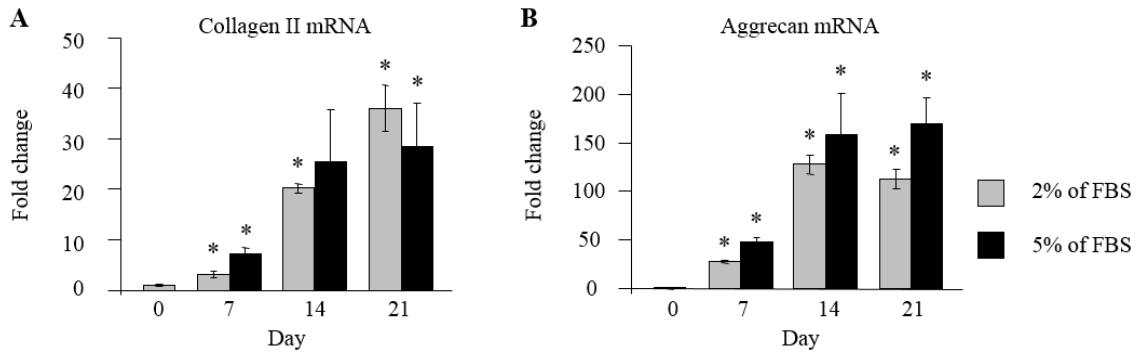


Figure IV-6. Collagen II (A) and aggrecan (B) mRNA expression. As a reference RPS29 mRNA expression was used. In the graphs, bars represent the average value \pm SEM of three independent experiments performed in duplicate for real time qPCR. Statistics were calculated with respect to the day 0. Statistical significant P-values ($*P < 0.05$) by Student t-Test are shown in bold.

Expression of terminal chondrocyte differentiation markers: collagen X and MMP13 is presented in figure IV-7. Collagen X, which is a marker of pre- and hypertrophic chondrocytes, increased as a function of time, reaching a maximum at day 21 (180 fold). This suggests that cells are in a pre-hypertrophic/hypertrophic stage. We did not notice differences in collagen X expression depending on different culture media. Nevertheless, expression of MMP13 by ATDC5 in culture was different depending on the content of FBS. Cells cultured with a medium containing 2% of FBS exhibited almost a 6 fold increase in MMP13 expression at day 21. In cells cultured with medium containing 5% of FBS expression of MMP13 increased almost 12 fold.

An increase in the MMP13 expression is necessary for the degradation of ECM components and future mineralization. The results presented in figure IV-7 suggest that cells have entered hypertrophy.

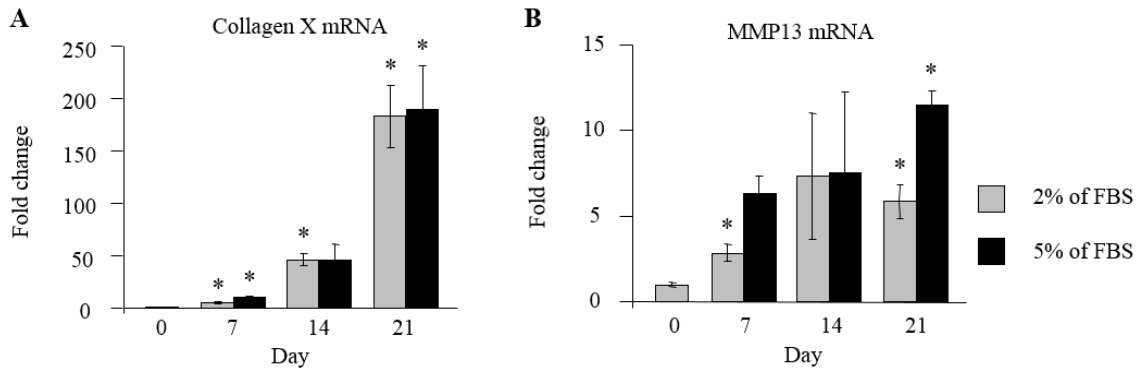


Figure IV-7. Collagen X (A) and MMP13 (B) mRNA expression. As a reference RPS29 mRNA expression was used. In the graphs, bars represent the average value \pm SEM of three independent experiments performed in duplicate for real time qPCR. Statistics were calculated with respect to the day 0. Statistical significant P-values ($*P < 0.05$) by Student t-Test are shown in bold.

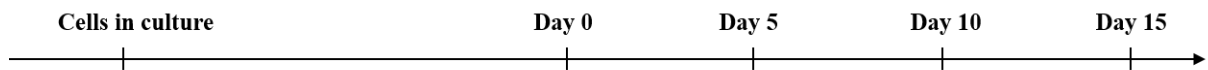
Final concentration of FBS in the culture medium had an influence on cell phenotype. Cells maintained with medium supplemented with 5%FBS presented a better profile of terminal cell differentiation.

Taken together, ATDC5 maintained in medium complemented with 5% of FBS presents a good profile of chondrocyte terminal differentiation described also in the literature. Nevertheless, the differences in tendency of chondrocyte marker expression between ATDC5 and chondrocytes in growth plates are remarkable.

For the determination of the *in vitro* chondrocyte differentiation model which will better reflect the process within the growth plate we have decided to perform a rat chondrocyte primary cell culture.

3.2.1.2. Primary rat chondrocytes culture

The second chondrocyte differentiation model used concerned rat chondrocytes cultured accordingly to the following protocols (Fig. IV-8):



Protocol	Medium	FBS	Supplements	Medium	FBS	Supplements	Supplements
1	DMEM/F12	10 %	P/S	DMEM/F12	10 %	P/S	-
2			L-glutamine	α -MEM	2 %	L-glutamine	+ insulin
3			Transferine	α -MEM	5 %	Transferine	+ insulin
			Sodium selenite			Sodium selenite	

Figure IV-8. The protocol used for chondrocytes differentiation.

In order to confirm the phenotype of chondrocytes in culture we studied cell morphology and the expression of chondrocyte markers: Sox9, collagen II and aggrecan and terminal chondrocyte differentiation markers: collagen X and MMP13.

As shown in figure IV-9, the cells were observed under phase-contrast microscopy. At day 0 (not shown but very similar to day 0, Fig. IV-4) cells had a round shape and presented chondrocyte-like morphology. During the differentiation protocols, depending on the culture medium, cells changed their morphology.

Cells cultured according to the first protocol (10% of FBS) were comparable at day 5 to those from day 0, then they presented a hypertrophic-like round shape at day 10. At day 15, cells lost the shape typical for chondrocytes.

Cells cultured with the second and the third differentiation protocols were larger at day 5 compared to cells from day 0. Since the 5th day until day 10 we noticed several cells with shapes characteristic of hypertrophy. Nevertheless, the cells at day 15 from these two cell cultures were not progressively larger but only similar to cells from the 5th day.

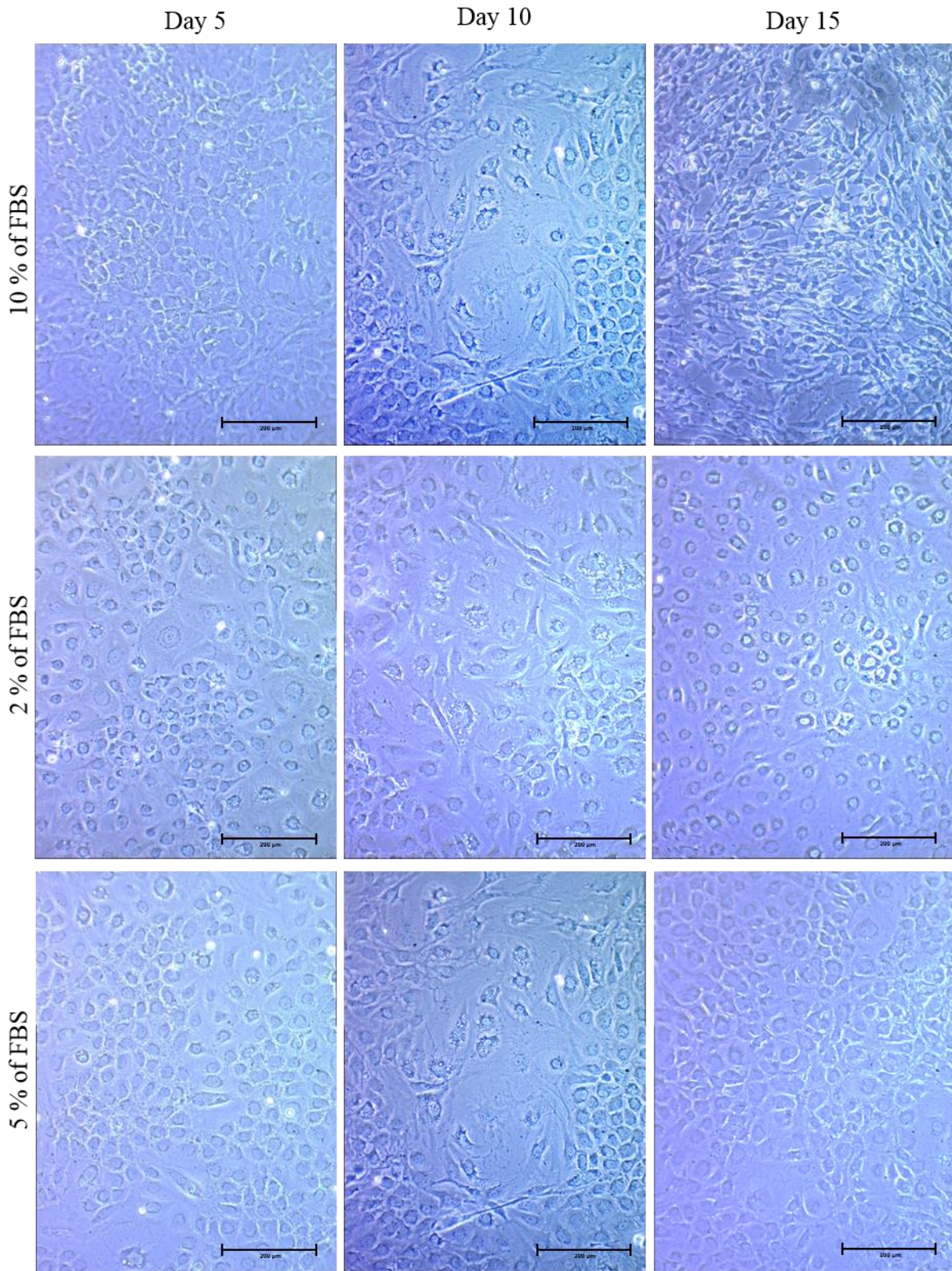


Figure IV-9. Phase-contrast microscopy of rat chondrocytes in culture as a function of time and culture medium composition. The micrographs were taken using Nikon Japan DIAPHOT 300 with magnification of 10x; the scale bar represents 200 μm .

In figure IV-10, Sox9 expression as a function of time is shown. Cells cultured according to protocol 1 (medium containing 10% of FBS) show an increase of Sox9 expression at the beginning of culture and, afterwards, a decrease with further culture time. Cells maintained with the second and third protocols (medium containing 2% or 5% of FBS) showed a decrease in Sox9 expression with culture time. Nevertheless, no large decrease was observed. This could be explained by a real decrease of Sox9 expression which had taken place just before day 0. To evaluate the protocols, expressions of other genes were also studied.

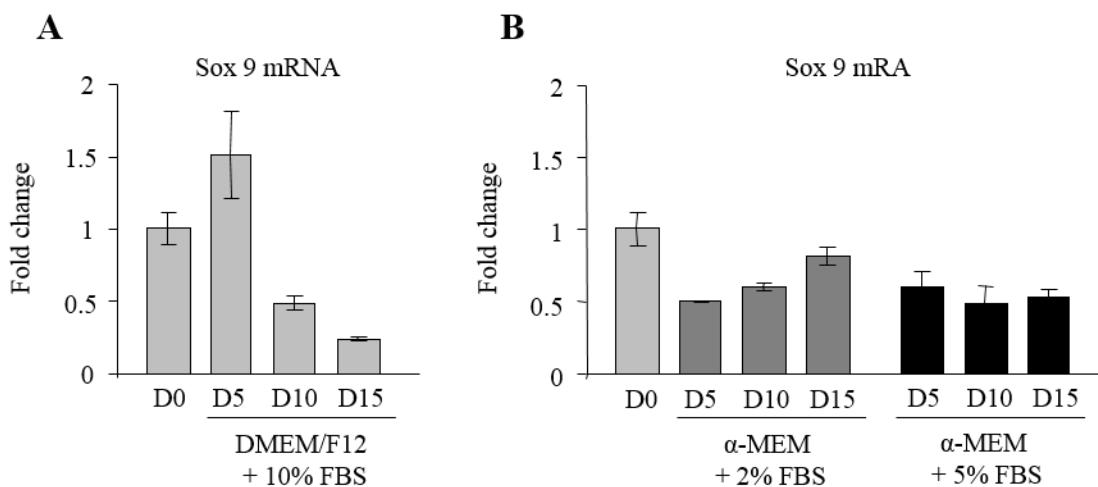


Figure IV-10. Sox9 expression in rat chondrocytes. As a reference RPS29 mRNA expression was used. In the graphs, bars represent experiments performed in duplicate for real time qPCR. Statistics are calculated with respect to the day 0. Statistical significant P-values ($*P < 0.05$) by Student t-Test are shown in bold.

Expression profiles of collagen I and II in three different cell culture conditions are presented in figure IV-11. Expression of collagen I in cells varied as a function of time of culture (Fig. IV-11A and IV-11B). This result cannot be unambiguously interpreted and cell dedifferentiation process cannot be excluded.

Cells cultured with the first protocol of chondrocytes differentiation (Fig. IV-11C) presented a decrease in collagen II expression from day 10 until day 15. Nonetheless, this is not an acceptable profile of terminal chondrocyte differentiation because of the increased expression of this marker at day 5 and 10 compared to day 0. Collagen II expression in cells from the two other cell cultures (Fig. IV-11D) were not consistent with the model of chondrocyte terminal differentiation presented in the literature.

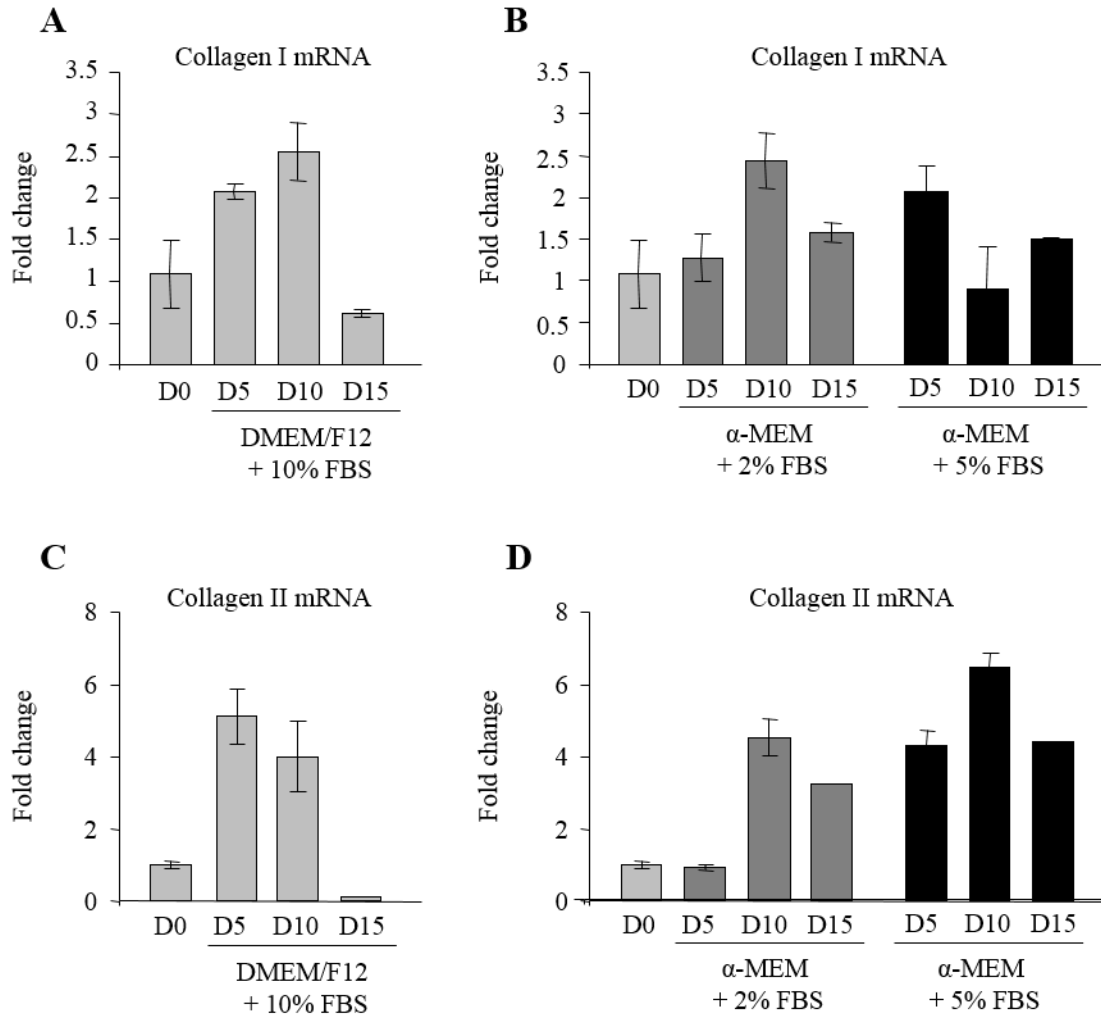


Figure IV-11. Collagen I and II expression in rat chondrocytes. As a reference RPS29 mRNA expression was used. In the graphs, bars represent experiments performed in duplicate for real time qPCR. Statistics are calculated with respect to the day 0. Statistical significant P-values (* $P < 0.05$) by Student t-Test are shown in bold.

Proteoglycan expression was studied (Fig. IV-12). In figure IV-12A and IV-12B aggrecan expression is presented. Cells maintained according to the first differentiation protocol (Fig. IV-12A) presented an expected decrease of aggrecan expression at day 10 and 15. In cells cultured according to the second and the third protocols (Fig. IV-12B) we have found the increase of aggrecan expression.

The decrease of aggrecan expression in chondrocytes undergoing terminal differentiation caused a short term expression of versican. Then its expression also decreased with the degree of terminal differentiation. In figure IV-12C and IV-12D versican expression as the function of time in three different cell culture conditions is presented. Cells in the first differentiation

protocol (Fig. IV-12C) showed an increase of versican expression at day 5 and day 15, but at day 10 we noticed expression on a level comparable with day 0. In the two other cell culture conditions (Fig. IV-12D), the expression of versican was not changed during the differentiation protocol.

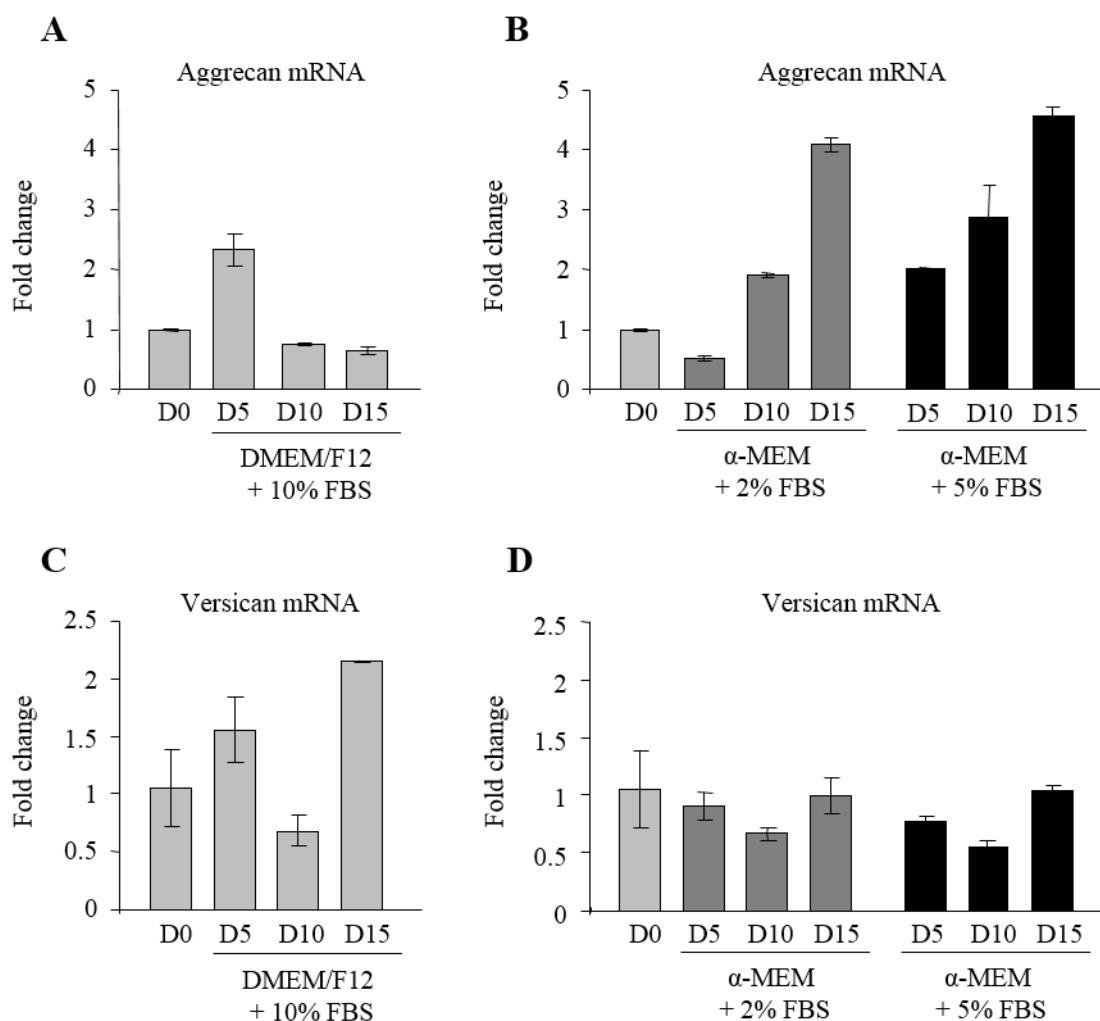


Figure IV-12. Aggrecan and versican expression in rat chondrocytes. As a reference RPS29 mRNA expression was used. In the graphs, bars represent experiments performed in duplicate for real time qPCR. Statistics are calculated with respect to the day 0. Statistical significant P-values (*P<0.05) by Student t-Test are shown in bold.

Then expression of chondrocyte prehypertrophy/hypertrophy markers like collagen X was measured (Fig. IV-13). In all cell cultures, an increase of this marker was observed, thus indicating that cells could reach the prehypertrophy stage. Moreover, cells in the first

differentiation medium (Fig. IV-13A), after the maximum of collagen X expression at day 10, presented a decrease of collagen X expression (day 15) which corresponds to the terminal hypertrophy stage, when chondrocytes decrease expression of extracellular matrix components.

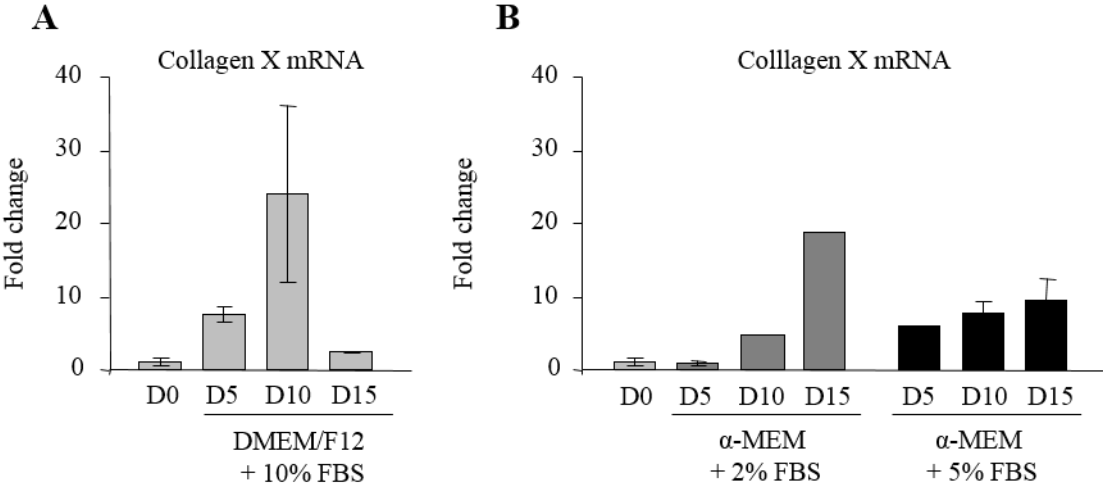
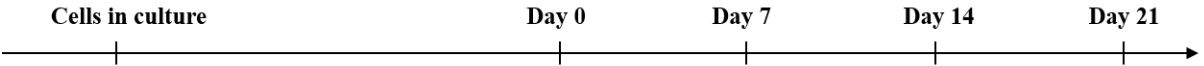


Figure IV-13. Collagen X expression in rat chondrocytes. As a reference RPS29 mRNA expression was used. In the graphs, bars represent experiments performed in duplicate for real time qPCR. Statistics are calculated with respect to the day 0. Statistical significant P-values (*P<0.05) by Student t-Test are shown in bold.

Taken together, chondrocytes maintained according to the first protocol of chondrocyte terminal differentiation have shown the best hypertrophic differentiation profile. Nevertheless, the expression of mature chondrocyte markers does not show clearly terminal differentiation. Because of this modification of this protocol was necessary.

For this purpose we have performed two chondrocyte cultures maintained according to the protocols presented in figure IV-14.



Protocol	Medium	FBS	Supplements	Medium	FBS	Supplements	Supplements

4	DMEM/F12	10 %	P/S	DMEM/F12	2%	P/S	-
5			L-glutamine			L-glutamine	+ Insulin
			Transferine			Transferine	+ Ascorbic acid
			Sodium selenite			Sodium selenite	

Figure IV-14. The chondrocyte culture protocols.

In figure IV-15, confluence stage (day 0) was observed using phase-contrast microscopy. Cells had a round shape as normal chondrocytes. At days 7, 14 and 21, chondrocytes treated with ins/asc, became progressively larger compared to day 0. At day 21, chondrocytes showed mostly a hypertrophic-like shape. Cells non-treated with ins/asc at day 7 were round and did not change in size, nonetheless at days 14 and 21 the cells are condensed and no longer visible.

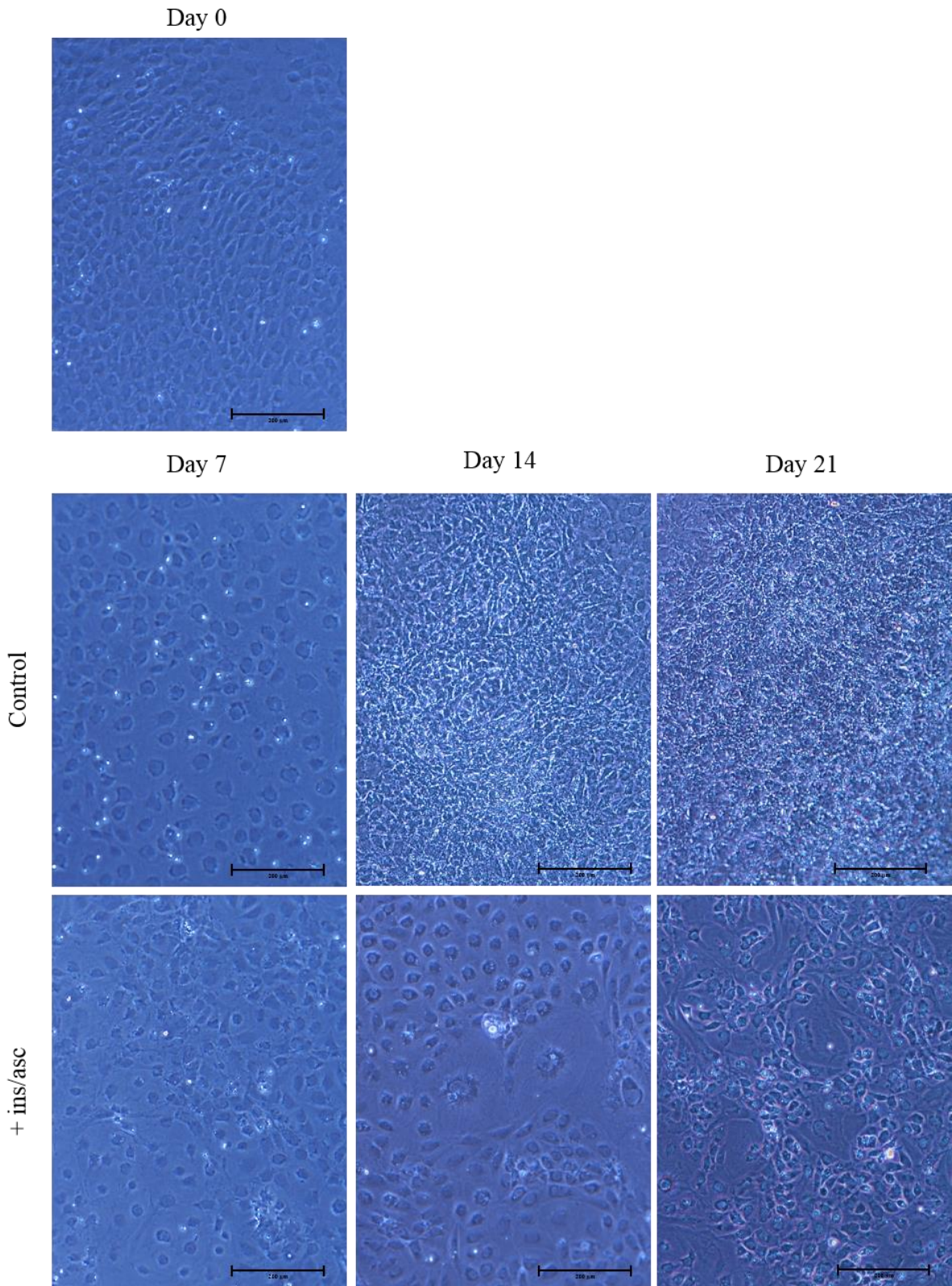


Figure IV-15. Phase-contrast microscopy of rat chondrocytes in culture, as a function of time and culture medium composition. The micrographs were taken using Nikon Japan DIAPHOT 300 with magnification of 10x; the scale bar represents 200 μm.

Figure IV-16 shows Sox9 expression as a function of time. The results clearly show that the expression level of the marker significantly decreased from day 0 until day 21 in the two different culture media indicating that cells entered the differentiation process.

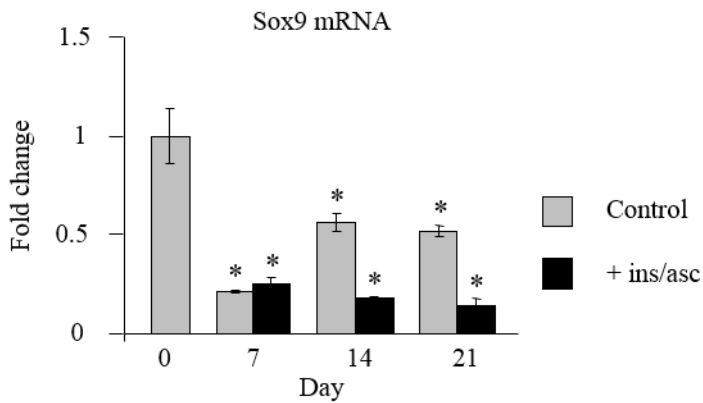


Figure IV-16. Sox9 expression in rat chondrocytes. As a reference RPS29 mRNA expression was used. In the graphs, bars represent the average value \pm SEM of three independent experiments performed in duplicate for real time qPCR. Statistics are calculated with respect to the day 0. Statistical significant P-values ($*P < 0.05$) by Student t-Test are shown in bold.

As figure IV-17A shows, the expression of collagen I was not changed whatever the culture condition, thus indicating that dedifferentiation did not take place.

Expression of collagen II decreased with the progression of cell differentiation (Fig. IV-17B), the maximum expression was observed at confluence day (day 0). In comparison with day 0, the expression of collagen II detected after 7 days presented a strong decline and this trend was further observed over the following days.

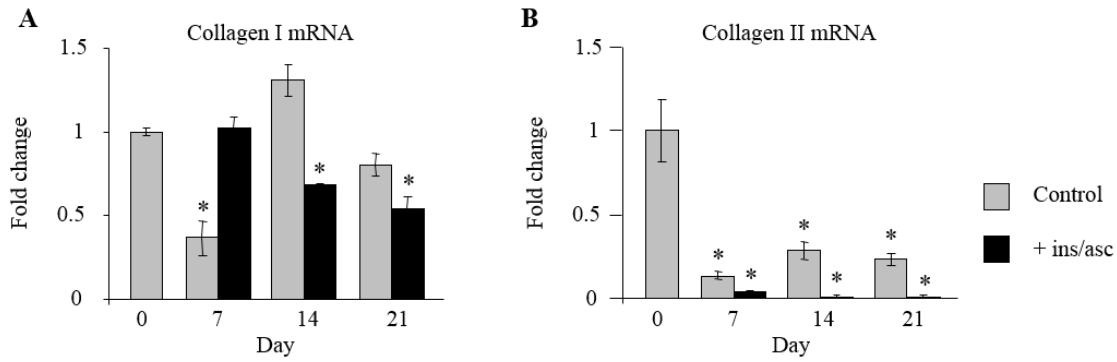


Figure IV-17. Collagen I (A) and II (B) expression during rat chondrocyte terminal differentiation. As a reference RPS29 mRNA expression was used. In the graphs, bars represent the average value \pm SEM of three independent experiments performed in duplicate for real time qPCR. Statistics are calculated with respect to the day 0. Statistical significant P-values ($*P < 0.05$) by Student t-Test are shown in bold.

Expression of genes encoding proteoglycans, like aggrecan and versican, were measured (Fig. IV-18). As expected, their expression decreased with time of culture indicating the progression of chondrocyte terminal differentiation.

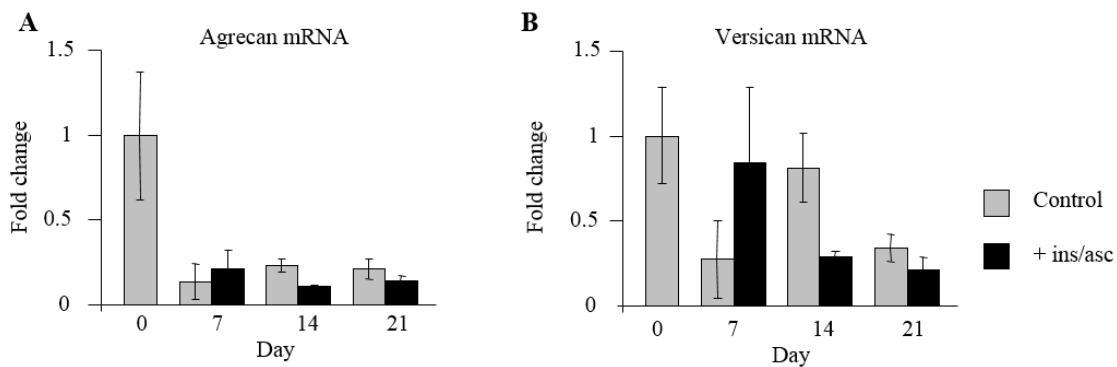


Figure IV-18. Aggrecan (A) and versican (B) expression during rat chondrocyte terminal differentiation. As a reference RPS29 mRNA expression was used. In the graphs, bars represent the average value \pm SEM of three independent experiments performed in duplicate for real time qPCR. Statistics are calculated with respect to the day 0. Statistical significant P-values ($*P < 0.05$) by Student t-Test are shown in bold.

Subsequently, the expression of pre- and hypertrophic markers was studied. Collagen X expression is presented in figure IV-19A. The maximum was obtained at day 21 (10 fold), where chondrocytes reached the pre-hypertrophic/hypertrophic stage, in medium supplemented or not with ins/asc. Expression of MMP13 (Fig. IV-19B) increased 8 fold at day 7 and 21 in cells maintained with supplemented medium (ins/asc). In cells cultured with medium not supplemented with ins/asc, we did not notice any increase of expression at day 7, nevertheless at day 21 cells reached hypertrophy.

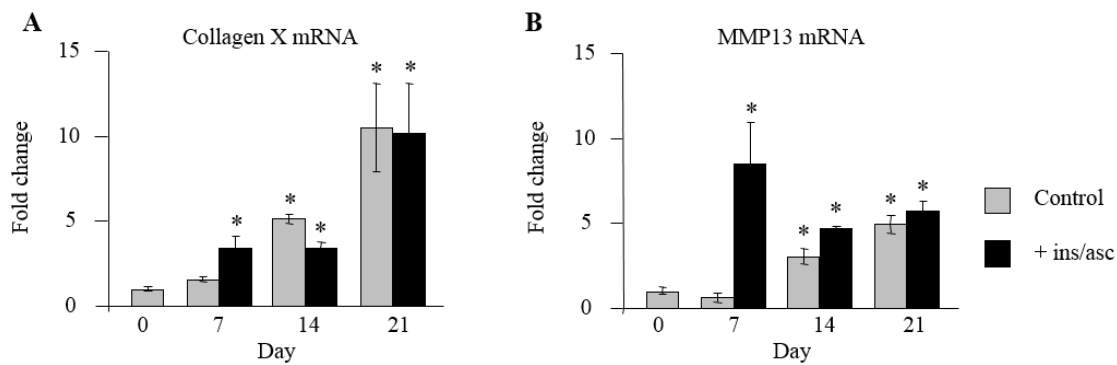


Figure IV-19. Collagen X (A) and MMP13 (B) expression during rat chondrocyte terminal differentiation. As a reference RPS29 mRNA expression was used. In the graphs, bars represent the average value \pm SEM of three independent experiments performed in duplicate for real time qPCR. Statistics are calculated with respect to the day 0. Statistical significant P-values (* $P < 0.05$) by Student t-Test are shown in bold.

3.2.2. Expression and enzyme activity of SSAO

Expression of the gene encoding SSAO and the activity of the enzyme were measured in the two differentiation cell models.

3.2.2.1. SSAO in ATDC5

Figure IV-20 presents SSAO expression in ATDC5 cultured in two differentiation media. Cells cultured with 2% FBS exhibited a 3 fold increase in SSAO expression at day 21 and cells cultured with 5% of FBS exhibited a 7 fold increase in SSAO expression in the same day.

Cells maintained with medium supplemented with 5% FBS presented a better profile of terminal cell differentiation with an important increase of SSAO expression.

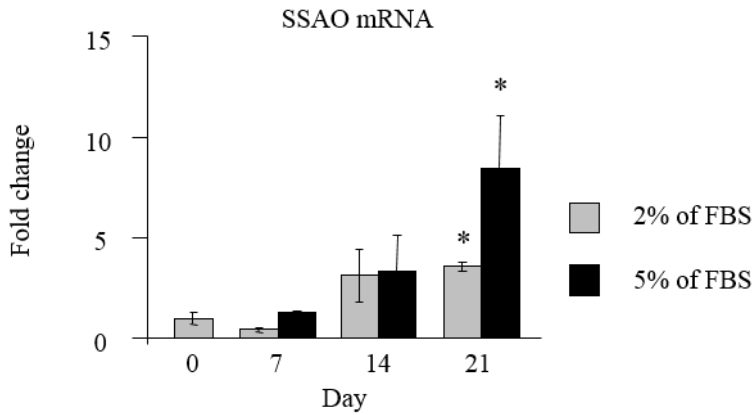


Figure IV-20. SSAO expression during rat chondrocyte terminal differentiation. As a reference RPS29 mRNA expression was used. In the graph, bars represent the average value \pm SEM of three independent experiments performed in duplicate for real time qPCR. Statistics are calculated with respect to the day 0. Statistical significant P-values (* $P < 0.05$) by Student t-Test are shown in bold.

3.2.2.2. SSAO expression and activity during primary chondrocyte differentiation.

Figure IV-21 presents the expression and the enzymatic activity of as a function of time. A 3 fold increase of SSAO expression by cells treated with ins/asc, from day 0 until day 7 was observed. From day 7 until 21, cells expressed SSAO constantly. Non-treated cells expressed SSAO constantly from day 0 until day 21.

Then, SSAO activity was measured. At day 0 we did not detect SSAO activity in chondrocytes. Cells non-treated with ins/asc showed SSAO activity at days 7 and 21. Cells treated by ins/asc showed SSAO activity at days 7 and 14, and in those cells enzymatic activity of SSAO was higher than in cells non-treated with ins/asc.

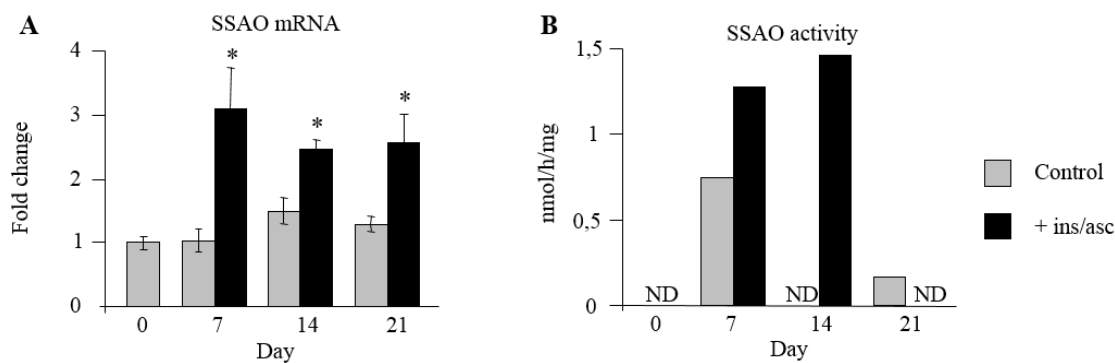


Figure IV-21. SSAO expression and activity during rat chondrocyte terminal differentiation. A: SSAO mRNA expression. As a reference RPS29 mRNA expression was used. In graph A, bars represent the average value \pm SEM of three independent experiments performed in duplicate for real time qPCR. B: SSAO enzymatic activity at day 7, 14 and 21. In graph B, bars represent the one experiment performed in duplicate for each sample. Statistics are calculated with respect to the day 0. Statistical significant P-values ($*P < 0.05$) by Student t-Test are shown in bold.

Then, we selected the chondrocyte hypertrophic differentiation protocol *in vitro* with the best pattern of marker expression and SSAO expression in the active form. Cells cultured according to the fifth protocol (DMEM/F12, 2% of FBS, P/S, L-glutamine, sodium selenite, transferrin, insulin and ascorbic acid) underwent hypertrophic chondrocyte differentiation.

The number of cells isolated from rat femoral head articular cartilage was limited, and the initial passage (P0) did not allow significantly to increase the number of cells. Thus we verified if for our studies it was possible to use rat chondrocytes from passages 2, 3, 4, and 5. For this purpose we established rat chondrocyte cultures for passages 1 to 5 and we studied the expression of the main chondrocyte markers (Sox9 and collagen II) and the main hypertrophic markers (collagen X and MMP13). Then the expression level of markers was compared to day 0 from passage 1. We had difficulties with the culture of cells from passages 4 and 5. At day 15 for passage 4, and at day 9 for passage 5 we noticed an increase in the death of cells in the media, thus we stopped the culture at these days.

In figure IV-22 expression of chondrocyte markers is presented. Sox9 expression decreased significantly during culture only in cells from passage 1 (Fig. IV-22A). In other passages the

expression of Sox9 was not changed during culture. In cells from passage 4 we noticed a significant increase in Sox9 expression. This result indicated that only the first passage of chondrocytes was acceptable for our studies. Nevertheless, we looked also at the expression of collagen II, as presented in figure IV-22B. The expression of collagen II decreased in culture time in cells from passages 1, 2 and 3. In cells from passage 4, the level of collagen II was not changed during culture time, and in cells from passage 5 we observed a significant increase in collagen II at day 9.

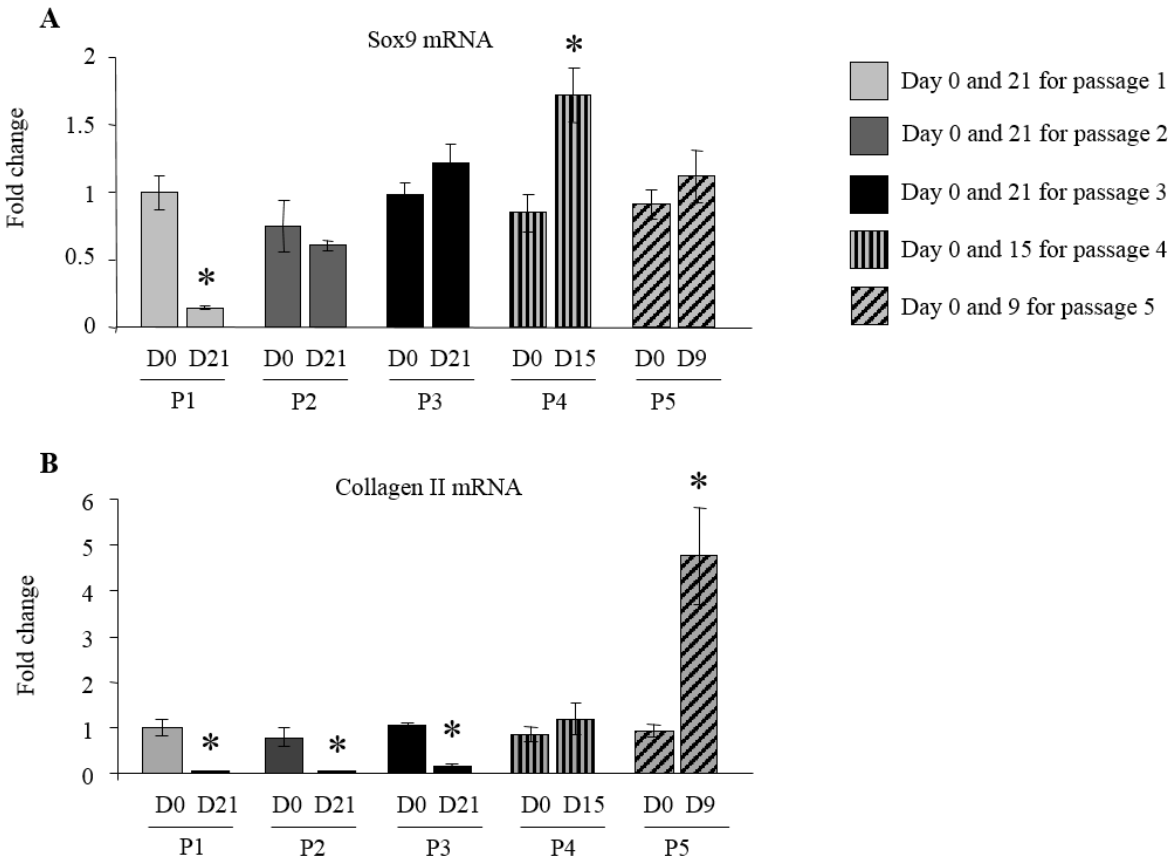


Figure IV-22. Sox9 (A) and collagen II (B) expression during rat chondrocyte terminal differentiation. As a reference RPS29 mRNA expression was used. In the graphs, bars represent the average value \pm SEM of three independent experiments performed in duplicate for real time qPCR. Statistics are calculated with respect to the day 0. Statistical significant P-values ($*P < 0.05$) by Student t-Test are shown in bold.

The expression of prehypertrophy and hypertrophy markers is presented in figure IV-23. A significant increase of collagen X expression was found in cells from passages 3 and 5 (Fig. IV-23A). In previous studies in cells from passage 1, we have found a significant increase of

collagen X expression. Nevertheless, we did not find this tendency in this cell culture, so we can suspect that the maximum of collagen X expression was before day 21.

Then we studied the second important hypertrophy marker, matrix metalloproteinase 13 (Fig. IV-23B). We noticed a significant matrix metalloproteinase 13 expression in cells from almost all different passages. Nonetheless, we can interpret these results only in combination with other marker expressions. Thus only cells from the first passage underwent hypertrophic differentiation during culture time.

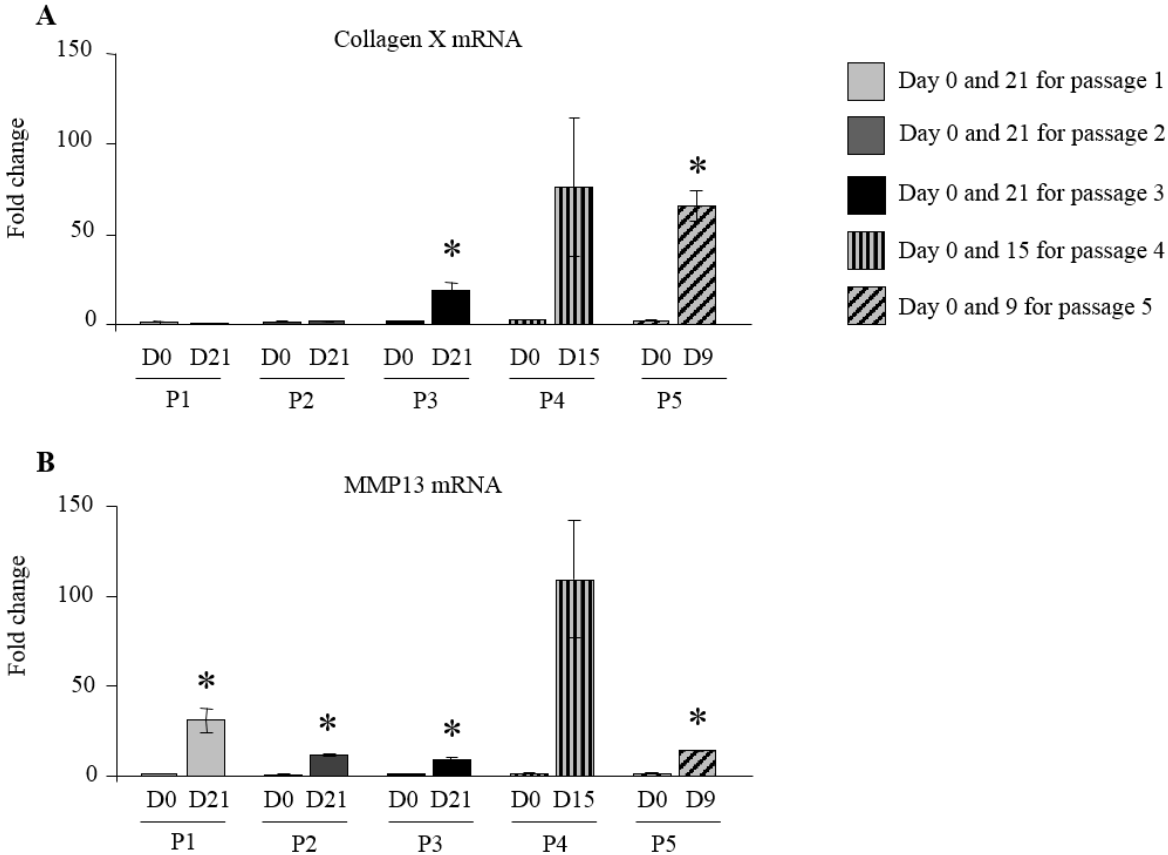


Figure IV-23. Collagen X (A) and MMP13 (B) expression during rat chondrocyte terminal differentiation. As a reference RPS29 mRNA expression was used. In the graphs, bars represent the average value \pm SEM of three independent experiments performed in duplicate for real time qPCR. Statistics are calculated with respect to the day 0. Statistical significant P-values ($*P < 0.05$) by Student t-Test are shown in bold.

The results presented confirmed that in our experiments we can use the first passage of rat chondrocytes. Thus, in order to confirm the protocol of terminal chondrocyte differentiation

with a significant increase in SSAO expression and in activity we performed four times the chondrocyte cultures according to the fifth protocol. The results presented below have been obtained from four independent cell cultures made in sextuplicate for each culture and analysis made in duplicate for each sample.

In figure IV-24A, chondrocytes morphology was observed under phase-contrast microscopy. As in a previous study, chondrocytes at the confluence stage were round. Then at days 7, 14 and 21, with time of differentiation cells became progressively larger. Chondrocytes at day 21 were characterized by cells with a hypertrophic-like shape.

Chondrocyte differentiation marker expression is present in figure IV-24B. The significant decrease of Sox9, collagen II and aggrecan expression indicated that chondrocytes lost their phenotype and entered the differentiation process. The increase of collagen X and matrix metalloproteinase expression indicated that chondrocytes reached hypertrophy. Moreover, we studied alkaline phosphatase and osteopontin expression which are necessary in terminal chondrocyte differentiation and indicate terminal hypertrophy and signal the mineralization process. Significant increases in alkaline phosphatase and osteopontin expressions show that cells are in the terminal phase of hypertrophy.

SSAO expression and its activity are shown in figure IV-24C and IV-24D, respectively. We confirm that during chondrocyte hypertrophic differentiation SSAO expression and activity are increased.

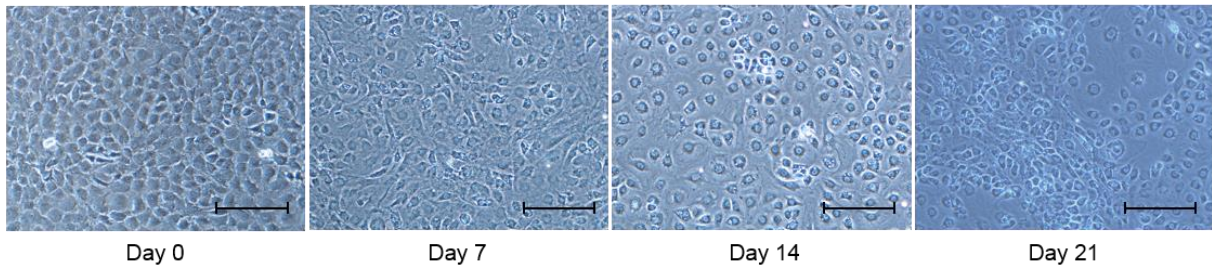
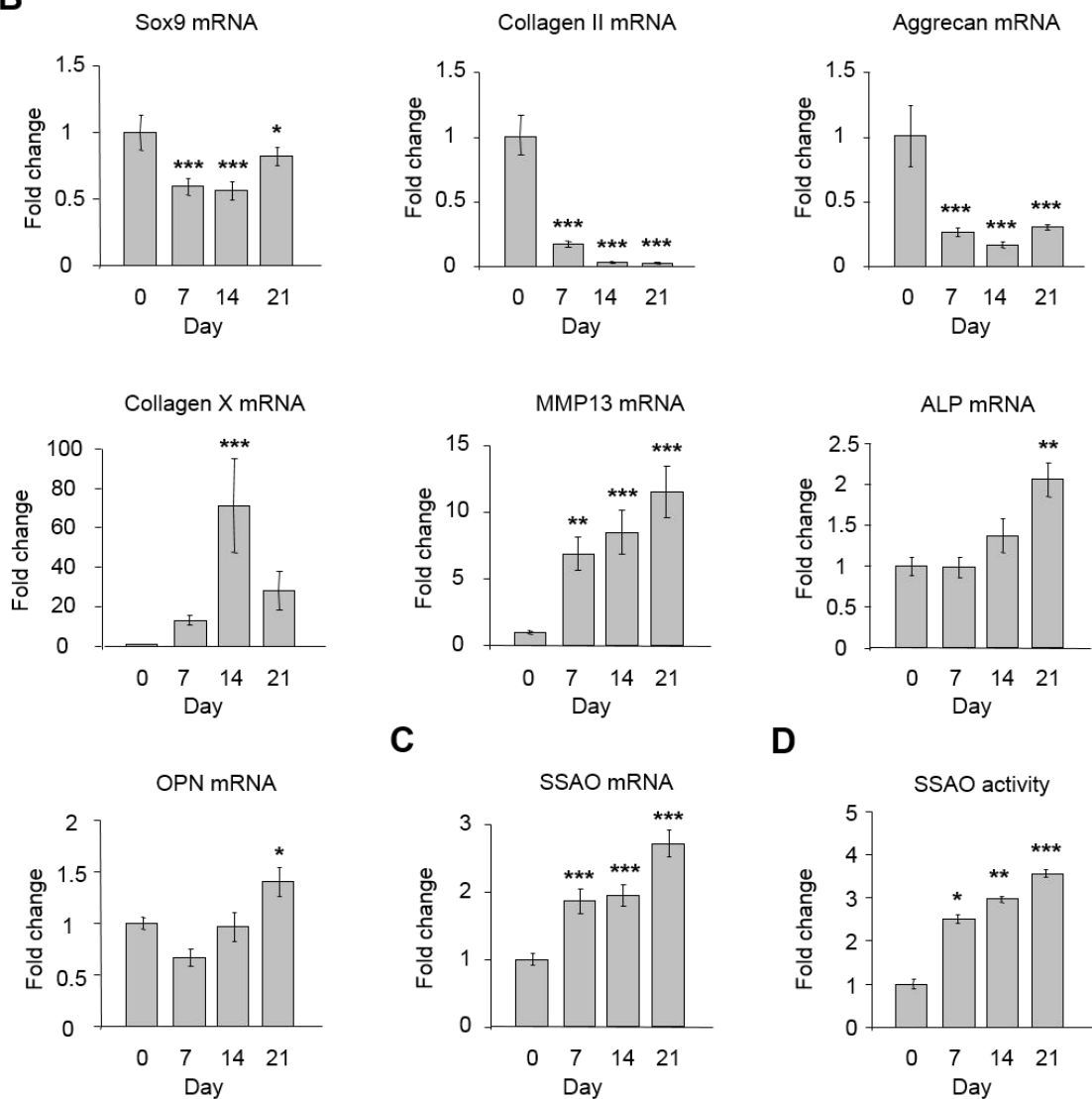
A**B**

Figure IV-24. Expression of SSAO as a function of terminal cell differentiation in primary chondrocyte culture. Rat chondrocytes were cultured from confluence from day 0 until day 21 in a differentiation medium containing insulin/ascorbate. Differentiation of chondrocytes was followed by the determination of mRNA expression of differentiation markers at day 7, 14 and 21, relatively to day 0. A: Representative images of chondrocytes in culture during differentiation protocol. The micrographs were taken using Nikon Japan DIAPHOT 300 with original magnification 10x and the scale present on the micrographs represent 200 μ m. B: mRNA expression of

chondrocyte differentiation markers: Sox 9, collagen II, matrix metalloproteinase 13, alkaline phosphatase and osteopontin. As a reference RP29 mRNA expression was used. The expression and enzyme activity of SSAO were concomitantly measured. C: SSAO mRNA expression at day 7, 14 and 21, relatively to day 0. D: SSAO enzyme activity at day 7, 14 and 21, relatively to day 0 (0.3 nmole/h/mg). In the graphs, bars represent the average value \pm SEM of twenty four (day: 0, 7 and 14) or eighteen (day 21) independent experiments performed in duplicate for real time qPCR and five (day 0, 7 and 14) or four (day 21) independent experiments performed in duplicate for enzyme activity assay. Statistics are calculated with respect to the day 0. Statistical significant P-values (*P<0.05, **P<0.01, ***P<0.001) by Fisher's LDS Multiple-Comparison Test are shown in bold.

Taken together, these results show that our model of hypertrophic differentiation of rat chondrocytes *in vitro* is characterized by

- a decrease of chondrocyte marker expression eg Sox9, collagen II and aggrecan
- an increase of hypertrophic chondrocyte marker expression eg collagen X, matrix metalloproteinase 13
- an increase of late hypertrophic chondrocyte marker expression eg alkaline phosphatase and osteopontine
- an increase in SSAO expression and activity in relation to the degree of differentiation

3.2.3. Effect of SSAO inhibition on terminal chondrocyte differentiation

Rat chondrocytes in the established and well characterized *in vitro* model of terminal differentiation were treated with different concentrations of LJP1586 [Z-3-Fluoro-2-(4-methoxybenzyl)allylamine hydrochloride], a selective SSAO inhibitor, and compared with the non-treated cells.

In order to confirm that LJP1586 did not affect chondrocyte viability and did not provoke cell death we performed a MTT assay which is shown in figure IV-25. The results show that LJP1586 did not affect viability of chondrocytes, moreover viability of cells treated with 1 μ M LJP1586 at day 21 increased significantly suggesting a delay in terminal differentiation.

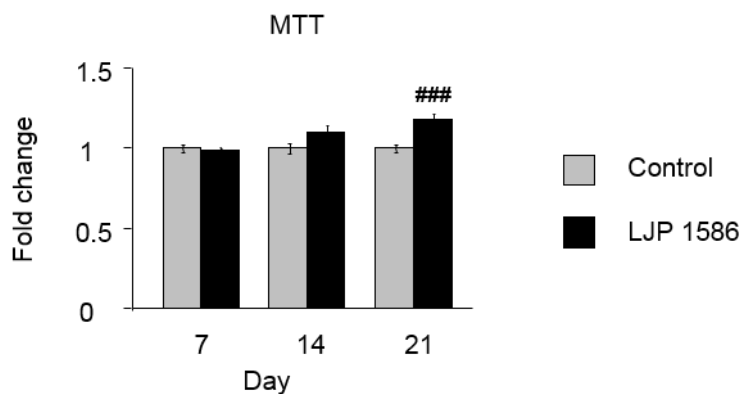


Figure IV-25. Cell viability. Cell viability was determined by MTT reduction at day 7, 14 and 21, relatively to non-treated cells. Chondrocytes were treated (black bars) or not (gray bars) with 1 μ M LJP 1586, [Z-3-Fluoro-2-(4-methoxybenzyl)allylamine hydrochloride] as selective SSAO inhibitor, from day 0 until day 21. Bars represent the average value \pm SEM of four independent experiments performed in duplicate. Statistics are calculated with respect to the day 0 (*) or non treated cells (#). Statistical significant P-values (*or # P<0.05, ** or ## P<0.01, *** or ### P<0.001) by Fisher's LDS Multiple-Comparison Test are shown in bold.

Then the efficacy of LJP1586 was confirmed by SSAO activity measurement. Cells treated with LJP did not show any detectable SSAO activity (Fig. IV-26), thus indicating that the 1 μ M concentration of LJP used in this study inhibited completely SSAO activity. Cells non-treated with LJP1586 exhibited an activity which linearly increased from day 0 until day 21.

Subsequently SSAO expression was studied. As expected, LJP inhibits activity of protein but has no effect on the transcription level (Fig. IV-26).

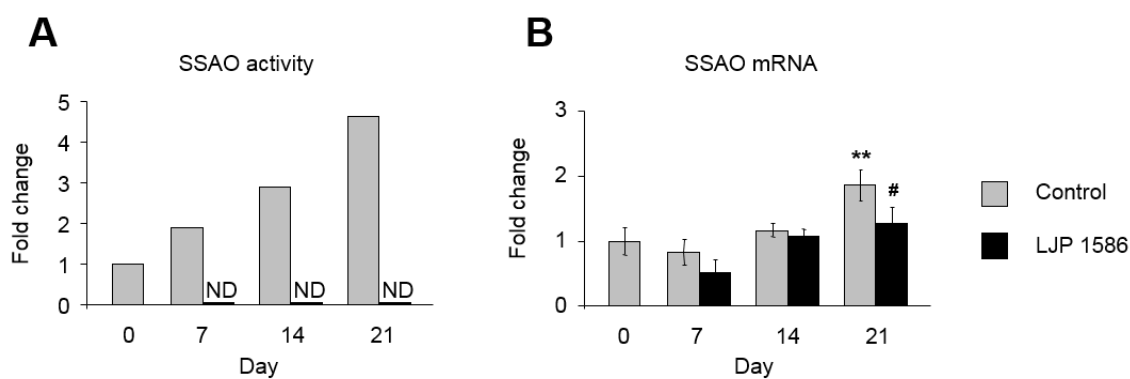


Figure IV-26. SSAO activity and SSAO mRNA expression. Chondrocytes were treated (black bars) or not (grey bars) with 1 μ M LJP 1586, [Z-3-Fluoro-2-(4-methoxybenzyl)allylamine hydrochloride] as selective SSAO inhibitor, from day 0 until day 21. A: SSAO enzyme activity at day 7, 14 and 21, relatively to day 0 (1.4 nmole/h/mg). One experiment was performed in duplicate for the enzyme activity assay to confirm efficacy of LJP 1586. B: SSAO mRNA expression at day 7, 14 and 21, relatively to day 0. Bars represent the average value \pm SEM of six independent experiments performed in duplicate for real time qPCR. Statistics are calculated with respect to the day 0 (*) or non-treated cells (#). Statistical significant P-values (*or # P<0.05, ** or ## P<0.01, *** or ### P<0.001) by Fisher's LDS Multiple-Comparison Test are shown in bold.

Figure IV-27 shows expression of late markers of chondrocyte hypertrophic differentiation, collagen X, MMP13, ALP and OPN respectively, by chondrocytes treated with LJP 1586, [Z-3-Fluoro-2-(4-methoxybenzyl)allylamine hydrochloride].

Collagen X is one of the most important markers of the pre-hypertrophic state of chondrocytes. It is known that its expression increases in pre-hypertrophic and hypertrophic chondrocytes and decreases when chondrocytes reach the terminal hypertrophy stage. In the presented results, a significant increase of collagen X expression in day 7 and day 14 by chondrocytes treated or not with LJP 1586 is seen. Then a significant decrease of collagen X expression was observed only in chondrocytes with the active form of SSAO (non-treated cells). Chondrocytes treated with LJP 1586 reached the maximum of collagen X expression on 14th day and then its decrease was not significant indicating that cells did not achieve the terminal stage of hypertrophy.

Then, we studied the expression of MMP13 in cells treated or not with LJP 1586. In the case of non-treated cells, expression of MMP13 significantly increased from day 7 until day 21. In contrast, cells treated by LJP 1586 presented a significant increase of MMP13 expression on

day 14 but this tendency was not maintained until day 21, thus confirming our hypothesis that inhibition of SSAO delays terminal chondrocyte hypertrophy.

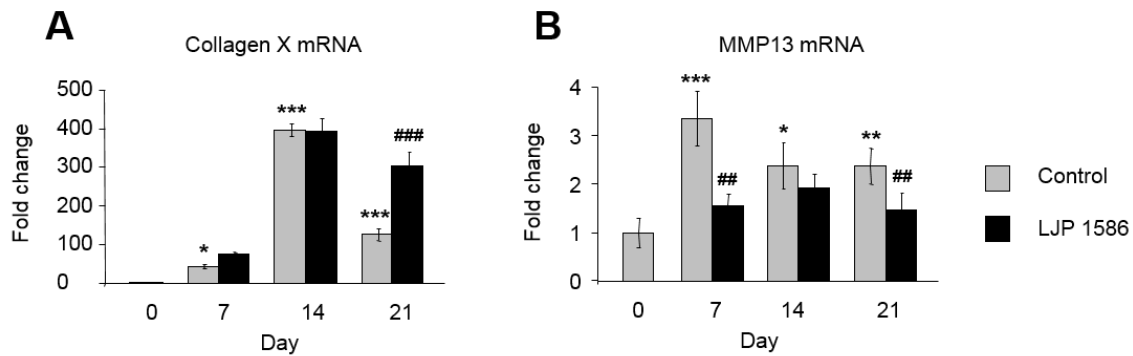


Figure IV-27. Expression of pre-hypertrophy/hypertrophy markers. Chondrocytes were treated (black bars) or not (gray bars) with 1 μ M LJP 1586, [Z-3-Fluoro-2-(4-methoxybenzyl)allylamine hydrochloride] as selective SSAO inhibitor, from day 0 until day 21. mRNA expression of chondrocyte differentiation markers: collagen X (A), matrix metalloproteinase 13 (B). In the graphs, bars represent the average value \pm SEM of six independent experiments performed in duplicate for real time qPCR. Statistics are calculated with respect to the day 0 (*) or non-treated cells (#). Statistical significant P-values (*or # P<0.05, ** or ## P<0.01, *** or ### P<0.001) by Fisher's LDS Multiple-Comparison Test are shown in bold.

The expression of late hypertrophic and mineralization markers was examined (alkaline phosphatase and osteopontin). As shown in figure IV-28, inhibition of SSAO expression delays the increase of alkaline phosphatase and osteopontin expression.

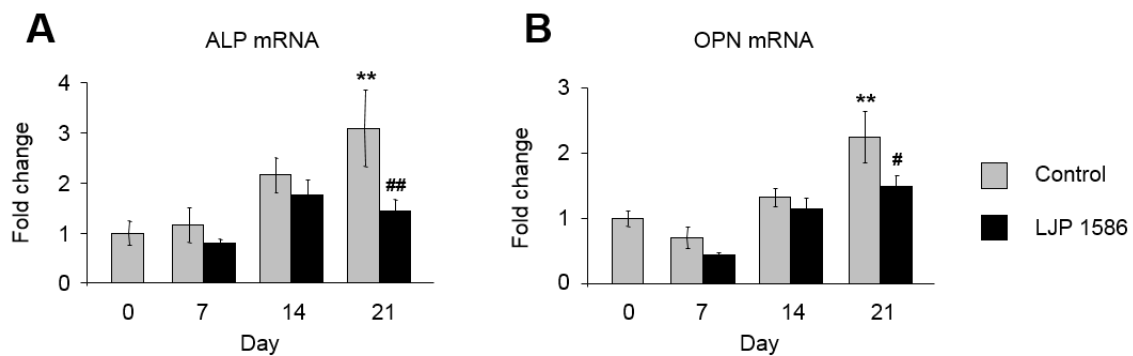


Figure IV-28. Expression of hypertrophy markers. Chondrocytes were treated (black bars) or not (gray bars) with 1 μ M LJP 1586, [Z-3-Fluoro-2-(4-methoxybenzyl)allylamine hydrochloride] as selective SSAO inhibitor, from day 0 until day 21. mRNA expression of chondrocyte differentiation markers: alkaline phosphatase (A) and osteopontin (B). In the graphs, bars represent the average value \pm SEM of six independent experiments performed

in duplicate for real time qPCR. Statistics are calculated with respect to the day 0 (*) or non-treated cells (#). Statistical significant P-values (*or # P<0.05, ** or ## P<0.01, *** or ### P<0.001) by Fisher's LDS Multiple-Comparison Test are shown in bold.

Taken together, in this part we have shown that SSAO in the active form is necessary in terminal chondrocyte differentiation. Complete inhibition of its activity delays the cells in hypertrophic differentiation.

3.2.4. The role of SSAO in terminal chondrocyte differentiation

Glucose transport (a preliminary study)

In next stage of our research, we wished to study the role of SSAO in chondrocyte hypertrophic differentiation. It is known that SSAO stimulates glucose transport in adipocytes and in VSMC by generation of H₂O₂ (Mercier et al., 2001; El Hadri et al., 2002).

Figure IV-29 shows glucose transport in chondrocytes treated or not during 21 days with 1 μM LJP1586. Basal glucose transport in chondrocytes treated chronically with the SSAO inhibitor is decreased compared to non-treated cells. Cells stimulated by BZM (a SSAO substrate) one hour prior to the measurement of glucose up-take did not show differences in glucose transport in the presence or in the absence of LJP1586. As a positive control, the chondrocytes were stimulated by LI-1β for 24 hours. A significant increase in glucose transport was observed in those cells compared to the control cells showing the efficiency of the experiment.

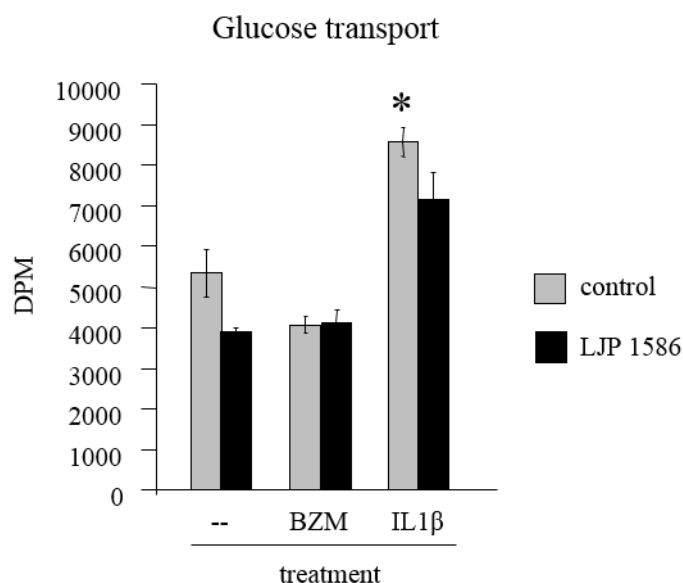


Figure IV-29. Glucose transport. Chondrocytes were treated (black bars) or not (gray bars) with 1 μ M LJP 1586, [Z-3-Fluoro-2-(4-methoxybenzyl)allylamine hydrochloride] as a selective SSAO inhibitor, from day 0 until day 21. In the graph, bars represent the average value \pm SEM of one experiment performed in triplicate for glucose transport. Statistics are calculated with respect to the basal glucose transport (non treated cells) Statistical significant P-values (* $P < 0.05$) by Student t-Test are shown in bold.

These results suggest that SSAO might participate in glucose up-take in hypertrophic chondrocytes. However, chondrocyte stimulation with IL-1 β was necessary to statistically increase glucose up-take in cells treated or not with LJP 1586.

3.3. The presence of SSAO in human OA cartilage

In order to explore the implication of SSAO in disease development, first we have examined if the level of SSAO expression and activity could be regulated as a function of the detection of OA in human cartilage biopsies.

3.3.1. SSAO in human more and less diseased cartilage

Samples of human cartilage were visually evaluated and divided into two groups: more and less affected cartilage. Then HES staining (cellular) and Safranin-O staining (proteoglycan content) were executed to assess the degree of disease progression. Safranin-O staining

confirmed that cartilage samples recognized before to be less affected were well selected. Nevertheless, it revealed that samples from different donors included in the same sample groups were very different in the degree of loss of proteoglycans and thus disease development (Fig. IV-30).

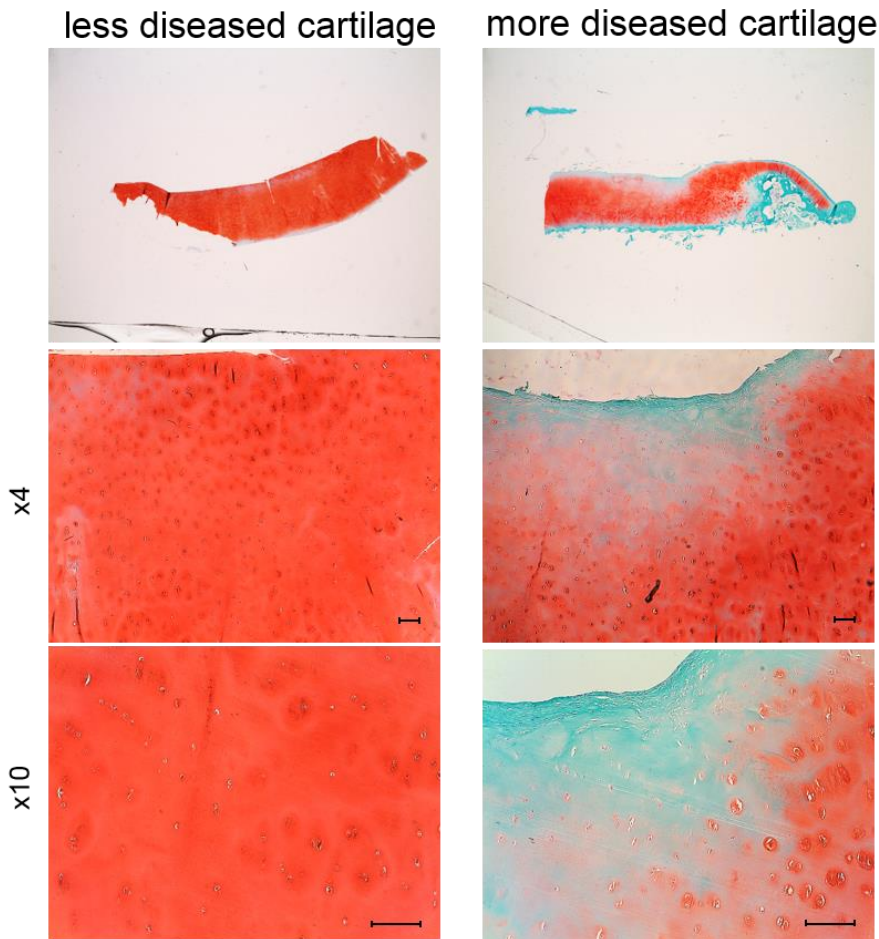


Figure IV-30. Characteristic of less/more diseased cartilage. Representative images of histological sections from osteoarthritic knee joint cartilages divided into two groups more or less affected cartilage, with Safranin O staining (proteoglycan content), where red staining reveals the proteoglycan presence. Micrographs were taken using DMD 108 Leica microscope with magnification 4x and 10x, the scale present on the micrographs represents 200 μ m.

Subsequently immunochemical staining was performed using anti-collagen X and anti-SSAO antibodies. The representative results shown in figure IV-31 indicate that collagen X increases in zones depleted of proteoglycans more so than in zones rich in these molecules. These data confirm that OA cartilage is characterized by chondrocyte hypertrophic differentiation.

SSAO localization was noticeably correlated with depletion of proteoglycans and expression of collagen X, visible in figure IV-31B. SSAO is richly present in diseased tissue, moreover, the immunochemical staining revealed the presence of this protein in cells as well as in the extracellular matrix.

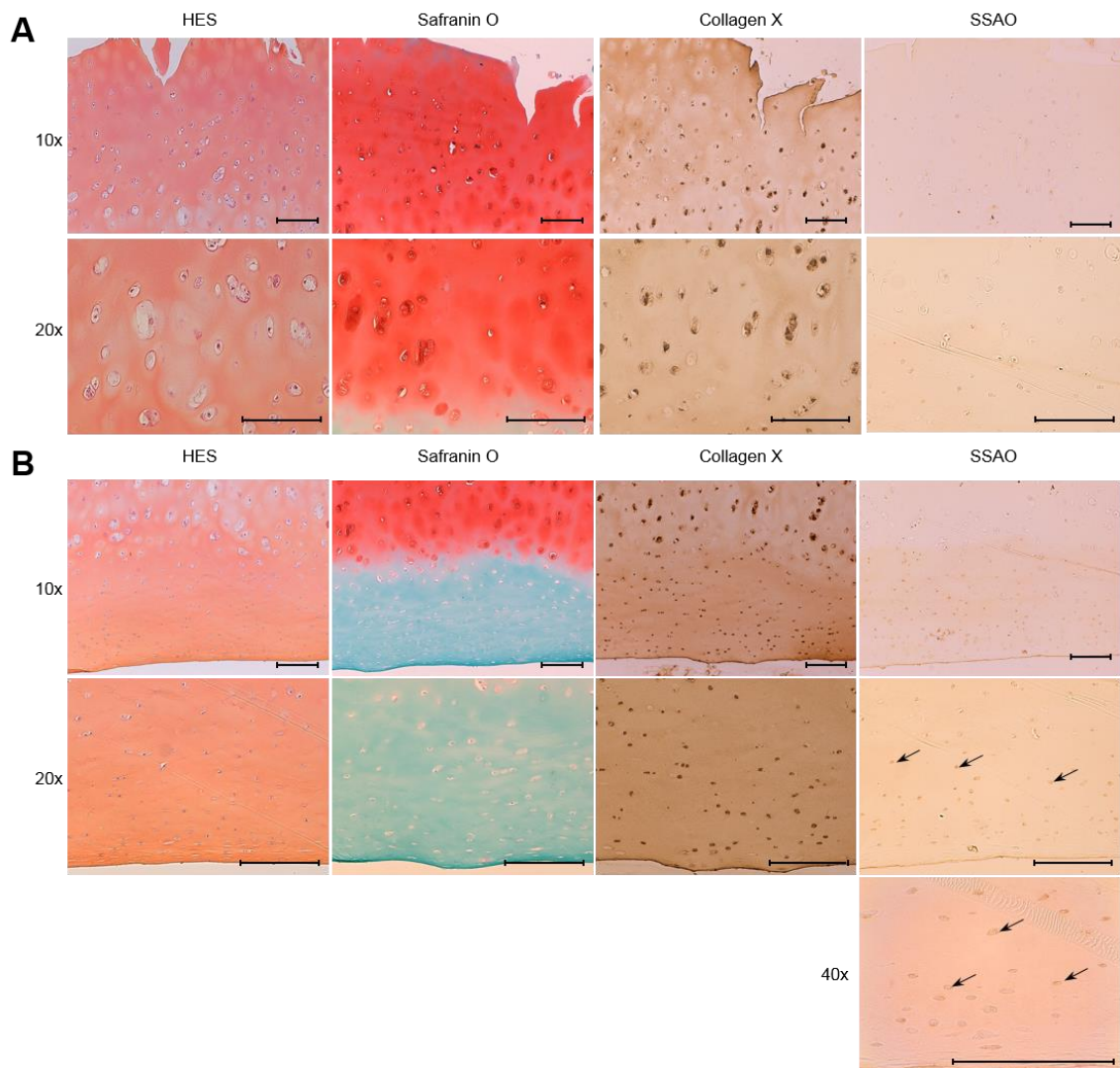


Figure IV-31. Expression of SSAO in human OA cartilage. A: Human less affected cartilage examination with HES (morphology), Safranin O (proteoglycan content) staining and immunohistochemical analysis using anti-type X collagen and anti-SSAO antibodies. B: Human more affected cartilage examination with HES (morphology), Safranin O (proteoglycan content) staining and immunohistochemical analysis using anti-type X collagen and anti-SSAO antibodies.

Arrows indicate anti-SSAO immunostaining. The micrographs were taken using a DMD 108 Leica microscope with magnification 10x, 20x and 40x, the scale present on the micrographs represent 200µm.

3.3.2. Expression and activity of SSAO in human more and less diseased cartilage

Following confirmation that SSAO is present in human cartilage, we performed a radiochemical assay to study enzymatic activity of SSAO. In figure IV-32 shows that enzymatic activity of SSAO is higher in cartilage more affected by OA than less affected by the disease, within the same patient. SSAO activity varies between samples in the same group but from different donors. Because of different stages of proteoglycan decline, lack of homogeneity in the same group of samples was expected.

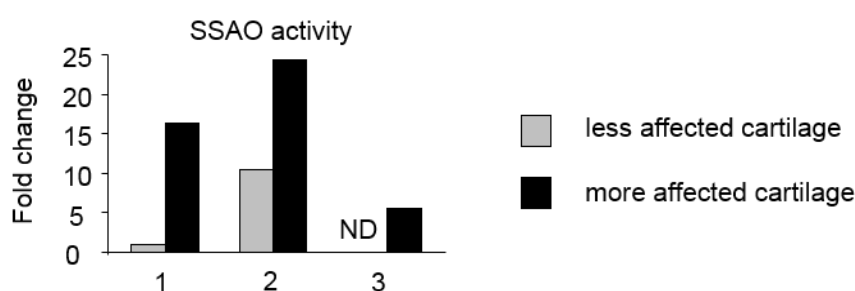


Figure IV-32. SSAO enzymatic activity in a human OA cartilage. The OA cartilage samples were obtained from knee joints of three patients after surgical intervention and divided into two groups of more or less affected cartilage. SSAO enzyme activity in less and more affected cartilage, relatively to patient-1 less affected cartilage (0.2 nmole/h/mg). One experiment was performed in duplicate for enzyme activity essay. Grey bars represent less affected cartilage and black bars more affected cartilage.

In the next step, the mRNA expression of SSAO and differentiation markers were studied. We did not find a difference in SSAO expression between cartilage more and less affected by the disease. Nevertheless, expression of chondrocyte terminal differentiation markers: collagen X, MMP13 and OPN are shown in figure IV-33. Studies of hypertrophic chondrocyte differentiation have confirmed diversity of cartilage samples from different donors. Collagen X is a marker of pre- and hypertrophic chondrocytes and its expression increases in more diseased cartilage. In OA cartilage from a zone more affected obtained from a second donor expression of collagen X increased more than 10 fold compared to cartilage less affected. MMP13 is the next marker of hypertrophy and terminal hypertrophy of chondrocytes. This matrix metalloproteinase cuts all components of the cartilage network and increases tissue degradation. In cartilage from a zone more affected of two of the three donors, levels of MMP13 expression were elevated (8 fold in cartilage more affected from the second donor).

Osteopontin is a marker of chondrocyte mineralization. It was shown by Oliver Pullig et al., (2000) that OPN increases with osteoarthritis. In the three OA cartilage samples we observed at least a 2 fold increase in MMP13 expression in more diseased cartilage.

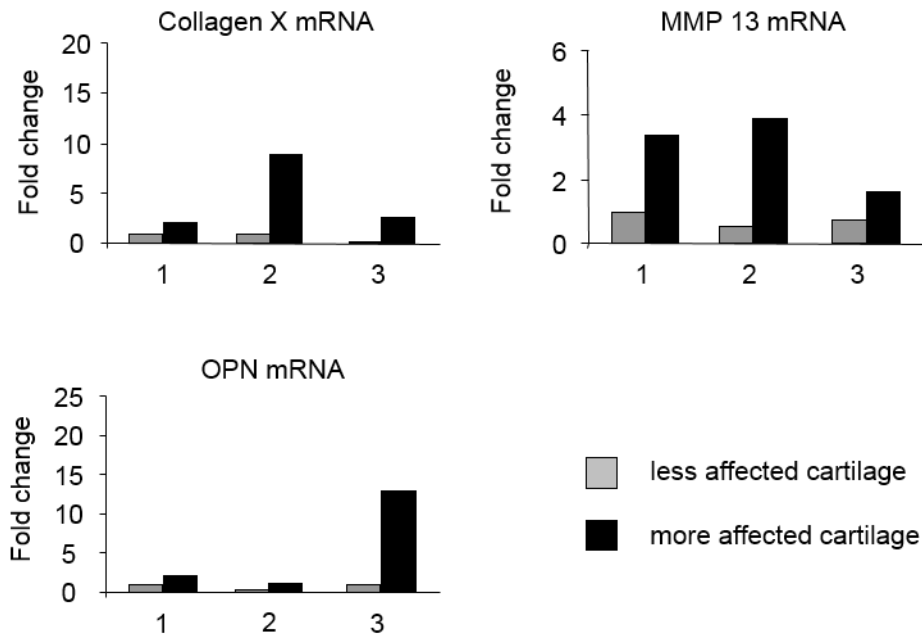


Figure IV-33. Expression of chondrocyte terminal differentiation markers. mRNA expression of collagen X, MMP13 and osteopontin in less (gray bars) and more injured (black bars) cartilage from three independent patients. Results are expressed relative to patient #1 less affected cartilage. The real time qPCR experiments were done in duplicate and results show the mean of 3 different samples taken from each zone.

We did not have a sample of healthy cartilage thus for the purposes of this research, we have used a reference cartilage from a zone less diseased from the same donor. Nevertheless, in this work we have confirmed that OA is characterised by hypertrophy of chondrocytes. Our results indicate that SSAO protein in the active form increases in osteoarthritic cartilage. But its role, substrate and source in this tissue are unknown. Marttila-Ichihara et al., (2006) have shown that inhibition of SSAO in the paw of animals with induced arthritis reduces visual inflammation. We know that SSAO is expressed by chondrocytes, but it can be robustly released by the synovial membrane, so it is important to identify the source of SSAO in ECM of OA cartilage.

3.4. Presence of SSAO in cartilage of the MIA rat model of cartilage degradation

In order to explain the role of SSAO in osteoarthritis development, we reproduced the MIA rat model in our laboratory. Cartilage treated by MIA in 0.9% NaCl was compared to cartilage treated with 0.9% NaCl.

Studies of the expression of chondrocyte terminal differentiation markers showed a decrease in cartilage treated by MIA (Fig. IV-34).

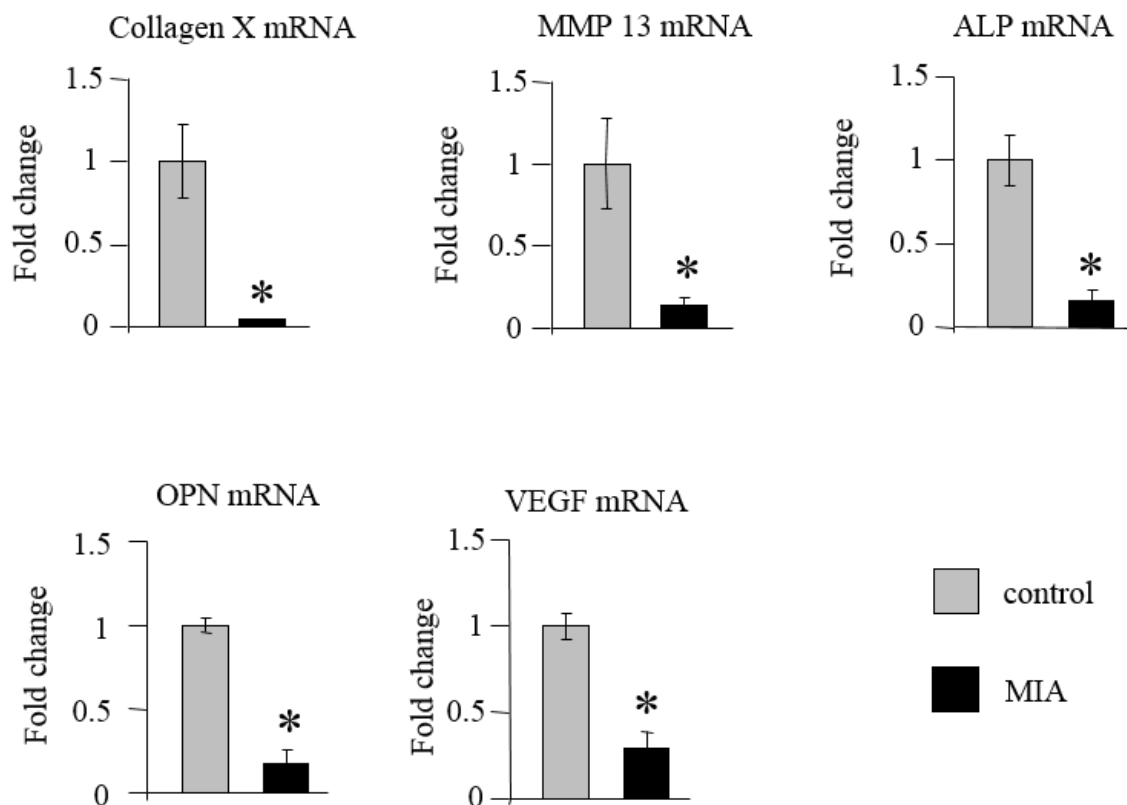


Figure IV-34. Expression of chondrocyte terminal differentiation markers in rat knee cartilage. The cartilage was treated (black bars) or not (gray bars) with MIA by one injection. After two weeks, expression of collagen X, MMP13, ALP, OPN and VEGF was studied. As a reference RPS29 mRNA expression was used. In the graphs, bars represent the average value \pm SEM of four animals, the experiments were performed in duplicate for real time qPCR. Statistical significant P-values ($*P < 0.05$) by Student t-Test are shown in bold.

Subsequently the expression of SSAO was studied (Fig. IV-35). Our results showed an decreased SSAO expression in rat cartilage treated with MIA. These results could be explained by apoptosis induced in time by MIA treatment.

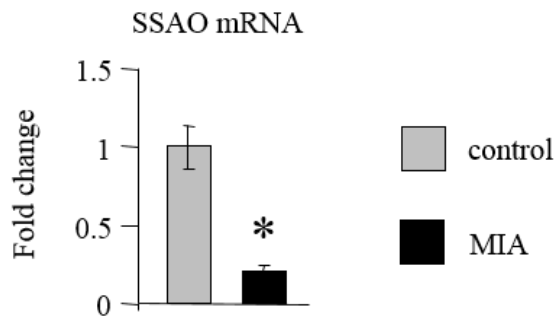


Figure IV-35. SSAO expression in rat knee cartilage. The cartilage was treated (black bars) or not (gray bars) with MIA by one injection. After two weeks SSAO expression was studied. As a reference RPS29 mRNA expression was used. In the graph, bars represent the average value \pm SEM of four animals, the experiments were performed in duplicate for real time qPCR. Statistical significant P-values ($*P<0.05$) by Student t-Test are shown in bold.

The enzymatic activity of SSAO was measured. As expected SSAO activity increased almost 10 fold in cartilage treated by MIA (Fig. IV-36).

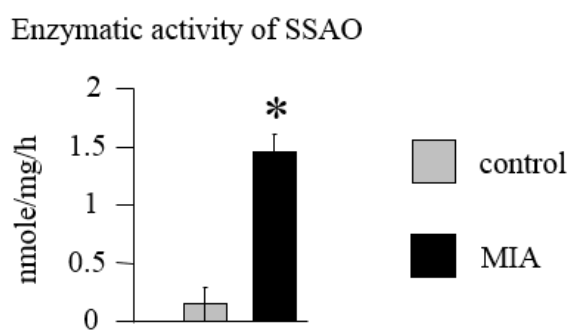


Figure IV-36. SSAO enzymatic activity in rat knee cartilage. The cartilage was treated (black bars) or not (gray bars) with MIA by one injection during two weeks. The SSAO activity is expressed in nmole/h/mg. In the graph, bars represent the average value \pm SEM of five animals, the experiments were performed in duplicate for each sample. Statistical significant P-values ($*P<0.05$) by Student t-Test are shown in bold.

Presented results again show an increase in SSAO in diseased cartilage. Nevertheless, this part of experiments must be continued to explain if the activity of SSAO accelerates cartilage degradation and if SSAO provokes an inflammation status which could be also one of the factors which participates in the development of the disease.

4. Discussion

There are many reports about the role of SSAO in vascularised tissues (Lyles et al., 1985, Enrique-Tarancon et al., 1998; Moldes et al., 1999). But, only a very few studies showed an expression or an activity of the enzyme in cartilage. Moreover, nobody has explored the role of SSAO in this conjunctive tissue.

In 1986, Lyles et al., reported in an abstract that SSAO activity was detectable in rat articular cartilage. Our work has confirmed that SSAO is expressed and is catalytically active in articular cartilage of rat and also in human. However, the expression was low when compared to that found in other tissues. Our results showed that expression and activity were 10 to 15 times lower in cartilage than tissues used as the control (vascular and adipose tissues). Immunohistochemical staining localized the SSAO in rat articular cartilage. The enzyme was associated with chondrocytes. We did not detect any SSAO expression in the extracellular matrix of cartilage. By contrast, bone marrow from the sub-chondral plate that provides support to cartilage was shown by immunohistochemistry to contain higher amounts of SSAO. Expression of the enzyme seems partly associated with the vascular channels present in this bone tissue.

In the literature, no information about the role of SSAO in cartilage has been provided. Recently, a study of SSAO/VAP-1 protein expression during mouse embryogenesis has shown that SSAO/VAP-1 appeared early in the development of cartilage sites (Valente et al., 2008). The authors detected a SSAO expression in chondrocytes in active differentiating process sites at day 12 of embryonic development (ED12) and ED14, mainly in the vertebrae and ribs, as well as in the vascular cells that surround the cartilage primordium of these skeletal sites. These results were in accordance with the human embryonic site of SSAO expression localised by immunohistochemistry by Salmi et al., (2006) and suggest an implication of SSAO in the building of cartilage skeleton.

It has been strongly suggested that SSAO could cross-link extracellular matrix proteins (Mercier et al., 2009). SSAO belongs to the same enzymatic family as lysyl oxidase, which has a crucial role in the building of mature and functional collagen and elastin proteins. Interaction of L-lysine and soluble elastin with SSAO was established by Olivieri et al., (2010). This *in vivo* binding of SSAO to lysyl residues in physiological targets might have a role in the maturation and maintenance of some extracellular matrix proteins. Interestingly, LOXL2, a member of the LOX family, regulates chondrocyte terminal differentiation and is re-expressed in a model of fracture healing (Iftikhar et al., 2011).

This knowledge allows us to hypothesize that SSAO could be implicated in chondrocyte maturation or in terminal differentiation as it has been shown for preadipocytes maturation (Mercier et al., 2001). Therefore, the role of SSAO in hypertrophic chondrocyte differentiation has been studied.

First, we determined the conditions of cell culture which allow cell hypertrophy. For this purpose we modified an *in vitro* model of hypertrophic chondrocyte differentiation from Gartland et al., (2005). A serum deprivation of up to 2% and supplemented with vitamins and insulin after confluence was permissive for terminal differentiation as found in other cell types (El Hadri et al., 2002; Mercier et al., 2001).

Rat chondrocytes in primary cell culture showed a good profile of chondrocyte hypertrophic differentiation. Expression of the specific markers for chondrocytes, like Sox9, collagen II and aggrecan, decreased during the time of culture which indicates a loss of the chondrocyte phenotype. Moreover, expression of collagen X and matrix metalloproteinase 13 increased compared to day 0, which is necessary for chondrocyte hypertrophy. We tested also markers of mineralization, and a significant increase of alkaline phosphatase and osteopontin at day 21 indicated that cells reached terminal hypertrophy. These results were corroborated by the morphological changes of the cell observed under the microscope. In the case of expression of several markers, the standard error of the mean was important. From one cell culture to another, kinetics of differentiation were slightly shifted earlier or later and the amplitude of the increase was also variable, leading to heterogeneity in the values.

When a model of chondrocyte terminal differentiation was validated, we investigated SSAO expression.

It was already reported that cells in primary culture lost the expression of SSAO (Yu et al., 1993, Sole et al., 2007). Nevertheless, we found expression of SSAO in chondrocytes. Furthermore, expression of SSAO increased significantly in accordance with the degree of cell differentiation. Next we studied the enzymatic activity of SSAO. Our results showed that SSAO was catalytically active in chondrocytes, and the maximum of activity was detected in hypertrophic cells.

Altogether, the results indicate that during *in vitro* terminal chondrocyte differentiation, induction of SSAO activity and expression was a differentiation-dependent event. This raises the question of whether SSAO is a marker of chondrocyte differentiation and what is its role in this process.

To establish whether SSAO could be involved in differentiation, cell cultures were performed in the absence or in the presence of LJP1586, a selective SSAO inhibitor (O'Rourke et al., 2008). LJP1586 was added to the culture medium throughout the differentiation protocol from day 0. At a concentration of 1 μ M, LJP1586 fully abolished enzyme activity without any toxicity toward the chondrocyte viability as shown by the MTT test.

In order to estimate chondrocyte differentiation, expression of markers of hypertrophic chondrocytes was measured. As we suspected, inhibition of SSAO activity delayed chondrocyte terminal differentiation.

Collagen X expression in control cells as well as in treated cells increased until day 14, and next in control cells decreased significantly at day 21. This result indicates that cells reduced the synthesis of matrix proteins and enhanced the synthesis of molecules that damage the cartilage network. It is noteworthy that at day 21 following the induction of terminal differentiation, the expression of collagen X mRNA levels was induced by LJP1586 treatment. This apparently paradoxical result is likely explained by a LJP1586-induced delay in chondrocyte differentiation, which maintains the cells in a pre-hypertrophic phenotype, with a related collagen X overexpression.

In the presence of LJP1586, the expressions of MMP13, alkaline phosphatase and osteopontin were decreased at day 21 of culture, compared to control cells. This confirms that cells treated by LJP1586 did not enter terminal hypertrophy.

SSAO expression at day 21 was also decreased in cells treated with LJP1586 compared to control cells. This result is in accordance with previous results where levels of SSAO expression were dependent on stage of chondrocytes differentiation.

Interestingly, chondrocyte viability was significantly enhanced by LJP1586 at the same time, although at a low level. These data show that LJP1586 exposure delayed the emergence of chondrocyte terminal maturation, and strongly suggest that SSAO is not only a marker of hypertrophic differentiation, but also participates in this process. Additionally, the anti-inflammatory properties of this compound (O'Rourke et al., 2008), by decreasing H₂O₂ production, may also have a beneficial effect on these cells.

Thus we have answered the question of whether SSAO is implicated in chondrocyte terminal differentiation, nevertheless we do not know the way by which its activity accelerates this process.

It was previously shown that SSAO activation promotes adipocyte maturation (Mercier et al., 2001; Fontana et al., 2001) and stimulates glucose transport through GLUT4 in pre-adipocytes (Mercier et al., 2001; Enrique-Tarancon et al., 1998). A methylamine-induced activation of SSAO can also increase glucose transport through GLUT1 in VSMC (El Hadri et al., 2002). In cartilage, glucose is of major importance for the biosynthesis of extracellular matrix glycosaminoglycans, as well as for the maturation of chondrocytes (Mobasheri et al., 2008). Inhibition of glucose is associated with growth impairment in cartilage (Leonard et al., 1989; Rodgers et al., 1995; Svenson et al., 1988). Ohara et al., (2001) have demonstrated that glucose transporters (GLUT) were differentially expressed in chondrocytes according to their cartilage localization in proliferative or hypertrophic zones. It is therefore possible that SSAO might increase terminal differentiation by activation of glucose transport. In our preliminary experiment, we have shown that a chronic inhibition of SSAO activity decreases basal glucose up-take. However, further studies are needed to verify SSAO involvement in this process.

The enzymatic action of SSAO led to the production of H₂O₂ and aldehyde. Therefore it is questioned whether SSAO overexpression could have the impact on development of the pathological conditions. Under physiological conditions, chondrocytes resident in articular cartilage are silenced, avoiding multiplication. The balance between degradation and synthesis of ECM proteins is tightly controlled (Goldring et al., 2006; Zuscik et al., 2008). During development of osteoarthritis this balance is deregulated.

When chondrocytes are activated, a reactivation of the cascade of chondrocyte hypertrophic differentiation in articular cartilage takes place. The chondrocytes express the hypertrophic markers, such as collagen X, matrix metalloproteinase 13 and Runx2 (Goldring, 2012). This event results in a loss of mechanical properties of cartilage and its degradation.

There are no reports on the role of SSAO in OA cartilage. In 2006 Marttila-Ichihara et al., have shown that in animal models of arthritis, an inhibitor of SSAO could diminish the extravasation of leukocytes from vessels to the inflamed joints. But they did not examine the articular cartilage specifically for the presence of SSAO and its activity. In our work we had the opportunity to examine human OA cartilage. From each biopsy from patients undergoing knee replacement we distinguished the tissue area with a more diseased cartilage (the degenerative tissue) from that of less diseased cartilage (outside the lesion).

Using chemical staining, we confirmed that the cartilage samples were well divided into more/less affected. Subsequently, we studied *hypertrophic chondrocyte marker expression and SSAO*. We were interested in SSAO expression and activity and localization of the SSAO as a function of more or less damaged cartilage. We demonstrated that SSAO activity highly increased in OA damaged cartilage. But its role remains unclear.

An implication of SSAO in neo-angiogenesis has been recently reported. SSAO inhibition was found to attenuate choroidal neovascularization (Yoshikawa et al., 2012). LJP1586 and also other SSAO-inhibitors could inhibit tumor growth (Marttila-Ichihara et al., 2010). In osteoarthritis, articular chondrocytes undergo phenotypic changes with the expression of hypertrophic differentiation markers leading to apoptosis. This effect is associated with subchondral bone remodelling and neo-vascularization of the tissue mediated by several factors including VEGF and VEGFR (Onyekwelu et al., 2009). These growth factors are required to convert the non-vascular and hypoxic cartilage tissue into bone through the combined actions of osteoclasts and osteoblasts (Onyekwelu et al., 2009). Thus, it is conceivable that SSAO might be implicated in vascularization of bone marrow from subchondral bone and osteoarthritis progression. Subsequently, SSAO inhibition could represent a relevant target to prevent the neo-vascularisation phenomenon and bone remodelling during osteoarthritis. This hypothesis has to be explored in future work.

Moreover, electrophilic species of aldehyde are prone to fairly and non-specifically react with proteins, whereby affecting their structure and function. On the other hand, SSAO activation

increases H₂O₂ production. Elevated levels of H₂O₂, a member of the reactive oxygen species (ROS), induces chondrocyte hypertrophy and also participates in cartilage degradation in OA (Kishimoto et al., 2010).

Moreover, immunohistochemical analysis disclosed that SSAO was present in more diseased cartilage. Staining was visible in chondrocytes but also in ECM what indicates the soluble form of SSAO (sSSAO).

The source of sSSAO in ECM is not known. Nevertheless, SSAO is also found in synovial liquid (Salmi et al., 1997) and serum (Boomsma et al., 2005). Elevation of its activity in serum has already been associated with several pathologies such as diabetes or cardiovascular diseases (Boomsma et al., 2005). It has been described that SSAO could be cleaved and released in the serum from adipocytes by MMP9 (Abella et al., 2004). Stolen et al., (2004b) revealed that in the mouse, endothelial cells could be the major source of soluble SSAO but in some diseases like diabetes, endothelial and adipose cells could also be a source of soluble SSAO. During OA, inflammation is a major factor associated with the risk of progression of cartilage loss and is a symptom of the disease (Goldring et al., 2010). The implication of SSAO in the inflammation has been well documented especially by Jalkanen's group (Marttila-Ichihara et al., 2006; Salmi et al., 2011). sSSAO increased during the inflammation phase and thus could be implicated in OA.

Taken together, SSAO over-activation and increased production of H₂O₂ could be implicated in the activation of phenotypical changes in chondrocytes observed in OA and the irreversible modification of ECM components.

In order to study the role of SSAO in the progression of cartilage disease, it is necessary to use an animal model of cartilage degradation.

In our work, we have reproduced the MIA rat model. By injection of MIA, the articular cartilage degrades and apparently decreases its thickness. The expression of chondrocyte hypertrophy markers but also SSAO were decreased. This could be explained by an advanced stage of the degradation process. Nevertheless, the SSAO activity was well elevated in cartilage treated by MIA. This result again confirms that SSAO increases with the development of the pathological condition.

Immunohistochemical analysis of cartilage revealed that SSAO expression was higher in MIA treated cartilage than in control cartilage. This can be due to inflammation which takes place in articulation and in chondrocyte hypertrophy.

This work needs be continued to study the role of SSAO and verify the potential effect of SSAO inhibition on disease development.

5. Conclusions

In this work we have explored the role of SSAO in rat and human cartilage. The *in vitro* and *in vivo* implication of SSAO in the process of chondrocyte differentiation has been detailed. The main results of this work are:

1. *SSAO is expressed in cartilage.*

The enzyme is associated with human and rat chondrocytes in articular cartilage. In healthy cartilage, it is not expressed in the extracellular matrix. The level of SSAO expression and activity is lower than that found in vascular or adipose tissues.

2. *SSAO is associated with the differentiation of chondrocytes.*

SSAO expression and activity increase in chondrocytes as a function of time in culture. This increase is paralleled by the expression profiles of markers of hypertrophic chondrocytes, particularly MMP13. Moreover, inhibition of its enzymatic activity decreases the level of chondrocyte terminal differentiation. Chondrocytes treated with LJP1586 do not reach the cell terminal hypertrophy stage. The expression of chondrocyte hypertrophic markers is delayed in time by abolishing SSAO activity. This study shows that induction of SSAO is a differentiation-dependent event and its activity is necessary for terminal hypertrophy accomplishment.

3. *SSAO stimulates glucose transport in hypertrophic chondrocytes.*

Inhibition of SSAO activity by LJP1586 decreased glucose transport in hypertrophic chondrocytes.

4. *SSAO is abundantly present in OA human cartilage.*

SSAO activity increases in OA cartilage compared to less affected cartilage regions. SSAO is detectable in chondrocytes (a cellular form of SSAO) and the extracellular matrix (a soluble form of SSAO) from OA cartilage.

5. *SSAO increases in an OA rat model.*

SSAO activity increases in MIA damaged rat cartilage.

6. Perspectives

Does SSAO stimulate glucose transport in chondrocyte by H₂O₂ production?

By the production of H₂O₂, SSAO might activate the glucose transporter GLUT4 as in other cell types. In our preliminary studies we have shown that it is possible that SSAO increases glucose transport in hypertrophic chondrocytes. However, the mechanism of this process needs to be studied.

What are the molecular targets of SSAO in cartilage?

In this work we have shown the role of SSAO in cartilage. Nevertheless, we did not characterize the consequences of its enzymatic action, namely the production of hydrogen peroxide and aldehydes and their effect on matrix macromolecules such as collagens and aggrecans. By modulation of the SSAO activity in cartilage tissue, the impact of its enzymatic action on matrix integrity will be better understood. The identification of the nature of SSAO ligands and substrates will be helpful to better elucidate SSAO action in cartilage (cross-link).

What is the role of SSAO in inflammation?

There are many reports about the role of SSAO in inflammation. As in osteoarthritis inflammation status is one of the factors contributing to the development of the disease. It is encouraging to speculate that soluble form of SSAO could represent a biomarker of inflamed joints. The follow-up of SSAO levels in serum and synovial liquid of patients from an early to a late stage of osteoarthritis represents an important issue. Moreover, as Marttila-Ichihara et al., 2006 have shown, inhibition of SSAO in arthritic joint disease decreases the inflammation status. It would be interesting to study in an animal model how inhibition of SSAO activity affects the development of chondrocyte terminal differentiation in cartilage and tissue degradation.

What is the precise role of SSAO in chondrogenic differentiation? Could SSAO be a new pharmacological target for the development of new treatments in OA?

SSAO is present in the sites of cartilage development during early embryogenesis in the mouse (Valente et al., 2008) and in humans (Salmi et al., 2006). But the role of SSAO in chondrogenic differentiation is still far from clear. We showed in preliminary studies that SSAO was expressed *in vitro* during chondrogenic differentiation of human MSC. Additional experiments are necessary to describe the role of SSAO in this process.

V. Vascular and atherosclerosis studies

1. Hypothesis

The homeostasis of the arterial wall is provided by the synthesis of tissue-specific matrix molecules by vascular smooth muscle cells (VSMC) as a function of their state of differentiation. VSMC phenotypic modification is a reversible process essential to the functioning of the cardiovascular system. An imbalance between the proliferative / synthetic and contractile phenotypes may lead to the development and/or progression of vascular disease in response to abnormal environmental signals. Thus, VSMCs dedifferentiate and may migrate into the neointima as in atherosclerosis or hypertrophy and modify their contractile properties as in hypertension, accompanied by modification of the extracellular matrix (ECM).

Oxidative stress has an important role in maintaining the differentiation of VSMC. In excess, it can lead to an increase in VSMC proliferation (Sung et al., 2005) and vascular calcification via osteogenic differentiation of VSMC (Byon et al., 2008). In contrast, a decrease in oxidative stress can lead to VSMC dedifferentiation in mice, such as in the *Nox4^{-/-}* model (Clempus et al., 2007). We have previously shown that SSAO increases during differentiation of vascular smooth muscle cells (El Hadri et al., 2002). SSAO can also accelerate adipocyte differentiation (Mercier et al., 2001). Several studies have suggested an involvement of SSAO in the organization of the ECM via the establishment of crosslinks or by altering the synthesis or organization of other matrix components such as proteoglycans (Mercier et al., 2006, 2007 and 2009). Finally, SSAO could also contribute to LDL oxidation and inflammation, particularly via the soluble form of SSAO present in the serum. Levels of soluble SSAO are increased in the plasma of patients with cardiovascular and inflammatory diseases.

SSAO is highly expressed in the VSMC in a differentiation-dependent manner, and may contribute to vascular remodelling observed in diseases associated with aging. Atherosclerosis is a chronic inflammatory disease of large arteries characterized by intimal thickening that grows by infiltration and proliferation of SMC, monocytes-macrophages and lymphocytes (Dzau et al., 2002; Wang et al., 2012). The development of atherosclerosis is promoted by various events such as oxidative stress that activates cell proliferation and lipid peroxidation.

It has been shown *in vivo* that incubation of methylamine and SSAO in the culture medium could induce cytotoxicity on endothelial cells (Yu et al., 1993) and to a lesser degree in the VSMCs (Langford and al., 2001), and apoptosis of VSMCs (Hernandez et al., 2006).

Thus, because SSAO (i) generates harmful reactive species (aldehydes, hydrogen peroxide), (ii) may be involved in the establishment of covalent bridges (crosslinks) proteins of the extracellular matrix, (iii) is important in extravasations of leukocytes into inflammatory tissues (Jalkanen et al., 2001; Salmi et al., 2001 and 2005) we hypothesize that SSAO could contribute to modifications of arterial matrix integrity during the process of cell differentiation in diseases related to aging and inflammation, like atherosclerosis.

2. Objectives and Strategies

So the first objective of this project was to demonstrate the involvement of SSAO in matrix remodelling of arterial tissue in an example of a pathology related to tissue inflammation and aging.

The second objective of this work was to study the role of SSAO in VSMC differentiation and the inflammatory response.

This project had two complementary approaches:

1) *in vivo*

In order to evaluate whether the absence of SSAO may modify the development of atherosclerosis by modulating inflammation and matrix remodeling, we established *ApoE*^{-/-} mice (which spontaneously develop atherosclerotic plaques) KO for the gene *SSAO* (mouse *ApoE*^{-/-}*SSAO*^{-/-}) in collaboration with Professor Sirpa Jalkanen.

We first studied the phenotype of the atherosclerotic plaques by measuring:

- the surface of the plaques in the aortic sinus and the total aorta (Oil Red O staining),
- infiltration of macrophages (MOMA-2) and lymphocytes (CD3),
- and the expression of alpha-actin (by immunohistochemistry).

We then studied the immune profile of mice by evaluating:

- the expression of pro- and anti- inflammatory cytokines in blood (by ELISA) and spleen (RT-qPCR) and in abdominal aorta (Mouse Atherosclerosis Antibody Array),
- the different populations of immune cells in blood and in spleen (FACS),
- the changes in the homing and trafficking of immune cells by injecting CFSE-labeled “peripheral bone marrow cells” (PBMC) in a spleen, an aorta and blood (FACS),
- splenocyte differentiation (TH1/Th2) after stimulation with inflammatory cytokines (FACS).

Because genetic manipulation could produce a situation slightly different from normal physiology and considering the two, adhesive and enzymatic SSAO functions, we decided to verify if:

a) the infusion of an SSAO inhibitor, the SCZ, could reproduce the phenotype obtained in *ApoE^{-/-}SSAO^{-/-}*. For this purpose, a first experiment was designed to evaluate the effect of an acute injection of SCZ on PBMC trafficking. A second was done with a 4 week-SCZ chronic infusion in mice fed with a high fat diet. Subsequently we have studied:

- plaque formation in SCZ-treated or not ApoE^{-/-} mice (Oil Red O staining)
- infiltration of macrophages (MOMA-2) (immunohistochemistry)
- the changes of immune cells trafficking (PBMC injection detected by FACS)
- the differences in populations of immune cells (FACS).

b) a combination of two anti-SSAO antibody injections which inhibit only the adhesive function of SSAO, we could modify the trafficking of PBMC monitored by FACS as previously described.

2) ex vivo

To investigate the consequences of SSAO deletion on the arterial cell response in inflammatory conditions, aortas from SSAO^{-/-} mice were treated with (TNF α). We are studying:

- the expression of cytokines (Mouse Atherosclerosis Antibody Array),
- the expression of various VSMC differentiation markers (RT-qPCR).

3. Results

3.1. Role of SSAO in plaque development: Invalidation of SSAO in *ApoE*^{-/-} mice

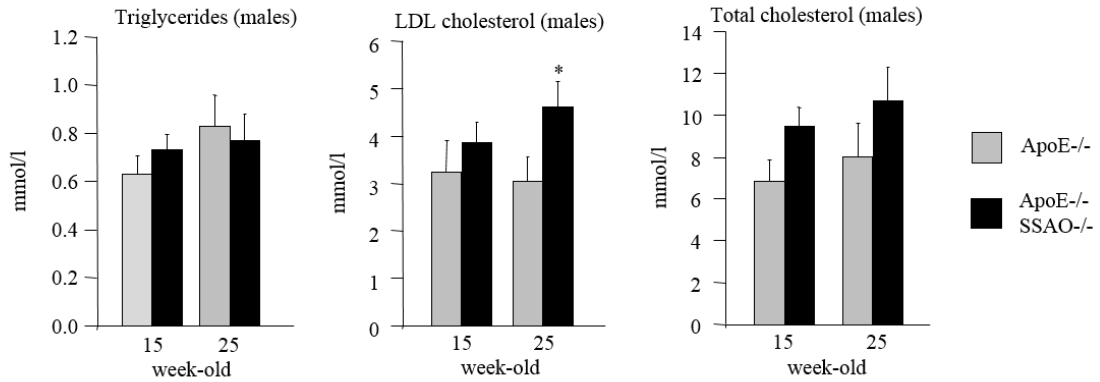
In order to study the potential implication of SSAO in the development of atherosclerosis, we established a mouse model for the invalidation of *ApoE* and for *SSAO* genes as explained in the Material and Methods sections. We thus compared first the kinetics of disease development and then the composition of the atheromas (plaque phenotype) in *ApoE*^{-/-} versus *ApoE*^{-/-} *SSAO*^{-/-} mice.

3.1.1. Lipid profile in *ApoE*^{-/-} and *ApoE*^{-/-} *SSAO*^{-/-} mice

Modification of the lipid profile could explain the difference in the plaque surface between *ApoE*^{-/-} et *ApoE*^{-/-} *SSAO*^{-/-} mice. We verified if the absence of SSAO in *ApoE*^{-/-} mice changed the lipid profile of *ApoE*^{-/-} mice. In figure V-1, triglyceride, LDL cholesterol and total cholesterol concentrations are presented in males and females. Triglyceride and total cholesterol levels were not changed depending on sex, genotype or mouse age. However, LDL cholesterol was increased in *ApoE*^{-/-} *SSAO*^{-/-} 25 week-old males but not in 15 week-old *ApoE*^{-/-} *SSAO*^{-/-} males compared to the control mice. LDL cholesterol in *ApoE*^{-/-} *SSAO*^{-/-} female mice was not modified compared to the *ApoE*^{-/-} control mice. Thus, a modification of the lipid profile cannot be the cause of the increase of the plaque surface in *ApoE*^{-/-} *SSAO*^{-/-} mice compared to *ApoE*^{-/-} mice.

Because female *ApoE*^{-/-} *SSAO*^{-/-} mice did not show modification in cholesterol levels and because it was reported that *ApoE*^{-/-} female mice with the C57BL/6 genetic background develop bigger atherosclerotic plaques in our future studies we used the *ApoE*^{-/-} and *ApoE*^{-/-} *SSAO*^{-/-} female mice.

A



B

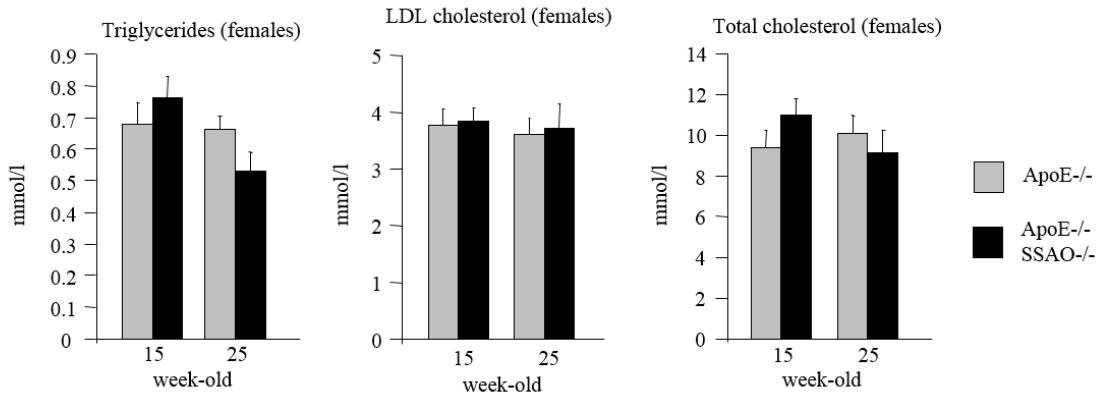


Figure V-1. Triglyceride, LDL cholesterol and total cholesterol concentrations in *ApoE*^{-/-} and *ApoE*^{-/-}*SSAO*^{-/-}, 15 and 25 week-old, male and female mice. In panel A the results for male mice and panel B the results for female mice. The concentration of lipids is expressed in mmol/l. Grey bars represent control mice *ApoE*^{-/-}, and black bars represent *ApoE*^{-/-}*SSAO*^{-/-} mice. In the graphs, bars represent the mean value \pm SEM of “n” animals (for 25 week-old males n= 9 *ApoE*^{-/-}, 7 *ApoE*^{-/-}*SSAO*^{-/-}; for 15 week-old males n= 6 mice per genotype; for 25 week-old females n= 6 *ApoE*^{-/-}, 7 *ApoE*^{-/-}*SSAO*^{-/-}; for 15 week-old females n= 7 mice per genotype). Statistical significant P-values (*P<0.05) by Student t-Test are shown in bold.

3.1.2. Kinetics of disease development

The atherosclerotic plaque size was quantified in the aortic sinus and the thoracic aorta of *ApoE*^{-/-}*SSAO*^{-/-} and *ApoE*^{-/-} mice by oil red O staining at 15 weeks-old. This corresponded to the early phase of atherosclerosis development and at 25 week-old when advanced plaques had formed. 15 week-old female mice did not present significant differences in plaque size neither in aortic sinus (Fig. V-2) nor in thoracic aorta in the two genotypes (Fig. V-3).

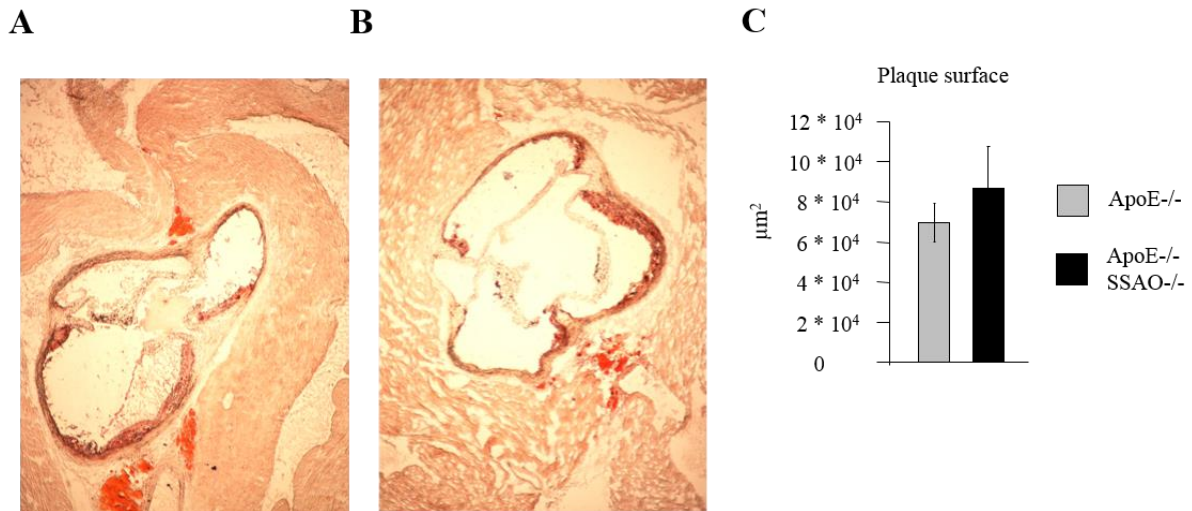


Figure V-2. Plaque quantification after oil red O staining in the aortic sinus from 15 week-old female mice. The representative micrographs of mouse aortic sinus. A: The aortic sinus of *ApoE*^{-/-} control mouse. B: The aortic sinus of *ApoE*^{-/-}*SSAO*^{-/-} mouse. C: Plaque surface quantification expressed in μm^2 . Grey bars represent control mice *ApoE*^{-/-}, black bars represent *ApoE*^{-/-}*SSAO*^{-/-} mice. In the graph, bars represent the mean value \pm SEM of six mice. Statistical significant P-values ($*P < 0.05$) by Fisher's LSD Multiple-Comparison Test are shown in bold. The micrographs were taken using Nikon Japan camera.

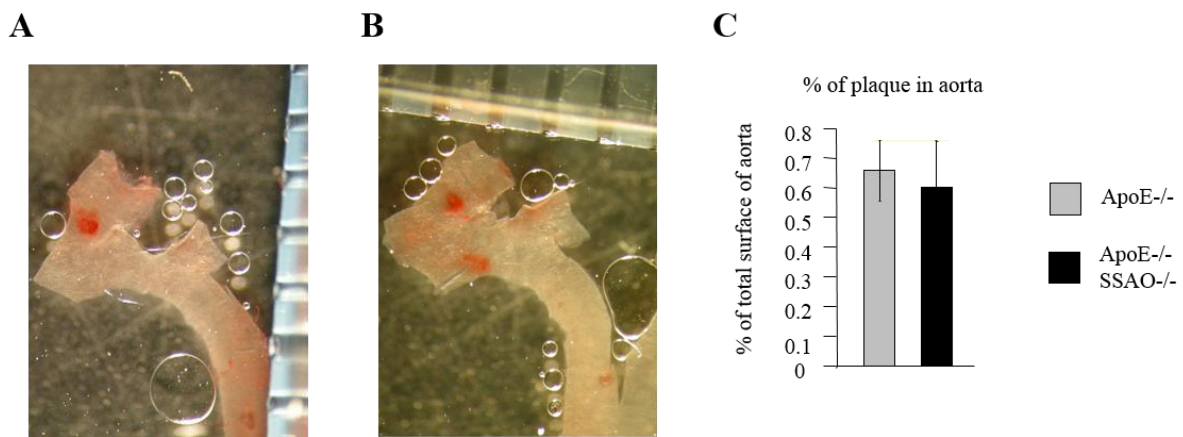


Figure V-3. Plaque quantification after oil red O staining in the thoracic aorta from 15 week-old female mice. The representative micrographs of mouse thoracic aortas. A: The thoracic aorta of *ApoE*^{-/-} control mouse. B: The thoracic aorta of *ApoE*^{-/-}*SSAO*^{-/-} mouse. C: Plaque quantification expressed as a percent of total surface of thoracic aorta. Grey bars represent control mice *ApoE*^{-/-}, black bars represent *ApoE*^{-/-}*SSAO*^{-/-} mice. In the graph, bars represent the mean value \pm SEM of six (*ApoE*^{-/-}) and nine (*ApoE*^{-/-}*SSAO*^{-/-}) mice. Statistical significant P-values ($*P < 0.05$) by Fisher's LSD Multiple-Comparison Test are shown in bold. The micrographs were taken using Nikon Japan camera.

However, 25 week-old *SSAO* deficient mice presented an increase in plaque surface compared to *ApoE*^{-/-} control mice, without any change in cholesterol levels. In the aortic sinus from *ApoE*^{-/-}*SSAO*^{-/-} mice, the plaque surface significantly increased by 1.38 (Fig. V-4).

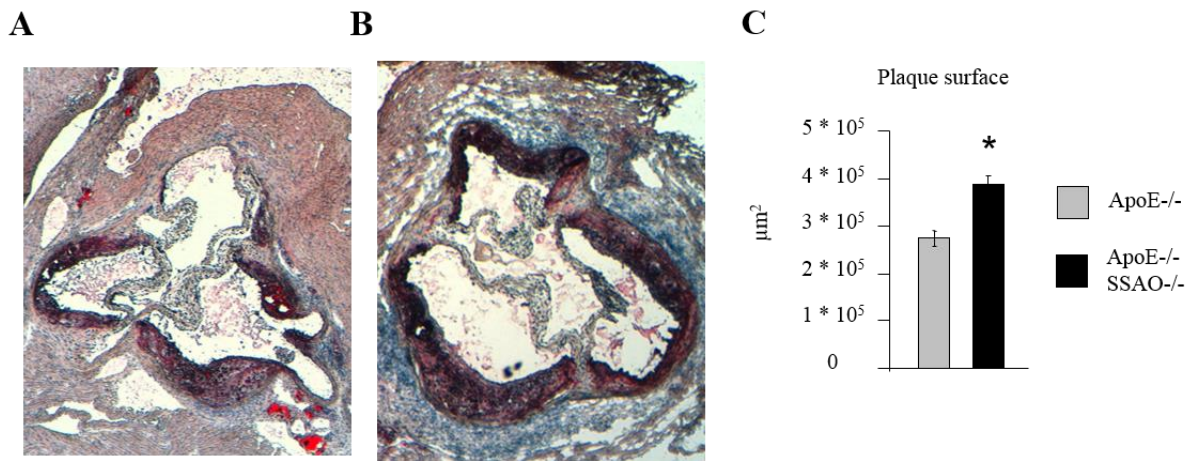


Figure V-4. Plaque quantification after oil red O staining in the aortic sinus from 25 week-old female mice. The representative micrographs of mouse aortic sinus. A: The aortic sinus of *ApoE*^{-/-} control mouse. B: The aortic sinus of *ApoE*^{-/-}*SSAO*^{-/-} mouse. C: Plaque surface quantification expressed in µm². Grey bars represent control mice *ApoE*^{-/-}, black bars represent *ApoE*^{-/-}*SSAO*^{-/-} mice. In the graph, bars represent the mean value ± SEM of six animals. Statistical significant P-values (*P<0.05) by Fisher's LSD Multiple-Comparison Test are shown in bold. The micrographs were taken using Nikon Japan DIAPHOT 300 with magnification of 4x.

Augmentation of plaque area was clearly marked in the thoracic aorta of double KO mice compared to their controls (2.2 fold increase) (Fig. V-5).

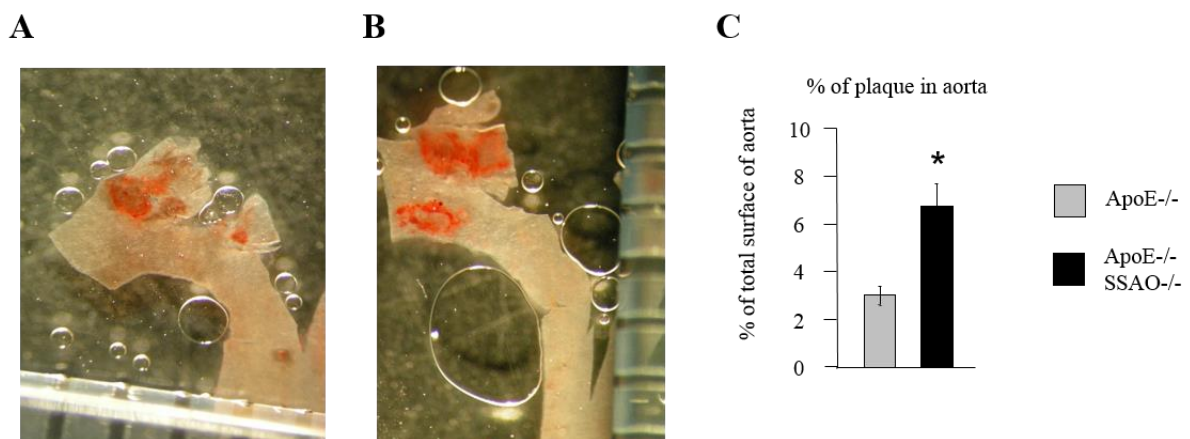


Figure V-5. Plaque quantification after oil red O staining in the thoracic aorta from 25 week-old female mice. The representative micrographs of mouse thoracic aortas. The thoracic aorta from *ApoE*^{-/-} control (A) and *ApoE*^{-/-}

SSAO^{-/-} (B) mouse. C: Plaque surface quantification expressed as a percent of total surface of the thoracic aorta. Grey bars represent control mice *ApoE*^{-/-}, black bars represent *ApoE*^{-/-}*SSAO*^{-/-} mice. In the graph, bars represent the mean value ± SEM for six animals. Statistical significant P-values (*P<0.05) by Fisher's LSD Multiple-Comparison Test are shown in bold. The micrographs were taken using Nikon Japan camera.

These results are contrary to our expectations. We hypothesized that the absence of SSAO would decrease atherosclerotic plaque development *via* a decreased production of aldehyde and hydrogen peroxide but also a reduction in of immune cell recruitment to the injury site.

3.1.3. Phenotype of atherosclerosis plaques and media

To better understand the unexpected increase of atherosclerotic plaque size in *ApoE*^{-/-}*SSAO*^{-/-} mice, the compositions of the atheroma and the media just under the plaque were studied. (i) We checked the infiltration of the intima by VSMC and their differentiation level (sm- α -actin) by monocytes/macrophages and CD3+ cells by immunodetection. (ii) The collagen content was evaluated by chemical staining with Sirius red.

3.1.3.1. α -actin expression in media of aortic sinus

During atherogenesis, VSMC from the media dedifferentiate and migrate in the neo-intima in formation. Immunohistochemical staining revealed that in young 15 week-old mice, the expression of α -actin was not changed in the two genotypes (Fig. V-6) and detected in the media layer, but not in the neointima.

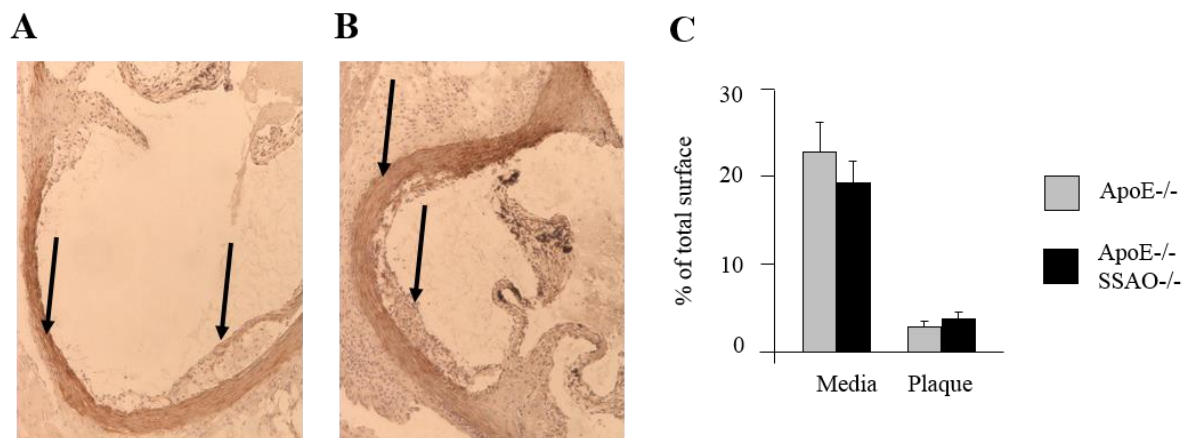


Figure V-6. α -actin staining in the aortic sinus of young, 15 week-old female mice. The representative micrographs of aortic sinus from *ApoE*^{-/-} control (A) and *ApoE*^{-/-}*SSAO*^{-/-} (B) mice. C: α -actin quantification expressed as percent

of total surface of tunica media or plaques. Grey bars represent control mice *ApoE*^{-/-}, black bars represent *ApoE*^{-/-} *SSAO*^{-/-} mice. In the graph, bars represent the mean value ± SEM of six animals. Statistical significant P-values (*P<0.05) by Fisher's LSD Multiple-Comparison Test are shown in bold. The micrographs were taken using Nikon Japan DIAPHOT 300 with magnification of 4x.

Nevertheless the α -actin expression in tunica media in old, 25 week-old, mice was decreased in *ApoE*^{-/-} *SSAO*^{-/-} mice, compared to *ApoE*^{-/-} mice (Fig. V-7). However, the quantity of α -actin in the plaque surface was not changed. These results indicate either a modification of vascular smooth muscle cell phenotype (dedifferentiation) or an increase in VSMC apoptosis in the absence of SSAO.

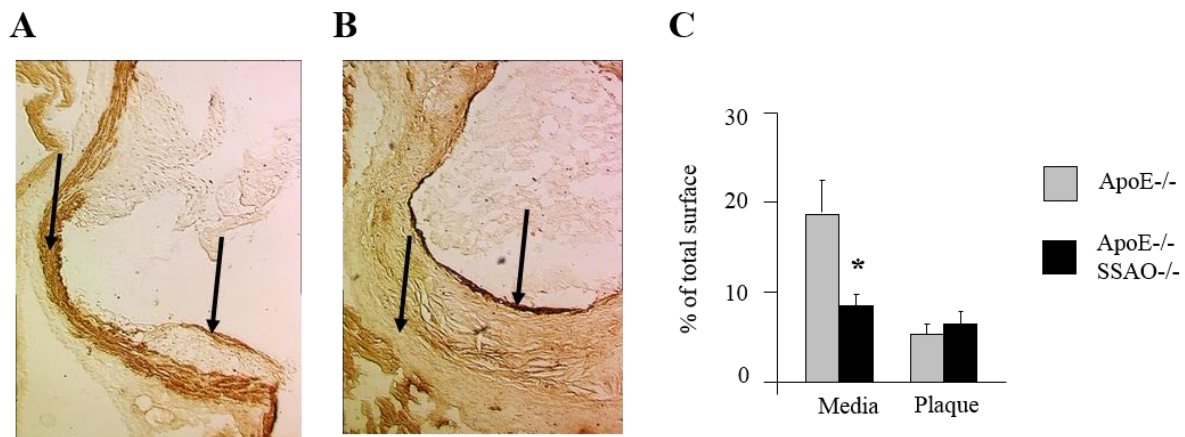


Figure V-7. α -actin IHC staining in the aortic sinus of old, 25 week-old female mice. The representative micrographs of mouse aortic sinus of *ApoE*^{-/-} control (A) and *ApoE*^{-/-} *SSAO*^{-/-} (B) mouse. C: α -actin stained surface expressed as a percent of total surface of tunica media or plaques. Grey bars represent control mice *ApoE*^{-/-}, black bars represent *ApoE*^{-/-} *SSAO*^{-/-} mice. In graph, bars represent the mean value ± SEM of six animals. Statistical significant P-values (*P<0.05) by Fisher's LSD Multiple-Comparison Test are shown in bold. The micrographs were taken using Nikon Japan DIAPHOT 300 with magnification of 10x.

3.1.3.2. Lymphocyte infiltration in media of aortic sinus

Then lymphocyte infiltration into the tunica media and plaques was studied (Fig. V-8). In 15 week-old mice, almost no CD3⁺ cells were found in the media which is in accordance with the immuno-privilege position of the media. However, the CD3⁺ cell number in the plaque was increased in *ApoE*^{-/-} *SSAO*^{-/-} mice compared to *ApoE*^{-/-} mice (Fig. V-8C).

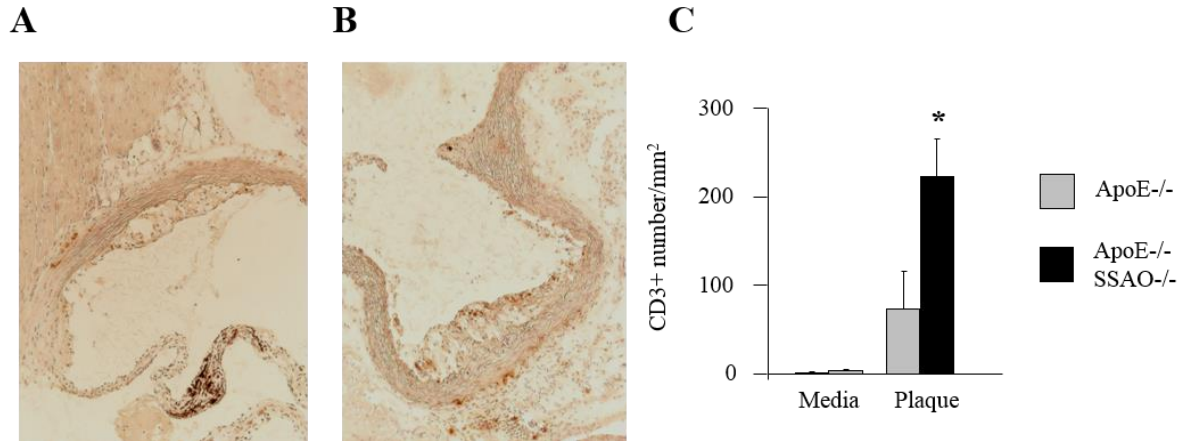


Figure V-8. Lymphocyte infiltration to plaques and tunica media in the aortic sinus of young, 15 week-old female mice. The representative micrographs of mouse aortic sinus. A: The aortic sinus of *ApoE*^{-/-} control mouse. B: The aortic sinus of *ApoE*^{-/-}*SSAO*^{-/-} mouse. C: CD3+ cells quantification expressed as CD3+ cell number per mm² of tunica media or plaques. Grey bars represent control mice *ApoE*^{-/-}, black bars represent *ApoE*^{-/-}*SSAO*^{-/-} mice. In the graph, bars represent the mean value \pm SEM of six (*ApoE*^{-/-}) and nine (*ApoE*^{-/-}*SSAO*^{-/-}) animals. Statistical significant P-values (*P<0.05) by Fisher's LSD Multiple-Comparison Test are shown in bold. The micrographs were taken using Nikon Japan DIAPHOT 300 with magnification of 10x.

Nevertheless, in 25 week-old *ApoE*^{-/-}*SSAO*^{-/-} mice, a significant increase in CD3+ cell number in the media but not in the plaques was found in figure V-9.

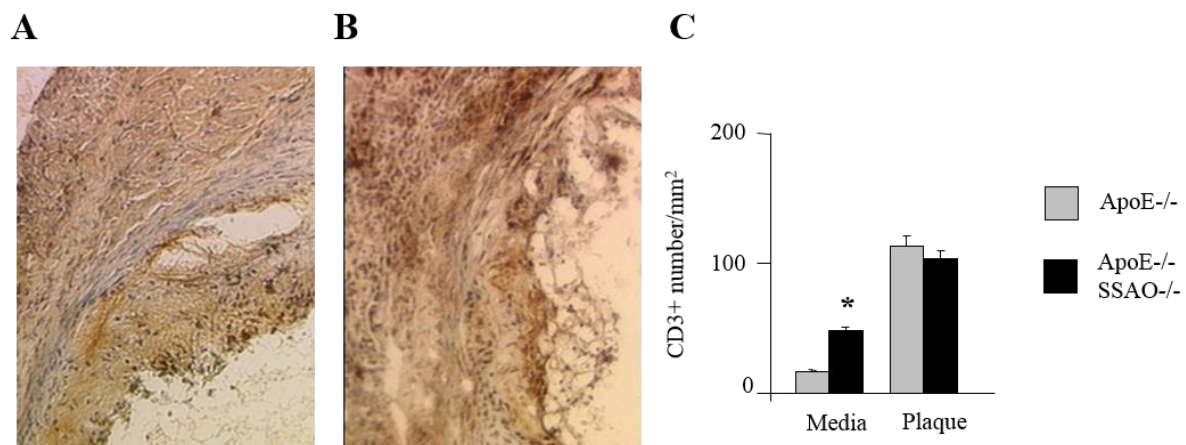


Figure V-9. Lymphocyte infiltration to plaques and tunica media in the aortic sinus of 25 female week-old mice. The representative micrographs of mouse aortic sinus. A: The aortic sinus of *ApoE*^{-/-} control mouse. B: The aortic sinus of *ApoE*^{-/-}*SSAO*^{-/-} mouse. C: CD3+ cells quantification expressed as CD3+ cell number per mm² of tunica media or plaques. Grey bars represent control mice *ApoE*^{-/-}, black bars represent *ApoE*^{-/-}*SSAO*^{-/-} mice. In the graph, bars represent the mean value \pm SEM of six animals. Statistical significant P-values (*P<0.05) by Fisher's LSD

Multiple-Comparison Test are shown in bold. The micrographs were taken using Nikon Japan DIAPHOT 300 with magnification of 10x.

3.1.3.3. Monocyte/macrophage presence in media of aortic sinus

In figure V-10, monocyte/macrophage infiltration into media and plaques of 25 week-old mice was monitored by MOMA positive staining. A strong positive staining was noticed in the neo-intima without any difference between the two genotypes.

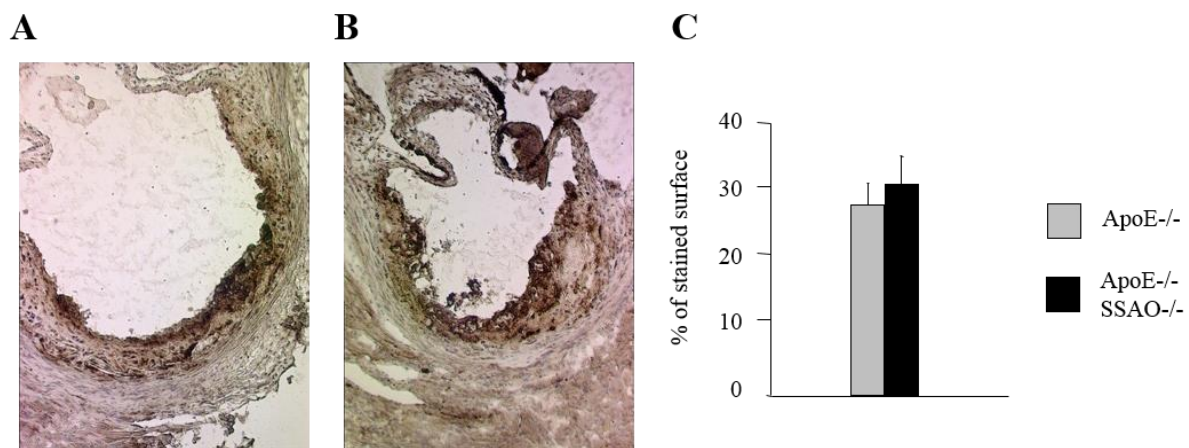


Figure V-10. Monocyte/macrophage infiltration to plaques in the aortic sinus of 25 week-old female mice. The representative micrographs of mouse aortic sinus. A: The aortic sinus of *ApoE*^{-/-} control mouse. B: The aortic sinus of *ApoE*^{-/-}*SSAO*^{-/-} mouse. C: MOMA staining quantification expressed as a percent of plaque stained surface. Grey bars represent control mice *ApoE*^{-/-}, black bars represent *ApoE*^{-/-}*SSAO*^{-/-} mice. In the graph, bars represent the mean value \pm SEM of six animals. Statistical significant P-values (***P**<0.05) by Fisher's LSD Multiple-Comparison Test are shown in bold. The micrographs were taken using Nikon Japan DIAPHOT 300 with magnification of 10x.

3.1.3.4. Collagen content in the media and the plaque of the aortic sinus

In order to study VSMC phenotype modification, we examined collagen content modification in the extracellular matrix in two genotypes by Sirius red staining. Figure V-11 shows no modification in the quantity of collagen in *ApoE*^{-/-}*SSAO*^{-/-} compared to *ApoE*^{-/-} mice, neither in tunica media nor in plaques in the aortic sinus of 25 week-old mice.

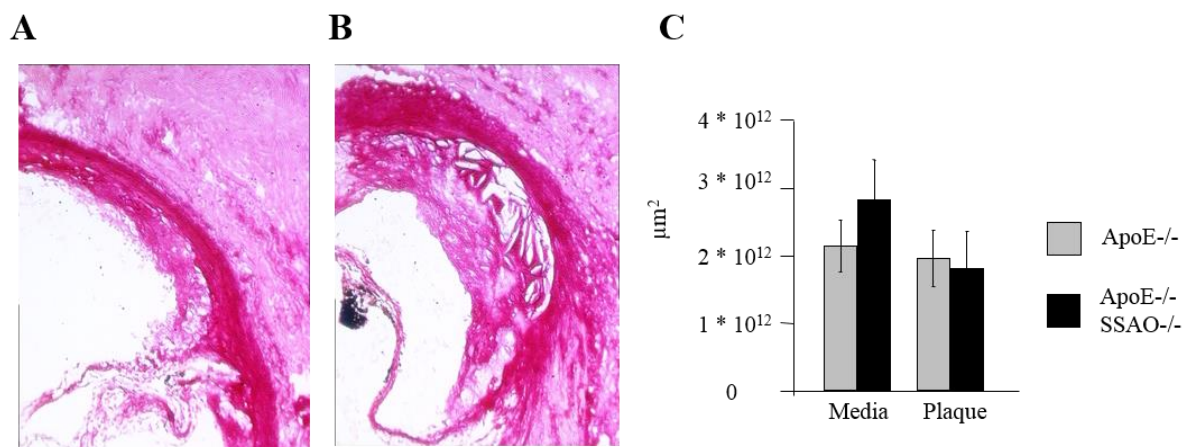


Figure V-11. Collagen content in plaques and tunica media in the aortic sinus of 25 week-old female mice. The representative micrographs of mouse aortic sinus. A: The aortic sinus of a *ApoE*^{-/-} control mouse. B: The aortic sinus of an *ApoE*^{-/-}*SSAO*^{-/-} mouse. C: collagen quantification in tunica media and plaques. Grey bars represent control mice *ApoE*^{-/-}, black bars represent *ApoE*^{-/-}*SSAO*^{-/-} mice. In the graph, bars represent the mean value \pm SEM of six animals. Statistical significant P-values ($*P < 0.05$) by Fisher's LSD Multiple-Comparison Test are shown in bold. The micrographs were taken using Nikon Japan DIAPHOT 300 with magnification of 10x.

Taken together, these results do not explain the role of SSAO in atherosclerosis development. Further experiments are necessary to study VSMC differentiation, calcification and inflammatory markers. In addition, modification in the immune response in the absence of SSAO needs to be explained.

3.1.4. Exploration of pro- and anti-inflammatory profiles

- in spleen

Then we were interested to study if absence of SSAO in *ApoE*^{-/-} mice causes and hastens plaque development via an increase in inflammatory status. So, gene expression of pro-inflammatory (TNF α and IFN γ), and anti-inflammatory (TGF β and IL-10) markers were measured in the spleen from the two genotypes in 15 (Fig. V-12) and 25 week-old mice (Fig. V-13).

No differences between the two genotypes were observed.

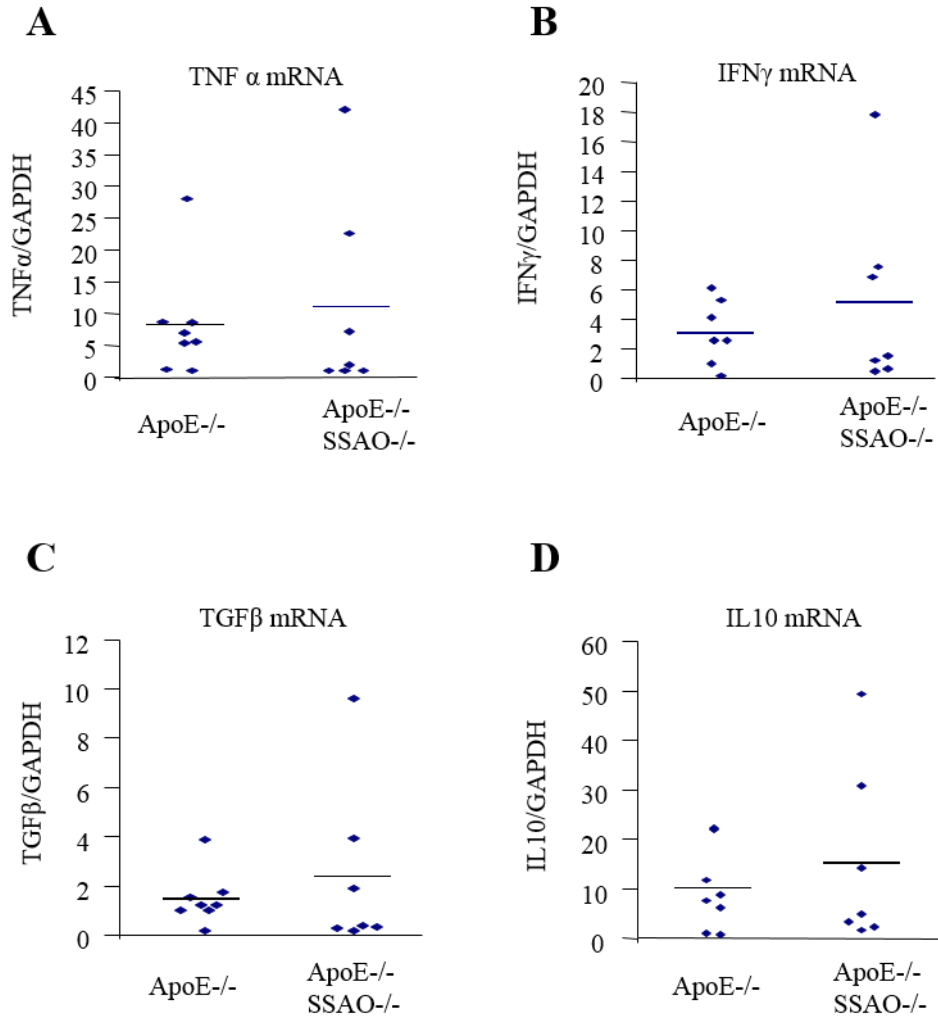


Figure V-12. Expression of pro-inflammatory markers (TNF α and IFN γ) and anti-inflammatory markers (TGF β and IL10) in spleen from *ApoE*^{-/-} and *ApoE*^{-/-}*SSAO*^{-/-} 15 week-old female mice. mRNA expression of A: TNF α , B: IFN γ , C: TGF β and D: IL10. As a reference GAPDH mRNA expression was used. In the graphs, the individual values for each animal and the average values are presented as a horizontal line for *ApoE*^{-/-} and *ApoE*^{-/-}*SSAO*^{-/-}. For each sample qPCR was performed in duplicate. Statistical significant P-values (*P<0.05) by Student t-Test are shown in bold.

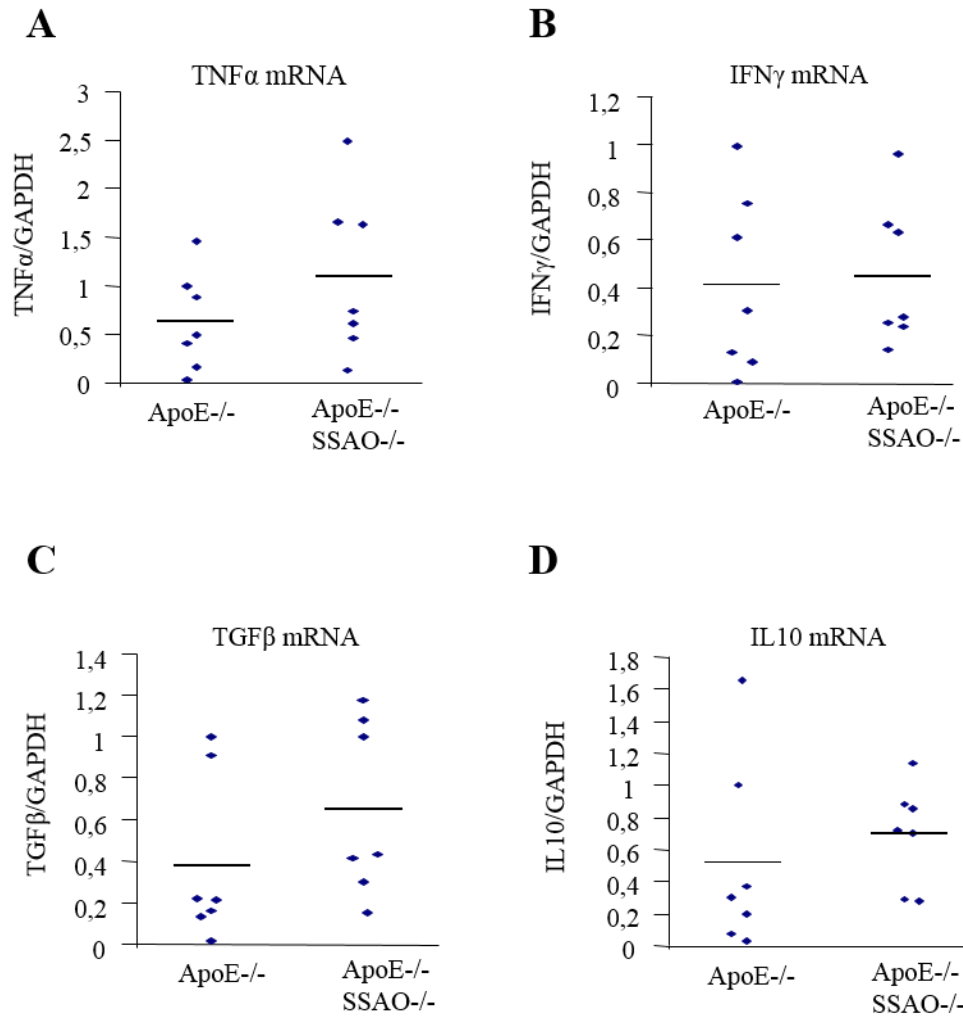


Figure V-13. Expression of pro-inflammatory markers (TNF α and IFN γ) and anti-inflammatory markers (TGF β and IL10) in the spleen from *ApoE* $^{-/-}$ and *ApoE* $^{-/-}$ SSAO $^{-/-}$ 25 week-old female mice. mRNA expression of A: TNF α , B: IFN γ , C: TGF β and D: IL10. As a reference GAPDH mRNA expression was used. In the graphs, the individual values for each animal and the average values are presented. For each sample qPCR was performed in duplicate. Statistics are calculated with respect to the *ApoE* $^{-/-}$ group. Statistical significant P-values (*P<0.05) by Student t-Test are shown in bold.

In order to study the differentiation of splenocytes, *ApoE* $^{-/-}$ and *ApoE* $^{-/-}$ SSAO $^{-/-}$ splenocytes were isolated and placed in culture under LPS+IFN- γ stimulation to induce an inflammation. The excretion of pro-inflammatory cytokine, interleukin 12 (which activates Th1 differentiation which are pro-atherogenic cells), and an athero-protective cytokine, interleukin 10, were measured in the medium. No differences in IL-10 and IL-12 were found between the two genotypes indicating no imbalance in the Th1/Th2 response.

- in aorta

Moreover, a “mouse atherosclerosis protein array” was performed with abdominal aortas from 15 (Fig. V-14) and 25 week-old (Fig. V-16) *ApoE*^{-/-} and *ApoE*^{-/-}*SSAO*^{-/-} mice in order to find if a modification in cytokine profil could explain the increase in plaque surface in the *ApoE*^{-/-}*SSAO*^{-/-} mice. The results are presented as a ratio of protein quantity in the aorta from *ApoE*^{-/-}*SSAO*^{-/-} to *ApoE*^{-/-}.

A decrease in bFGF, GM-CSF, INF γ , IL1b, MIP-3 α and RANTES expression and an increase in MCP-1 expression were found in aorta from *ApoE*^{-/-}*SSAO*^{-/-} 15 week-old mice compared to *ApoE*^{-/-} mice (Fig. V-15). Thus based on these result we cannot elucidate if inflammatory status was modified in the absence of SSAO in *ApoE*^{-/-} mice.

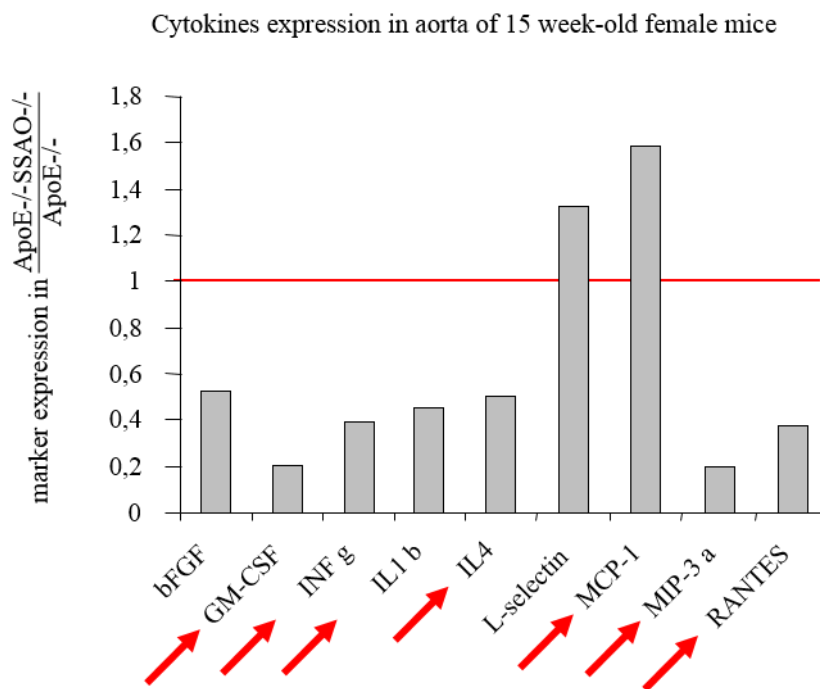


Figure V-14. Mouse atherosclerosis array was performed with abdominal aortas from 15 week-old female mice. In the graph, the results are presented as the ratio between the marker expression in *ApoE*^{-/-}*SSAO*^{-/-} aorta and the marker expression in *ApoE*^{-/-}. 7 abdominal aortas per groups were homogenized separately and an equal amount of proteins were pooled together in each group. The results present the pool of seven or eight independent aorta samples. The red arrows indicate a modification higher than 50% in the expression marker ratio. The horizontal red line symbolizes no change in expression (ratio = 1).

3.1.5. Exploration of the VSMC phenotype

We suspected that the significant increase of atherosclerosis in *ApoE*^{-/-} mice in absence of SSAO could be caused by VSMC phenotype modulation. To study VSMC phenotype modification we performed WB and we quantified the presence of differentiated VSMC markers: smMHC and α -actin. In *ApoE*^{-/-}*SSAO*^{-/-} 25 week-old female mice, we found a significant decrease of smMCH protein level although α -actin was unchanged (Fig. V-15). The decrease of smMHC indicates that cells may lose their differentiated phenotype.

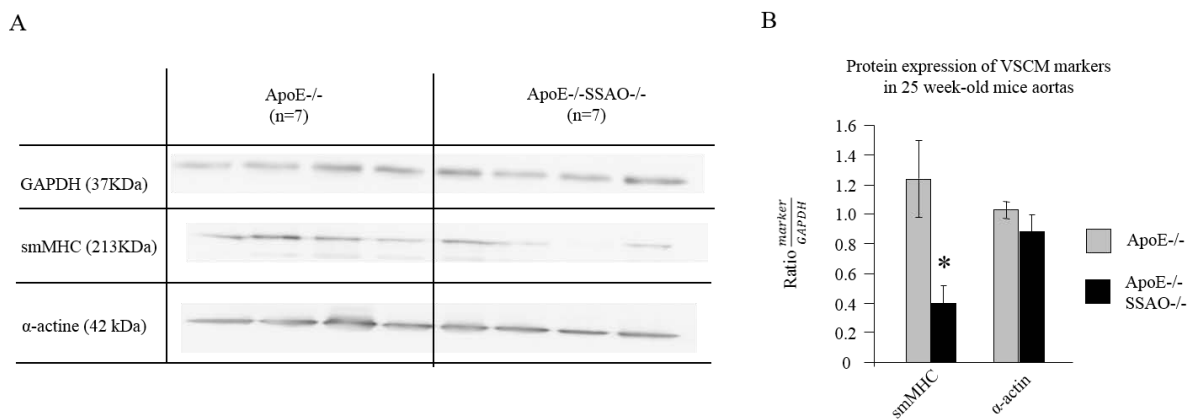


Figure V-15. Western blot was performed to study protein presence in abdominal aortas from 25 week-old female mice. A: the representative WB membranes for each marker and B: protein quantification. As a reference GAPGH expression was used. The grey bar represents control *ApoE*^{-/-} mice, the black bar represents *ApoE*^{-/-}*SSAO*^{-/-} mice. In the graph, bars represent the mean value \pm SEM of seven (*ApoE*^{-/-}) and seven (*ApoE*^{-/-}*SSAO*^{-/-}) animals. Statistical significant P-values (*P<0.05) by Student t-Test are shown in bold.

3.1.6. Role of SSAO in cellular trafficking in *ApoE*^{-/-}*SSAO*^{-/-} mice vs *ApoE*^{-/-} mice - in mice under HFD

The other hypothesis that could explain the differences in atherosclerotic plaque size in *ApoE*^{-/-}*SSAO*^{-/-} mice compared to *ApoE*^{-/-} mice could be a modification of immune cell recruitment to the lesion area. After 4 weeks on a high fat diet, young mice (early stage of atherosclerosis) were injected with peripheral bone marrow cells from *ApoE*^{-/-} CD45.1 mice. Five days after

the injection, the presence of CD45.1 cells was monitored in the blood, the spleen and the aorta by FACS.

As the principal characteristic of this group of animals, we did not find modification in cholesterol levels in *ApoE*^{-/-}*SSAO*^{-/-} mice compared to *ApoE*^{-/-} mice (Fig V-16A). In addition, the atherosclerotic plaque surface was unchanged in the absence of SSAO in *ApoE*^{-/-} mice (Fig V-16B).

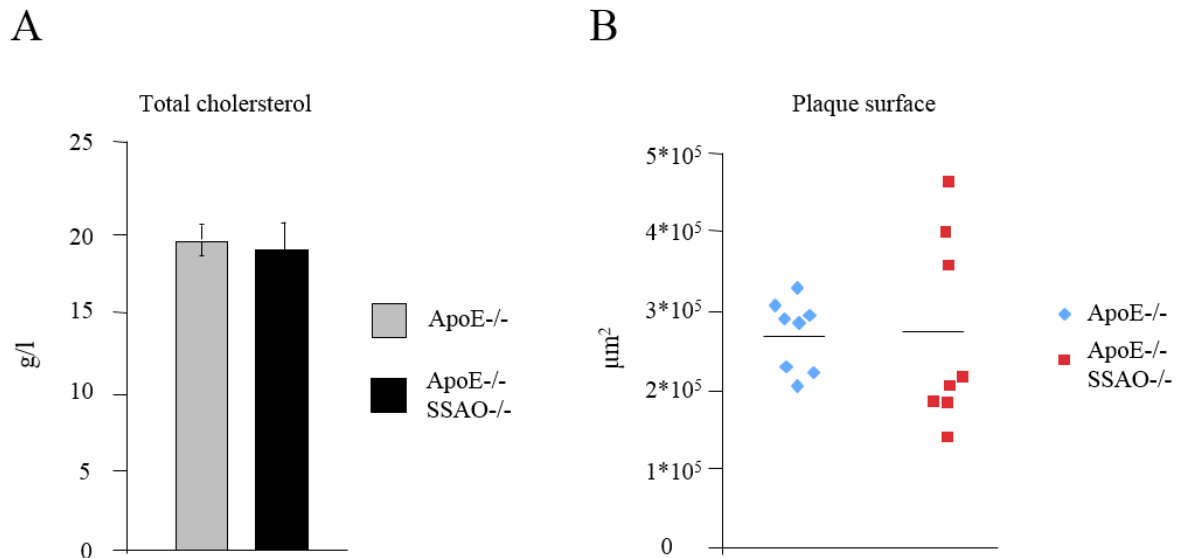


Figure V-16. General characteristic of *ApoE*^{-/-} and *ApoE*^{-/-}*SSAO*^{-/-} young female mice. The results present, A: cholesterol levels and B: atherosclerotic plasue size in *ApoE*^{-/-} and *ApoE*^{-/-}*SSAO*^{-/-} mice. Grey bars (dots) represent control mice *ApoE*^{-/-}, black bars (dots) represent *ApoE*^{-/-}*SSAO*^{-/-} mice. In graph A, bars represent the mean value ± SEM of eight animals. In graph B, the independent values of eight animals in each genotype, and the mean values (horizontal line) are presented.

However, a modification in CD45.1 cell trafficking was found. Our results show a significant decrease of the CD45.1 cell percentage in the blood and a significant increase of the CD45.1 percentage in the aorta wall (Fig. V-17). This suggests that the absence of SSAO in *ApoE*^{-/-} mice increases the recruitment of immune cells from blood to the arterial wall.

Nevertheless, we did not find differences between the two genotypes in the CD45.1 cell percentage in the spleen.

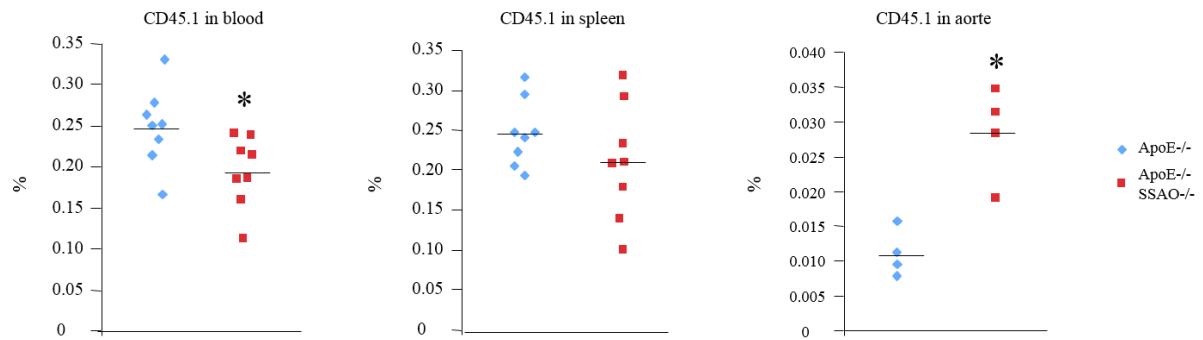


Figure V-17. CD45.1 peripheral bone marrow cells (PBMC) distribution in *ApoE*^{-/-} and *ApoE*^{-/-}*SSAO*^{-/-} young female mice. After 4 weeks of a high fat diet, *ApoE*^{-/-} and *ApoE*^{-/-}*SSAO*^{-/-} mice were injected with PBMC isolated from *ApoE*^{-/-} CD45.1 mice. Subsequently, the percentage of CD45.1 cells in the blood, the spleen and the aorta was counted by FACS. In the graphs, the independent values of eight animals in each genotype, and the mean values (horizontal line) are presented in the blood and the spleen. In the FACS analysis for aorta samples, each result (dot) represents the mean of two pooled aortas. For each sample FACS was performed in duplicate. Statistical significant P-values (*P<0.05) by Student t-Test are shown in bold.

Studies of CD45.1 cell populations have shown significant increases of CD4 percent in blood from *ApoE*^{-/-}*SSAO*^{-/-} mice and significant increase of CD3 percent in aortic wall (Fig. V-18).

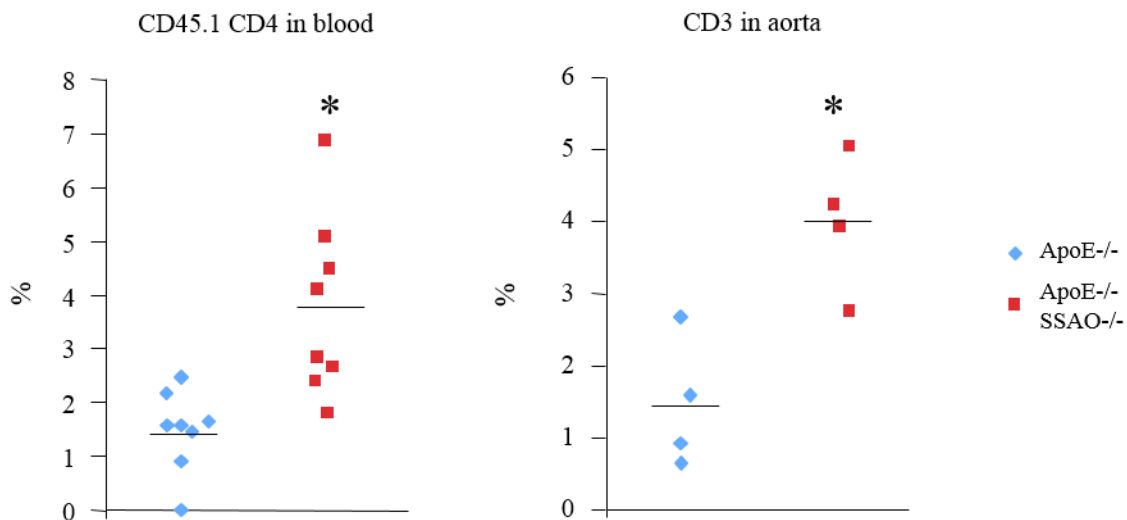


Figure V-18. Immune cell populations in *ApoE*^{-/-} and *ApoE*^{-/-}*SSAO*^{-/-} young mice. The percentage of CD4 in blood (A) and CD3 in aorta (B). Grey bars (dots) represent control mice *ApoE*^{-/-}, black bars (dots) represent *ApoE*^{-/-}*SSAO*^{-/-} mice. In graph, the independent values of eight animals in each genotype, and the mean values (horizontal line) are presented. In the FACS analysis for aorta samples, each result (dot) represents the mean of two pooled aortas. For each sample FACS was performed in duplicate. Statistical significant P-values (*P<0.05) by Student t-Test are shown in bold.

The spleen weight was significantly increased in *ApoE^{-/-}SSAO^{-/-}* mice, compared to *ApoE^{-/-}* mice without any difference in body weight and cholesterol level. In addition, the number of splenocytes was also significantly increased in *ApoE^{-/-}SSAO^{-/-}* mice, compared to the control group.

4. Discussion

Many reports exist about the elevated soluble form of SSAO in blood of patients with diabetes, congestive heart failure, cerebral infarct and atherosclerosis. Studies of Yu et al., (1998b) have shown that the C57BL/6 mouse strain, which is more susceptible to atherosclerosis (even if mice are naturally resistant to atherosclerosis), presented a significant increase in SSAO activity and an higher rate of SSAO-dependent MA turnover and an higher production of formaldehyde than other strains more resistant to atherosclerosis (IE, Balb/c and CD1). The authors suggested that this increase in formaldehyde production could result in some vascular disorders (Yu et al., 2003).

In addition, SSAO is also known to play a role in immune cell trafficking *in vivo* in normal conditions and at the inflammation site (Salmi et al., 2001; Stolen et al., 2005).

So the hypothesis of our research was that the absence of SSAO would decrease atherosclerosis in *ApoE*^{-/-} mice *via* limitation of inflammation and a reduction of immune cell infiltration into lesion sites. In order to study our hypothesis we generated *SSAO*-deficient *ApoE*^{-/-} mice with the C57BL/6 genetic background, and we have studied plaque development. As found in the literature, female *ApoE*^{-/-} mice with the C57BL/6 genetic background develop better atherosclerosis than male *ApoE*^{-/-} mice with the same genetic background (Surra et al., 2010). For the purposes of our experiment we used only female mice. We have used young female mice (15 week-old) where the lesion area was small in order to study the early stage of disease development. In order to study the later stage of atherosclerosis we have used older, 25 week-old female mice.

In order to confirm that SSAO plays a role in atherosclerosis we studied plaques size in the aortic sinus and the thoracic aorta. We did not notice differences in plaque size between the two genotypes in 15 week-old mice. However, examination of 25 week-old mice, contrary to our predication, have shown that the absence of SSAO increased atherosclerotic plaque

development in *ApoE^{-/-}* mice. The plaque size was studied in aortic sinus where we noticed a significant 1.4 fold increase, and in thoracic aorta where a 2.2 fold increase was noted.

These results were contradictory with our hypothesis based on the literature that suggested that the absence of SSAO would limit inflammation development and limit immune cell infiltration into inflamed tissue.

In the literature we find that increased activity of the soluble form of SSAO in inflammatory conditions could participate in endothelium damage, protein crosslinkage and atherosclerosis development by toxic product generation. Increased, SSAO-dependent, MA oxidative deamination increased cytotoxicity in endothelial cells *in vitro* (Yu et al., 1993). As reported by Yu et al., (1998b) their studies have shown that MA-treated mice increase SSAO activity and it is associated with vulnerability to atherosclerosis in C57BL/6 mice. In addition, atherosclerotic plaque surface area increased in mice treated with MA vs non-treated mice. And overexpression of SSAO in endothelial cells in mice decreased the number of atherosclerotic lesions whereas the total surface area of atherosclerosis remained unchanged, compared to normal mice. Thus SSAO overexpression and its elevated activity modified plaque development (Stolen et al., 2004b). Recently it was reported that inhibition of SSAO gene expression and enzymatic activity by liver X receptor agonist T0901317 shows the atheroprotective effect *in vivo* (Dai et al., 2008). *In vitro* studies have confirmed that aldehyde and H₂O₂ formation by soluble SSAO increased apoptosis in vascular smooth muscle cells. However, the formaldehyde indicated higher cytotoxicity than H₂O₂ and it seems to be the main contributor to cell death by altering mitochondria homeostasis (Hernandez et al., 2006). Aortic smooth muscle cells transfected with human SSAO cDNA express a membrane form of SSAO and also an increase in cell death under acute MA treatment. The enzymatic action of membrane SSAO by formation of formaldehyde is involved in the toxicity process. Removal of H₂O₂ by catalase addition probably increases MA oxidation thus more formaldehyde is generated and higher cytotoxicity was detected (Sole et al., 2008).

Further, since the level of serum SSAO activity was shown to be associated with the severity of atherosclerosis it has been proposed that determination of sSSAO activity could be marker of atherosclerosis (Kardi et al., 2002).

All these reports about enzymatic action of a soluble or membrane form of SSAO show that aldehyde formation is the principal cause the cell dysfunction and can lead to disease development. Thus absence of SSAO should decrease atherosclerosis development.

In 2004, Koskinen et al., confirmed that SSAO plays an important role in immune cell emigration. Its activity on the luminal surface of endothelial cells was a precondition for adhesive function, and regulated polymorphonuclear leukocytes extravasation *in vitro* and *in vivo*.

In addition, SSAO regulates granulocyte transmigration through the endothelium (Tohka et al., 2001; Koskinen et al., 2004). When SSAO activity is blocked, a great reduction in the number of granulocytes infiltrating into an inflamed tissue was observed. The same studies have shown that SSAO has a role in the initiation of rolling and then leads to adhesion and extravasation of granulocytes (Tohka et al., 2001). Blockade of SSAO adhesion leads to significant decreases of T-lymphocyte infiltration *in vivo* (Martelius et al., 2004).

The absence of SSAO impairs the capacity of lymphocytes and polymorphonuclear leukocytes to interact with the vascular endothelium and manifests as highly increased rolling velocity, diminished firm adhesion and reduced transmigration (Stolen et al., 2005). And blockade of SSAO activity attenuates granulocyte-dependent inflammatory responses *in vivo* (Tohka et al., 2001).

In atherosclerotic plaque formation and development, immune cell recruitment to a lesion site is the crucial event. The aim of the immune response is the elimination of inflammation and to limit disease development. Nevertheless, monocytes recruited to the arterial wall in contact with oxLDL differentiate into macrophages and by phagocytosis form the foam cells. Subsequently foam cells form the fatty streaks and the atherosclerotic plaque develops.

In next stage of our work, by injection of peripheral bone marrow cells from CD45.1 *ApoE*^{-/-} mice we studied SSAO involvement in modulation of immune cell trafficking in young *ApoE*^{-/-} mice on a high fat diet. In this group of mice, atherosclerosis development was in an early stage and we did not notice any difference in plaque surface between two genotypes. Interestingly, the results have shown that in the absence of SSAO in *ApoE*^{-/-} mice the number of CD45.1 cells significantly decreased in blood and significantly increased in the thoracic aorta. This result indicates that when SSAO is absent, immune cells are directed from blood to the arterial wall.

Thus we decided that studies of the VSMC phenotype were necessary to clarify the cause of inflammatory cell recruitment in the absence of SSAO.

Salmi et al., (2001) and Stolen et al., (2005) have reported that SSAO controls lymphocyte migration, and other studies have confirmed that SSAO enzymatic activity or *SSAO* gene elimination, decrease lymphocyte infiltration. Our results described below show the contrary effect of SSAO absence suggesting that in atherosclerosis other mechanisms of immune cells recruitment can play an important role. So we decided to study pro- and anti-inflammatory marker expression and cytokines involved in atherosclerosis present in aortas from 15 and 25 week-old *ApoE^{-/-}SSAO^{-/-}* and *ApoE^{-/-}* mice. In our results, no significant difference in gene expression of pro- and anti-inflammatory markers was found between the two genotypes for the two different age groups.

Then we studied the presence of atherosclerosis-related cytokines in aorta of 15 and 25 week-old *ApoE^{-/-}SSAO^{-/-}* and *ApoE^{-/-}* mice.

In literature we found reports showing that chemokine monocyte chemoattractant protein-1 (MCP-1) specifically attracts monocytes, memory T lymphocytes and NK cells. It was also involved in the recruitment of leukocytes to sites of inflammation (Zittermann et al., 2006). Moreover, the absence of MCP-1 reduces atherosclerosis (Gu et al., 1998). Our studies have shown that in the early stage of atherosclerosis absence of SSAO in 15 week-old *ApoE^{-/-}* mice increased MCP-1 in the aortic wall. In 25 week-old *ApoE^{-/-}SSAO^{-/-}* mice there was a significant increase in plaque surface area, even if the increase of MCP-1 was not preserved.

We observed also a diminution of granulocyte macrophage-colony stimulating factor (GM-CSF) in the arterial wall of young, 15 week-old *ApoE^{-/-}SSAO^{-/-}* mice, compared to control mice. There exist many reports about the role of GM-CSF in atherosclerosis where it is abundantly present. The treatment of male *ApoE^{-/-}* mice with murine GM-CSF increased the atherosclerotic lesion area by 2-fold. In contrast, genetic deletion of GM-CSF in *ApoE^{-/-}* mice increased atherosclerotic lesion size (Kleemann et al., 2008). In our research we noticed a decrease in GM-CSF in the arterial wall of young *ApoE^{-/-}SSAO^{-/-}* mice and subsequently an increase of atherosclerotic plaques in older mice. Our results are in accordance with those presented for GM-CSF-deficient *ApoE^{-/-}* mice.

Nevertheless, the decrease of interferon γ and basic fibroblast growth factor (bFGF), and increase in interleukin 5 are not well correlated with an increase in plaque surface in *ApoE^{-/-}SSAO^{-/-}* mice. IFN γ is a pro-inflammatory mediator and is expressed at high levels in atherosclerotic lesions by various cells (Kleemann et al., 2008), so a decrease of its expression should provide the limitation of atherosclerosis development. Subsequently, a decrease of

bFGF which synergistically enhances the recruitment of monocytes, T cells, and PMNs in response to a variety of inflammatory mediators (Zittermann et al., 2006) should result in a decrease but should not support lesion area development in *ApoE^{-/-}SSAO^{-/-}* mice. In addition, IL-5 is reported to play overall atheroprotective role (Kleemann et al., 2008). However, an increase in its expression was not sufficient to prevent atherosclerosis development in 25 week-old *ApoE^{-/-}SSAO^{-/-}* mice. We noticed also an increase of VEGF in 25 week-old *ApoE^{-/-}SSAO^{-/-}* mice, a factor known to be correlated with new plaque formation and increased neovascularization.

Taken together, the VSMC phenotype markers need to be studied for a better understanding of the increase of atherosclerosis in SSAO-deficient *ApoE^{-/-}* mice. Moreover, the modification of immune cells recruitment to the lesion site in the absence of SSAO can clarify the increased promotion of atherosclerosis.

To better understand our results we have studied plaque composition and modification in tunica media.

In the first instance a significant decrease of α -actin expression by smooth muscle cells was detected in tunica media of aortic sinus from 25 week-old *ApoE^{-/-}SSAO^{-/-}* mice compared to *ApoE^{-/-}* mice. As the aorta is the major source of SSAO activity, and it is expressed by VSMC, we can suspect that SSAO plays a role in the maintenance of the cell phenotype. Thus the absence of SSAO could cause the switching of the VSMC contractile phenotype to a synthetic one.

In the literature we found reports on SSAO expression in VSMC where it plays a role in glucose transport. Nevertheless, involvement of SSAO in cell differentiation was not shown (El Hadri et al., 2002). However, the glucose transported to the cell may act as a signal modulating the expression of genes coding for differentiation markers and extracellular matrix proteins (Mercier et al., 2009; Bartz et al., 2010).

Furthermore, studies underway for atherosclerotic plaque characterization have shown in tunica media in aortic sinus from 25 week-old *ApoE^{-/-}SSAO^{-/-}* mice an increase of lymphocyte infiltration. Nevertheless no differences in monocytes/macrophages recruitment were noted. In addition, the collagen content in the extracellular matrix was not changed in the absence of SSAO in aortic sinus of 25 week-old *ApoE^{-/-}* mice.

In addition, the product of SSAO enzymatic action, H₂O₂, is known to be a signaling molecule in the appropriate concentration. It was also suggested that optimal health may require a certain amount of oxidative stress (Bartz et al., 2010; Marinho et al., 2014). Cell exposure to a small dose of H₂O₂ can induce a favorable biological response thus deletion of the enzyme which generates this molecule could have a negative impact on the cell phenotype. Because of that in our future studies we wish to study the role of VSMC SSAO in normal and in the inflammatory condition.

For the purpose of studying VSMC phenotype modulation we decided to treat the aortas from 15 and 25 week-old, WT and *SSAO*^{-/-} female mice with the pro-inflammatory molecule, TNF α . We wished to find modulation of phenotype-specific marker expressions in aortas from *SSAO*^{-/-} female mice compared to WT female mice of the same age.

5. Conclusion

In this work we have explored the role of SSAO in atherosclerosis development in *ApoE^{-/-}* mice. *In vivo* the implication of SSAO in the process of atherosclerotic plaque formation was shown. The main results of this work are:

1. *SSAO activity in $ApoE^{-/-}$ mice was not changed when compared to WT mice.*

The enzyme activity was measured in several tissues such as: aorta, adipose tissue, lung and heart from *ApoE^{-/-}* and WT mice. The level of SSAO activity was not significantly changed in transgenic animals compared to WT mice.

2. *The absence of SSAO did not change the lipid profile in $ApoE^{-/-}$ 15 week-old and 25 week-old female mice.*

In order to study atherosclerotic plaque development in *ApoE^{-/-}SSAO^{-/-}* mice compared to *ApoE^{-/-}* in the first instance we have confirmed that the absence of SSAO modified the lipid profile which could explain the differences in plaque surface area. Our results have shown unchanged lipid profiles in 15 week-old and 25 week-old female mice.

3. *The absence of SSAO in $ApoE^{-/-}$ increases atherosclerosis development.*

ApoE^{-/-}SSAO^{-/-} mice presented significant increase of atherosclerotic plaque surface in aortic sinus and thoracic aorta compared to *ApoE^{-/-}* mice. The differences in plaque surface were accompanied by decreases of α -actin expression and increased CD3+ infiltration in plaques (15 week-old) and in media (25 week-old) from aortic sinus of *ApoE^{-/-}SSAO^{-/-}* mice compared to *ApoE^{-/-}* mice. Nevertheless, monocyte/macrophage infiltration to the plaques was unchanged, as well as the collagen content in media and plaques.

4. *The inflammatory profile was unchanged in spleen but not in aorta.*

No differences in expression of pro- and anti-inflammatory cytokines were found in the spleen from the two different genotypes. However, differences in cytokines present in the abdominal aortas between the genotypes were found.

5. *Absence of SSAO has an influence on VSMC phenotype.*

In the late stages of atherosclerosis the VSMC, in the absence of SSAO, expressed less sm-MCH which could indicate dedifferentiation of cells. In later stages of the disease the α -actin in aortas from *ApoE^{-/-}SSAO^{-/-}* mice is unchanged compared to aortas from *ApoE^{-/-}* mice.

6. *SSAO absence changes the trafficking of immune cells in ApoE^{-/-} mice on a high fat diet.*

Labelled PBMC injected into the *ApoE^{-/-}SSAO^{-/-}* mice are increased in the aortic wall and decreased in blood compared to *ApoE^{-/-}* mice. Moreover, an increase of the number of CD4 in blood and CD3⁺ in the aortic wall of *ApoE^{-/-}SSAO^{-/-}* mice was found compared to *ApoE^{-/-}* mice.

6. Perspectives

How VSMC in aortas from SSAO^{-/-} mice change their phenotype under inflammatory conditions?

SSAO in aortas from WT mice is abundantly expressed, nevertheless only its role in glucose transport for these cells is known. Nobody has explored its role in VSMC differentiating phenotypes. In the next stage of our research, we wish to study modulation of the smooth muscle cell phenotype under inflammatory conditions *in vitro*, in the presence or absence of SSAO (cells from aortas of *ApoE^{-/-}* and *ApoE^{-/-}SSAO^{-/-}* mice). For this purpose isolation of VSMC from several aortas was performed. Cells were cultured *in vitro*, and several passages were performed to obtain a sufficient number of cells. Nonetheless, during the second passage cells stopped proliferation and they had a star-shaped form which indicated loss of the differentiation phenotype. Moreover, they did not express α -actin/SM-MHC. After several attempts we were not able to have a sufficient number of cells with a good phenotype. Because of that we decided to treat *ex vivo* whole thoracic aortas from WT and *SSAO^{-/-}* mice of 15 and 25 week-old with the inflammatory agent TNF α . Several experimental groups were provided (Tab. III-1). The general characteristics of the mice are presented in figure V-27 for 15 week-old mice and in figure V-28 for 25 week-old mice.

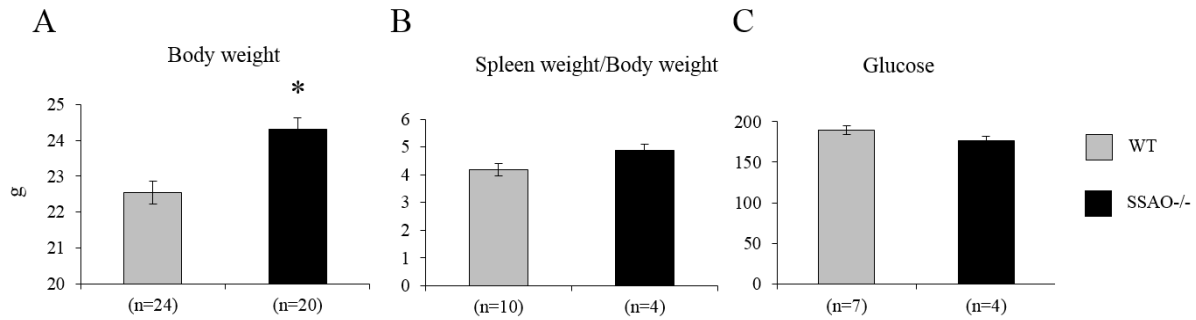


Figure V-19. General WT and *SSAO*^{-/-} 15 week-old female mice characteristics. A: body weight expressed in grams. B: ratio of spleen weight to body weight and C: glucose level in blood, after 4 hours of fasting. Grey bars represent control, WT mice, black bars represent *SSAO*^{-/-} mice. In the graphs, bars represent the mean value \pm SEM of “n” independent animals. N-value is different for each group therefore indicated below each bar. Statistical significant P-values (*P<0.05) by Student t-Test are shown in bold.

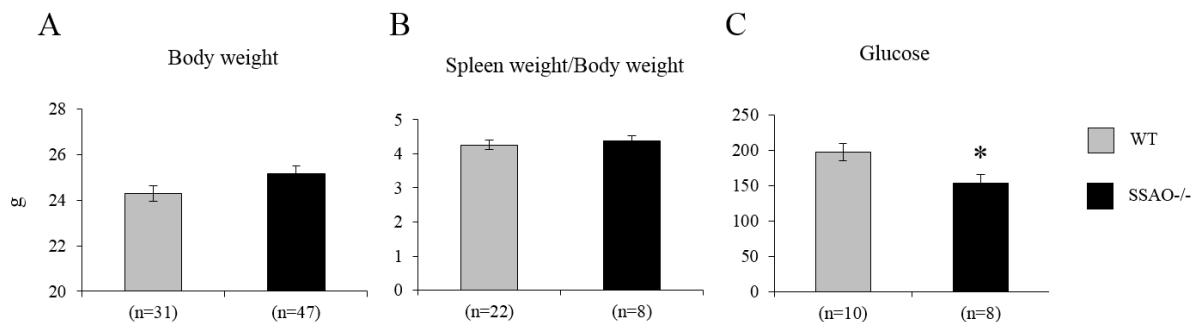


Figure V-20. General WT and *SSAO*^{-/-} 25 week-old female mice characteristics. A: body weight expressed in grams. B: ratio of spleen weight to body weight and C: glucose level in blood, after 4 hours of fasting. Grey bars represent control, WT mice, black bars represent *SSAO*^{-/-} mice. In the graphs, bars represent the mean value \pm SEM of “n” independent animals. N-value is different for each group therefore indicated below each bar. Statistical significant P-values (*P<0.05) by Student t-Test are shown in bold.

What is the role of SSAO in VSMC?

In order to answer this question cell cultures of VSMC need to be established in permissive conditions for cell differentiation. Then modulation of SSAO activity by substrate/selective inhibitors needs to be performed in order to clarify its role in this cell type.

VI. General discussion

The extracellular matrix (ECM) plays an important role in many tissues, especially in cartilage and in blood vessels, where it not only provides mechanical properties like elasticity but also ensures integrity and functionality. The integrity of the macromolecular network can be altered during aging or in pathophysiological situations leading to cardiovascular (atherosclerosis, arteriosclerosis) or joint (osteoarthritis, arthritis) diseases. These age-related diseases are highly prevalent in today's population. They greatly affect the quality of life of patients and are sources of important economic costs.

Homeostasis of the arterial wall and cartilage is provided by synthesis of tissue-specific matrix molecules by resident cells, in vessels: vascular smooth muscle cells (VSMC) and in cartilage: chondrocytes. Quality of ECM proteins depends on the state of cell differentiation/phenotype which can be affected during aging or during diseases development (osteoarthritis/arthritis and atherosclerosis).

As we have already shown in this work, SSAO expression/activity was reported in many tissues where under physiological condition it plays different roles. SSAO increases during differentiation of VSMC where, similarly to adipocytes, it promotes glucose transport. In addition, SSAO can accelerate adipocyte differentiation (Mercier et al., 2001; El Hadri et al. 2002). Several studies have suggested an involvement of SSAO in the organization of the ECM *via* the establishment of crosslinks or altering the synthesis or organization of other matrix components such as proteoglycans (Mercier et al., 2006, 2007 and 2009). Finally, SSAO may also participate in the oxidation of LDL and in inflammation, in particular *via* the soluble form of SSAO in serum. The soluble form of SSAO is increased in the plasma of patients with cardiovascular and inflammatory diseases.

Because of SSAO differentiation-dependent expression and potential roles in matrix organization, we have studied in this work SSAO implication in the differentiation process of VSMC and chondrocytes in physiological and pathological conditions in animals and in man.

Many reports show toxicity of products generated by SSAO. So overexpression of SSAO in tissues like cartilage or arteries may cause progression of the lesion area.

The results of our studies have shown that SSAO is implicated in chondrocyte differentiation and its expression and activity are elevated in osteoarthritic human cartilage.

In addition, we can suspect that an increase of SSAO activity is involved in extracellular matrix modification.

On the other hand, inhibition of SSAO activity or blockade of its adhesive function did not decrease atherosclerosis. Moreover, the absence of SSAO in *ApoE*^{-/-} mice increased disease development. These results are contradictory to our assumption that SSAO by generation of aldehydes and increased immune response will increase atherosclerotic plaque development. So we can suspect that SSAO has roles other than the increase of inflammation in this pathology.

Taken together, these results show that SSAO plays an important role in diseases such as osteoarthritis and atherosclerosis. The explanation of the mechanism and role of SSAO in those diseases may be useful to identify new targets at the origin of medical treatments. Indeed, SSAO has already been considered as a new therapeutic target. At the moment human monoclonal antibodies targeting SSAO have been investigated in small clinical trials in rheumatoid arthritis and psoriasis patients. And research is advancing (phase II) in the fibrotic condition.

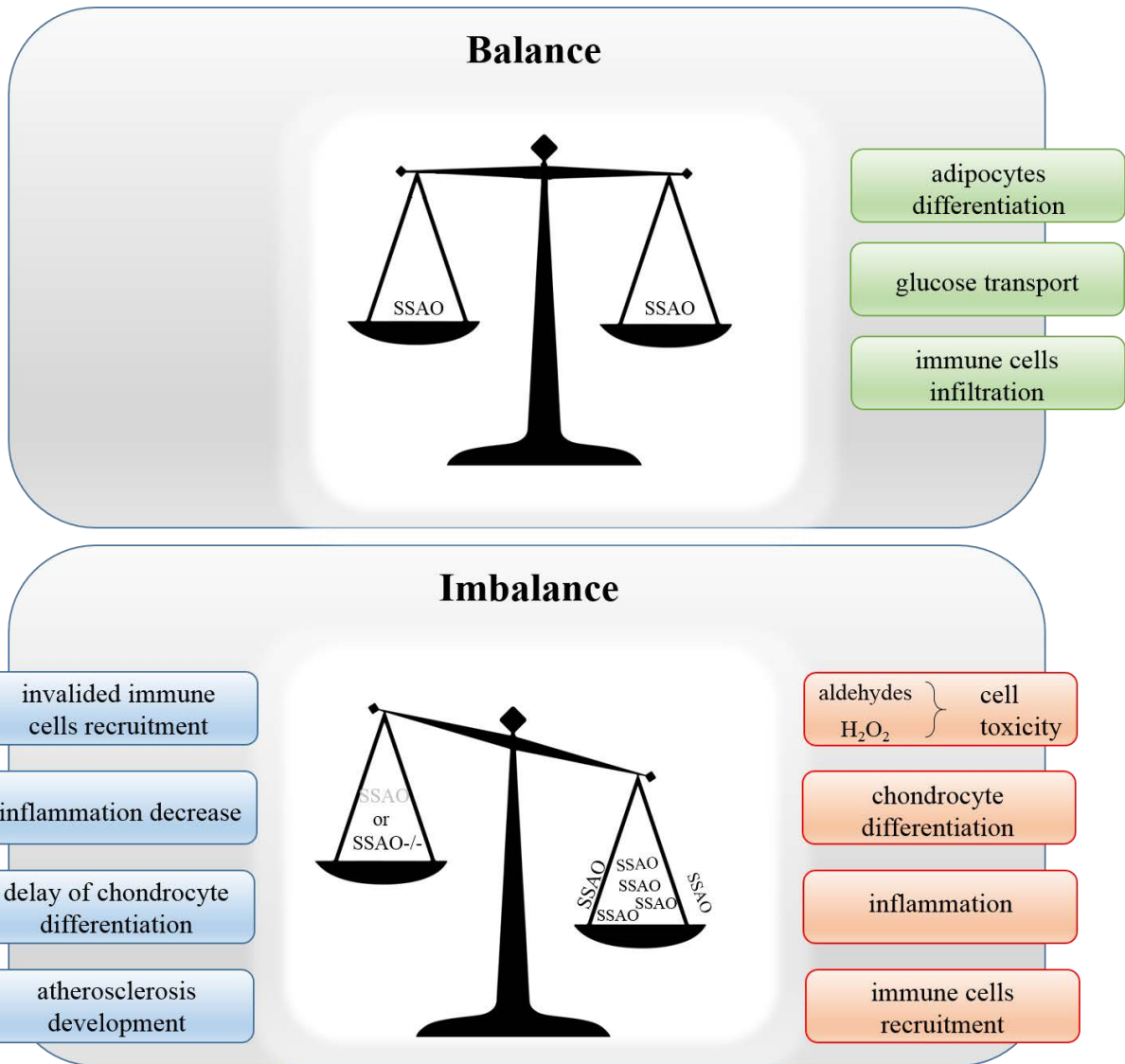


Figure V-1. The general schema of the consequences of SSAO action.

VII. References

- Abella, A., García-Vicente, S., Viguierie, N., Ros-Baró, A., Camps, M., Palacín, M., Zorzano, A., and Marti, L. (2004). Adipocytes release a soluble form of VAP-1/SSAO by a metalloprotease-dependent process and in a regulated manner. *Diabetologia* 47, 429-438.
- Abouhamed, M., Reichenberg, S., Robenek, H., and Plenz, G. (2003). Tropomyosin 4 expression is enhanced in dedifferentiating smooth muscle cells in vitro and during atherogenesis. *Eur J Cell Biol* 82, 473-482.
- Adams, B.D., Samani, J.E., and Holley, K.A. (1996). Triangular fibrocartilage injury: a laboratory model. *J Hand Surg Am* 21, 189-193.
- Aigner, T., Glückert, K., and von der Mark, K. (1997). Activation of fibrillar collagen synthesis and phenotypic modulation of chondrocytes in early human osteoarthritic cartilage lesions. *Osteoarthritis Cartilage* 5, 183-189.
- Airenne, T.T., Nymalm, Y., Kidron, H., Smith, D.J., Pihlavisto, M., Salmi, M., Jalkanen, S., Johnson, M.S., and Salminen, T.A. (2005). Crystal structure of the human vascular adhesion protein-1: unique structural features with functional implications. *Protein Sci* 14, 1964-1974.
- Akhavanpoor, M., Wangler, S., Gleissner, C.A., Korosoglou, G., Katus, H.A., and Erbel, C. (2014). Adventitial inflammation and its interaction with intimal atherosclerotic lesions. *Front Physiol* 5, 296.
- Akiyama, H., Chaboissier, M.C., Martin, J.F., Schedl, A., and de Crombrughe, B. (2002). The transcription factor Sox9 has essential roles in successive steps of the chondrocyte differentiation pathway and is required for expression of Sox5 and Sox6. *Genes Dev* 16, 2813-2828.
- Alberts, B., and May, R.M. (2002). Scientist support for biological weapons controls. *Science* 298, 1135.
- Albrecht, J. (1998). Roles of neuroactive amino acids in ammonia neurotoxicity. *J Neurosci Res* 51, 133-138.
- Alexander, M.R., and Owens, G.K. (2012). Epigenetic control of smooth muscle cell differentiation and phenotypic switching in vascular development and disease. *Annu Rev Physiol* 74, 13-40.

- Asai, K., Kudej, R.K., Shen, Y.T., Yang, G.P., Takagi, G., Kudej, A.B., Geng, Y.J., Sato, N., Nazareno, J.B., Vatner, D.E., *et al.* (2000). Peripheral vascular endothelial dysfunction and apoptosis in old monkeys. *Arterioscler Thromb Vasc Biol* 20, 1493-1499.
- Barrand, M.A., and Callingham, B.A. (1982). Monoamine oxidase activities in brown adipose tissue of the rat: some properties and subcellular distribution. *Biochem Pharmacol* 31, 2177-2184.
- Barrand, M.A., and Callingham, B.A. (1984). Solubilization and some properties of a semicarbazide-sensitive amine oxidase in brown adipose tissue of the rat. *Biochem J* 222, 467-475.
- Barrand, M.A., and Fox, S.A. (1984). Amine oxidase activities in brown adipose tissue of the rat: identification of semicarbazide-sensitive (clorgyline-resistant) activity at the fat cell membrane. *J Pharm Pharmacol* 36, 652-658.
- Bartz, R.R., and Piantadosi, C.A. (2010). Clinical review: oxygen as a signaling molecule. *Crit Care* 14, 234.
- Bendele, A.M. (2001). Animal models of osteoarthritis. *J Musculoskelet Neuronal Interact* 1, 363-376.
- Bertrand, J., Cromme, C., Umlauf, D., Frank, S., and Pap, T. (2010). Molecular mechanisms of cartilage remodelling in osteoarthritis. *Int J Biochem Cell Biol* 42, 1594-1601.
- Bird, M.I., Nunn, P.B., and Lord, L.A. (1984). Formation of glycine and aminoacetone from L-threonine by rat liver mitochondria. *Biochim Biophys Acta* 802, 229-236.
- Birukov, K.G., Frid, M.G., Rogers, J.D., Shirinsky, V.P., Koteliansky, V.E., Campbell, J.H., and Campbell, G.R. (1993). Synthesis and expression of smooth muscle phenotype markers in primary culture of rabbit aortic smooth muscle cells: influence of seeding density and media and relation to cell contractility. *Exp Cell Res* 204, 46-53.
- Blicharski, J.R., and Lyles, G.A. (1990). Semicarbazide-sensitive amine oxidase activity in rat aortic cultured smooth muscle cells. *J Neural Transm Suppl* 32, 337-339.
- Boehm, M., and Nabel, E.G. (2001). Cell cycle and cell migration: new pieces to the puzzle. *Circulation* 103, 2879-2881.
- Bonder, C.S., Norman, M.U., Swain, M.G., Zbytnuik, L.D., Yamanouchi, J., Santamaria, P., Ajuebor, M., Salmi, M., Jalkanen, S., and Kubes, P. (2005). Rules of recruitment for Th1 and Th2 lymphocytes in inflamed liver: a role for alpha-4 integrin and vascular adhesion protein-1. *Immunity* 23, 153-163.
- Bono, P., Salmi, M., Smith, D.J., and Jalkanen, S. (1998a). Cloning and characterization of mouse vascular adhesion protein-1 reveals a novel molecule with enzymatic activity. *J*

- Immunol *160*, 5563-5571.
- Bono, P., Salmi, M., Smith, D.J., Leppänen, I., Horelli-Kuitunen, N., Palotie, A., and Jalkanen, S. (1998b). Isolation, structural characterization, and chromosomal mapping of the mouse vascular adhesion protein-1 gene and promoter. *J Immunol* *161*, 2953-2960.
- Boomsma, F., Bhaggoe, U.M., van der Houwen, A.M., and van den Meiracker, A.H. (2003). Plasma semicarbazide-sensitive amine oxidase in human (patho)physiology. *Biochim Biophys Acta* *1647*, 48-54.
- Boomsma, F., de Kam, P.J., Tjeerdsma, G., van den Meiracker, A.H., and van Veldhuisen, D.J. (2000). Plasma semicarbazide-sensitive amine oxidase (SSAO) is an independent prognostic marker for mortality in chronic heart failure. *Eur Heart J* *21*, 1859-1863.
- Boomsma, F., Hut, H., Bagghoe, U., van der Houwen, A., and van den Meiracker, A. (2005). Semicarbazide-sensitive amine oxidase (SSAO): from cell to circulation. *Med Sci Monit* *11*, RA122-126.
- Boomsma, F., van den Meiracker, A.H., Winkel, S., Aanstoot, H.J., Batstra, M.R., Man in 't Veld, A.J., and Bruining, G.J. (1999). Circulating semicarbazide-sensitive amine oxidase is raised both in type I (insulin-dependent), in type II (non-insulin-dependent) diabetes mellitus and even in childhood type I diabetes at first clinical diagnosis. *Diabetologia* *42*, 233-237.
- Boomsma, F., van Veldhuisen, D.J., de Kam, P.J., Man in't Veld, A.J., Mosterd, A., Lie, K.I., and Schalekamp, M.A. (1997). Plasma semicarbazide-sensitive amine oxidase is elevated in patients with congestive heart failure. *Cardiovasc Res* *33*, 387-391.
- Boor, P.J., Hysmith, R.M., and Sanduja, R. (1990). A role for a new vascular enzyme in the metabolism of xenobiotic amines. *Circ Res* *66*, 249-252.
- Bour, S., Prévot, D., Guigné, C., Stolen, C., Jalkanen, S., Valet, P., and Carpené, C. (2007). Semicarbazide-sensitive amine oxidase substrates fail to induce insulin-like effects in fat cells from AOC3 knockout mice. *J Neural Transm* *114*, 829-833.
- Bove, S.E., Calcaterra, S.L., Brooker, R.M., Huber, C.M., Guzman, R.E., Juneau, P.L., Schrier, D.J., and Kilgore, K.S. (2003). Weight bearing as a measure of disease progression and efficacy of anti-inflammatory compounds in a model of monosodium iodoacetate-induced osteoarthritis. *Osteoarthritis Cartilage* *11*, 821-830.
- Boyle, J.J. (2005). Macrophage activation in atherosclerosis: pathogenesis and pharmacology of plaque rupture. *Curr Vasc Pharmacol* *3*, 63-68.
- Bretón-Romero, R., and Lamas, S. (2014). Hydrogen peroxide signaling in vascular endothelial cells. *Redox Biol* *2*, 529-534.

- Bronckers, A.L., Goei, W., Luo, G., Karsenty, G., D'Souza, R.N., Lyaruu, D.M., and Burger, E.H. (1996). DNA fragmentation during bone formation in neonatal rodents assessed by transferase-mediated end labeling. *J Bone Miner Res* *11*, 1281-1291.
- Brownlee, M. (2001). Biochemistry and molecular cell biology of diabetic complications. *Nature* *414*, 813-820.
- Bruckner, P., Hörler, I., Mandler, M., Houze, Y., Winterhalter, K.H., Eich-Bender, S.G., and Spycher, M.A. (1989). Induction and prevention of chondrocyte hypertrophy in culture. *J Cell Biol* *109*, 2537-2545.
- Buckwalter, J.A., Mankin, H.J., and Grodzinsky, A.J. (2005). Articular cartilage and osteoarthritis. *Instr Course Lect* *54*, 465-480.
- Bui, Q.T., Prempeh, M., and Wilensky, R.L. (2009). Atherosclerotic plaque development. *Int J Biochem Cell Biol* *41*, 2109-2113.
- Burdan, F., Szumiło, J., Korobowicz, A., Farooquee, R., Patel, S., Patel, A., Dave, A., Szumiło, M., Solecki, M., Klepacz, R., *et al.* (2009). Morphology and physiology of the epiphyseal growth plate. *Folia Histochem Cytobiol* *47*, 5-16.
- BURTON, A.C. (1954). Relation of structure to function of the tissues of the wall of blood vessels. *Physiol Rev* *34*, 619-642.
- Byon, C.H., Javed, A., Dai, Q., Kappes, J.C., Clemens, T.L., Darley-Usmar, V.M., McDonald, J.M., and Chen, Y. (2008). Oxidative stress induces vascular calcification through modulation of the osteogenic transcription factor Runx2 by AKT signaling. *J Biol Chem* *283*, 15319-15327.
- Cai, D., and Klinman, J.P. (1994). Evidence of a self-catalytic mechanism of 2,4,5-trihydroxyphenylalanine quinone biogenesis in yeast copper amine oxidase. *J Biol Chem* *269*, 32039-32042.
- Callingham, B.A., Crosbie, A.E., and Rous, B.A. (1995). Some aspects of the pathophysiology of semicarbazide-sensitive amine oxidase enzymes. *Prog Brain Res* *106*, 305-321.
- Carpéné, C., Daviaud, D., Boucher, J., Bour, S., Visentin, V., Grès, S., Duffaut, C., Fontana, E., Testar, X., Saulnier-Blache, J.S., *et al.* (2006). Short- and long-term insulin-like effects of monoamine oxidases and semicarbazide-sensitive amine oxidase substrates in cultured adipocytes. *Metabolism* *55*, 1397-1405.
- Carter, D.R., and Wong, M. (2003). Modelling cartilage mechanobiology. *Philos Trans R Soc Lond B Biol Sci* *358*, 1461-1471.
- Chassande, O., Renard, S., Barbry, P., and Lazdunski, M. (1994). The human gene for diamine oxidase, an amiloride binding protein. Molecular cloning, sequencing, and

- characterization of the promoter. *J Biol Chem* 269, 14484-14489.
- Chen, F.H., Rousche, K.T., and Tuan, R.S. (2006). Technology Insight: adult stem cells in cartilage regeneration and tissue engineering. *Nat Clin Pract Rheumatol* 2, 373-382.
- Cines, D.B., Pollak, E.S., Buck, C.A., Loscalzo, J., Zimmerman, G.A., McEver, R.P., Pober, J.S., Wick, T.M., Konkle, B.A., Schwartz, B.S., *et al.* (1998). Endothelial cells in physiology and in the pathophysiology of vascular disorders. *Blood* 91, 3527-3561.
- Clarke, D.E., Lyles, G.A., and Callingham, B.A. (1982). A comparison of cardiac and vascular clorgyline-resistant amine oxidase and monoamine oxidase. Inhibition by amphetamine, mexiletine and other drugs. *Biochem Pharmacol* 31, 27-35.
- Clarke, M.C., Figg, N., Maguire, J.J., Davenport, A.P., Goddard, M., Littlewood, T.D., and Bennett, M.R. (2006). Apoptosis of vascular smooth muscle cells induces features of plaque vulnerability in atherosclerosis. *Nat Med* 12, 1075-1080.
- Clempus, R.E., Sorescu, D., Dikalova, A.E., Pounkova, L., Jo, P., Sorescu, G.P., Schmidt, H.H., Lassègue, B., and Griendling, K.K. (2007). Nox4 is required for maintenance of the differentiated vascular smooth muscle cell phenotype. *Arterioscler Thromb Vasc Biol* 27, 42-48.
- Crelin, E.S., and Southwick, W.O. (1960). Mitosis of Chondrocytes Induced in the Knee Joint Articular Cartilage of Adult Rabbits. *Yale J Biol Med* 33, 243-244.241.
- Cronin, C.N., Zhang, X., Thompson, D.A., and McIntire, W.S. (1998). cDNA cloning of two splice variants of a human copper-containing monoamine oxidase pseudogene containing a dimeric Alu repeat sequence. *Gene* 220, 71-76.
- Dai, X., Ou, X., Hao, X., Cao, D., Tang, Y., Hu, Y., Li, X., and Tang, C. (2008). Synthetic liver X receptor agonist T0901317 inhibits semicarbazide-sensitive amine oxidase gene expression and activity in apolipoprotein E knockout mice. *Acta Biochim Biophys Sin (Shanghai)* 40, 261-268.
- DAVIS, E.J., and DE ROPP, R.S. (1961). Metabolic origin of urinary methylamine in the rat. *Nature* 190, 636-637.
- Dawkes, H.C., and Phillips, S.E. (2001). Copper amine oxidase: cunning cofactor and controversial copper. *Curr Opin Struct Biol* 11, 666-673.
- de Crombrughe, B., Lefebvre, V., and Nakashima, K. (2001). Regulatory mechanisms in the pathways of cartilage and bone formation. *Curr Opin Cell Biol* 13, 721-727.
- de Crombrughe, B., Lefebvre, V., Behringer, R.R., Bi, W., Murakami, S., and Huang, W. (2000). Transcriptional mechanisms of chondrocyte differentiation. *Matrix Biol* 19, 389-394.

- DeLise, A.M., Fischer, L., and Tuan, R.S. (2000). Cellular interactions and signaling in cartilage development. *Osteoarthritis Cartilage* 8, 309-334.
- Deng, Y., and Yu, P.H. (1999). Assessment of the deamination of aminoacetone, an endogenous substrate for semicarbazide-sensitive amine oxidase. *Anal Biochem* 270, 97-102.
- Deng, Y., Boomsma, F., and Yu, P.H. (1998). Deamination of methylamine and aminoacetone increases aldehydes and oxidative stress in rats. *Life Sci* 63, 2049-2058.
- Doege, K.J., Sasaki, M., Kimura, T., and Yamada, Y. (1991). Complete coding sequence and deduced primary structure of the human cartilage large aggregating proteoglycan, aggrecan. Human-specific repeats, and additional alternatively spliced forms. *J Biol Chem* 266, 894-902.
- Donato, A.J., Gano, L.B., Eskurza, I., Silver, A.E., Gates, P.E., Jablonski, K., and Seals, D.R. (2009). Vascular endothelial dysfunction with aging: endothelin-1 and endothelial nitric oxide synthase. *Am J Physiol Heart Circ Physiol* 297, H425-432.
- Doran, A.C., Meller, N., and McNamara, C.A. (2008). Role of smooth muscle cells in the initiation and early progression of atherosclerosis. *Arterioscler Thromb Vasc Biol* 28, 812-819.
- Dreier, R. (2010). Hypertrophic differentiation of chondrocytes in osteoarthritis: the developmental aspect of degenerative joint disorders. *Arthritis Res Ther* 12, 216.
- Dreier, R., Günther, B.K., Mainz, T., Nemere, I., and Bruckner, P. (2008). Terminal differentiation of chick embryo chondrocytes requires shedding of a cell surface protein that binds 1,25-dihydroxyvitamin D3. *J Biol Chem* 283, 1104-1112.
- Dubois, J.L., and Klinman, J.P. (2005). Mechanism of post-translational quinone formation in copper amine oxidases and its relationship to the catalytic turnover. *Arch Biochem Biophys* 433, 255-265.
- Dunkel, P., Balogh, B., Meleddu, R., Maccioni, E., Gyires, K., and Mátyus, P. (2011). Semicarbazide-sensitive amine oxidase/vascular adhesion protein-1: a patent survey. *Expert Opin Ther Pat* 21, 1453-1471.
- Dy, P., Wang, W., Bhattaram, P., Wang, Q., Wang, L., Ballock, R.T., and Lefebvre, V. (2012). Sox9 directs hypertrophic maturation and blocks osteoblast differentiation of growth plate chondrocytes. *Dev Cell* 22, 597-609.
- Dzau, V.J., Braun-Dullaeus, R.C., and Sedding, D.G. (2002). Vascular proliferation and atherosclerosis: new perspectives and therapeutic strategies. *Nat Med* 8, 1249-1256.
- El Hadri, K., Moldes, M., Mercier, N., Andreani, M., Pairault, J., and Feve, B. (2002).

- Semicarbazide-sensitive amine oxidase in vascular smooth muscle cells: differentiation-dependent expression and role in glucose uptake. *Arterioscler Thromb Vasc Biol* 22, 89-94.
- ELLIOTT, W.H. (1960). Aminoacetone formation by *Staphylococcus aureus*. *Biochem J* 74, 478-485.
- Enomoto, H., Furuichi, T., Zanma, A., Yamana, K., Yoshida, C., Sumitani, S., Yamamoto, H., Enomoto-Iwamoto, M., Iwamoto, M., and Komori, T. (2004). Runx2 deficiency in chondrocytes causes adipogenic changes in vitro. *J Cell Sci* 117, 417-425.
- Enrique-Tarancón, G., Castan, I., Morin, N., Marti, L., Abella, A., Camps, M., Casamitjana, R., Palacín, M., Testar, X., Degerman, E., *et al.* (2000). Substrates of semicarbazide-sensitive amine oxidase co-operate with vanadate to stimulate tyrosine phosphorylation of insulin-receptor-substrate proteins, phosphoinositide 3-kinase activity and GLUT4 translocation in adipose cells. *Biochem J* 350 Pt 1, 171-180.
- Enrique-Tarancón, G., Marti, L., Morin, N., Lizcano, J.M., Unzeta, M., Sevilla, L., Camps, M., Palacín, M., Testar, X., Carpéné, C., *et al.* (1998). Role of semicarbazide-sensitive amine oxidase on glucose transport and GLUT4 recruitment to the cell surface in adipose cells. *J Biol Chem* 273, 8025-8032.
- Erlebacher, A., Filvaroff, E.H., Gitelman, S.E., and Derynck, R. (1995). Toward a molecular understanding of skeletal development. *Cell* 80, 371-378.
- Finney, J., Moon, H.J., Ronnebaum, T., Lantz, M., and Mure, M. (2014). Human copper-dependent amine oxidases. *Arch Biochem Biophys* 546, 19-32.
- Fontana, E., Boucher, J., Marti, L., Lizcano, J.M., Testar, X., Zorzano, A., and Carpéné, C. (2001). Amine oxidase substrates mimic several of the insulin effects on adipocyte differentiation in 3T3 F442A cells. *Biochem J* 356, 769-777.
- Fuerst, M., Bertrand, J., Lammers, L., Dreier, R., Echtermeyer, F., Nitschke, Y., Rutsch, F., Schäfer, F.K., Niggemeyer, O., Steinhagen, J., *et al.* (2009a). Calcification of articular cartilage in human osteoarthritis. *Arthritis Rheum* 60, 2694-2703.
- Fuerst, M., Niggemeyer, O., Lammers, L., Schäfer, F., Lohmann, C., and Rüther, W. (2009b). Articular cartilage mineralization in osteoarthritis of the hip. *BMC Musculoskelet Disord* 10, 166.
- Fukumoto, T., Sperling, J.W., Sanyal, A., Fitzsimmons, J.S., Reinholz, G.G., Conover, C.A., and O'Driscoll, S.W. (2003). Combined effects of insulin-like growth factor-1 and transforming growth factor-beta1 on periosteal mesenchymal cells during chondrogenesis in vitro. *Osteoarthritis Cartilage* 11, 55-64.

- Gartland, A., Mechler, J., Mason-Savas, A., MacKay, C.A., Mailhot, G., Marks, S.C., and Odgren, P.R. (2005). In vitro chondrocyte differentiation using costochondral chondrocytes as a source of primary rat chondrocyte cultures: an improved isolation and cryopreservation method. *Bone* 37, 530-544.
- Getz, G.S., and Reardon, C.A. (2012). Animal models of atherosclerosis. *Arterioscler Thromb Vasc Biol* 32, 1104-1115.
- Giachelli, C.M., Schwartz, S.M., and Liaw, L. (1995). Molecular and cellular biology of osteopontin Potential role in cardiovascular disease. *Trends Cardiovasc Med* 5, 88-95.
- Gleissner, C.A., von Hundelshausen, P., and Ley, K. (2008). Platelet chemokines in vascular disease. *Arterioscler Thromb Vasc Biol* 28, 1920-1927.
- Göktürk, C., Nilsson, J., Nordquist, J., Kristensson, M., Svensson, K., Söderberg, C., Israelson, M., Garpenstrand, H., Sjöquist, M., Orelund, L., *et al.* (2003). Overexpression of semicarbazide-sensitive amine oxidase in smooth muscle cells leads to an abnormal structure of the aortic elastic laminae. *Am J Pathol* 163, 1921-1928.
- Gokturk, C., Sugimoto, H., Blomgren, B., Roomans, G.M., Forsberg-Nilsson, K., Orelund, L., and Sjoquist, M. (2007). Macrovascular changes in mice overexpressing human semicarbazide-sensitive amine oxidase in smooth muscle cells. *Am J Hypertens* 20, 743-750.
- Goldring, M.B. (2000a). Osteoarthritis and cartilage: the role of cytokines. *Curr Rheumatol Rep* 2, 459-465.
- Goldring, M.B. (2000b). The role of the chondrocyte in osteoarthritis. *Arthritis Rheum* 43, 1916-1926.
- Goldring, M.B. (2006). Update on the biology of the chondrocyte and new approaches to treating cartilage diseases. *Best Pract Res Clin Rheumatol* 20, 1003-1025.
- Goldring, M.B. (2012). Articular cartilage degradation in osteoarthritis. *HSS J* 8, 7-9.
- Goldring, M.B., and Goldring, S.R. (2010). Articular cartilage and subchondral bone in the pathogenesis of osteoarthritis. *Ann N Y Acad Sci* 1192, 230-237.
- Gong, B., and Boor, P.J. (2006). The role of amine oxidases in xenobiotic metabolism. *Expert Opin Drug Metab Toxicol* 2, 559-571.
- Gordon, S. (2003). Alternative activation of macrophages. *Nat Rev Immunol* 3, 23-35.
- Gregory, M.H., Capito, N., Kuroki, K., Stoker, A.M., Cook, J.L., and Sherman, S.L. (2012). A review of translational animal models for knee osteoarthritis. *Arthritis* 2012, 764621.
- Grönvall-Nordquist, J.L., Bäcklund, L.B., Garpenstrand, H., Ekblom, J., Landin, B., Yu, P.H., Orelund, L., and Rosenqvist, U. (2001). Follow-up of plasma semicarbazide-sensitive

- amine oxidase activity and retinopathy in Type 2 diabetes mellitus. *J Diabetes Complications* 15, 250-256.
- Gu, L., Okada, Y., Clinton, S.K., Gerard, C., Sukhova, G.K., Libby, P., and Rollins, B.J. (1998). Absence of monocyte chemoattractant protein-1 reduces atherosclerosis in low density lipoprotein receptor-deficient mice. *Mol Cell* 2, 275-281.
- Gubisne-Haberle, D., Hill, W., Kazachkov, M., Richardson, J.S., and Yu, P.H. (2004). Protein cross-linkage induced by formaldehyde derived from semicarbazide-sensitive amine oxidase-mediated deamination of methylamine. *J Pharmacol Exp Ther* 310, 1125-1132.
- Hahn, C., and Schwartz, M.A. (2009). Mechanotransduction in vascular physiology and atherogenesis. *Nat Rev Mol Cell Biol* 10, 53-62.
- Hansson, G.K. (2005). Inflammation, atherosclerosis, and coronary artery disease. *N Engl J Med* 352, 1685-1695.
- Hansson, G.K., and Libby, P. (2006). The immune response in atherosclerosis: a double-edged sword. *Nat Rev Immunol* 6, 508-519.
- Hargus, G., Kist, R., Kramer, J., Gerstel, D., Neitz, A., Scherer, G., and Rohwedel, J. (2008). Loss of Sox9 function results in defective chondrocyte differentiation of mouse embryonic stem cells in vitro. *Int J Dev Biol* 52, 323-332.
- Henn, V., Slupsky, J.R., Gräfe, M., Anagnostopoulos, I., Förster, R., Müller-Berghaus, G., and Kroczeck, R.A. (1998). CD40 ligand on activated platelets triggers an inflammatory reaction of endothelial cells. *Nature* 391, 591-594.
- Hernandez, M., Solé, M., Boada, M., and Unzeta, M. (2006). Soluble semicarbazide sensitive amine oxidase (SSAO) catalysis induces apoptosis in vascular smooth muscle cells. *Biochim Biophys Acta* 1763, 164-173.
- Høgdall, E.V., Houen, G., Borre, M., Bundgaard, J.R., Larsson, L.I., and Vuust, J. (1998). Structure and tissue-specific expression of genes encoding bovine copper amine oxidases. *Eur J Biochem* 251, 320-328.
- Horton, W.E., Feng, L., and Adams, C. (1998). Chondrocyte apoptosis in development, aging and disease. *Matrix Biol* 17, 107-115.
- Huber, P.A. (1997). Caldesmon. *Int J Biochem Cell Biol* 29, 1047-1051.
- Hunziker, E.B., Lippuner, K., and Shintani, N. (2014). How best to preserve and reveal the structural intricacies of cartilaginous tissue. *Matrix Biol* 39C, 33-43.
- Hysmith, R.M., and Boor, P.J. (1987). In vitro expression of benzylamine oxidase activity in cultured porcine smooth muscle cells. *J Cardiovasc Pharmacol* 9, 668-674.
- Hysmith, R.M., and Boor, P.J. (1988a). Purification of benzylamine oxidase from cultured

- porcine aortic smooth muscle cells. *Biochem Cell Biol* 66, 821-829.
- Hysmith, R.M., and Boor, P.J. (1988b). Role of benzylamine oxidase in the cytotoxicity of allylamine toward aortic smooth muscle cells. *Toxicology* 51, 133-145.
- Iftikhar, M., Hurtado, P., Bais, M.V., Wigner, N., Stephens, D.N., Gerstenfeld, L.C., and Trackman, P.C. (2011). Lysyl oxidase-like-2 (LOXL2) is a major isoform in chondrocytes and is critically required for differentiation. *J Biol Chem* 286, 909-918.
- Iglesias-Osma, M.C., Bour, S., Garcia-Barrado, M.J., Visentin, V., Pastor, M.F., Testar, X., Marti, L., Enrique-Tarancon, G., Valet, P., Moratinos, J., *et al.* (2005). Methylamine but not mafenide mimics insulin-like activity of the semicarbazide-sensitive amine oxidase-substrate benzylamine on glucose tolerance and on human adipocyte metabolism. *Pharmacol Res* 52, 475-484.
- Iglesias-Osma, M.C., Garcia-Barrado, M.J., Visentin, V., Pastor-Mansilla, M.F., Bour, S., Prévot, D., Valet, P., Moratinos, J., and Carpené, C. (2004). Benzylamine exhibits insulin-like effects on glucose disposal, glucose transport, and fat cell lipolysis in rabbits and diabetic mice. *J Pharmacol Exp Ther* 309, 1020-1028.
- Imamura, Y., Kubota, R., Wang, Y., Asakawa, S., Kudoh, J., Mashima, Y., Oguchi, Y., and Shimizu, N. (1997). Human retina-specific amine oxidase (RAO): cDNA cloning, tissue expression, and chromosomal mapping. *Genomics* 40, 277-283.
- Imamura, Y., Noda, S., Mashima, Y., Kudoh, J., Oguchi, Y., and Shimizu, N. (1998). Human retina-specific amine oxidase: genomic structure of the gene (AOC2), alternatively spliced variant, and mRNA expression in retina. *Genomics* 51, 293-298.
- Jaakkola, K., Kaunismäki, K., Tohka, S., Yegutkin, G., Vääntinen, E., Havia, T., Pelliniemi, L.J., Virolainen, M., Jalkanen, S., and Salmi, M. (1999). Human vascular adhesion protein-1 in smooth muscle cells. *Am J Pathol* 155, 1953-1965.
- Jaakkola, K., Nikula, T., Holopainen, R., Vähäsilta, T., Matikainen, M.T., Laukkanen, M.L., Huupponen, R., Halkola, L., Nieminen, L., Hiltunen, J., *et al.* (2000). In vivo detection of vascular adhesion protein-1 in experimental inflammation. *Am J Pathol* 157, 463-471.
- Jackson, S.P. (2011). Arterial thrombosis--insidious, unpredictable and deadly. *Nat Med* 17, 1423-1436.
- Jakobsson, E., Nilsson, J., Källström, U., Ogg, D., and Kleywegt, G.J. (2005). Crystallization of a truncated soluble human semicarbazide-sensitive amine oxidase. *Acta Crystallogr Sect F Struct Biol Cryst Commun* 61, 274-278.
- Jalkanen, S., and Salmi, M. (2001). Cell surface monoamine oxidases: enzymes in search of a function. *EMBO J* 20, 3893-3901.

- Janes, S.M., Mu, D., Wemmer, D., Smith, A.J., Kaur, S., Maltby, D., Burlingame, A.L., and Klinman, J.P. (1990). A new redox cofactor in eukaryotic enzymes: 6-hydroxydopa at the active site of bovine serum amine oxidase. *Science* 248, 981-987.
- Jawień, J., Nastalek, P., and Korbut, R. (2004). Mouse models of experimental atherosclerosis. *J Physiol Pharmacol* 55, 503-517.
- Jiang, L., Li, L., Geng, C., Gong, D., Ishikawa, N., Kajima, K., and Zhong, L. (2013). Monosodium iodoacetate induces apoptosis via the mitochondrial pathway involving ROS production and caspase activation in rat chondrocytes in vitro. *J Orthop Res* 31, 364-369.
- Kagan, H.M., and Trackman, P.C. (1991). Properties and function of lysyl oxidase. *Am J Respir Cell Mol Biol* 5, 206-210.
- Kaitaniemi, S., Grön, K., Elovaara, H., Salmi, M., Jalkanen, S., and Elimä, K. (2013). Functional modulation of vascular adhesion protein-1 by a novel splice variant. *PLoS One* 8, e54151.
- Kamiya, N., Watanabe, H., Habuchi, H., Takagi, H., Shinomura, T., Shimizu, K., and Kimata, K. (2006). Versican/PG-M regulates chondrogenesis as an extracellular matrix molecule crucial for mesenchymal condensation. *J Biol Chem* 281, 2390-2400.
- Karádi, I., Mészáros, Z., Csányi, A., Szombathy, T., Hosszúfalusi, N., Romics, L., and Magyar, K. (2002). Serum semicarbazide-sensitive amine oxidase (SSAO) activity is an independent marker of carotid atherosclerosis. *Clin Chim Acta* 323, 139-146.
- Kawakami, Y., Capdevila, J., Büscher, D., Itoh, T., Rodríguez Esteban, C., and Izpisua Belmonte, J.C. (2001). WNT signals control FGF-dependent limb initiation and AER induction in the chick embryo. *Cell* 104, 891-900.
- Kemp, P.R., Grainger, D.J., Shanahan, C.M., Weissberg, P.L., and Metcalfe, J.C. (1991). The Id gene is activated by serum but is not required for de-differentiation in rat vascular smooth muscle cells. *Biochem J* 277 (Pt 1), 285-288.
- Khaidakov, M., Wang, X., and Mehta, J.L. (2011). Potential involvement of LOX-1 in functional consequences of endothelial senescence. *PLoS One* 6, e20964.
- Kirkham, S.G., and Samarasinghe, R.K. (2009). Review article: Glucosamine. *J Orthop Surg (Hong Kong)* 17, 72-76.
- Kirsch, T., Nah, H.D., Shapiro, I.M., and Pacifici, M. (1997). Regulated production of mineralization-competent matrix vesicles in hypertrophic chondrocytes. *J Cell Biol* 137, 1149-1160.
- Kishimoto, H., Akagi, M., Zushi, S., Teramura, T., Onodera, Y., Sawamura, T., and Hamanishi,

- C. (2010). Induction of hypertrophic chondrocyte-like phenotypes by oxidized LDL in cultured bovine articular chondrocytes through increase in oxidative stress. *Osteoarthritis Cartilage* 18, 1284-1290.
- Kleemann, R., Zadelaar, S., and Kooistra, T. (2008). Cytokines and atherosclerosis: a comprehensive review of studies in mice. *Cardiovasc Res* 79, 360-376.
- Klinman, J.P. (1996). New quinocofactors in eukaryotes. *J Biol Chem* 271, 27189-27192.
- Klinman, J.P. (2003). The multi-functional topa-quinone copper amine oxidases. *Biochim Biophys Acta* 1647, 131-137.
- Komori, T., Yagi, H., Nomura, S., Yamaguchi, A., Sasaki, K., Deguchi, K., Shimizu, Y., Bronson, R.T., Gao, Y.H., Inada, M., *et al.* (1997). Targeted disruption of *Cbfa1* results in a complete lack of bone formation owing to maturational arrest of osteoblasts. *Cell* 89, 755-764.
- Koskinen, K., Nevalainen, S., Karikoski, M., Hänninen, A., Jalkanen, S., and Salmi, M. (2007). VAP-1-deficient mice display defects in mucosal immunity and antimicrobial responses: implications for antiadhesive applications. *J Immunol* 179, 6160-6168.
- Koskinen, K., Vainio, P.J., Smith, D.J., Pihlavisto, M., Ylä-Herttuala, S., Jalkanen, S., and Salmi, M. (2004). Granulocyte transmigration through the endothelium is regulated by the oxidase activity of vascular adhesion protein-1 (VAP-1). *Blood* 103, 3388-3395.
- Kronenberg, H.M. (2003). Developmental regulation of the growth plate. *Nature* 423, 332-336.
- Kurkijärvi, R., Adams, D.H., Leino, R., Möttönen, T., Jalkanen, S., and Salmi, M. (1998). Circulating form of human vascular adhesion protein-1 (VAP-1): increased serum levels in inflammatory liver diseases. *J Immunol* 161, 1549-1557.
- Kurkijärvi, R., Yegutkin, G.G., Gunson, B.K., Jalkanen, S., Salmi, M., and Adams, D.H. (2000). Circulating soluble vascular adhesion protein 1 accounts for the increased serum monoamine oxidase activity in chronic liver disease. *Gastroenterology* 119, 1096-1103.
- Lacolley, P., Regnault, V., Nicoletti, A., Li, Z., and Michel, J.B. (2012). The vascular smooth muscle cell in arterial pathology: a cell that can take on multiple roles. *Cardiovasc Res* 95, 194-204.
- Lalor, P.F., Edwards, S., McNab, G., Salmi, M., Jalkanen, S., and Adams, D.H. (2002). Vascular adhesion protein-1 mediates adhesion and transmigration of lymphocytes on human hepatic endothelial cells. *J Immunol* 169, 983-992.
- Lee, J.W., Kim, Y.H., Kim, S.H., Han, S.H., and Hahn, S.B. (2004). Chondrogenic differentiation of mesenchymal stem cells and its clinical applications. *Yonsei Med J* 45 *Suppl*, 41-47.

- Lefebvre, F., Graillat, N., Cherin, E., Berger, G., and Saïed, A. (1998). Automatic three-dimensional reconstruction and characterization of articular cartilage from high-resolution ultrasound acquisitions. *Ultrasound Med Biol* *24*, 1369-1381.
- Lefebvre, V., Behringer, R.R., and de Crombrughe, B. (2001). L-Sox5, Sox6 and Sox9 control essential steps of the chondrocyte differentiation pathway. *Osteoarthritis Cartilage* *9 Suppl A*, S69-75.
- Lefebvre, V., Huang, W., Harley, V.R., Goodfellow, P.N., and de Crombrughe, B. (1997). SOX9 is a potent activator of the chondrocyte-specific enhancer of the pro alpha1(II) collagen gene. *Mol Cell Biol* *17*, 2336-2346.
- Leonard, C.M., Bergman, M., Frenz, D.A., Macreery, L.A., and Newman, S.A. (1989). Abnormal ambient glucose levels inhibit proteoglycan core protein gene expression and reduce proteoglycan accumulation during chondrogenesis: possible mechanism for teratogenic effects of maternal diabetes. *Proc Natl Acad Sci U S A* *86*, 10113-10117.
- Lewinsohn, R. (1981). Amine oxidase in human blood vessels and non-vascular smooth muscle. *J Pharm Pharmacol* *33*, 569-575.
- Lewinsohn, R. (1984). Mammalian monoamine-oxidizing enzymes, with special reference to benzylamine oxidase in human tissues. *Braz J Med Biol Res* *17*, 223-256.
- Libby, P. (2002). Inflammation in atherosclerosis. *Nature* *420*, 868-874.
- Libby, P., Ridker, P.M., and Hansson, G.K. (2011). Progress and challenges in translating the biology of atherosclerosis. *Nature* *473*, 317-325.
- Little, C.B., and Zaki, S. (2012). What constitutes an "animal model of osteoarthritis"--the need for consensus? *Osteoarthritis Cartilage* *20*, 261-267.
- Liu, X., Liu, J., Kang, N., Yan, L., Wang, Q., Fu, X., Zhang, Y., Xiao, R., and Cao, Y. (2014). Role of insulin-transferrin-selenium in auricular chondrocyte proliferation and engineered cartilage formation in vitro. *Int J Mol Sci* *15*, 1525-1537.
- Lizcano, J.M., Balsa, D., Tipton, K.F., and Unzeta, M. (1991a). The oxidation of dopamine by the semicarbazide-sensitive amine oxidase (SSAO) from rat vas deferens. *Biochem Pharmacol* *41*, 1107-1110.
- Lizcano, J.M., Escrich, E., Ribalta, T., Muntané, J., and Unzeta, M. (1991b). Amine oxidase activities in rat breast cancer induced experimentally with 7,12-dimethylbenz(alpha)anthracene. *Biochem Pharmacol* *42*, 263-269.
- Lotz, M.K., and Caramés, B. (2011). Autophagy and cartilage homeostasis mechanisms in joint health, aging and OA. *Nat Rev Rheumatol* *7*, 579-587.
- Lunelli, M., Di Paolo, M.L., Biadene, M., Calderone, V., Battistutta, R., Scarpa, M., Rigo, A.,

- and Zanotti, G. (2005). Crystal structure of amine oxidase from bovine serum. *J Mol Biol* 346, 991-1004.
- Lyles, G.A. (1996). Mammalian plasma and tissue-bound semicarbazide-sensitive amine oxidases: biochemical, pharmacological and toxicological aspects. *Int J Biochem Cell Biol* 28, 259-274.
- Lyles, G.A., and Chalmers, J. (1992). The metabolism of aminoacetone to methylglyoxal by semicarbazide-sensitive amine oxidase in human umbilical artery. *Biochem Pharmacol* 43, 1409-1414.
- Lyles, G.A., and Pino, R. (1998). Properties and functions of tissue-bound semicarbazide-sensitive amine oxidases in isolated cell preparations and cell cultures. *J Neural Transm Suppl* 52, 239-250.
- Lyles, G.A., and Singh, I. (1985). Vascular smooth muscle cells: a major source of the semicarbazide-sensitive amine oxidase of the rat aorta. *J Pharm Pharmacol* 37, 637-643.
- Lyles, G.A., Holt, A., and Marshall, C.M. (1990). Further studies on the metabolism of methylamine by semicarbazide-sensitive amine oxidase activities in human plasma, umbilical artery and rat aorta. *J Pharm Pharmacol* 42, 332-338.
- Lyles, G.A., Marshall, C.M., McDonald, I.A., Bey, P., and Palfreyman, M.G. (1987). Inhibition of rat aorta semicarbazide-sensitive amine oxidase by 2-phenyl-3-haloallylamines and related compounds. *Biochem Pharmacol* 36, 2847-2853.
- M. Atanasova, A. Dimitrova, B. Ruseva, A. Stoyanova, M. Georgieva and E. Konova, Quantification of Elastin, Collagen and Advanced Glycation End Products as Functions of Age and Hypertension. Intechopen (2012).
- Ma, H.L., Hung, S.C., Lin, S.Y., Chen, Y.L., and Lo, W.H. (2003). Chondrogenesis of human mesenchymal stem cells encapsulated in alginate beads. *J Biomed Mater Res A* 64, 273-281.
- Majesky, M.W., Dong, X.R., Hognlund, V., Mahoney, W.M., and Daum, G. (2011). The adventitia: a dynamic interface containing resident progenitor cells. *Arterioscler Thromb Vasc Biol* 31, 1530-1539.
- Mallat, Z., Besnard, S., Duriez, M., Deleuze, V., Emmanuel, F., Bureau, M.F., Soubrier, F., Esposito, B., Duez, H., Fievet, C., *et al.* (1999). Protective role of interleukin-10 in atherosclerosis. *Circ Res* 85, e17-24.
- Mano, T., Luo, Z., Malendowicz, S.L., Evans, T., and Walsh, K. (1999). Reversal of GATA-6 downregulation promotes smooth muscle differentiation and inhibits intimal hyperplasia in balloon-injured rat carotid artery. *Circ Res* 84, 647-654.

- Marinho, H.S., Real, C., Cyrne, L., Soares, H., and Antunes, F. (2014). Hydrogen peroxide sensing, signaling and regulation of transcription factors. *Redox Biol* 2, 535-562.
- Martelius, T., Salaspuro, V., Salmi, M., Krogerus, L., Höckerstedt, K., Jalkanen, S., and Lautenschlager, I. (2004). Blockade of vascular adhesion protein-1 inhibits lymphocyte infiltration in rat liver allograft rejection. *Am J Pathol* 165, 1993-2001.
- Martel-Pelletier, J. (1999). Pathophysiology of osteoarthritis. *Osteoarthritis Cartilage* 7, 371-373.
- Marti, L., Morin, N., Enrique-Tarancon, G., Prevot, D., Lafontan, M., Testar, X., Zorzano, A., and Carpené, C. (1998). Tyramine and vanadate synergistically stimulate glucose transport in rat adipocytes by amine oxidase-dependent generation of hydrogen peroxide. *J Pharmacol Exp Ther* 285, 342-349.
- Martin, J.A., and Buckwalter, J.A. (1998). Effects of fibronectin on articular cartilage chondrocyte proteoglycan synthesis and response to insulin-like growth factor-I. *J Orthop Res* 16, 752-757.
- Marttila-Ichihara, F., Castermans, K., Auvinen, K., Oude Egbrink, M.G., Jalkanen, S., Griffioen, A.W., and Salmi, M. (2010). Small-molecule inhibitors of vascular adhesion protein-1 reduce the accumulation of myeloid cells into tumors and attenuate tumor growth in mice. *J Immunol* 184, 3164-3173.
- Marttila-Ichihara, F., Smith, D.J., Stolen, C., Yegutkin, G.G., Elima, K., Mercier, N., Kiviranta, R., Pihlavisto, M., Alaranta, S., Pentikäinen, U., *et al.* (2006). Vascular amine oxidases are needed for leukocyte extravasation into inflamed joints in vivo. *Arthritis Rheum* 54, 2852-2862.
- Mathys, K.C., Ponnampalam, S.N., Padival, S., and Nagaraj, R.H. (2002). Semicarbazide-sensitive amine oxidase in aortic smooth muscle cells mediates synthesis of a methylglyoxal-AGE: implications for vascular complications in diabetes. *Biochem Biophys Res Commun* 297, 863-869.
- Mátyus, P., Dajka-Halász, B., Földi, A., Haider, N., Barlocco, D., and Magyar, K. (2004). Semicarbazide-sensitive amine oxidase: current status and perspectives. *Curr Med Chem* 11, 1285-1298.
- Mau, E., Whetstone, H., Yu, C., Hopyan, S., Wunder, J.S., and Alman, B.A. (2007). PTHrP regulates growth plate chondrocyte differentiation and proliferation in a Gli3 dependent manner utilizing hedgehog ligand dependent and independent mechanisms. *Dev Biol* 305, 28-39.
- McEwen, C.M. (1965). Human plasma monoamine oxidase. 1. Purification and identification.

- J Biol Chem 240, 2003-2010.
- MCEWEN, C.M. (1965). HUMAN PLASMA MONOAMINE OXIDASE. II. KINETIC STUDIES. J Biol Chem 240, 2011-2018.
- McGuirl, M.A., and Dooley, D.M. (1999). Copper-containing oxidases. Curr Opin Chem Biol 3, 138-144.
- Mercier, N., El Hadri, K., Osborne-Pellegrin, M., Nehme, J., Perret, C., Labat, C., Regnault, V., Lamazière, J.M., Challande, P., Lacolley, P., *et al.* (2007). Modifications of arterial phenotype in response to amine oxidase inhibition by semicarbazide. Hypertension 50, 234-241.
- Mercier, N., Kakou, A., Challande, P., Lacolley, P., and Osborne-Pellegrin, M. (2009). Comparison of the effects of semicarbazide and beta-aminopropionitrile on the arterial extracellular matrix in the Brown Norway rat. Toxicol Appl Pharmacol 239, 258-267.
- Mercier, N., Moldes, M., El Hadri, K., and Fève, B. (2001). Semicarbazide-sensitive amine oxidase activation promotes adipose conversion of 3T3-L1 cells. Biochem J 358, 335-342.
- Mercier, N., Moldes, M., El Hadri, K., and Fève, B. (2003). Regulation of semicarbazide-sensitive amine oxidase expression by tumor necrosis factor-alpha in adipocytes: functional consequences on glucose transport. J Pharmacol Exp Ther 304, 1197-1208.
- Mercier, N., Osborne-Pellegrin, M., El Hadri, K., Kakou, A., Labat, C., Loufrani, L., Henrion, D., Challande, P., Jalkanen, S., Fève, B., *et al.* (2006). Carotid arterial stiffness, elastic fibre network and vasoreactivity in semicarbazide-sensitive amine-oxidase null mouse. Cardiovasc Res 72, 349-357.
- Merinen, M., Irjala, H., Salmi, M., Jaakkola, I., Hänninen, A., and Jalkanen, S. (2005). Vascular adhesion protein-1 is involved in both acute and chronic inflammation in the mouse. Am J Pathol 166, 793-800.
- Mészáros, Z., Karádi, I., Csányi, A., Szombathy, T., Romics, L., and Magyar, K. (1999a). Determination of human serum semicarbazide-sensitive amine oxidase activity: a possible clinical marker of atherosclerosis. Eur J Drug Metab Pharmacokinet 24, 299-302.
- Mészáros, Z., Szombathy, T., Raimondi, L., Karádi, I., Romics, L., and Magyar, K. (1999b). Elevated serum semicarbazide-sensitive amine oxidase activity in non-insulin-dependent diabetes mellitus: correlation with body mass index and serum triglyceride. Metabolism 48, 113-117.
- Mizuno, M., Takebe, T., Kobayashi, S., Kimura, S., Masutani, M., Lee, S., Jo, Y.H., Lee, J.I.,

- and Taniguchi, H. (2014). Elastic cartilage reconstruction by transplantation of cultured hyaline cartilage-derived chondrocytes. *Transplant Proc* 46, 1217-1221.
- Mobasheri, A., Bondy, C.A., Moley, K., Mendes, A.F., Rosa, S.C., Richardson, S.M., Hoyland, J.A., Barrett-Jolley, R., and Shakibaei, M. (2008). Facilitative glucose transporters in articular chondrocytes. Expression, distribution and functional regulation of GLUT isoforms by hypoxia, hypoxia mimetics, growth factors and pro-inflammatory cytokines. *Adv Anat Embryol Cell Biol* 200, 1 p following vi, 1-84.
- Moore, K.J., Sheedy, F.J., and Fisher, E.A. (2013). Macrophages in atherosclerosis: a dynamic balance. *Nat Rev Immunol* 13, 709-721.
- Morgan, K.G., and Gangopadhyay, S.S. (2001). Invited review: cross-bridge regulation by thin filament-associated proteins. *J Appl Physiol* (1985) 91, 953-962.
- Mörgelin, M., Paulsson, M., Hardingham, T.E., Heinegård, D., and Engel, J. (1988). Cartilage proteoglycans. Assembly with hyaluronate and link protein as studied by electron microscopy. *Biochem J* 253, 175-185.
- Morris, N.J., Ducret, A., Aebersold, R., Ross, S.A., Keller, S.R., and Lienhard, G.E. (1997). Membrane amine oxidase cloning and identification as a major protein in the adipocyte plasma membrane. *J Biol Chem* 272, 9388-9392.
- Mu, D., Janes, S.M., Smith, A.J., Brown, D.E., Dooley, D.M., and Klinman, J.P. (1992). Tyrosine codon corresponds to topa quinone at the active site of copper amine oxidases. *J Biol Chem* 267, 7979-7982.
- Mu, D., Medzihradzky, K.F., Adams, G.W., Mayer, P., Hines, W.M., Burlingame, A.L., Smith, A.J., Cai, D., and Klinman, J.P. (1994). Primary structures for a mammalian cellular and serum copper amine oxidase. *J Biol Chem* 269, 9926-9932.
- Muñoz-Espín, D., and Serrano, M. (2014). Cellular senescence: from physiology to pathology. *Nat Rev Mol Cell Biol* 15, 482-496.
- Muzykantov, V.R. (2001). Targeting of superoxide dismutase and catalase to vascular endothelium. *J Control Release* 71, 1-21.
- Neogi, T., and Zhang, Y. (2013). Epidemiology of osteoarthritis. *Rheum Dis Clin North Am* 39, 1-19.
- Ng, L.J., Wheatley, S., Muscat, G.E., Conway-Campbell, J., Bowles, J., Wright, E., Bell, D.M., Tam, P.P., Cheah, K.S., and Koopman, P. (1997). SOX9 binds DNA, activates transcription, and coexpresses with type II collagen during chondrogenesis in the mouse. *Dev Biol* 183, 108-121.
- Niswander, L. (2002). Interplay between the molecular signals that control vertebrate limb

- development. *Int J Dev Biol* 46, 877-881.
- Norqvist, A., Fowler, C.J., and Orelund, L. (1981). The deamination of monoamines by pig dental pulp. *Biochem Pharmacol* 30, 403-409.
- Norqvist, A., Orelund, L., and Fowler, C.J. (1982). Some properties of monoamine oxidase and a semicarbazide sensitive amine oxidase capable of the deamination of 5-hydroxytryptamine from porcine dental pulp. *Biochem Pharmacol* 31, 2739-2744.
- Ochiai, Y., Itoh, K., Sakurai, E., and Tanaka, Y. (2005). Molecular cloning and characterization of rat semicarbazide-sensitive amine oxidase. *Biol Pharm Bull* 28, 413-418.
- Ohara, H., Tamayama, T., Maemura, K., Kanbara, K., Hayasaki, H., Abe, M., and Watanabe, M. (2001). Immunocytochemical demonstration of glucose transporters in epiphyseal growth plate chondrocytes of young rats in correlation with autoradiographic distribution of 2-deoxyglucose in chondrocytes of mice. *Acta Histochem* 103, 365-378.
- Olivieri, A., O'Sullivan, J., Fortuny, L.R., Vives, I.L., and Tipton, K.F. (2010). Interaction of L-lysine and soluble elastin with the semicarbazide-sensitive amine oxidase in the context of its vascular-adhesion and tissue maturation functions. *Biochim Biophys Acta* 1804, 941-947.
- Onyekwelu, I., Goldring, M.B., and Hidaka, C. (2009). Chondrogenesis, joint formation, and articular cartilage regeneration. *J Cell Biochem* 107, 383-392.
- O'Rourke, A.M., Wang, E.Y., Miller, A., Podar, E.M., Scheyhing, K., Huang, L., Kessler, C., Gao, H., Ton-Nu, H.T., Macdonald, M.T., *et al.* (2008). Anti-inflammatory effects of LJP 1586 [Z-3-fluoro-2-(4-methoxybenzyl)allylamine hydrochloride], an amine-based inhibitor of semicarbazide-sensitive amine oxidase activity. *J Pharmacol Exp Ther* 324, 867-875.
- O'Rourke, M.F., and Hashimoto, J. (2007). Mechanical factors in arterial aging: a clinical perspective. *J Am Coll Cardiol* 50, 1-13.
- O'Rourke, M.F., and Nichols, W.W. (2005). Aortic diameter, aortic stiffness, and wave reflection increase with age and isolated systolic hypertension. *Hypertension* 45, 652-658.
- O'Sullivan, J., Unzeta, M., Healy, J., O'Sullivan, M.I., Davey, G., and Tipton, K.F. (2004). Semicarbazide-sensitive amine oxidases: enzymes with quite a lot to do. *Neurotoxicology* 25, 303-315.
- Otto, F., Thornell, A.P., Crompton, T., Denzel, A., Gilmour, K.C., Rosewell, I.R., Stamp, G.W., Beddington, R.S., Mundlos, S., Olsen, B.R., *et al.* (1997). *Cbfa1*, a candidate gene for cleidocranial dysplasia syndrome, is essential for osteoblast differentiation and bone

- development. *Cell* 89, 765-771.
- Owens, G.K. (1998). Molecular control of vascular smooth muscle cell differentiation. *Acta Physiol Scand* 164, 623-635.
- Owens, G.K., and Wise, G. (1997). Regulation of differentiation/maturation in vascular smooth muscle cells by hormones and growth factors. *Agents Actions Suppl* 48, 3-24.
- Owens, G.K., Kumar, M.S., and Wamhoff, B.R. (2004). Molecular regulation of vascular smooth muscle cell differentiation in development and disease. *Physiol Rev* 84, 767-801.
- P. Berillis, The Role of Collagen in the Aorta's Structure. *The Open Circulation and Vascular Journal*, 6, 1-8 (2013).
- Palfrey, A.J., and Davies, D.V. (1966). The fine structure of chondrocytes. *J Anat* 100, 213-226.
- Paulsen, F., and Tillmann, B. (1999). Composition of the extracellular matrix in human cricoarytenoid joint articular cartilage. *Arch Histol Cytol* 62, 149-163.
- Pearle, A.D., Warren, R.F., and Rodeo, S.A. (2005). Basic science of articular cartilage and osteoarthritis. *Clin Sports Med* 24, 1-12.
- Penraat, J.H., Allen, A.L., Fretz, P.B., and Bailey, J.V. (2000). An evaluation of chemical arthrodesis of the proximal interphalangeal joint in the horse by using monoiodoacetate. *Can J Vet Res* 64, 212-221.
- Perrotta, I. (2013). Ultrastructural features of human atherosclerosis. *Ultrastruct Pathol* 37, 43-51.
- Pizette, S., and Niswander, L. (2000). BMPs are required at two steps of limb chondrogenesis: formation of prechondrogenic condensations and their differentiation into chondrocytes. *Dev Biol* 219, 237-249.
- Pober, J.S., and Sessa, W.C. (2007). Evolving functions of endothelial cells in inflammation. *Nat Rev Immunol* 7, 803-815.
- Poliseno, L., Cecchetti, A., Mariani, L., Evangelista, M., Ricci, F., Giorgi, F., Citti, L., and Rainaldi, G. (2006). Resting smooth muscle cells as a model for studying vascular cell activation. *Tissue Cell* 38, 111-120.
- Precious, E., Gunn, C.E., and Lyles, G.A. (1988). Deamination of methylamine by semicarbazide-sensitive amine oxidase in human umbilical artery and rat aorta. *Biochem Pharmacol* 37, 707-713.
- Pritchett, J., Athwal, V., Roberts, N., Hanley, N.A., and Hanley, K.P. (2011). Understanding the role of SOX9 in acquired diseases: lessons from development. *Trends Mol Med* 17,

166-174.

- Pullig, O., Weseloh, G., Gauer, S., and Swoboda, B. (2000). Osteopontin is expressed by adult human osteoarthritic chondrocytes: protein and mRNA analysis of normal and osteoarthritic cartilage. *Matrix Biol* 19, 245-255.
- Quinn, T.M., Häuselmann, H.J., Shintani, N., and Hunziker, E.B. (2013). Cell and matrix morphology in articular cartilage from adult human knee and ankle joints suggests depth-associated adaptations to biomechanical and anatomical roles. *Osteoarthritis Cartilage*.
- Raimondi, L., Pirisino, R., Ignesti, G., Capecchi, S., Banchelli, G., and Buffoni, F. (1991). Semicarbazide-sensitive amine oxidase activity (SSAO) of rat epididymal white adipose tissue. *Biochem Pharmacol* 41, 467-470.
- Rieppo, J., Töyräs, J., Nieminen, M.T., Kovanen, V., Hyttinen, M.M., Korhonen, R.K., Jurvelin, J.S., and Helminen, H.J. (2003). Structure-function relationships in enzymatically modified articular cartilage. *Cells Tissues Organs* 175, 121-132.
- Roach, H.I., and Clarke, N.M. (1999). "Cell paralysis" as an intermediate stage in the programmed cell death of epiphyseal chondrocytes during development. *J Bone Miner Res* 14, 1367-1378.
- Roach, H.I., and Clarke, N.M. (2000). Physiological cell death of chondrocytes in vivo is not confined to apoptosis. New observations on the mammalian growth plate. *J Bone Joint Surg Br* 82, 601-613.
- Rodgers, B.D., Strack, A.M., Dallman, M.F., Hwa, L., and Nicoll, C.S. (1995). Corticosterone regulation of insulin-like growth factor I, IGF-binding proteins, and growth in streptozotocin-induced diabetic rats. *Diabetes* 44, 1420-1425.
- Rosenfeld, M.E., Polinsky, P., Virmani, R., Kauser, K., Rubanyi, G., and Schwartz, S.M. (2000). Advanced atherosclerotic lesions in the innominate artery of the ApoE knockout mouse. *Arterioscler Thromb Vasc Biol* 20, 2587-2592.
- Roughley, P.J. (2006). The structure and function of cartilage proteoglycans. *Eur Cell Mater* 12, 92-101.
- Roy, S.G., Nozaki, Y., and Phan, S.H. (2001). Regulation of alpha-smooth muscle actin gene expression in myofibroblast differentiation from rat lung fibroblasts. *Int J Biochem Cell Biol* 33, 723-734.
- Rudijanto, A. (2007). The role of vascular smooth muscle cells on the pathogenesis of atherosclerosis. *Acta Med Indones* 39, 86-93.
- Ruhlen, R., and Marberry, K. (2014). The chondrocyte primary cilium. *Osteoarthritis Cartilage* 22, 1071-1076.

- Rzucidlo, E.M., Martin, K.A., and Powell, R.J. (2007). Regulation of vascular smooth muscle cell differentiation. *J Vasc Surg 45 Suppl A*, A25-32.
- Safar, M.E., London, G.M., Asmar, R., and Frohlich, E.D. (1998). Recent advances on large arteries in hypertension. *Hypertension 32*, 156-161.
- Salmi, M., and Jalkanen, S. (1992). A 90-kilodalton endothelial cell molecule mediating lymphocyte binding in humans. *Science 257*, 1407-1409.
- Salmi, M., and Jalkanen, S. (2001). VAP-1: an adhesin and an enzyme. *Trends Immunol 22*, 211-216.
- Salmi, M., and Jalkanen, S. (2005). Cell-surface enzymes in control of leukocyte trafficking. *Nat Rev Immunol 5*, 760-771.
- Salmi, M., and Jalkanen, S. (2006). Developmental regulation of the adhesive and enzymatic activity of vascular adhesion protein-1 (VAP-1) in humans. *Blood 108*, 1555-1561.
- Salmi, M., and Jalkanen, S. (2011). Homing-associated molecules CD73 and VAP-1 as targets to prevent harmful inflammations and cancer spread. *FEBS Lett 585*, 1543-1550.
- Salmi, M., and Jalkanen, S. (2012). Ectoenzymes controlling leukocyte traffic. *Eur J Immunol 42*, 284-292.
- Salmi, M., Kalimo, K., and Jalkanen, S. (1993). Induction and function of vascular adhesion protein-1 at sites of inflammation. *J Exp Med 178*, 2255-2260.
- Salmi, M., Rajala, P., and Jalkanen, S. (1997). Homing of mucosal leukocytes to joints. Distinct endothelial ligands in synovium mediate leukocyte-subtype specific adhesion. *J Clin Invest 99*, 2165-2172.
- Salmi, M., Stolen, C., Jousilahti, P., Yegutkin, G.G., Tapanainen, P., Janatuinen, T., Knip, M., Jalkanen, S., and Salomaa, V. (2002). Insulin-regulated increase of soluble vascular adhesion protein-1 in diabetes. *Am J Pathol 161*, 2255-2262.
- Salmi, M., Tohka, S., and Jalkanen, S. (2000). Human vascular adhesion protein-1 (VAP-1) plays a critical role in lymphocyte-endothelial cell adhesion cascade under shear. *Circ Res 86*, 1245-1251.
- Salmi, M., Yegutkin, G.G., Lehtonen, R., Koskinen, K., Salminen, T., and Jalkanen, S. (2001). A cell surface amine oxidase directly controls lymphocyte migration. *Immunity 14*, 265-276.
- Salminen, T.A., Smith, D.J., Jalkanen, S., and Johnson, M.S. (1998). Structural model of the catalytic domain of an enzyme with cell adhesion activity: human vascular adhesion protein-1 (HVAP-1) D4 domain is an amine oxidase. *Protein Eng 11*, 1195-1204.
- Sandell, L.J., Nalin, A.M., and Reife, R.A. (1994a). Alternative splice form of type II

- procollagen mRNA (IIA) is predominant in skeletal precursors and non-cartilaginous tissues during early mouse development. *Dev Dyn* 199, 129-140.
- Sandell, L.J., Sugai, J.V., and Trippel, S.B. (1994b). Expression of collagens I, II, X, and XI and aggrecan mRNAs by bovine growth plate chondrocytes in situ. *J Orthop Res* 12, 1-14.
- SCHAYER, R.W., SMILEY, R.L., and KAPLAN, E.H. (1952). The metabolism of epinephrine containing isotopic carbon. II. *J Biol Chem* 198, 545-551.
- Schwelberger, H.G. (2006). Origins of plasma amine oxidases in different mammalian species. *Inflamm Res* 55 Suppl 1, S57-58.
- Schwelberger, H.G. (2007). The origin of mammalian plasma amine oxidases. *J Neural Transm* 114, 757-762.
- Seki, K., Fujimori, T., Savagner, P., Hata, A., Aikawa, T., Ogata, N., Nabeshima, Y., and Kaechoong, L. (2003). Mouse Snail family transcription repressors regulate chondrocyte, extracellular matrix, type II collagen, and aggrecan. *J Biol Chem* 278, 41862-41870.
- Shea, C.M., Edgar, C.M., Einhorn, T.A., and Gerstenfeld, L.C. (2003). BMP treatment of C3H10T1/2 mesenchymal stem cells induces both chondrogenesis and osteogenesis. *J Cell Biochem* 90, 1112-1127.
- Sherwood, J.C., Bertrand, J., Eldridge, S.E., and Dell'Accio, F. (2014). Cellular and molecular mechanisms of cartilage damage and repair. *Drug Discov Today* 19, 1172-1177.
- Shi, Q., Aida, K., Vandeberg, J.L., and Wang, X.L. (2004). Passage-dependent changes in baboon endothelial cells--relevance to in vitro aging. *DNA Cell Biol* 23, 502-509.
- Shibata, S., Fukada, K., Imai, H., Abe, T., and Yamashita, Y. (2003). In situ hybridization and immunohistochemistry of versican, aggrecan and link protein, and histochemistry of hyaluronan in the developing mouse limb bud cartilage. *J Anat* 203, 425-432.
- Sies, H. (2014). Role of metabolic H₂O₂ generation: redox signaling and oxidative stress. *J Biol Chem* 289, 8735-8741.
- Smith, D.J., Salmi, M., Bono, P., Hellman, J., Leu, T., and Jalkanen, S. (1998). Cloning of vascular adhesion protein 1 reveals a novel multifunctional adhesion molecule. *J Exp Med* 188, 17-27.
- Smith, G.N. (2006). The role of collagenolytic matrix metalloproteinases in the loss of articular cartilage in osteoarthritis. *Front Biosci* 11, 3081-3095.
- Solé, M., Hernandez, M., Boada, M., and Unzeta, M. (2007). Characterization of A7r5 cell line transfected in a stable form by hSSAO/VAP-1 gene (A7r5 hSSAO/VAP-1 cell line). *J Neural Transm* 114, 763-767.

- Solé, M., Hernandez-Guillamon, M., Boada, M., and Unzeta, M. (2008). p53 phosphorylation is involved in vascular cell death induced by the catalytic activity of membrane-bound SSAO/VAP-1. *Biochim Biophys Acta* 1783, 1085-1094.
- Steinberg, D. (2002). Atherogenesis in perspective: hypercholesterolemia and inflammation as partners in crime. *Nat Med* 8, 1211-1217.
- Steinberg, D., and Witztum, J.L. (2002). Is the oxidative modification hypothesis relevant to human atherosclerosis? Do the antioxidant trials conducted to date refute the hypothesis? *Circulation* 105, 2107-2111.
- Stolen, C.M., Madanat, R., Marti, L., Kari, S., Yegutkin, G.G., Sariola, H., Zorzano, A., and Jalkanen, S. (2004a). Semicarbazide sensitive amine oxidase overexpression has dual consequences: insulin mimicry and diabetes-like complications. *FASEB J* 18, 702-704.
- Stolen, C.M., Marttila-Ichihara, F., Koskinen, K., Yegutkin, G.G., Turja, R., Bono, P., Skurnik, M., Hänninen, A., Jalkanen, S., and Salmi, M. (2005). Absence of the endothelial oxidase AOC3 leads to abnormal leukocyte traffic in vivo. *Immunity* 22, 105-115.
- Stolen, C.M., Yegutkin, G.G., Kurkijärvi, R., Bono, P., Alitalo, K., and Jalkanen, S. (2004b). Origins of serum semicarbazide-sensitive amine oxidase. *Circ Res* 95, 50-57.
- Strolin Benedetti, M., Tipton, K.F., and Whomsley, R. (2007). Amine oxidases and monooxygenases in the in vivo metabolism of xenobiotic amines in humans: has the involvement of amine oxidases been neglected? *Fundam Clin Pharmacol* 21, 467-480.
- Subra, C., Fontana, E., Visentin, V., Testar, X., and Carpené, C. (2003). Tyramine and benzylamine partially but selectively mimic insulin action on adipose differentiation in 3T3-L1 cells. *J Physiol Biochem* 59, 209-216.
- Sugiki, T., Uyama, T., Toyoda, M., Morioka, H., Kume, S., Miyado, K., Matsumoto, K., Saito, H., Tsumaki, N., Takahashi, Y., *et al.* (2007). Hyaline cartilage formation and enchondral ossification modeled with KUM5 and OP9 chondroblasts. *J Cell Biochem* 100, 1240-1254.
- Sumpio, B.E., Riley, J.T., and Dardik, A. (2002). Cells in focus: endothelial cell. *Int J Biochem Cell Biol* 34, 1508-1512.
- Sun, J., Sukhova, G.K., Wolters, P.J., Yang, M., Kitamoto, S., Libby, P., MacFarlane, L.A., Mallen-St Clair, J., and Shi, G.P. (2007). Mast cells promote atherosclerosis by releasing proinflammatory cytokines. *Nat Med* 13, 719-724.
- Sung, H.J., Eskin, S.G., Sakurai, Y., Yee, A., Kataoka, N., and McIntire, L.V. (2005). Oxidative stress produced with cell migration increases synthetic phenotype of vascular smooth muscle cells. *Ann Biomed Eng* 33, 1546-1554.

- Surra, J.C., Guillén, N., Arbonés-Mainar, J.M., Barranquero, C., Navarro, M.A., Arnal, C., Orman, I., Segovia, J.C., and Osada, J. (2010). Sex as a profound modifier of atherosclerotic lesion development in apolipoprotein E-deficient mice with different genetic backgrounds. *J Atheroscler Thromb* *17*, 712-721.
- Svenson, K.L., Pollare, T., Lithell, H., and Hällgren, R. (1988). Impaired glucose handling in active rheumatoid arthritis: relationship to peripheral insulin resistance. *Metabolism* *37*, 125-130.
- Tábi, T., Szökő, E., Mérey, A., Tóth, V., Mátyus, P., and Gyires, K. (2013). Study on SSAO enzyme activity and anti-inflammatory effect of SSAO inhibitors in animal model of inflammation. *J Neural Transm* *120*, 963-967.
- Taleb, S., Herbin, O., Ait-Oufella, H., Verreth, W., Gourdy, P., Barateau, V., Merval, R., Esposito, B., Clément, K., Holvoet, P., *et al.* (2007). Defective leptin/leptin receptor signaling improves regulatory T cell immune response and protects mice from atherosclerosis. *Arterioscler Thromb Vasc Biol* *27*, 2691-2698.
- Taleb, S., Tedgui, A., and Mallat, Z. (2008). Regulatory T-cell immunity and its relevance to atherosclerosis. *J Intern Med* *263*, 489-499.
- ten Dijke, P., and Arthur, H.M. (2007). Extracellular control of TGFbeta signalling in vascular development and disease. *Nat Rev Mol Cell Biol* *8*, 857-869.
- Tickle, C. (2002). Molecular basis of vertebrate limb patterning. *Am J Med Genet* *112*, 250-255.
- Tickle, C. (2003). Patterning systems--from one end of the limb to the other. *Dev Cell* *4*, 449-458.
- Tickle, C., and Münsterberg, A. (2001). Vertebrate limb development--the early stages in chick and mouse. *Curr Opin Genet Dev* *11*, 476-481.
- Tohka, S., Laukkanen, M., Jalkanen, S., and Salmi, M. (2001). Vascular adhesion protein 1 (VAP-1) functions as a molecular brake during granulocyte rolling and mediates recruitment in vivo. *FASEB J* *15*, 373-382.
- Tsamis, A., Krawiec, J.T., and Vorp, D.A. (2013). Elastin and collagen fibre microstructure of the human aorta in ageing and disease: a review. *J R Soc Interface* *10*, 20121004.
- Ushijima, T., Okazaki, K., Tsushima, H., Ishihara, K., Doi, T., and Iwamoto, Y. (2014). CCAAT/enhancer binding protein β regulates expression of Indian hedgehog during chondrocytes differentiation. *PLoS One* *9*, e104547.
- Valente, T., Solé, M., and Unzeta, M. (2008). SSAO/VAP-1 protein expression during mouse embryonic development. *Dev Dyn* *237*, 2585-2593.

- van der Kraan, P.M., Vitters, E.L., van de Putte, L.B., and van den Berg, W.B. (1989). Development of osteoarthritic lesions in mice by "metabolic" and "mechanical" alterations in the knee joints. *Am J Pathol* 135, 1001-1014.
- van Varik, B.J., Rennenberg, R.J., Reutelingsperger, C.P., Kroon, A.A., de Leeuw, P.W., and Schurgers, L.J. (2012). Mechanisms of arterial remodeling: lessons from genetic diseases. *Front Genet* 3, 290.
- Virmani, R., Avolio, A.P., Mergner, W.J., Robinowitz, M., Herderick, E.E., Cornhill, J.F., Guo, S.Y., Liu, T.H., Ou, D.Y., and O'Rourke, M. (1991). Effect of aging on aortic morphology in populations with high and low prevalence of hypertension and atherosclerosis. Comparison between occidental and Chinese communities. *Am J Pathol* 139, 1119-1129.
- von der Mark, H., von der Mark, K., and Gay, S. (1976). Study of differential collagen synthesis during development of the chick embryo by immunofluorescence. I. Preparation of collagen type I and type II specific antibodies and their application to early stages of the chick embryo. *Dev Biol* 48, 237-249.
- Wallis, G.A. (1996). Bone growth: coordinating chondrocyte differentiation. *Curr Biol* 6, 1577-1580.
- Wang, J.C., and Bennett, M. (2012). Aging and atherosclerosis: mechanisms, functional consequences, and potential therapeutics for cellular senescence. *Circ Res* 111, 245-259.
- Ward, M.R., Pasterkamp, G., Yeung, A.C., and Borst, C. (2000). Arterial remodeling. Mechanisms and clinical implications. *Circulation* 102, 1186-1191.
- Weyand, C.M., and Goronzy, J.J. (2013). Immune mechanisms in medium and large-vessel vasculitis. *Nat Rev Rheumatol* 9, 731-740.
- Weyrich, A.S., Schwertz, H., Kraiss, L.W., and Zimmerman, G.A. (2009). Protein synthesis by platelets: historical and new perspectives. *J Thromb Haemost* 7, 241-246.
- Wibo, M., Duong, A.T., and Godfraind, T. (1980). Subcellular location of semicarbazide-sensitive amine oxidase in rat aorta. *Eur J Biochem* 112, 87-94.
- Williams, J.M., and Brandt, K.D. (1985). Triamcinolone hexacetonide protects against fibrillation and osteophyte formation following chemically induced articular cartilage damage. *Arthritis Rheum* 28, 1267-1274.
- Wong, M., and Carter, D.R. (2003). Articular cartilage functional histomorphology and mechanobiology: a research perspective. *Bone* 33, 1-13.
- Yoong, K.F., McNab, G., Hübscher, S.G., and Adams, D.H. (1998). Vascular adhesion protein-1 and ICAM-1 support the adhesion of tumor-infiltrating lymphocytes to tumor

- endothelium in human hepatocellular carcinoma. *J Immunol* *160*, 3978-3988.
- Yoshida, C.A., Yamamoto, H., Fujita, T., Furuichi, T., Ito, K., Inoue, K., Yamana, K., Zanma, A., Takada, K., Ito, Y., *et al.* (2004). Runx2 and Runx3 are essential for chondrocyte maturation, and Runx2 regulates limb growth through induction of Indian hedgehog. *Genes Dev* *18*, 952-963.
- Yoshikawa, N., Noda, K., Ozawa, Y., Tsubota, K., Mashima, Y., and Ishida, S. (2012). Blockade of vascular adhesion protein-1 attenuates choroidal neovascularization. *Mol Vis* *18*, 593-600.
- YOUNG, R.W. (1962). Cell proliferation and specialization during endochondral osteogenesis in young rats. *J Cell Biol* *14*, 357-370.
- Young, S.N., Davis, B.A., and Gauthier, S. (1982). Precursors and metabolites of phenylethylamine, m and p-tyramine and tryptamine in human lumbar and cisternal cerebrospinal fluid. *J Neurol Neurosurg Psychiatry* *45*, 633-639.
- Yu, P.H. (1998). Increase of formation of methylamine and formaldehyde in vivo after administration of nicotine and the potential cytotoxicity. *Neurochem Res* *23*, 1205-1210.
- Yu, P.H., and Deng, Y.L. (1998). Endogenous formaldehyde as a potential factor of vulnerability of atherosclerosis: involvement of semicarbazide-sensitive amine oxidase-mediated methylamine turnover. *Atherosclerosis* *140*, 357-363.
- Yu, P.H., and Zuo, D.M. (1993). Oxidative deamination of methylamine by semicarbazide-sensitive amine oxidase leads to cytotoxic damage in endothelial cells. Possible consequences for diabetes. *Diabetes* *42*, 594-603.
- Yu, P.H., and Zuo, D.M. (1996). Formaldehyde produced endogenously via deamination of methylamine. A potential risk factor for initiation of endothelial injury. *Atherosclerosis* *120*, 189-197.
- Yu, P.H., and Zuo, D.M. (1997). Aminoguanidine inhibits semicarbazide-sensitive amine oxidase activity: implications for advanced glycation and diabetic complications. *Diabetologia* *40*, 1243-1250.
- Yu, P.H., Fang, C.Y., and Yang, C.M. (1992). Semicarbazide-sensitive amine oxidase from the smooth muscles of dog aorta and trachea: activation by the MAO-A inhibitor clorgyline. *J Pharm Pharmacol* *44*, 981-985.
- Yu, P.H., Lai, C.T., and Zuo, D.M. (1997). Formation of formaldehyde from adrenaline in vivo; a potential risk factor for stress-related angiopathy. *Neurochem Res* *22*, 615-620.
- Yu, P.H., Wang, M., Deng, Y.L., Fan, H., and Shira-Bock, L. (2002). Involvement of semicarbazide-sensitive amine oxidase-mediated deamination in atherogenesis in KKAY

- diabetic mice fed with high cholesterol diet. *Diabetologia* 45, 1255-1262.
- Yu, P.H., Wang, M., Fan, H., Deng, Y., and Gubisne-Haberle, D. (2004). Involvement of SSAO-mediated deamination in adipose glucose transport and weight gain in obese diabetic KKAY mice. *Am J Physiol Endocrinol Metab* 286, E634-641.
- Yu, P.H., Wright, S., Fan, E.H., Lun, Z.R., and Gubisne-Harberle, D. (2003). Physiological and pathological implications of semicarbazide-sensitive amine oxidase. *Biochim Biophys Acta* 1647, 193-199.
- Zeisel, S.H., and DaCosta, K.A. (1986). Increase in human exposure to methylamine precursors of N-nitrosamines after eating fish. *Cancer Res* 46, 6136-6138.
- Zeisel, S.H., DaCosta, K.A., and Fox, J.G. (1985). Endogenous formation of dimethylamine. *Biochem J* 232, 403-408.
- Zeisel, S.H., Wishnok, J.S., and Blusztajn, J.K. (1983). Formation of methylamines from ingested choline and lecithin. *J Pharmacol Exp Ther* 225, 320-324.
- Zhang, X., and McIntire, W.S. (1996). Cloning and sequencing of a copper-containing, topa quinone-containing monoamine oxidase from human placenta. *Gene* 179, 279-286.
- Zhao, Q., Eberspaecher, H., Lefebvre, V., and De Crombrughe, B. (1997). Parallel expression of Sox9 and Col2a1 in cells undergoing chondrogenesis. *Dev Dyn* 209, 377-386.
- Zittermann, S.I., and Issekutz, A.C. (2006). Basic fibroblast growth factor (bFGF, FGF-2) potentiates leukocyte recruitment to inflammation by enhancing endothelial adhesion molecule expression. *Am J Pathol* 168, 835-846.
- Zou, H., Wieser, R., Massagué, J., and Niswander, L. (1997). Distinct roles of type I bone morphogenetic protein receptors in the formation and differentiation of cartilage. *Genes Dev* 11, 2191-2203.
- Zuscik, M.J., Hilton, M.J., Zhang, X., Chen, D., and O'Keefe, R.J. (2008). Regulation of chondrogenesis and chondrocyte differentiation by stress. *J Clin Invest* 118, 429-438.
- Zwilling, E. (1972). Limb morphogenesis. *Dev Biol* 28, 12-17.

Annex
